Discovery of small-molecule AR-V7 inhibitors for castration-resistant prostate cancer

Qianhui Yi

Division of Experimental Medicine

Faculty of Medicine, McGill University, Montreal August 2022

A thesis submitted to the Faculty of Graduate Studies and Research in partial fulfillment of requirements of the degree of Doctor of Philosophy

Discovery of small-molecule AR-V7 inhibitors for castration-resistant prostate cancer

THESIS FOR DOCTORAL DEGREE (Ph. D.)

By

Qianhui Yi

Principal supervisor:
Professor Jian Hui Wu
McGill University
Department of Medicine - Division of Experimental Medicine

This thesis is dedicated to my beloved husband Henry and my dear daughter Calia. This work was finished during a particularly difficult time of my life, both post-COVID19 pandemic and post-partum. I thank them for their love and support. I am also grateful for my supervisor Dr. Wu; this work would not be possible without his selfless guidance.

Acknowledgements

I would like to foremost offer my deepest gratitude to my supervisor Dr. Jian Hui Wu for taking me along an intellectually stimulating journey into the field of cancer research. His constant support, patience, and guidance throughout my project solidified my passion for drug discovery. I would also like to thank my academic advisor Dr. Andrew Mouland and my committee members Dr. Nicoletta Eliopoulos, Dr. Hua Gu, and Dr. Moulay Alaoui-Jamali for offering me advice and encouragement during my stay. Also innumerable thanks to all my lab mates, Xiaojun Han, Hui-Yue Chen, Jung Hwa Seo, Dinghong Qiu, Xiaohong Tian and Mao Li for their everyday support and cooperation in my project.

Abstract

Castration-resistant prostate cancer (CRPC) is a relapsed form of prostate cancer from initial androgen deprivation therapies (ADT), its progression manifests reactivated androgen receptor (AR) signaling activity despite the castration level of androgen. When CRPC develops, second-line ADT is offered to patients for regaining AR signaling blockade, including androgen biosynthesis inhibitor abiraterone (Abi); and the antiandrogens, such as enzalutamide (ENZ), which compete for the androgen binding pocket in the AR ligand-binding domain (LBD). However, resistance almost always occurs after a brief response period, featured with rising PSA as a sign of restored AR signaling activity. The AR splice variants with LBD truncated, majorly, AR-V7 is becoming a well-established driver of the persistent AR signaling in CRPC. On the molecular basis, AR-V7 sustains AR signaling by leveraging the loss of LBD to stay constitutively active and bypass all the currently available ADTs. From the clinical perspective, AR-V7 mRNA and protein were both found overexpressed in Abi and ENZ-treated CRPC patients and were predictive of worse outcomes. Although mounting evidence highlighted the urgency of AR-V7 inhibition, AR-V7 is still undrugged.

In **Chapter 1** of this thesis, the first part comprises a comprehensive review of prostate cancer epidemiology, oncogenesis, diagnosis, treatment landscape, drug resistance, and corresponding resistant mechanisms. In the second part, I discussed the biology of AR-V7 and its role as a resistance driver in CRPC. Lastly, I summarized the emerging approaches of AR-V7 targeting, and reviewed recent literature reporting their potency in preclinical models and clinical trials.

Developing chemical inhibitors against AR-V7 as CRPC therapeutics has been the major focus of my Ph.D. study. **Chapter 2** and **Chapter 3** are manuscripts reporting the discovery of two novel small molecules SC428 and SC912, individually. SC428 and SC912 have completely different chemical scaffolds and target different regions of the AR N-terminal domain. Both compounds potently inhibited AR-V7 mediated AR signaling and demonstrated efficacy against CRPC models *in vitro* and *in vivo*, suggesting their therapeutic potential in overcoming drug resistance in CRPC.

One may also wonder about the potential of immunotherapies against prostate cancer. Therefore, in **Chapter 4,** we described the progress of a side project during my Ph.D. study, which is to develop small-molecule STING agonists to stimulate anti-cancer immunity. We discovered an initial hit compound that activated STING and enhanced tumor antigen-specific T cell generation in mice.

Résumé

Le cancer de la prostate résistant à la castration (CRPC) est une forme récidivante du cancer de la prostate des thérapies initiales de privation d'androgènes (ADT), sa progression manifeste une activité de signalisation des récepteurs aux androgènes (AR) réactivée malgré le niveau de castration des androgènes. Lorsque le CPRC se développe, l'ADT de deuxième ligne est proposé aux patients pour rétablir le blocage de la signalisation AR, y compris l'abiratérone (Abi), inhibiteur de la biosynthèse des androgènes ; et les anti-androgènes, tels que l'enzalutamide (ENZ), qui entrent en compétition pour la poche de liaison aux androgènes dans le domaine de liaison au ligand AR (LBD). Cependant, la résistance survient presque toujours après une brève période de réponse, caractérisée par une augmentation du PSA comme signe d'une activité de signalisation AR restaurée. Les variantes d'épissage AR avec LBD tronqué, principalement, AR-V7 devient un pilote bien établi de la signalisation AR persistante dans le CRPC. Sur la base moléculaire, AR-V7 soutient la signalisation AR en tirant parti de la perte de LBD pour rester constitutivement actif et contourner tous les ADT actuellement disponibles. Du point de vue clinique, l'ARNm et la protéine AR-V7 ont tous deux été trouvés surexprimés chez les patients atteints de CPRC traités par Abi et ENZ et étaient prédictifs d'un résultat pire. Bien que de plus en plus de preuves aient mis en évidence l'urgence de l'inhibition de l'AR-V7, l'AR-V7 n'est toujours pas médicamenté.

Dans le **chapitre 1** de cette thèse, la première partie comprend un examen complet de l'épidémiologie du cancer de la prostate, de l'oncogenèse, du diagnostic, du paysage thérapeutique, de la résistance aux médicaments et des mécanismes de résistance correspondants. Dans la deuxième partie, j'ai discuté de la biologie de l'AR-V7 et de son rôle en tant que moteur de résistance dans le CRPC. Enfin, j'ai résumé les approches émergentes du ciblage AR-V7, passé en

revue la littérature récente rapportant leur puissance dans les modèles précliniques et les essais cliniques.

Le développement d'inhibiteurs chimiques contre l'AR-V7 en tant que thérapie CRPC a été l'objectif principal de mon doctorat. Les **chapitres 2 et 3** nos deux manuscrits rapportent la découverte de deux nouvelles petites molécules SC428 et SC912, individuellement. SC428 et SC912 ont des échafaudages chimiques complètement différents et ciblent différentes régions du domaine AR N-terminal. Les deux composés ont puissamment inhibé la signalisation AR médiée par AR-V7 et ont démontré leur efficacité contre les modèles de CRPC in vitro et in vivo, suggérant leur potentiel thérapeutique pour surmonter la résistance aux médicaments dans le CRPC.

On peut aussi s'interroger sur le potentiel des immunothérapies contre le cancer de la prostate. Donc, dans le **chapitre 4**, nous avons décrit l'avancement d'un projet parallèle au cours de mon doctorat. Étude, qui développe des agonistes STING à petites molécules pour stimuler l'immunité anticancéreuse. Nous avons découvert un composé à succès initial qui a activé STING et amélioré la génération de lymphocytes T spécifiques de l'antigène tumoral chez la souris.

Table of Contents

ACKNOWLEDGEMENTS **4**

ABSTRACT **5**

RÉSUMÉ **7**

TABLE OF CONTENTS **9**

LIST OF SCIENTIFIC PUBLICATIONS **11**

CONTRIBUTION TO ORIGINAL KNOWLEDGE **12**

CONTRIBUTION OF AUTHORS **13**

LIST OF FIGURES **15**

LIST OF KEY ABBREVIATIONS **18**

CHAPTER 1: INTRODUCTION **19**

1.1. Prostate cancer 19
1.2. FDA-approved drugs for CRPC treatment 41
1.3. Continued AR signaling activity as a main drug-resistant mechanism in CRPC 50
1.4. The biology of AR-V7 57
1.5. Emerging approaches for pharmacological inhibition of AR-V7 activity 62
1.6. Our research rationale and objectives 72

CHAPTER 2: DISCOVERY OF A SMALL-MOLECULE INHIBITOR TARGETING THE ANDROGEN RECEPTOR N-TERMINAL DOMAIN FOR CASTRATION-RESISTANT PROSTATE CANCER **73**

2.1. Abstract 75
2.2. Introduction 76
2.3. Materials and Methods 78
2.4. Results 83
2.5. Discussion 92
2.6. Figures 96
2.7. Supplementary information 108
2.8. Manuscript 1 References 118

BRIDGING TEXT 1 ..... **123**

CHAPTER 3: SC912 INHIBITS AR-V7 ACTIVITY IN CASTRATION-RESISTANT PROSTATE CANCER BY TARGETING ANDROGEN RECEPTOR N-TERMINAL DOMAIN **124**

3.1. Abstract 126
3.2. Introduction 127
3.3. Result 129
3.4. Discussion 135
3.5. Materials and Methods 138
3.6. Figures 142
3.7. Supplementary Information 154
3.8. Manuscript 2 References 159

BRIDGING TEXT 2 ..... **164**

CHAPTER 4: STIMULATION OF STING BY NOVEL SMALL MOLECULES FOR ANTITUMOR IMMUNITY **179**

4.1. Abstract 181
4.2. Introduction 182
4.3. Materials and Methods 184
4.4. Result 187
4.5. Discussion 193
4.6. Figures 195
4.7. Manuscript 3 References 201

COMPREHENSIVE DISCUSSION 204

CONCLUSION AND SUMMARY 209

REFERENCES FOR BACKGROUND AND DISCUSSION 210

List of Scientific Publications

1. Discovery of a small-molecule inhibitor targeting the androgen receptor N-terminal domain for castration-resistant prostate cancer Qianhui Yi[1,2], Weiguo Liu[1], Jung Hwa Seo[1], Jie Su[1], Moulay A. Alaoui-Jamali[1,2], Jun Luo[3], Rongtuan Lin[1,2] and Jian Hui Wu[1,2]*

- Manuscript accepted by Molecular Cancer Therapeutics January 22th, 2023

2. SC912 inhibits AR-V7 activity in castration-resistant prostate cancer by targeting androgen receptor N-terminal domain

Qianhui Yi[1,2], Xiaojun Han[1], Henry G. Yu[1,2], Huei-Yu Chen[1,2], Dinghong Qiu[1], Jie Su[1], Moulay A. Alaoui-Jamali[1,2], Rongtuan Lin[1,2], Gerald Batist[1,2], and Jian Hui Wu[1,2]*

- Manuscript ready for submission to Oncogene

3. **Stimulation of STING by Novel Small Molecules for Antitumor Immunity** Qianhui Yi[1,2], Xiaojun Han[1], Rongtuan Lin[1,2], Gerald Batist[1,2]and Jian Hui Wu[1,2]*

- Manuscript in preparation

Contribution to original knowledge

Androgen receptor is presently the most crucial therapeutic target for advanced prostate cancer. However, current mainstay therapies are not effective against truncated, constitutively active forms of AR, including AR-V7, which drives drug resistance in the terminal form of prostate cancer called castration-resistant prostate cancer (CRPC). The N-terminal domain (NTD) is crucial to AR activity and is retained in AR-V7, but the intrinsically disordered nature of this domain imposes severe challenge to drugging this region. In this thesis, we describe the discovery and characterization of two novel lead compounds (SC428 and SC912) that are effective in targeting the AR NTD, leading to substantial inhibition of AR-V7 activity, thus reducing CRPC growth *in vitro* and *in vivo*. Importantly, SC428 and SC912 have completely different chemical scaffolds and target different regions of the AR N-terminal domain, which have opened up avenues for further development of AR-V7 inhibitors.

Contribution of authors

Chapter 1 (Introduction)

Q. Yi: Gathering and reviewing the literatures, writing original draft. **J. H. Wu**: manuscript editing.

Chapter 2 (Discovery of a small-molecule inhibitor targeting the androgen receptor N-terminal domain for castration-resistant prostate cancer)

Q. Yi: Design of experiments, compound design and screening. *In vitro* characterization, including all western blots, proliferation assay, reporter assay, immunofluorescence, chromatin immunoprecipitation, co-immunoprecipitation, quantitative PCR, and nuclear localization assay. *In vivo* evaluation, including implantation of tumor cells, measurement of tumor, animal sacrifice, tumor harvest, and western blot analysis of tumor samples. Additionally, data interpretation, and writing original draft. **W. Liu**: Compound synthesis. **J.H. Seo**: Immunofluorescence in figure 3c **J. Su**: Animal surgery, animal and tumor monitoring. **M.A. Jamali**: Resource, *in vivo* protocol assembly. **J. Luo**: Resource, result interpretation. **R. Lin**: Resource, plasmids construction. **J. H. Wu**: Conceptualization, funding acquisition, supervision, data interpretation and manuscript editing.

Chapter 3 (SC912 inhibits AR-V7 activity in castration-resistant prostate cancer by targeting androgen receptor N-terminal domain)

Q. Yi: Design of experiments, compound design and screening. *In vitro* characterization, including all western blots, proliferation assay, reporter assay, immunofluorescence, chromatin immunoprecipitation, co-immunoprecipitation, quantitative PCR, and nuclear localization assay. *In vivo* evaluation, including implantation of tumor cells, measurement of tumor cells, animal

sacrifice, tumor harvest, and western blot analysis of tumor samples. Additionally, data interpretation, and writing original draft. **X. Han:** Compound synthesis. **H. Yu:** building up shAR-FL and shAR-V7 22Rv1 cell lines**. H. Chen:** Reporter assay in figure 2a. **D. Qiu:** plasmid construction, **J. Su**: Animal surgery, animal and tumor monitoring. **M.A. Jamali**: Resource, *in vivo* protocol assembly. **R. Lin**: Resource, plasmids construction. **G. Batist:** Resource, result interpretation **J. H. Wu**: Conceptualization, funding acquisition, supervision, data interpretation and manuscript editing.

Chapter 4: Stimulation of STING by Novel Small Molecules for Antitumor Immunity:

Q. Yi: Gathering and reviewing the literature for the bridging text. Design of experiments, compound design and screening. *In vitro* characterization, including all western blots, proliferation assay, reporter assay, quantitative PCR, and flow cytometry. *In vivo* evaluation, including implantation of tumor cells, measurement of tumor, animal sacrifice, tumor harvest, western blot and flow cytometric analysis of tumor samples. Additionally, data interpretation, and writing original draft. **X. Han:** Compound synthesis. **R. Lin**: Conceptualization, data interpretation, resource, plasmids construction. **G. Batist:** Resource, result interpretation **J. H. Wu**: Conceptualization, funding acquisition, supervision, data interpretation and manuscript editing.

List of Figures

Chapter 1

Figure 1: Prostate cancer overview

Figure 2: Androgen receptor domains and its assembly at androgen response elements

Table 1: Risk stratification of patients for prostate cancer

Figure 3: Overview of localized prostate cancer management strategies

Figure 4: Overview of advanced prostate cancer management strategies

Figure 5: Composition of androgen receptor (full length: AR-FL), and a selection of clinically observable constitutively active splice variants (AR-V's).

Figure 6: Spliceosome assembly and generation of splice variants

Chapter 2

Figure M1-1. SC428 inhibits the transactivation of AR-V7, ARv567es and directly targets the AR N-terminal domain.

Figure M1-2. SC428 antagonized the WT and clinically relevant mutants of AR-FL and showed antiproliferative activity towards AR-positive prostate cancer cells.

Figure M1-3. SC428 inhibited AR-FL transcriptional activity, attenuated AR-FL chromatin binding, and impaired its nuclear localization.

Figure M1-4. SC428 suppressed the AR signaling in AR-V7 high-expressing PCa cells and suppressed their ENZ-resistant proliferation.

Figure M1-5. SC428 disrupted AR-V7 homodimerization and nuclear localization.

Figure M1-6. SC428 inhibits 22Rv1 xenograft growth in vivo.

Figure M1-S1. Chemical structures of SC428 and its analogs.

Figure M1-S2. SC428 potently inhibits the transactivation of AR but is inactive against PR and GR.

Figure M1-S3. SC428 exhibits full antagonist activity against the AR F877L mutant.

Figure M1-S4. SC428 induces modest degradation of AR-FL, but not AR-V7.

Figure M1-S5. SC428 hampered the phosphorylation of S81 and S210/213 located in AR-NTD.

Chapter 3

Figure M2-1. SC912 inhibited AR-V7 and AR-FL transactivation without cross-reactivity to other hormone receptors.

Figure M2-2. AR-NTD amino acids 507-531 are indispensable for SC912's full inhibitory capacity

Figure M2-3. SC912 blocked AR-V7 driven AR signaling in CRPC cells.

Figure M2-4. SC912 hampered the nuclear localization and chromatin binding for both AR-V7 and AR-FL.

Figure M2-5. SC912 caused proliferation arrest and apoptosis in AR-V7 positive CRPC cells.

Figure M2-6. SC912 repressed tumor growth and interrupted AR signaling in AR-V7 expressing CRPC xenografts.

Figure M2-S1. SC912 inhibited the transactivation of AR-FL and its clinically relevant LBD mutants.

Figure M2-S2. SC912 inhibited the androgen-independent AR signaling in CRPC cell lines.

Figure M2-S3. Estimated antiproliferation IC50 of SC912 in CRPC cell lines.

Figure M2-S4. SC912 caused cell cycle arrest in CRPC cell lines.

Chapter 4

Figure M3-1. Initial candidate molecule directly bound to hSTING and stimulated the STING signaling pathway.

Figure M3-2. Compound #716 demonstrated substantially improved STING agonist potency.

Figure M3-3. Compound #716 induced STING-dependent signaling in human immune cells and enhanced immune cell-mediated prostate cancer cell killing

Figure M3-4. Compound # 716 exhibited anti-tumor efficacy in murine TRAMP-C1 prostate cancer and trigged cytokine production in tumor-bearing mice.

Figure M3-5. #716 stimulated the generation of tumor antigen-specific CD8+ T cells in mice.

List of Key Abbreviations

ADT Androgen deprivation therapy
AF1 Transactivation function-1
AR Androgen receptor
AR-V AR splice variant
AREs Androgen response elements
CRPC Castration resistant prostate cancer
DBD DNA-binding domain
DHT 5α-dihydrotestosterone
DRE Digital rectal exam
FOXA1 Forkhead box protein A
GATA2 GATA binding protein 2
HOXB13 Homobox protein 13
HSP90 Heat shock protein 90
IL-6 Interleukin 6
LBD Ligand-binding domain
NTD N-terminal domain
NLS Nuclear localization signal
PCa Prostate Cancer
PSA Prostate specific antigen
RT Radiation therapy
RP Radical prostatectomy
TAUs Transcription activation units
TMPRSS2 The transmembrane protease, serine2

Chapter 1: Introduction

1.1.Prostate cancer

1.1.1. Prostate cancer epidemiology

Prostate cancer is the second most frequent malignancy with the fifth highest mortality rate in men globally. In 2020, prostate cancer caused 1,414,259 new cases and 375,304 new deaths, accounting for 14.1% of cancer incidence and 6.8% of cancer mortality in men, respectively. The incidence rates of prostate cancer are highly variable worldwide, with the highest rates (70-85 per 100,000 people) found in Northern and Eastern Europe, the Caribbean, Australia/New Zealand, and Northern America, and the lowest rates (5–20 per 100,000 people) in Asia and Northern Africa. The geographic disparity might be attributed to international differences in prostate cancer diagnostic practice, including more widespread PSA testing in high-income countries. Prostate cancer mortality rates also vary considerably across regions. In 2020, the highest mortality rate was recorded in the Caribbean (27.9 per 100,000 people), followed by Africa (Middle, 24.8; Southern, 22.0; Western, 20.0 and Eastern, 16.3), Europe (Eastern, 13.7; Northern, 13.0 and Western, 9.8), America (South, 13.6; Central, 10.8 and Northern 8.3) and Australia/New Zealand (10.3). The lowest rate was reported in the countries of Asia (South-Central, 3.1; Eastern, 4.7 and South-Eastern, 5.4). Over the last 20 years, the mortality rates in most western countries, such as Northern America, and in Northern, and Western Europe have been steadily declining, which likely reflects both treatment improvement and earlier detection[1].

The etiology of prostate cancer remains largely unknown, and the well-established risk factors are limited to advancing age, African ethnicity, family history, and genetic mutations (eg, *BRCA1* and *BRCA2*). The mortality rate of prostate cancer was found to rise with age, the risk was

observed to increase especially after 50 years of age in white men and 40 years of age in black men or men with a family history of prostate cancer. Moreover, black men in the Caribbean and America have the highest incidence and mortality rate, supporting Western African ancestry as a risk factor for prostate cancer. Therefore, the current guideline from the American Cancer Society recommends informed/shared decision-making for PSA testing in men at average risk beginning at age 50 years, and men at higher risk (African American or men with family history) beginning at age 45 years. Lastly, other emerging risk factors were found positively associated with prostate cancer development including a high-fat diet, obesity, physical inactivity, infection, and inflammation[2].

1.1.2. Prostate cancer carcinogenesis

The prostate gland is a male reproductive organ located within the pelvis beneath the bladder. It functions to secrete semen which formulates ejaculate and facilitates sperm viability. The prostate itself is composed of branching glands with ducts lined with a single layer of columnar epithelium and embedded in the stroma. The most important cellular composition of the epithelium is: (1) secretory luminal cells, (2) secretory basal cells, and (3) neuroendocrine cells[3]. Prostatic epithelial cells express a high level of androgen receptor (AR) and predominantly depend on androgen stimulation for growth and differentiation. Therefore, the AR regulated gene prostate-specific antigen (PSA), whose protein is secreted by these epithelial cells, is widely used as a diagnostic marker for prostate disorders. The stroma, a network of connective tissue surrounding the prostate outside the epithelial layer, contains fibroblasts that secrete growth and survival factors to sustain ducts through paracrine signalling. Moreover, the stromal smooth muscles encourage spontaneous contractility and avoid fluid stagnation. The interaction between epithelial cells and

stromal cells provides essential crosstalk to maintain the prostate gland homeostasis, and disruption of which could lead to tissue dedifferentiation and malignant proliferation.

Prostatic carcinogenesis is thought to originate from the luminal or basal prostate epithelial cells acquiring stromal cell-independent AR-stimulated growth. Such epithelial cell-autonomous proliferation also involves losing normal AR function as a growth suppressor, but conversely, utilizing AR signaling to prevent their apoptotic cell death and promote lethal growth[4]. This tumorigenic transformation of epithelial cells is believed to result from the accumulation of somatic genetic changes, leading to the inactivation of tumor-suppressor genes and activation of oncogenes[5, 6]. For instance, the most frequently detected genetic change in the early malignant stage is gene fusion of AR-regulated *TMPRSS2* promoter regions with transcription factors *ERG*[7, 8]. In addition, other genetic alterations that are commonly found in localized prostate cancer and have a role in early progression include *PTEN* and *RB1* deletion, *TP53* mutation, *MYC* amplification, and loss-of-function mutation in *SPOP* that has been linked to promoting genomic instability[9, 10]. In contrast, the AR gene alteration, such as copy number gain and structural rearrangements, is mostly enriched in the advanced stage of prostate cancer[11-13]. Lastly, prostate cancer is highly heterogenous and patients can have a combination of genetic changes, multiple epithelial cell populations often arise independently through different sets of disease-driven genes. Therefore, in the initial stage of prostate cancer, lacking broadly targetable genes adds to the challenge of early disease control.

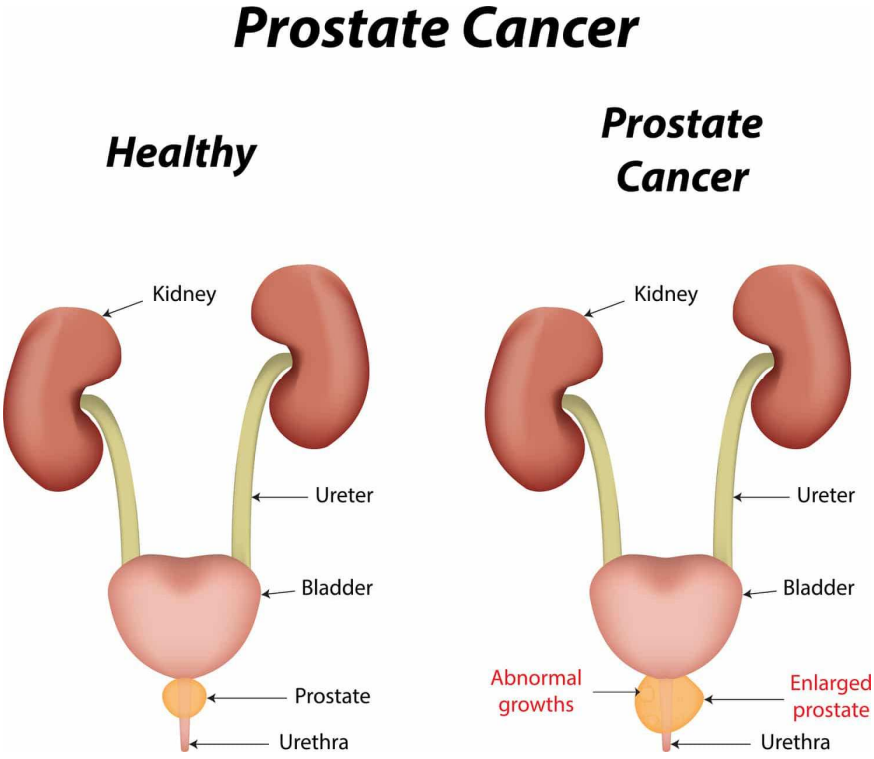

Figure 1: Prostate cancer overview

The prostate gland is a male reproductive organ located within the pelvis, beneath the bladder. It is composed of branching glands with ducts lined with a single layer of columnar epithelium and embedded in the stroma. Indicators of prostate cancer include discharge of blood in semen, pain in the pelvic region, erectile dysfunction, bone and muscle aches, and problems with urination. A common initial diagnosis for prostate cancer is to check for external signs of prostate gland enlargement, followed by a prostate-specific antigen test. This figure is reproduced from an online source: http://www.vims.ac.in/blog/prostate-cancer/.

1.1.3. AR signaling pathway as the core driver of prostate cancer oncogenesis

Evidence of androgen's importance to prostate cancer growth came over 70 years ago, when Charles Huggins demonstrated that surgical removal of the testes (eliminating a major source of androgen production) caused prostate cancer to regress [14]. Androgen and AR play a key role in the physiological maintenance of normal prostate gland cells, both by stimulating cell proliferation, and by inhibiting programmed cell death [15]. Prostate cancer arises when the rate between cell proliferation and cell death becomes imbalanced, resulting in a state of persistent net growth. The most prominent mechanism of prostate cancer initiation is a gene fusion between the TMPRSS2 gene promoter and the coding region of ERG, occurring in ~50% of all cases. This fusion-gene is responsive to AR via the TMPRSS2 gene promoter and produces a gene product that drives cell-cycle progression, fueling tumor growth. This translocation event appears to be facilitated by AR's DNA binding activity, which predisposes AR-regulated genetic elements to intra- and inter-molecular actions [16], and requires the co-recruitment of the DNA-cutting enzyme topoisomerase II beta to generate double-strand breaks [17]. Aside from TMPRSS2-ERG gene fusion, other components of the AR pathways, such as NCOR2, are mutated in ~56% of primary and ~100% of metastatic prostate cancer cases) [18], emphasizing AR signaling as a crucial regulator of prostate cancer initiation and progression.

1.1.4. Androgen receptor biology

1.1.4.1. AR structure and domains

AR is located on the chromosome X, cytoband Xq11-Xq12, of the human genome. It is composed of 2758 nucleotides, organized into eight exons, which encodes a 919 amino acids protein (molecular weight: 110kDa) [19]. The AR protein is organized into three major domains –

a NH-2 terminus domain (NTD), a DNA-binding domain (DBD) and a ligand-binding domain (LBD), each composed of highly conserved motifs and serving a distinct function. Amino acids 6-449 (protein family database code: pfam02166) of human AR located within androgen receptor's N-terminal domain is highly conserved across mammals but is absent in more distant ancestors such as birds or reptiles. Amino acids 555-636 (conserved domain database code: cd07173) within the DNA-binding domain is highly conserved across all jawed vertebrates including certain amphibians and bony fishes (such as zebrafish). Amino acids 673-918 (conserved domain database code: cd07073) resides within the ligand binding domain is also highly conserved across jawed vertebrates but diverges in bony fishes [20, 21].

The NTD (residues 1-555) is the largest domain and encoded entirely by exon 1. The N-terminal domain is intrinsically highly disordered [22, 23], a protein state which favors folding plasticity and the formation of highly-specific but low-affinity interactions with a wide range of binding partners[24]. The NTD also contains a poly-glutamine (polyQ) chain of varying length. Longer AR PolyQ is linked to the neuromuscular disease spinal and bulbar muscular atrophy [25], while shorter AR PolyQ is associated with better protections against severe acute respiratory syndrome coronavirus 2 (SARS-CoV-2)-mediated disease [26]. Despite the intrinsically disordered nature of AR-NTD, light-based structural analysis of NTD regions indicate that certain regions within the NTD are relatively stable [23, 27], thus exposing potential avenues to target this domain.

The DBD is highly conserved across nuclear receptors and is characterized by 9 conserved cysteine residues. 8 of these cysteine residues are distributed across two zinc-fingers, which stabilizes the DBD fold through coordinating two zinc-ions. The first of the zinc fingers is crucial for recognizing the binding of DNA-response elements via a "P-box" motif consisting of Gly578,

Ser579, and Val582. The second zinc-finger contains the "D-box" (Ala597-Ser-Arg-Asn-Asp601) required for AR receptor dimerization at the DNA-interface. The DBD also has a carboxy-terminal extension that is loosely structured and contributes to specificity of DNA-recognition [28].

The LBD (residues 666-919) is the domain whose 3D structure is best understood due to extensive crystallography studies. The three-dimensional structure of LBD is composed of 9 alpha helices, two 3_{10} helices, and four β-strands; the helices are arranged as a three-layered anti-parallel sandwich while the β-strands form two separate anti-parallel sheets [28]. The ligand-binding pocket is spanned by H3, H5, and H11; H12, which contains the core of AF2, encloses the binding pocket once the ligand is docked [28].

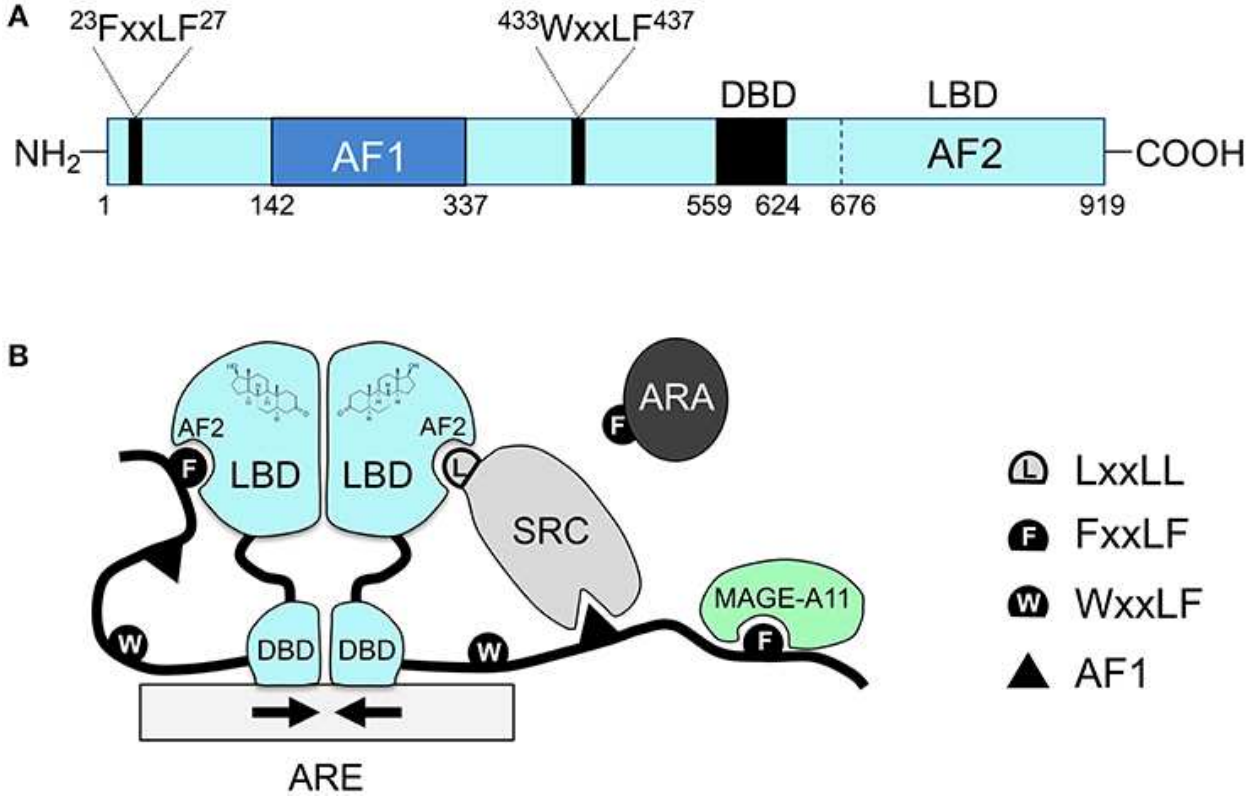

Figure 2: Androgen receptor domains and its assembly at androgen response elements A) Androgen receptor is composed of three major domains of which the N-terminal domain (NTD) harbours an activation function 1 (AF1) that mediates AR's interaction with basal transcription factors such as TATA binding protein. The NTD also contains two distinct motifs (FxxLF and WxxLF) that mediates AR dimerization. The DNA-binding binding domain (DBD) is separated from the ligand binding domain (LBD) by a small hinge region that contains the nuclear localization sequence. The LBD domain contains the second activation function domain (AF2) that primarily mediates AR dimerization. **B)** Following ligand-stimulation, the androgen receptor forms an intramolecular N/C interaction through the binding of AF2 to the FxxLF domain. AR dimerization is formed through both the LBD and DBD. Both the AF1 and AF2 can mediate interaction with cofactors containing the FxxLF sequence such as SRC. Additionally, the FxxLF domain in the AR NTD can also mediate interaction with an AR-specific cofactor MAGE-A11. This figure is reproduced from " Androgen Receptor Signaling in the Development of Castration-Resistant Prostate Cancer" by Qin Feng and Bin He, Frontiers in Oncology (2019) under the terms of the Creative Commons Attribution License (http://creativecommons.org/licenses/by/4.0/).

1.1.4.2. AR activation

Activation of AR signaling is crucial in many physiological processes including male sexual differentiation, pubertal maturation, and spermatogenesis [29]. Loss-of-function mutations in AR which weakens its ability to be activated by ligands can result in male infertility or androgen insensitivity syndrome [30, 31]. Activation of androgen receptor is primarily governed by exposure to forms of testosterone, produced by the testes and, to a lesser extent, the adrenal glands. In many tissues, including prostate, skin, and the scalp, testosterone is subsequently converted to a more potent AR agonist dihydrotestosterone (DHT) by the activity of 5 alpha-reductase [32]. While both testosterone and DHT binds to AR with similar affinity, their binding kinetics are drastically different, with DHT having a much slower rate of dissociation compared to testosterone [33].

As with all known steroid receptors, AR resides primarily in the cytoplasm in the absence of ligand, where it's bound to chaperone proteins such as the heat shock proteins ((HSP90, HSP70, HSP56) [34]. AR activation following the entry of ligands into the cell results in conformational change and dissociation of chaperone proteins. AR activation can be further modulated by post-translational modifications such as phosphorylation [35].

AR possesses two main activation domains. Activation function (AF)-1 found in the NTD governs most of AR's interaction with co-factors such as transcription factor II, and is required for maximize the transcriptional activity of AR [36]. The second, AF-2, resides in the LBD and primarily governs AR's ability to dimerize with another AR monomer, though certain co-factors such as TRIM24 can bind to AF2 [37] [38] [39]. Upon ligand-induced activation, AR's LBD undergoes a conformational change at helices 3, 4 and 12 within the LBD, leading to Hsp90 release. This energy-consuming step requires hydrolysis of ATP at the nucleotide-binding domains of

Hsp90 [40]. Once release from the chaperone, the AF-2 domain in the AR's C-terminus preferentially engages with the FXXLF motif, and to a lesser extent the WHTLF motif, in the AR NTD [41]. This "intracellular N/C interaction" likely enhances AR signaling by stabilizing the protein and reducing the rate of ligand dissociation [42, 43]. In this manner, AR's intramolecular N/C interaction distinguishes it from other nuclear hormone receptors, whose LBD instead has higher affinity for LxxLL motif, such those found in p160 cofactors. That said, AR can still weakly interact with LxxLL motifs [44], leading to activation of oncogenic signaling pathways such as Akt and Erk [45-47]. In the absence of androgen, these interactions, mediated through a variety of AR-post translational modifications (e.g. S81), permits AR activation by coactivators such as SRC and IL-6 [48].

1.1.4.3. AR dimerization

A critical component of the AR signaling axis is the ability of this nuclear receptor to dimerize. Three forms of AR dimerization have been observed that are relevant to its function as a transcription factor.

The first is a form of anti-parallel dimer formed from N/C interactions between two separate AR monomers. This occurs when, upon ligand binding, the AF-2 in AR LBD interacts with the FQNLF motif in the AR NTD of a second AR monomer. Fluorescence resonance energy transfer experiments suggests that this interaction occurs only until the point where AR interacts with DNA [49], suggesting that this form of dimer might functions to limit unfavorable cofactor binding.

The second type of dimerization occurs via a DNA-dependent dimerization through AR's DBD. As with other hormone responsive elements, androgen response elements (ARE's) are

generally composed of two hexametric half-sites (5'-AGAACA-3') spaced out by three extra nucleotides. Typically, two hormone receptor units would each interact with opposite DNA strands. For AR, however, only one of the AR monomers interacts with DNA, while the second AR monomer instead binds to the first AR. While ARE's are classically palindromic in nature, crystal structure of AR-DBD dimers showed that AR can also bind to direct repeat DNA elements as head-to-head arrangements. This form of dimerization is strengthened by the van der Waals contact between the Serine-580 residues between two AR dimers [50]. This mismatch in orientation between DNA element and dimer pattern means that, in some cases, only one AR monomer forms a high-affinity bond with DNA, while the second AR monomer forms a lower affinity bond [50, 51]. In patients with androgen-insensitivity syndrome, mutations in the DBD dimer interface is much higher than average (http://androgendb.mcgill.ca/), highlighting the importance of this interaction to proper AR activity [51].

Lastly, the AR LBD can also dimerize, though the mechanistic details of this form of dimerization is poorly understood. Recent crystal structure studies indicate that AR LBD dimerization is inducible by agonists and might be reliant on the residue P767, as a point mutation in this area impairs with dimer formation and normal development in *male* mice [52, 53].

1.1.4.4. AR translocation

AR nuclear localization is essential for its activity as a transcription factor. AR possesses multiple nuclear localization signals (NLS). The small hinge region between the DBD and LBD (residues 624-676) contains a bipartite nuclear localization signal (NLS) that become exposed once AR dissociates from chaperon proteins and interacts with the f-actin cross-linking protein filamin A to promote AR nuclear import [54]. Two additional NLS exist in the NTD and LBD which

regulate AR nuclear import in a Ran GTPase-dependent manner [55]. The latter two NLS regions can mediate AR nuclear import in the absence of androgen [55], and represents an avenue through which androgen nuclear localization is maintained in recurrent prostate cancer [56].

Negative regulation of AR nuclear translocation exists in the form of AR active nuclear export and AR degradation. AR can be actively exported out of the nuclear via a leptomycin B-insensitive nuclear export signal found at residues 743-817 of the LBD, which enhances the export, polyubiquitination, and cytoplasmic degradation of AR in the absence of androgen [57]. AR can also be degraded directly in the nucleus following polyubiquitination in the nucleus by the E3 ligase MDM2 [58]. Overall, the subcellular localization of AR is dynamically regulated through its dimerization, cytoskeletal transport, and factors that govern its stability.

1.1.4.5. AR chromatin binding

Once inside the nucleus, AR functions as a transcription factor by binding to androgen response elements: two hexameric motifs separated by a short ~3bp spacer [59]. However, chromosome-wide AR-occupancy studies have shown that the majority of ARs do not bind to conventional AREs but rather to half-AREs composed of only one hexameric motif [60-62]. The ability of AR to bind to these enhancer elements is influenced by the state of chromatin accessibility, histone modifications, and possible competition or cooperation with other transcription factors or chromatin remodelers **[63]** [64].

While many details of AR's dynamics with DNA and chromatin are unclear, there are numerous studies which have delineated some of the important factors. Early chromatin immunoprecipitation studies showed that AR's ability to bind chromatin is impaired by mutations that limited N/C interactions [65]. Overexpression of AR also increases its binding affinity for chromatin [66]. Genome-wide chromatin accessibility studies showed that activated and

inactivated AR can bind to distinct regions of chromatin [67]. Additionally, pioneer factors, such as FoxA1 and GATA2, can enhance AR's chromatin binding by inducing chromatin remodeling to increase AR access **[60, 68-70]**. These pioneering factors can, to some extent, rescue AR chromatin binding in the absence of ligand, and therefore are frequently overexpressed in recurrent prostate cancer [71]. The specificity of pioneer factors are influenced by histone epigenetic marks, such as histone H3 lysine 4 demethylation[72]. As a result of these mechanisms, AR can regulate gene expression in a cell/tissue-type specific manner.

1.1.4.6. AR regulated transcription

Unlike most nuclear receptors, the transcriptional activity of AR is conferred by its NTD rather than LBD due to having a strong AF1 and a comparatively weak AF2, due to the latter's affinity for FXXLF motifs rather than LXXLL motifs. Within the AF1 of AR NTD are two transcription activation units, Tau-1 (residues 100-370) and Tau-5 (residues 360-485), which are indispensable for full AR transactivation. AR transcriptional activity is also influenced by the length of the polyQ region in the NTD, whereby shorter polyQs generally correlate with increased transactivation [73].

The majority of AR binding sites are not within cis promoter regions, but rather distal enhancer sites [61, 74]. At target promoters, the AR NTD interacts with the RAP74 subunit of transcription factor II (TFIIF) and TATA-box binding protein (TBP) to form the preinitiation complex [75]. Simultaneously, AR is also recruited to distal enhancer sites where it assembles an AR coactivator complex composed of factors such as p160/p300 [28, 75]. Recruitment of AR cofactors is further optimized by pioneer factors including GATA2 and FoxA1 [76]. These events lead to the formation of a chromosome loop which facilitates RNA polymerase II's tracking from

promoter to enhancer [77]. AR-mediated chromatin looping has been shown to be further enhanced by enhancer RNAs, a class of long non-coding RNA [78].

1.1.5. Prostate cancer diagnosis and risk stratification

The modern-day paradigm for general cancer treatment is based on proper diagnosis and classification of cancer progression stage. The two cornerstones for early detection of prostate cancer in clinics are DRE (digital rectal exam) and PSA (prostate-specific antigen) blood test. DRE is physical palpation of the prostate to assess gland enlargement and texture change, which is a preliminary indicator of malignancy presence. *PSA* is a positive AR-regulated gene, its expressed protein is secreted by the prostate epithelial cells and subsequently released into the bloodstream. Therefore, elevated serum PSA level is predictive of excessive AR signaling activity owing to abnormal prostate epithelial cell proliferation. Patients with suspicious findings on DRE and PSA tests are further subjected to higher precision tests such as bone scan, pelvic CT (computed tomography), and MRI (magnetic resonance imaging), for the purpose of visualizing the potential cancerous lesion. Lastly, targeted biopsy is performed on the confirmed lesion sites for final diagnosis. Each biopsy site is characterized and reported individually with location, differentiation grade, and extent, therefore providing guidance for the risk classification and treatment selection[79].

According to the standard American Joint Committee on Cancer (AJCC) TNM system, prostate cancer clinical stages contain three major categories[80]: (1) T category describes clinically localized and locally advanced prostate tumor, where the tumor is mainly confined to the prostate gland or slightly spread to the adjacent structures like the seminal vesicle, rectum,

bladder and/or the pelvis wall; (2) N category is for describing the primarily metastatic prostate cancer, where the cancer has already spread to the nearby lymph nodes is the main standard; (3) M category is for aggressively metastatic prostate cancer, where the prostate cancer has already spread to distant parts of the body. The most common prostate cancer metastatic sites are bones and distant lymph nodes, organ metastasis is also frequently observed, especially in the lungs, liver, and/or brain; The three main categories T, N, and M each contains subcategories as well.

The Gleason system is a clinical golden standard for determining the aggressiveness of prostate cancer[81]. By assessing the histological feature of tumor tissue under microscopy, prostate cancers can thereby be classified as well-differentiated (the lowest grade) to poorly differentiated (highest grade). The Gleason Score ranges from 6-10, and the higher scored lesion contain less normal tissue structure and are more likely to grow and spread quickly. The summation of Gleason scores from the most and second most prominent lesions gives the result of Gleason grade to corresponding prostate cancer case. The grading system recommended by World Health Organization subdivides prostate cancer into five categories described as[82]: (1) Grade 1 (Gleason score $\leqslant$6) - Only individual discrete well-formed glands; (2) Grade 2 (Gleason score 3+4=7) - Predominantly well-formed glands with fewer component of poorly formed/fused/cribriform glands; (3) Grade 3 (Gleason score 4+3=7) - Predominantly poorly-formed/fused/cribriform glands with a less component of well-formed glands; (4) Grade 4 (Gleason score 8)- Only poorly-formed/fused/cribriform glands or predominantly well-formed glands with a less component lacking glands or predominantly lacking glands with a less component of well-formed glands; (5) Grade 5 (Gleason scores 9-10) - Lacks gland formation or with necrosis, and with or without poorly-formed/fused/cribriform glands.

Traditionally, prostate cancers are classified into low, intermediate, and high-risk groups based on the sum of PSA level, clinical stage, and Gleason Score. Because heterogeneity exists within each risk group, the year 2018-updated National Comprehensive Cancer Network risk stratification uses an 8-tier system that subdivides the localized prostate cancer groups and added advanced disease groups (Table 1) [83].

Risk Group	Clinical/Pathologic Features	Imaging	Molecular Testing of Tumor	Genetic Testing of Tumor
Very low	All of the following: • T1c • Gleason score ≤6/grade group 1 • PSA <10ng/mL • <3 prostate biopsy fragments/ cores positive, ≤50% cancer in each fragment/core • PSA density <0.15 ng/mL/g	Not indicated	Not indicated	Consider if there's a strong family history
Low	All of the following: • T1-T2a • Gleason score ≤6/grade group 1 • PSA <10ng/mL	Not indicated	Consider if life expectancy is ≥10 years	Consider if there's a strong family history
Intermediate-favorable	Any of the following: • T2b-T2c • Gleason score 3+4=7/grade group 2 • PSA 10-20 ng/mL PLUS percentage of positive biopsy cores <50%	• Bone imaging: not recommended for staging • Pelvic ± abdominal imaging: recommended if nomogram predicts >10% probability of pelvic lymph node involvement	Consider if life expectancy is ≥10 years	Consider if there's a strong family history
Intermediate-unfavorable	Any of the following: • T2b-T2c • Gleason score 3+4=7/grade group 2 or Gleason score 4+3=7/grade group 3 • PSA 10-20 ng/mL	• Bone imaging: recommended if T2 and PSA >10 ng/mL • Pelvic ± abdominal imaging: recommended if nomogram predicts >10% probability of pelvic lymph node involvement	Not routinely recommended	Consider if there's a strong family history
High	Any of the following: • T3a • Gleason score 8/grade group 4 or Gleason score 4+5=9/grade group 5 • PSA >20 ng/mL	• Bone imaging: recommended • Pelvic ± abdominal imaging: recommended if nomogram predicts >10% probability of pelvic lymph node involvement	Not routinely recommended	Consider
Very high	Any of the following: • T3b-T4 • Primary Gleason pattern 5 • >4 cores with Gleason core 8-10/ grade group 4 or 5	• Bone imaging: recommended • Pelvic ± abdominal imaging: recommended if nomogram predicts >10% probability of pelvic lymph node involvement	Not routinely recommended	Consider
Regional	Any T, N1, M0	Already performed	Consider tumor testing for: • homologous recombination gene mutations • MSI/dMMR	Consider
Metastatic	Any T, any N, M1	Already performed	Consider tumor testing for: • homologous recombination gene mutations • MSI/dMMR	Consider

Table 1: Risk stratification of patients for prostate cancer

1.1.6. Localized prostate cancer

Active surveillance is conservative management for low-risk prostate cancers, which allows sufficient monitoring of disease progression *via* routine DRE, PSA testing, and tumor imaging while avoiding overtreatment. The survival rate of patients at this stage is as high as 93% at 15-year follow-up[84]. Patients who are diagnosed with intermediate-risk, high-risk or regional prostate cancer may be offered local therapies, such as radical prostatectomy (RP) to remove the cancer-containing prostate gland, and pelvic lymph node dissection (PLND) to prevent potential lymph node spreading. These surgeries are only modestly invasive but highly effective with a patient survival rate of higher than 80% at 10-year follow-up, and on average entail no loss of well-being or life quality. For patients with high-risk prostate cancer, regional prostate cancer, or cancer relapse after local therapy, local salvage treatment like radiation therapy (RT), and systemic treatment like androgen deprivation therapy (ADT) are also applied after RP for long-term disease control. In summary, prostate cancer at early stages is highly treatable with the standard of care, 10-year or longer lifespan can be achieved in 80% –100% of patients[85].

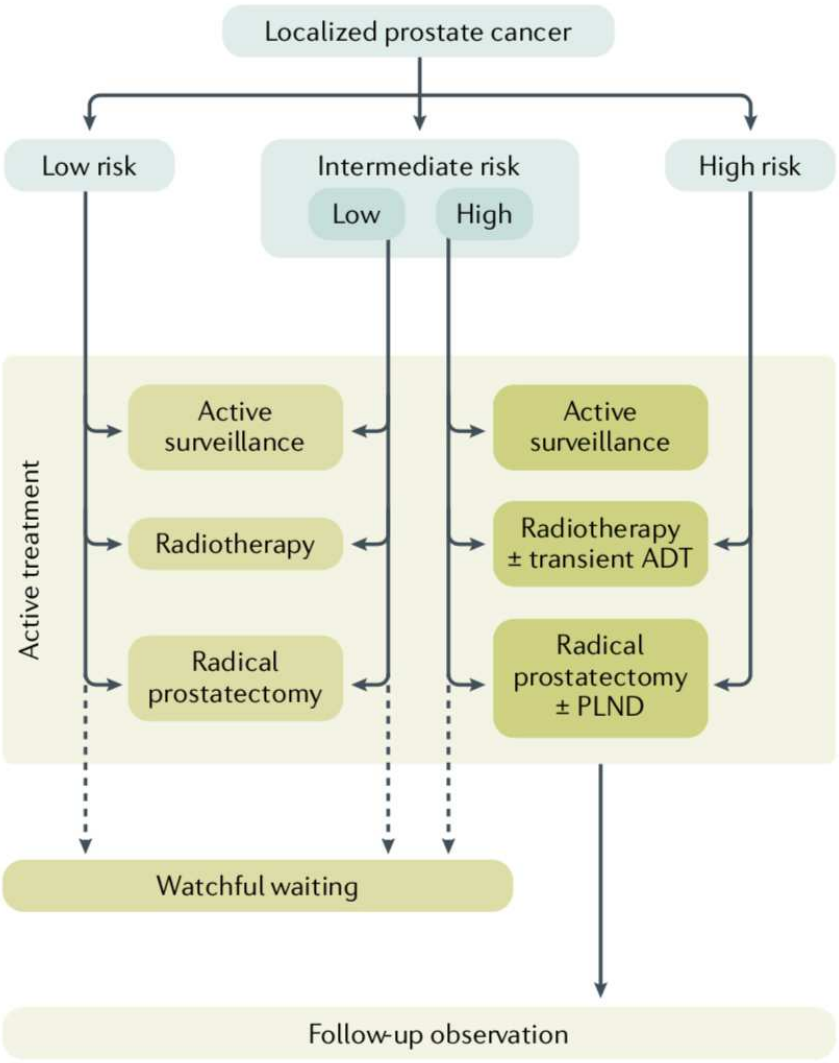

Figure 3: Overview of localized prostate cancer management strategies Based on the tests results including prostate-specific antigen (PSA) levels and Gleason score, patients are stratified into different risk groups, with low risks being managed primarily through active surveillance or radical local treatment. While low-risks patients may also be offered radiotherapy, low-dose brachytherapy, radical proctectomy, and/or transient androgen deprivation therapy (ADT), these treatments are more commonly used on intermediate/high risk patients. Under the active surveillance regime, new treatments are offered when the disease progresses, which can be indicated for instance by increasing PSA levels. Follow-up treatments are not always necessary. This figure is reproduced from Prostate Cancer by Richard J. Rebello et al, Nature Reviews Disease Primers (2021) with permission from Springer Nature.

1.1.7. Metastatic prostate cancer

Metastatic prostate cancer patients may present with de novo metastatic disease at the time of initial diagnosis, or they may develop distant metastases at a later stage after having had localized prostate cancer. When metastases are found in presenting, immediate and systemic androgen-deprivation therapy (ADT) is offered to patients. In the last 20 years, ADT with either luteinizing hormone-releasing hormone (LHRH) agonists/antagonists (chemical castration) or bilateral orchiectomy (surgical castration) has been the standard of care for metastatic prostate cancer. By inhibiting the testicular androgen synthesis with LHRH, or by surgically removing patients' testicles, the main source of androgen supply could be effectively cut off, hence suppressing the AR-dependent proliferation of tumor cells. Recently, the addition of chemotherapy (docetaxel) or AR signaling inhibitors (abiraterone, enzalutamide, apalutamide) to ADT has demonstrated survival benefits in multiple clinical trials for patients with either *de novo* metastatic disease or progression after local therapy. However, whether the triple combination of ADT plus docetaxel plus an AR signaling inhibitor adds further benefit is currently not clear as a longer follow-up is needed. Therefore, combinational treatment of ADT with either docetaxel or one of the AR signaling inhibitors is currently replacing ADT monotherapy as the new standard of care for metastatic prostate cancer, achieving 3-year survival in 60%–80% of patients[86].

Metastatic disease is the lethal form of prostate cancer. Recent improvements in treatment regimens and patient care were only found effective in slowing-down progression and prolonging survival by a couple of months, nonetheless, prostate cancer is incurable at this stage. Treatment resistance almost always occurs after a brief period of the initial response to ADT, and cancer progressing to the final stage, named castration-resistant prostate cancer, is inevitable.

1.1.8. Castration-resistant prostate cancer

When prostate cancer progresses despite ADT treatments, patients are reclassified as having castration-resistant prostate cancer (CRPC), either with or without metastatic disease. Approximately 10–20% of patients with prostate cancer will develop castration resistance within 5 years and 84% of patients have metastatic disease at the time of CRPC diagnosis[87], plus, the non-metastatic CRPC will eventually become metastatic CRPC. CRPC is defined as the disease progresses, evidenced by either rising PSA or new lesions, under castration level of androgen; Its precise clinical description is castrated serum testosterone <50 ng/dl or 1.7 nmol/l plus one of the following types of progression: (1) Biochemical progression, demonstrated by three consecutive rises in PSA 1-week apart, resulting in two 50% increases over the nadir, and PSA > 2 ng/mL; (2) Radiological progression demonstrated by the appearance of new lesions—either two or more new bone lesions on bone scan or a soft tissue lesion using the Response Evaluation Criteria in Solid Tumours[86].

Current CRPC-treating strategies lack standardization compared to that for earlier stages of prostate cancer. Thus, the treatment prescription for a specific patient is highly customized based on various parameters including responding time to previous ADT therapy, tumor burden, the pace of progression, location and extent of disease, cancer genomic profile, and patient overall physical condition. In general, ADT is continually given to patients on a lifelong basis because AR signaling activity remains a driving force of prostate cancer cell survival and proliferation even in the CRPC stage. Moreover, taxanes such as docetaxel are commonly added to ADT for further suppression of cancer cell growth; and AR signaling inhibitors like abiraterone or enzalutamide are also offered before or after docetaxel for enhanced blockade of AR signaling. Beyond these first-in-line treatments, other therapeutic approaches are also becoming available in the clinic and included for

treating a subset of CRPC patients, who fulfill certain criteria, like disease relapse after first-in-line treatments, and/or showed minimal symptoms, metastasized to bone, harbored a specific gene mutation, etcetera. Their mechanisms and efficacy in prolonging survival or as supportive care will be discussed in the next section. Lastly, the optimal incorporation of CRPC drugs into the conventional treatment regimen remains undetermined. Especially for the common scenario where patients, having been previously treated with certain agents, are found less responsive to the agents sharing a similar mechanism of action at the CRPC stage[88, 89]. The selection of the next-in-line treatment is an ongoing debate. For instance, docetaxel seems to be less efficacious in CRPC when it had previously been used in the earlier stages, but abiraterone and enzalutamide remain active. Likewise, CRPC patients who have been previously treated with enzalutamide are less likely to benefit from abiraterone than from docetaxel[90, 91]. Taken together, though a few new drugs have been added to the toolbox of treating CRPC besides AR signaling inhibitors and taxanes, they are only appliable to a small group of patients and lack generalizability to the broader CRPC population. Furthermore, the right combination and sequencing of various treatment options remain unclear and are currently under intensive investigation. Prostate cancer, especially when evolved to the metastatic CRPC stage, is most aggressive and deadly. The currently available therapeutic options are only moderately effective, and the treatment paradigm requires further optimization. Hence, treatments are almost always accompanied by rapidly developed resistance, resulting in a patient's median overall survival of fewer than 2 years.

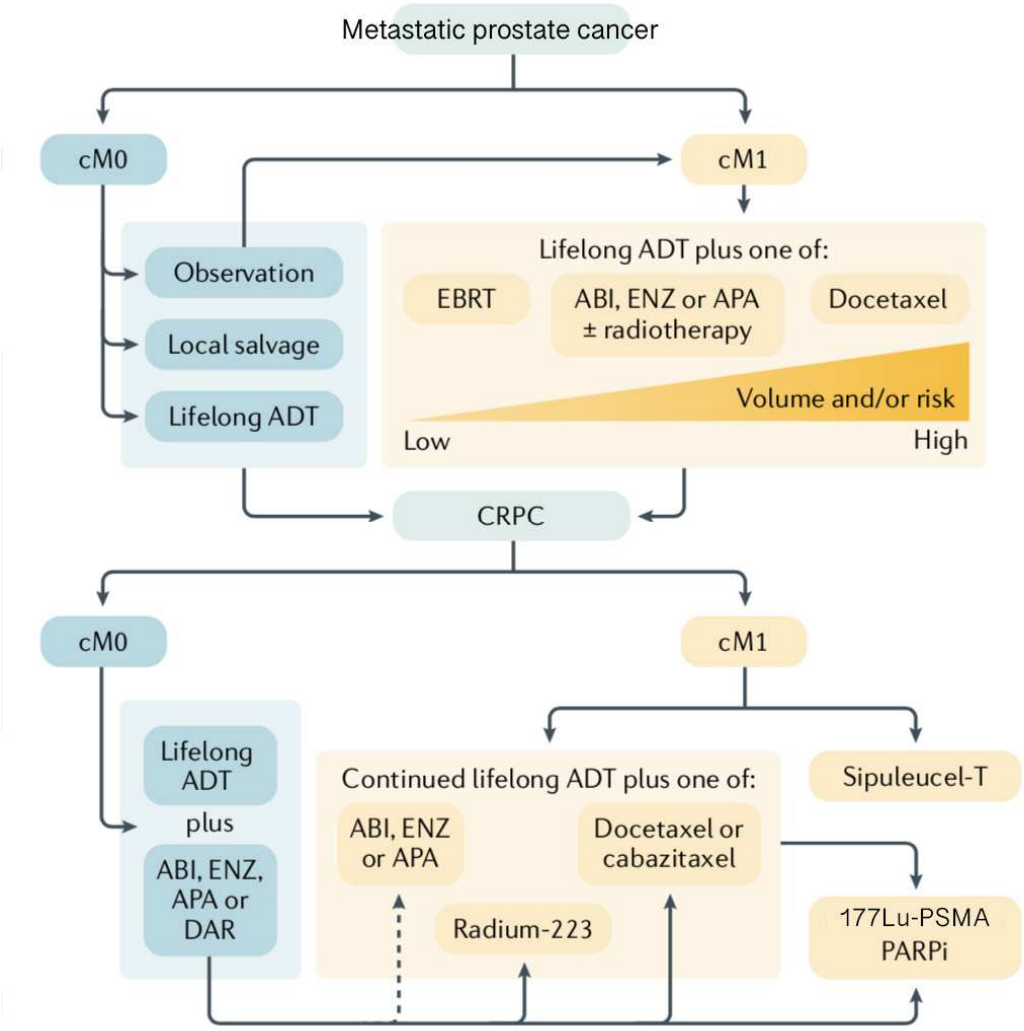

Figure 4: Overview of advanced prostate cancer management strategies

Advanced prostate cancer, which is no longer confined to the prostate gland, is generally presented with micrometastasis (cM0) or overtly metastasis (cM1). cM0 patients continue to receive salvage treatments similar to localized prostate cancer until disease progresses, while cM1 patients are treated with lifelong androgen deprivation therapy (ADT) combined with one of docetaxel or androgen signaling inhibitor (e.g., Enzalutamide; ENZ). Disease that progresses beyond this stage is named castration resistant prostate cancer (CRPC) and is treated with continued lifelong ADT alongside numerous other agents, including novel options such as PARP inhibitors. This figure is reproduced with modifications from Prostate Cancer by Richard J. Rebello et al, Nature Reviews Disease Primers (2021) with permission from Springer Nature.

1.2. FDA-approved drugs for CRPC treatment

1.2.1. AR signaling inhibitors: abiraterone, enzalutamide, apalutamide and darolutamide

AR signaling inhibitors could be broadly categorized as androgen biosynthesis inhibitor (abiraterone) that target the testosterone biosynthesis pathway, and antiandrogens (enzalutamide, apalutamide, and darolutamide) that act on inhibiting the androgen receptor directly by impeding the androgen binding.

Androgen deprivation therapy blocks the majority of androgen supply, which is generated in the testicle. However, a significant amount of androgen is still synthesized by the adrenal gland and sometimes even by the prostate cancer cells[92], which cannot be affected by ADT, thus fuel to sustain basal AR signaling activity in CRPC. Studies showed elevated expression of enzyme genes related to androgen synthesis in CRPC tissues. Intra-tumoral androgen levels in recurrent tumors post-ADT frequently surpass the androgen level in normal prostate tissue and untreated primary prostate cancer[93]. These studies suggested that ADT induces upregulation of androgen production in the tumor cells or adrenal gland, helping the tumor survive the treatment and accelerating the development of resistance. In order to combat the mechanisms of persistent androgen synthesis, novel classes of drugs such as abiraterone were developed to target the androgen biosynthesis pathways.

Abiraterone inhibits CYP17 (cytochrome P450), an enzyme that catalyzes the conversion of pregnenolone and progesterone to their 17-alpha-hydroxylase, 17,20-lyase forms during androgen biosynthesis, thus blocking adrenal and intra-tumoral androgen production[94, 95]. In the preclinical study, abiraterone significantly reduced plasma testosterone concentrations for at least 24 h in adult male mice[96]. This was associated with reduced weights of the ventral prostate,

seminal vesicles, kidneys, and testis, which are expected effects corresponding to decreased androgen levels. Furthermore, animal toxicology studies found no effects on hematological, biochemical, or renal function. Abiraterone was therefore considered safe enough to be studied in humans. In the first phase 3 trial, where 1195 CRPC patients who had previously received docetaxel were offered abiraterone or placebo, the overall survival was significantly longer in the abiraterone group (14.8 months) than in the placebo–prednisone group (10.9 months), with all secondary endpoints, including time to PSA progression, progression-free survival, and PSA response rate, favor the treatment group[97]. In the second phase 3 trial, abiraterone was assessed in an earlier disease setting, whereby 1,088 men with late-stage, castration-resistant prostate cancer who are asymptomatic or mildly symptomatic and had not previously received chemotherapy were enrolled. The study found that median overall survival was significantly longer in the abiraterone group (34.7 months) than in the placebo group (30.3 months)[98]. These two phase III studies collectively established the effectiveness of abiraterone and led to the FDA approval for treating CRPC patients both prior to and post receiving chemotherapy in the year 2011–2012.

Enzalutamide is a second-generation antiandrogen that was approved by FDA for treating late-stage CRPC in the year 2012. Upon the initial approval, enzalutamide quickly replaced the first-generation antiandrogens such as bicalutamide in clinical application owing to its higher potency of AR inhibition[99, 100], thus being subsequently also approved for treating non-metastatic CRPC as well as metastatic castration sensitive prostate cancer. Mechanistically, enzalutamide competes with androgen for the ligand-binding pocket located in the AR C-terminal, therefore, preventing the androgen binding induced AR activation and downstream cascade including AR nuclear translocation, chromatin binding, and regulated gene transcription[101]. In addition, enzalutamide is capable of retaining activity in the presence of increased AR expression,

which is often seen in CRPC patients and known to be one of the driving mechanisms for resistance[102]. In the first large-scale phase 3 trial of enzalutamide, 1199 patients with CRPC after chemotherapy were enrolled for evaluating its efficacy and safety. The result demonstrated that enzalutamide extended the median overall survival of patients from 13.6 months (placebo group) to 18.4 months (enzalutamide group). Furthermore, the superiority of enzalutamide over placebo was shown with respect to all secondary endpoints in the same trial, including the proportion of patients with a $\geq$ 50% reduction in the PSA level (54% vs. 2%), the soft-tissue response rate (29% vs. 4%), the quality-of-life response rate (43% vs. 18%), the time to PSA progression (8.3 vs. 3.0 months), radiographic progression-free survival (8.3 vs. 2.9 months), and the time to the first skeletal-related event (16.7 vs. 13.3 months). The common side effects observed in this trial are fatigue, diarrhea, and hot flashes, while the most alarming one was seizures, which were reported in five patients (0.6%) receiving enzalutamide[103].

More recently developed antiandrogens such as apalutamide demonstrated improved pharmacokinetics, and *in vivo* efficacy relative to enzalutamide[60]. Another novel antiandrogen darolutamide has greater binding affinity to AR compared to enzalutamide and do not cross the blood-brain barrier which decreases the likelihood of seizures[104, 105]. In clinical trials, these new antiandrogens have shown comparable efficacy to enzalutamide with a favorable safety profile[106, 107]. Moreover, darolutamide has been proven to be effective at overcoming resistance to enzalutamide in multiple preclinical models[108]. Apalutamide and darolutamide received FDA approval for treating CRPC in the year 2018 and 2019, respectively. However, the approval was limited to only a subgroup of patients with non-metastatic CRPC, arguing their improvement of overall survival is likely insignificant for patients at the final metastatic-CRPC stage when compared with the traditional antiandrogen enzalutamide.

1.2.2. Taxane-based chemotherapy: docetaxel, cabazitaxel

Docetaxel is a widely used antimitotic cancer drug that binds to intracellular microtubules and suppresses their dynamics. Docetaxel binding stabilizes microtubules and prevents depolymerization from calcium ions, hence inhibiting the disassembly of tubulin from microtubules. Eventually, the disrupted natural dynamics of microtubules hampers correct spindle formation during cell mitosis, leading to mitotic failure and cell death[109]. Furthermore, docetaxel could directly promote cell apoptosis *via* inducing the phosphorylation and inactivation of Bcl-2[110]. For more than a decade, docetaxel has been used as the standard first-line chemotherapy for advanced prostate cancer, including metastatic CRPC[111].

Cabazitaxel is a derivative of docetaxel with similar microtubule-stabilizing potency, nonetheless, comprises improved pharmacologic properties demonstrated by both preclinical and clinical studies. In particular, cabazitaxel sustains its antitumor activity in docetaxel-resistant animal models and patients, leading to its FDA approval in the year 2010 for CRPC patients whose disease progressed during or after docetaxel[112, 113]. The first-line chemotherapy, docetaxel has a high affinity for P-glycoprotein (P-gp), an ATP-dependent drug efflux pump that decreases the intracellular concentrations of these drugs. Given that P-glycoprotein was found widely overexpressed in prostate cancers, it is believed to be a major driver of docetaxel failure in CRPC patients. In contrast, cabazitaxel showed a poor affinity for P-gp, therefore has the potential of offering a more long-lasting response in prostate cancer[114, 115]. In preclinical studies, cabazitaxel showed potent *in vitro* and *in vivo* activity against a wide range of docetaxel-sensitive and -resistant tumor cell lines[114, 116]. Notably, cabazitaxel was significantly more potent than docetaxel in cancer cell lines with P-gp-mediated acquired resistance to docetaxel[114].

Cabazitaxel was next studied in a large-scale phase 3 trial with 755 metastatic CRPC patients, who had progressed after or during docetaxel-based chemotherapy. The median survival was 15.1 months in the cabazitaxel group and 12.7 months in the control group. Moreover, cabazitaxel treatment also improved median progression-free survival from 1.4 months to 2.8 months, thus suggesting significant antitumor activity and survival benefits[117]. However, cabazitaxel did not outperform docetaxel as a first-line treatment in another clinical trial[118] and is therefore only offered as second-line chemotherapy to CRPC patients with docetaxel-refractory disease.

1.2.3. Cell-based immunotherapy: sipuleucel-T

Sipuleucel-T was granted approval by FDA in the year 2010 and up to date, is the only cell-based immunotherapy for treating prostate cancer. Sipuleucel-T is a cell vaccine formulated to stimulate an adaptive immune response to prostate cancer by targeting the prostate tissue-specific antigen prostate acid phosphatase (PAP)[119]. The therapeutic intent is to generate PAP-antigen presenting cells *in vitro* from autologous peripheral blood mononuclear cells, and then fuse them back into the patients. These PAP-antigen presenting cells will subsequently activate and induce the amplification of PAP antigen-specific cytotoxic T cells, which eventually facilitate targeted tumor cell killing by recognizing the PAP antigen that is specifically expressed on the surface of prostate cancer cells[120].

The most convincing clinical data supporting the therapeutic potential of spiuleaucel-T is from a double-blind, placebo-controlled, multicenter phase 3 trial. 512 asymptomatic or minimally symptomatic patients with metastatic CRPC were randomly assigned to receiving sipuleucel-T or placebo, the sipuleucel-T infusion was administered every 2 weeks for 3 total doses. After a median follow-up of 34 months, the median survival was 25.8 months in the sipuleucel-T group

compared with 21.7 months in the placebo group. However, no PSA decline was observed in the sipuleucel-T arm, and the progression-free survival was similar in both study arms. Lacking the PSA response raised skepticism regarding the clinical benefit of this therapy[121]. Although sipuleucel-T was approved by FDA for the treatment of patients with asymptomatic or minimally symptomatic metastatic CRPC in 2010, it is not adopted for clinical usage outside of America. Additionally, the prohibitive cost and complicated manufacturing procedure also severely limited the application of sipuleucel-T in the clinic[122]. Sipuleucel-T was even more subsided for treatment prescription after other CRPC therapies came into the market, such as cabazitaxel in 2010, abiraterone in 2011, and enzalutamide in 2012.

1.2.4. Bone-targeted radionuclide therapy: Radium-233

More than 90% of patients with metastatic CRPC have imaging evidence of bone metastases, which are a major cause of death and decreased quality of life[123]. Once seeded on the bone, prostate cancer cells secrete cytokines and growth factors to activate the osteoblasts and promote their proliferation. In turn, osteoblasts control bone matrix resorption and create an extracellular matrix that is prone to accommodate more prostate cancer cells, forming a sizeable metastatic lesion *via* this vicious cycle[124]. Therefore, a bone-targeted therapy functioning to disrupt the prostate cancer cell and osteoblast co-stimulating loop, could theoretically reduce bone metastasis and its associated death in CRPC.

Radium-223 is developed as a bone-seeking calcium mimetic that selectively binds to areas of increased bone turnover and produces localized radiation[125]. After intravenous injection, Radium-223, being a calcium analog, is taken up by bone as a calcium substitute. It, therefore, concentrates in sites of active mineralization, especially within the microenvironment of high

osteoblastic activity[126]. Subsequently, Radium-223, being a radioactive isotope, will decay to the stable lead ^{207}Pb while emitting high-energy alpha-particle radiation to the surrounding areas. This process eventually causes double-stranded DNA breaks within the locally resident tumor cells, offering a potent and specific cytotoxic effect on cancer bone metastasis[127, 128]. In a large phase 3 trial, 921 patients with symptomatic metastatic CRPC, who failed docetaxel, received Radium-223 or placebo. Radium-223 significantly improved median overall survival by 3.6 months (14.9 months vs. 11.3 months) and was also associated with prolonged time to metastasis, improvement in pain scores, and quality of life[129]. In the year 2013, Radium-223 was FDA approved for the treatment of symptomatic metastatic CRPC that has spread to the bones but not to any other organs. However, later studies uncovered that Radium-223 also accumulates tremendously in the part where the bone is already damaged, thus increasing the risk of fracture[130]. Strikingly, when co-administrated with abiraterone, Radium-223 caused the reduction of lifespan by 2.6 months[131]. Owing to bone safety concerns, the use of Radium-223 was recently restricted in Europe[132].

1.2.5. Tumor-targeted radionuclide therapy: ^{177}Lu-PSMA

^{177}Lu-PSMA is designed based on a novel treatment concept of tumor-targeted radioligand therapy, whereby the ^{177}Lu radioisotope is conjugated with a monoclonal antibody against the prostate-specific membrane antigen (PSMA). PSMA is highly expressed on the prostate cancer cell surface; in particular, the metastatic lesions are PSMA-positive in most metastatic CRPC patients. Upon docking on the cell surface through the PSMA antigen-antibody binding, ^{177}Lu-PSMA emits beta-particle radiation to facilitate the recipient cell killing, thus, providing selective radiation targeting the prostate cancer cells while minimizing disturbance on normal tissue[133].

In a recently published phase 3 trial, ^{177}Lu-PSMA was evaluated in 831 patients who were previously treated with AR signaling inhibitors and taxane agents and had metastatic CRPC that were confirmed PSMA-positive by CT scan. ^{177}Lu-PSMA combined with standard of care improved median overall survival from 11.3 to 15.3 months, with prolonged progression-free survival and better PSA response. However, no significant improvement in the quality of life was observed in this study, and the incidence of severe adverse events was higher in the ^{177}Lu-PSMA group[134]. In 2022, the FDA approved ^{177}Lu-PSMA for the treatment of patients with metastatic CRPC in the post androgen receptor pathway inhibition, post-taxane-based chemotherapy setting, therefore, for the first time, offering a last-line therapeutic option to these heavily pretreated CRPC patients. However, the clinical availability may be largely delayed and limited owing to the high costs for production and administration[135], additionally, its efficacy and safety in the real-world setting require further investigation.

1.2.6. PARP inhibitors for homologous recombination repair (HRR) gene mutated tumor: olaparib, rucaparib

Loss of function mutation in DNA repair genes is very common in cancer, as insufficient repair of DNA damage leads to genomic instability and promotes the acquisition of oncogenic mutations[136, 137]. Conversely, more recent studies discovered that the DNA repair deficit also renders cancer cells hypersensitive to genotoxic agents and DNA repair pathway inhibitors, therefore has been exploited as a novel targeting strategy[138]. The two common types of DNA damage: single-strand break and double-strand break are each covered by unique repair pathways. For instance, the single-strand break can be repaired by poly (ADP-ribose) polymerase (PARP) binding to the nick and reconnecting the breaks, which is simple but prone to introducing

errors[139]. Whereas homologous recombination repairs (HRR) the double-strand break enables high fidelity, *via* using the homologous chromosome as a template to recreate an exact replica[140]. In cancer, when left unrepaired, the DNA single-strand breaks can be quickly converted into double-strand breaks, which are far more toxic and trigger cell death[141]. Over 10 years of studies in breast cancer revealed that HRR gene mutations, for example, the *BRAC1* and *BRAC2* mutations drive cancer development but also lead to HRR deficiency[138, 142]. These HRR-deficient cancer cells avoid DNA damage-induced cell death by depending on the PARP pathway as compensation, therefore, are particularly vulnerable to PARP inhibition[143, 144]. Given that the HRR gene mutation happens in 20%–30% of tumors from metastatic CRPC patients[11, 145-147], there is also substantial enthusiasm for developing PARP inhibitors as CRPC treatment.

Olaparib is the first PARP inhibitor that entered Phase 3 trial for CRPC. The study contains two cohorts that enrolled patients with the same disease conditions but different sets of HRR gene mutations. The first cohort of 245 metastatic CRPC patients who had disease progression while receiving enzalutamide or abiraterone, harbour at least one of the 3 HRR gene mutations intratumorally: *BRAC1*, *BRAC2,* and *ATM*. Olaparib was compared to enzalutamide or abiraterone as control. The median overall survival was 18.5 months in the olaparib group and 15.1 months in the control group, with the secondary endpoints: progression-free survival and PSA concentration also significantly improved in the olaparib group. Of note, the survival benefits were strongest in those with *BRAC2* mutations, whereas little benefit was seen in those with *ATM* mutations. Moreover, in the second cohort of 142 patients with HRR gene mutations other than *BRAC1*, *BRAC2,* and *ATM*, olaparib treatment has achieved no overall survival benefit and a less meaningful response rate[148]. Similarly, the other PARP inhibitor, rucaparib, examined in a phase 2 trial, also showed the highest responses in those with *BRCA1* or *BRCA2* mutations.

Responses in CRPC patients with other HRR gene mutations like *ATM*, *CHEK2,* or *CDK12* mutations but without mutated *BRCA1* or *BRCA2* were less frequent[149, 150].

Olaparib and rucaparib were both licensed by the FDA in the year 2020. Olaparib is approved for metastatic CRPC patients with deleterious HRR gene mutations, who have progressed following prior treatment with enzalutamide or abiraterone. Rucaparib is approved for metastatic CRPC patients with deleterious *BRCA* mutation, who have been treated with androgen signaling inhibitors and taxane-based chemotherapy. Both agents offer an exciting new opportunity for customized therapy based on the mutation profile (mainly *BRCA1/2*) contained within a tumor or germline. As newly approved drugs, more clinical trials for PARP inhibitors in CRPC patients are still ongoing, such as direct comparison with taxane agents, abiraterone, and enzalutamide; or combination with abiraterone as earlier in line treatment. Due to the high responding rate in CRPC patients with deleterious *BRCA1/2* mutations, olaparib and rucaparib are becoming the new standard of care for this patient group. However, it is worth noting that, *BRCA1/2* mutated patients only account for less than 20% of all CRPCs, therefore, novel therapeutic strategies that offer survival improvement to a broader patient population are urgently needed.

1.3. Continued AR signaling activity as a main drug-resistant mechanism in CRPC

1.3.1. AR overexpression

AR overexpression due to AR gene amplification was one of the first mechanisms that was discovered to confer resistance to anti-androgen treatments in CRPC. The reported incidence of

AR gene amplification based on biopsy is ~20-30% in CRPC, while being rare in untreated primary prostate cancer [151, 152]. Later studies found that circulating tumor cells from patients receiving second-line hormone therapy exhibited even higher rate of AR gene copy gains [153, 154]. AR gene amplification was well correlated with an increase in both AR mRNA and protein levels [155].

A seminal study by Sawyers' group demonstrated that increased AR expression was sufficient and necessary to confer resistance to first-generation antiandrogens [156]. The overexpression of AR renders prostate cancer cells hypersensitive to androgen, allowing them to sustain cell proliferation even with low levels of androgen, which is a case in the castration-resistant prostate cancer (CRPC) patients. [56, 157]. Moreover, AR overexpression in prostate cancer cells can also cause antagonist to agonist conversion of first line antiandrogen bicalutamide[156]. Clinical solution for AR overexpressed CRPC cases is using second line antiandrogen enzalutamide, which has 10-fold higher binding affinity to AR than bicalutamide[101].

1.3.2. AR ligand-binding domain mutation

Several point-mutations in AR-LBD have been associated with resistance to anti-androgens. The first LBD-mutant discovered was AR T878A, discovered in LNCaP cells and subsequently in CRPC patients, which conferred resistance to abiraterone [158, 159]. Deep-coverage next-generation sequencing further revealed three additional point mutations (L702H, W742C, H875Y), and these four-point mutations have been shown to occur in ~15-20% of CRPC cases [11, 12, 18, 146, 160]. Notably, flutamide and nilutamide behave as AR agonist rather than antagonist against T878A and H875Y mutants. Likewise, this antagonist-to-agonist switch also

occurred for AR W742C against bicalutamide, and for AR F877L against enzalutamide. However, W742C and F877L mutations are only rarely detected in biopsies of patients that previously received bicalutamide/enzalutamide. Another aspect to consider is that certain LBD mutants, such as H875Y, T878A, or L702H, can also sensitize AR to promiscuous activation by non-canonical ligands, thus aiding cancer cells to survive anti-androgen treatment without necessarily interfering with anti-androgen activity[161, 162].

Collectively, these discoveries demonstrated that, in the absence of androgen and presence of certain type of antiandrogen, AR-LBD mutants which get activated by using the antiandrogen as ligand are selectively enriched, thus convey resistance to the antiandrogen and sustains cancer growth. The recently approved third line antiandrogen darolutamide possesses inhibitory effect against all the currently discovered AR-LBD mutants[104], therefore is expected to overcome drug resistance driven by LBD mutation.

1.3.3. AR splicing variants: AR-V7

Alternative RNA splicing is a physiologically relevant process whereby, during the processing of pre-mRNA into mature mRNA, some exons are excluded and/or introns included, resulting in a protein product that is partially distinct from the wildtype form. DNA segments that are introns in the wildtype transcript that become exons in splice variants are called "cryptic exons", or pseudo-exons. Around 20 AR splice variants have been identified in human prostate cancer samples, which lack either some, or all, of the LBD.

Most clinically detected AR splice variants lose exons 4 onwards. Since the AR NLS is partially encoded by exon 4 (and partially by exon 3), these splice variants have compromised nuclear localization capacity except in the cases where the NLS is restored via a cryptic exon. In

AR-V7, the NLS is restored by a unique C-terminal peptide sequence in cryptic exon 3. Likewise, AR-V9 also regains constitutive activation through cryptic exon 5, though this effect appears cell-type specific. In the case of AR-V3 and AR-V4, constitutive activation is achieved through splicing of cryptic exon 4 to exon 2 and 3 respectively. In other cases, such as with AR-V1 and AR-V6, the splicing of cryptic exons does not reconstitute the NLS, resulting in these variants being primarily cytoplasmic and inactive for AR transcriptional activity. Among the AR splice variants, AR-V7 is exceptionally well-characterized, which is in part attributed to the existence of a V7-specific antibody that allows for its immunohistochemical detection in clinical samples, as well as it being generally one the most highly expressed variants [102, 163].

.

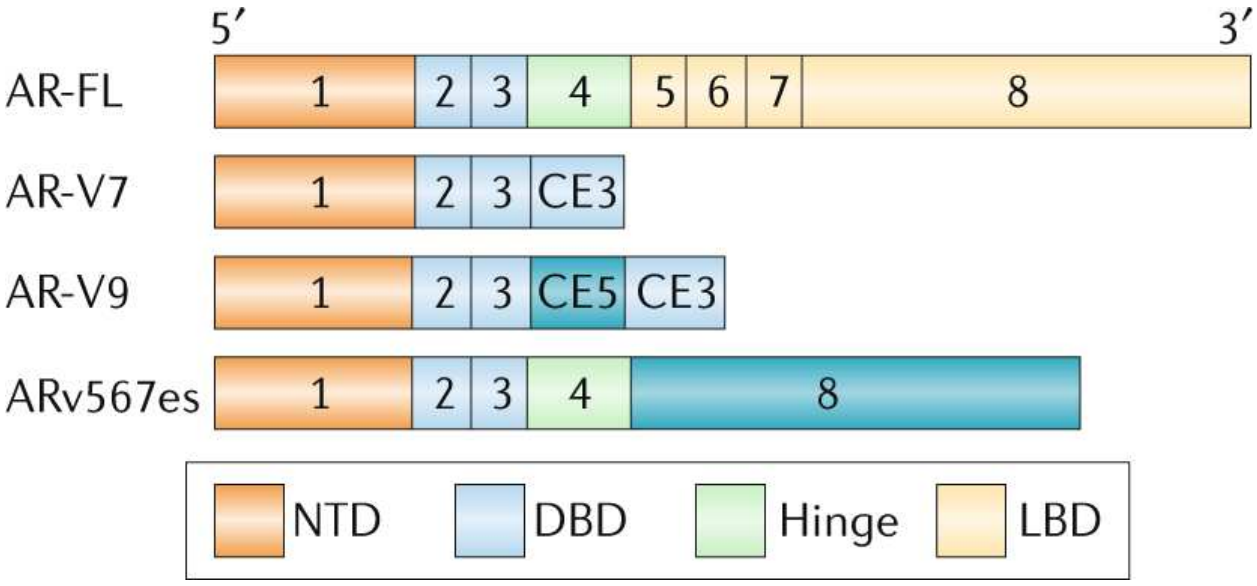

Figure 5: Composition of androgen receptor (full length: AR-FL), and a selection of clinically observable constitutively active splice variants (AR-V's).
These variants all lack the exons which code for the ligand binding domain (LBD), but retain exon 1, which codes for the N-terminal domain (NTD), and exons 2-3, which codes for the DNA-binding domain (DBD). Note that exon 4 codes for part of the hinge region, which contains a key nuclear localization sequence (NLS) required for AR to enter the nucleus. In the case of AR-V7 and AR-V9, the NLS is reconstituted via a cryptic exon 3 (CE3) and cryptic exon 5 (CE5) respectively, while in the case of Arv567es, the hinge region is retained. These features allow AR splice variants to enter the nucleus regardless of ligand. This figure is reproduced from " Androgen Receptor Signaling in the Development of Castration-Resistant Prostate Cancer" by Alec Paschalis et al, Nature Reviews Clinical Oncology (2018) with permission from Springer Nature.

1.3.4. AR-V7 abundance in CRPC patients

AR-V7 expression in prostate cancer specimens was firstly identified by immunohistochemistry analysis on prostate tissue microarray. AR-V7 protein was found significantly overexpressed in samples from patients who received initial ADT treatment, and AR-V7 expression level was correlated with the risk of tumor recurrence after radical prostatectomy[164]. This discovery was immediately confirmed by another study reporting that, when comparing ADT-relapsed prostate cancer patients with the ADT-naïve patients, AR-V7 mRNA showed an average 20-fold higher expression[163]. Therefore, these pioneering studies concluded that AR-V7 was barely detectable in ADT-naïve patients, however, its expression was drastically greater in ADT-treated prostate cancer patients, indicating a role of AR-V7 in prostate cancer progression.

The follow-up studies sought to answer if AR-V7 upregulation was actually inducible by ADT in prostate cancer patients. Therefore, serval studies were set up to monitor AR-V7 expression change in different stages of prostate cancer[165-167]. By assessing the autopsies acquired prior to and post CRPC progression from the same patient, one study revealed that AR-V7 protein expression was significantly higher in CRPC versus castration-sensitive prostate cancer stage[165]. Moreover, another study further dissected that AR-V7 protein is rarely expressed (<1%) in primary prostate cancer but became frequently detectable (75%) following ADT, with further significant increase in expression following second-generation ADT like abiraterone or enzalutamide treatments[167]. Taken together, these analytical studies on CRPC tissue confirmed clinical significance of AR-V7 expression during CRPC progression and suggested AR-V7's correlation to abiraterone and enzalutamide resistance.

1.3.5. Clinical evidence of AR-V7 as a driver of therapy resistance

The technological advances on enriching circulating tumor cells (CTC) from patient plasma allowed higher throughput analysis of patient specimens. Therefore, assessing the AR-V7 status in patient CTCs could provide a powerful means of studying AR-V7's role in CRPC with unprecedented statistical power. Luo et al. evaluated this approach by detecting AR-V7 mRNA in CTC from CRPC patients, and their results demonstrated, for the first time, that AR-V7 expression in CRPC patients is associated with enzalutamide and abiraterone resistance. Men with detectable AR-V7 in their CTC had lower PSA response rate and shorter overall survival from enzalutamide or abiraterone treatment[168]. This discovery was then validated by subsequent studies with larger scale[169], and the knowledge was further extended to that AR-V7 is not associated with unfavorable survival on taxane chemotherapy[170-172] nor ^{177}Lu-PSMA-617 radionuclide therapy[173], highlighting that AR-V7 associated resistance is very specific to AR-targeted therapy.

Earlier research laid the foundation for the development of AR-V7 as a biomarker to direct treatment choices for CRPC. As a result, there has been some diversification in the techniques used to identify circulating tumour cell AR-V7. Scher and colleagues assessed the nuclear expression of AR-V7 protein in CTC and uncovered that nuclear-localized AR-V7 protein in CTC can determine differential overall survival among CRPC patients treated with taxanes versus AR-targeted therapy[174, 175]. CRPC patients with positive nuclear AR-V7 had superior overall survival on taxanes over enzalutamide or abiraterone. On the contrary, CRPC patients with negative nuclear AR-V7 treated with enzalutamide or abiraterone had superior overall survival

relative to those treated with taxanes[176]. Collectively, these studies firmly established that AR-V7 is upregulated in CRPC patients and drives drug resistance against second generation-ADT, including enzalutamide and abiraterone.

1.4. The biology of AR-V7

1.4.1 AR-V7 occurrence

It was originally hypothesized that ARs which lacked LBD were isoforms that were generated by calpain-based cleavage of full-length AR [177]. This concept that was later rectified by PCR-based experiments demonstrating that constitutively activated AR were rather generated by alternative mRNA splicing [163]. Physiologically, the existence of alternatively spliced proteins is a normal phenomenon, and concordantly, AR-V7 is detectable in normal prostate cells [164]. However, CRPC cells can often accumulate much higher level of AR splice variants compared to normal prostate tissues. This is partially due to an increase in AR transcription that occurs under castration condition, which leads to an increase in the absolute level of AR-V7 [178]. For instance, AR-FL imposes negative feedback on total AR transcription via LSD1; consequently, decreased AR-FL activation drives AR transcription and, concordantly, an overall increase in AR-V7 [179, 180].

The ratio of AR-V7 to AR-FL can also increase in malignant tissues. Numerous factors have been identified that regulate RNA splicing pathways to favor AR-V7 genesis. In response to androgen deprivation and increased AR transcription, U2AF65 and SRSF1 is recruited the AR 3' splicing site to promotes splicing of exon 3 to cryptic exon 3 (CE3) rather than exon 4 [181]. Evidence suggests that U2AF65 activity is further dependent on SAP155 to facilitate its physical interaction with the polypyrimidine tract near the 3' splice site [182]. Additionally, SRSF1

expression is enhanced by Aurora Kinase A [183, 184] - a cell-cycle related oncogenic kinase overactive in many cancer models, including prostate cancer [185]. AR-V7 splicing is also enhanced by RNA-binding protein A1 (hnRNPA1) via NF-κB2/p52 and c-Myc, but here the mechanistic details at the level of splicing is unclear [186]. AR splicing has also been shown to be modulated by long-coding RNAs, including PCGEM1 and Malat1, through interactions with the aforementioned splicing factors [187, 188].

AR-Vs can also be increased through intragenic rearrangement. The 22Rv1 cell line carries a 35kd tandem duplication surrounding exon 3, and it has been shown that using TALEN to genetically correct this duplication resulted in a markedly decreased AR-V7 levels. Another cell line, CWR-R1, has a 48kb deletion within intron-1, which also enhances AR-V7 alternative splicing [189]. A recent study using liquid-phase AR bait panel combined with high-coverage sequencing of AR gene locus found that around one in three CRPC metastases (n=30) contained detectable AR genomic structural rearrangements (GSR); furthermore, presence of GSR correlated with increased expression of constitutively active AR splice variants [190]. Likewise, deep sequencing of AR circulating DNA found that ~11% of metastatic CRPC harboured AR gene rearrangement at baseline, which increased to >20% following antiandrogen treatment.

Lastly, AR-V7's level also depends on its stability, which is largely determined by the ubiquitin–proteasome system. In prostate cancer cells, both AR-V7 and AR-FL is stabilized by the chaperone protein HSP70 [191]. Additional factors including AKR1C3 and [192] and KIF15 [193] have also been identified as regulators of AR ubiquitination/stability. Conversely, the E3 ubiquitin ligase STUB1 disrupts AR's interaction with HSP70, leading to AR degradation [191]. Other mechanisms of AR stability have been observed to specifically affect AR-V7, such as its regulation by the deubiquitases USP14 and USP22 **[194]**.

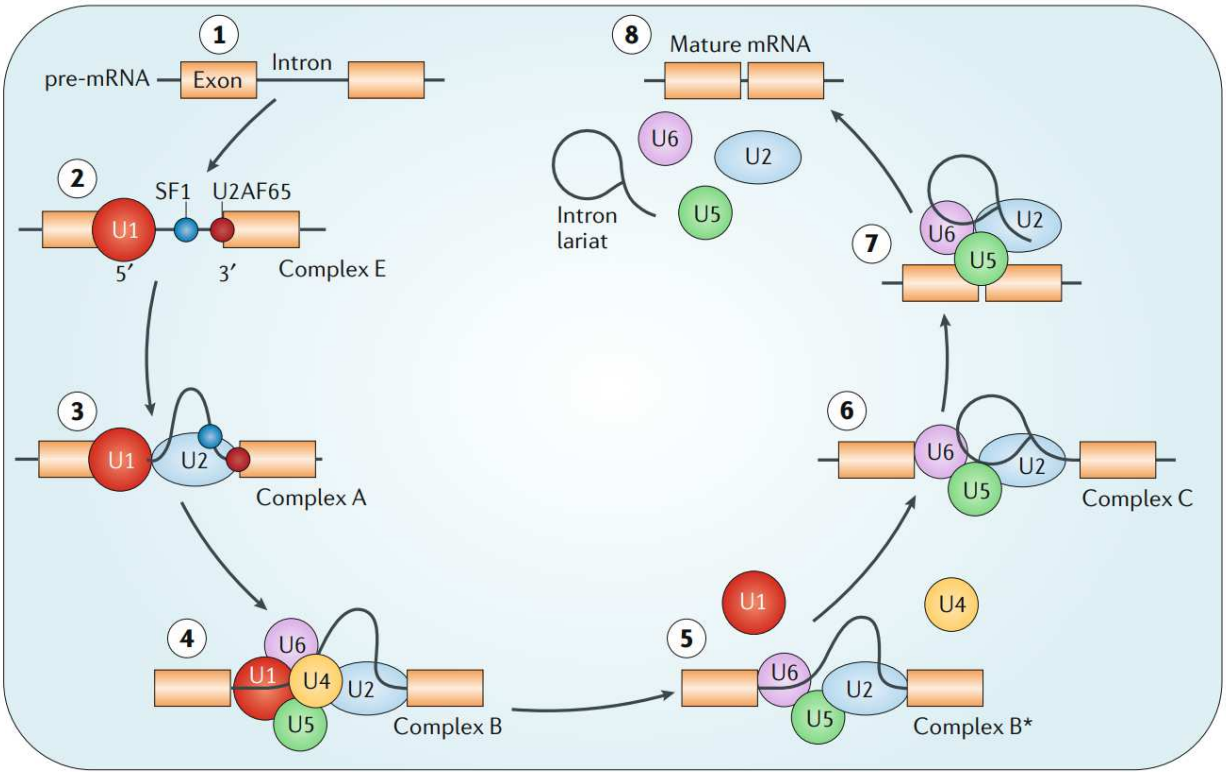

Figure 6: Spliceosome assembly and generation of splice variants
Step 1) Small nuclear ribonucleoprotein (snRNP) U1 couples with the intron 5' splice site **Step 2)** The complex is stabilized by splicing factor 1 (SF1), and splicing factor U2AF 65kDa subunit (u2AF65) is recruited to the 3' splice site. **Step 3)** snRNP U2 is recruited to the intron branch point in an ATP-dependent manner. **Step 4)** a U4-U6-U5 triRNP complex is recruit to the spliceosome, inducing a conformational change. **Step 5)** U1 and U4 is released from the spliceosome, forming a catalytically active complex (complex B*) **Step 6)** Catalytic activity of Complex B* forms an intron–exon lariat intermediate from the 5' end of the intron **Step 7)** Second catalytic reaction results in the complete formation of the mature mRNA and the entire looped intron-lariat. **Step 8)** The components are then released from the spliceosome to be recycled for additional splicing reactions. This figure is reproduced from " Androgen Receptor Signaling in the Development of Castration-Resistant Prostate Cancer" by Alec Paschalis et al, Nature Reviews Clinical Oncology (2018) with permission from Springer Nature.

1.4.2 AR-V7 structure and activity

Like most AR-V's, AR-V7 retains from the full-length AR the NTD, DBD, while losing the LBD and part of the hinge region. Consequently, AR-V7 possesses the full transcriptional activity conferred by the AR N-terminal domain, as well as the potential to bind androgen response elements [7]. The loss of LBD critically means that AR-V7 is not constrained by the requirement of ligand-dependent activation, nor is it targetable by any anti-androgens that directly target the AR-ligand interaction [8]. At the C-terminus-end, AR-V7 possesses a unique basic peptide sequence that reconstitutes the NLS lost through truncation of exon 4, thus permitting AR-V7 nuclear localization [9]. AR-V7 can continue to interact with co-activators that binds to AR AF-1 (in NTD) such as SRC-1 and CBP, while losing interactivity with co-activators that bind to AR AF-2 [37].

1.4.3 AR-V7 activation, localization, and dimerization

While it is generally accepted that AR-V7 is a form that is active in the absence of AR, many aspects of its functions are still under investigation. The constitutively active nature of AR-V7 is largely due to its ability to localize to the nucleus in the absence of androgen, unlike full-length AR where the nuclear localization signal (NLS) becomes exposed only after ligand-induced conformational changes. Some studies show that AR-V7 isn't exclusively nuclear, which might be indicative of additional non-androgen factors that contribute to its nuclear localization, though the specificity of the antibody used in those studies were not entirely validated [164, 165]. Cytoplasmic AR-V7 has been proposed to be a consequence of its ubiquitination, such that it becomes exported out of the nucleus for degradation [195].

Given that since AR-V7 is always expressed alongside AR-FL the question of whether AR-V7 acts primarily as a homodimer or heterodimer has been a focus of several recent studies. These studies offer the consensus that AR-V7 forms both homodimers as well as heterodimer with full-length AR, but that AR-FL is dispensable to AR-V7's gene transcription activity [196, 197]. Furthermore, mutation at AR-V7's dimerization interface impaired its activity, supporting the notion that AR-V7 relies on homodimers for its biological activity. AR-V7 can form both types of dimers via DBD-DBD interaction, as well as heterodimers with AR-FL via an N-C interaction **[197-200]**. By forming heterodimers, AR-V7 also facilitates full-length AR's nuclear translocation in the absence of androgen [200], though upon binding DNA, AR-V7 quickly dissociates from the DNA while AR-FL remains bound longer [197].

1.4.4 AR-V7 regulated gene transcription

Since AR-V7 retains the AR NTD, which is the region largely responsible for assembly of the general transcription and coactivator complex, it is inferred that AR-V7 retains these functions - a notion that is supported by observations that impairing AR coactivator activity affects both AR-FL and AR-V7 mediated transcription [76, 201, 202].

Despite AR-FL and AR-V7 sharing many target genes, they do not fully overlap. It has been observed early on that inhibition of AR-FL via anti-androgens, resulting in AR-V7 upregulation, results in cells adopting a distinct transcriptomic profile compared to cells that receive adequate amount of androgen [203][108]. Efforts to understand how AR-V7 distinctly regulates transcription is complicated by AR-V7 cistrome being highly heterogeneous among CRPC patients [204]. The homeobox protein B13 (HOXB13) may be a key player in this regard,

as it's been demonstrated to be an upstream regulator of AR-V7 mediated transcription; moreover, germline mutation in HOXB13 (G84E) is associated with higher risk of prostate cancer [204, 205].

Inducible expression of AR-V7 has shown that AR-V7, in addition to driving expression of canonical AR-regulated genes, also promotes expression of genes that are unique to AR-V7, such as EDN2, BIRC3, and HSP27 [206]. Likewise, global differential gene expression analysis combined with targeted knockdown of AR-FL and AR-V7 revealed both similarities and differences in gene regulation profiles; notably, AR-V7 preferentially represses rather than promotes transcription, including those of genes that suppresses tumor growth such *SLC30A7*, *B4GALT1*, *HIF1A*, and *SNX14* [207]. One possibility is that the difference in occupancy between AR-V7 and AR-FL is contributed by an unresolved role for the LBD in recruiting co-factors that enhance AR binding at low-occupancy AREs [197].

1.5. Emerging approaches for pharmacological inhibition of AR-V7 activity

1.5.1. Targeting AR N-terminal domain

The N-terminal domain (NTD) is the largest domain of AR (amino acid 1–547) and represents nearly 60% of the receptor proteins. More importantly, all the transcriptional activity of AR resides in its NTD[208]. The activation function (AF) 1 located in NTD is the predominant site for the transcriptional machinery interaction and coregulatory binding. As a result, the NTD is indispensable for the transcriptional activity of AR[209]. Given that AR-NTD contains a potent transactivation function that is independent of the androgen and ligand-binding domain, targeting NTD will substantially inhibit AR signaling activity in CRPC[210]. In addition, AR mutants, especially AR-V7, still retain the NTD, therefore, an inhibitor targeting this domain should

theoretically block the transcriptional activities for all forms of AR. Lastly, compared to AR LBD and DBD, AR NTD shares relatively little sequence homology with other hormone receptors such as progesterone receptor (PR) and glucocorticoids receptor (GR)[50], hence, targeting AR NTD is also expected to achieve high selectivity.

However, pharmacological inhibition of AR through its NTD is extremely challenging, because AR NTD is composed entirely of intrinsically disordered protein which is considered undruggable[211]. Intrinsically disordered protein does not adopt a fixed, ordered structure under physiological conditions, instead, its conformation is highly variable depending on the environmental factors and the cofactors it interacts with[212]. This structural plasticity enables the intrinsically disordered protein to bind to a wide spectrum of molecular partners in a reversible fashion, thus mediating the fast assembly and disassembly of multi-protein complexes, but technically, also imposes a great challenge for its pharmacological targeting[213]. Firstly, the three-dimensional structure of an intrinsically disordered protein cannot be resolved by X-ray crystallography, thus the conventional drug screening method using virtual docking to identify the putative target-inhibitor binding is not feasible. Secondly, lacking a stable binding pocket reflects its biological nature of being difficult to form a high affinity and selectivity bond with a drug molecule[212]. As a result, besides AR NTD, numerous other oncogenic or tumor suppressor proteins such as P53 and c-Myc, remain undrugged owing to their high composition of intrinsically disordered proteins[214]. To date, few compounds designed to target the intrinsically disordered proteins have reached clinical trial, and none has achieved FDA approval.

EPI-001 and its analogs were developed by Sadar's group as AR NTD inhibitors; they are the only class of drug binding to an intrinsically disordered protein that has proceeded to human

clinical trial. Interestingly, rather than having the conventional linear amino acids as binding sites, EPI-001 and its stereoisomer EPI-002 were shown by NMR to covalently binds three regions within the AF-1 of AR NTD[214]. All three regions within the amino acids 354 – 448 must be simultaneously present for the binding to form, and EPI compounds do not bind to any of these regions individually, suggesting the presence of a binding pocket within this segment for EPI compounds. EPI-001 and EPI-002 were characterized in cellular models to inhibit the transcriptional activity of AR-FL and AR variants, including AR-V7[215, 216]; and they have no effect on the activities of other hormonal receptors. Moreover, EPI compounds were proven to block the binding of AR-FL to DNA and disrupt the recruitment of transcriptional coregulators like CREB-binding protein and P300 to AR NTD. The potential efficacy of EPI compounds as therapeutics for CRPC has also been evidenced by their inhibition of androgen-independent growth of prostate cancer cells *in vitro* and in xenograft models[217].

However, skepticism of EPI compounds arises largely due to their effective concentration being in the high micromolar range (> 10 μM). In most cell-based assays, such as for assessing EPI inhibited AR transcription, AR transactivation, cancer cell proliferation, etcetera, the IC50 of EPI-001 and EPI-002 ranges between 25 μM to 50 μM. In contrast, the IC50 of enzalutamide in similar assays is no more than 10 μM. Therefore, the requirement for high drug concentration reflects a modest binding affinity of EPI-001 and EPI-002 to the AR-NTD. Moreover, as insufficient data on EPI's potency in AR-V7 driven CRPC models are published, the inhibitory extent of EPI compounds against AR-V7, and how it intervenes in the biological function of AR-V7 remain unanswered questions. Lastly, EPI-001 was reported to also hit additional targets, which modulates peroxisome proliferator-activated receptor-gamma (PPARγ) activity to lower the

expression of AR[218], thus interrogating EPI compounds' targeting specificity and mechanism of action.

In the year 2017, the results of an open-label, single-arm phase 1/2 clinical trial, evaluating the safety, pharmacokinetics, and maximum tolerated dose of EPI-002 were disclosed. 21 patients with metastatic CRPC who had progressed on enzalutamide or abiraterone received once-daily oral administration of EPI-002 (80 mg –2400 mg) for 87 days on average. PSA decline was observed in 4/8 patients who received the highest dosages of EPI-002 (1280 mg and 2400 mg), but 0/13 patients in the lower dose cohorts (<1280 mg) had a PSA response[219]. Though EPI-002 is well-tolerated with an acceptable safety profile, this trial was terminated early due to the high pill burden which likely resulted from insufficient potency and poor pharmacokinetics. The next generation of EPI analogs is currently under development and investigation[220].

1.5.2. Targeting AR DNA binding domain

As with the N-terminal domain, most AR mutants, including AR-V7 also retain the DNA binding domain (DBD). The AR DBD is quite short relative to the other domains (amino acid 558–624) accounting for less than 10% of the whole AR protein. This region contains two important functional units: P-box (aa 577-581) and D-box (aa 596-600), which are essential for AR to recognize its binding sites on the DNA[50, 221]. More recently, the D-box was found to be indispensable for the dimerization of AR-FL, as well as for the AR splicing variants[198]. Therefore, drug design against AR-DBD would be an approach to block the transcriptional activity for all forms of AR *via* disrupting their DNA binding and/or dimerization. However, because of the high sequence homology of AR-DBD with that of the other hormone receptors (77%–80%)[50], finding a drug with both high affinity and high specificity may be difficult. Nonetheless, efforts have been dedicated to the discovery of AR antagonists for the AR DBD, and a number of

compounds targeting this domain have been published, though their developments are currently staying at the preclinical stage.

In the year 2017, Dalal and colleagues developed a small molecule compound VPC-14449 that inhibits AR-DBD by targeting the P-box[222]. VPC-14449 was found to directly interact with AR amino acids Q592/Y594 that are near the P-box recognition helix. Moreover, the proximal residues K591-L595 are also indispensable for facilitating the binding, indicating the existence of a compound binding pocket in this region. Mechanistically, VPC-14449 reduced the ability of full-length AR as well as AR variants to interact with chromatin, but somehow, the effect on AR-V7 is less pronounced than on full-length AR. Concordantly, VPC-14449 inhibits AR transactivation with IC50 of 0.1–1 μM and cell viability with IC50 of 1-5 μM in multiple prostate cancer cell lines; however, its efficacy is significantly mitigated in the AR-V7 high-expressing cell line, showed an IC50 much higher than 10 μM.

In the year 2018, Dalal and colleagues reported the development of the other small molecule VPC-17005 that targets the AR dimerization interface within the AR D-box[223]. The putative binding pocket of VPC-17005 is between amino acids L594-S613, within which L594, A596, T602, and N610 residues were predicted to directly contact the compound. Moreover, three non-conserved amino acids are in this segment which forms a conceptual basis for AR targeting selectivity without cross-reactivity towards other hormone receptors. At the concentration of 25 μM, VPC-17005 suppressed the AR-FL and AR-V7 homodimerization by ~50% and ~40%, when assessed by fluorescence resonance energy transfer-based assay. VPC-17005 was also demonstrated to inhibit AR-FL transactivation with sub-micromolar IC50 in androgen-sensitive prostate cancer cell line LNCaP, while its inhibition against AR-V7 transactivation is relatively modest (IC50=10 μM). Lastly, VPC-17005 suppressed LNCaP cell proliferation with the IC50 of

1.46 μM, in contrast to a 10-fold higher IC50 (15.2 μM) for AR-V7 expressing cell line 22Rv1, hinting more chemical modification might be necessary for improving inhibitory activity specifically towards AR-V7. Very recently, an analogue of VPC-17005 named VPC-17281 was published by the same research group[224]. VPC-17281 showed improved efficacy in inhibiting AR-FL homodimerization relative to VPC-17005 (IC50: 20 μM versus 25 μM). Likewise, VPC-17281 also demonstrated greater inhibition towards AR-V7 transactivation when compared to VPC-17005 (IC50: 6 μM versus 10 μM). More importantly, VPC-17281 possesses greater microsomal stability alongside improved antiproliferative activity against both LNCaP and 22Rv1 cells. Contradictory to the results mentioned above, when compared to VPC-17005, the potency of VPC-17281 for inhibiting AR-FL transactivation somehow drastically decreased by almost 10 folds (IC50: 6 μM versus 0.7 μM), highlighting that more detailed dissection for this series of compounds' mechanism of action is needed.

1.5.3. Inducing AR-V7 protein degradation

Niclosamide is originally an FDA-approved anti-helminthic drug that was later discovered by Gao's group to degrade AR-V7 protein in prostate cancer cells[225]. Niclosamide downregulates AR-V7 protein level *via* HSP70/STUB1 mediated ubiquitin-proteasome pathway[226]; 1μM of the compound could start lowering AR-V7 level at 4 hours of treatment and inhibit approximately 50% of AR-V7 transactivation activity in the ectopic expressing cellular model. Niclosamide inhibited the proliferation of ENZ-resistant CRPC cells, and was demonstrated to enhance the ENZ treatment effect both *in vitro* and *in vivo*. In a phase Ib trial, CRPC patients who were abiraterone naïve but could have received antiandrogen therapy or chemotherapy were enrolled[227]. Patients orally received escalating doses of niclosamide (400-

1600 mg daily) combined with a standard dose of abiraterone (1000 mg daily). While this trial is still ongoing, the early disclosed results for a small cohort of patients showed a promising PSA response rate (5 out of 9 patients). However, the limits of this preliminary clinical study could be that the AR-V7 status of recruited patients was not tested, and niclosamide was co-administrated with abiraterone, therefore the therapeutic effect of niclosamide in AR-V7 positive CRPC patients, especially as monotherapy is yet to be determined.

MTX-23 is a recently developed AR-V7 degrader by Kim's group using the principle of proteolysis targeting chimeras (PROTAC)[228]. A PROTAC molecule generally comprises three key structural components: a ligand of the target protein, a ubiquitin E3 ligase ligand, and a linker[229]. Functionally, the PROTAC compound can bind to the target protein and subsequently recruit ubiquitin E3 ligases to promote polyubiquitination of the target protein, thus eventually causing the target protein degradation in the proteasome. After that, the PROTAC molecule can be released and free to bind the next round of target protein. Thus, a single PROTAC molecule can be repeatedly used to degrade multiple targets. Consequently, a relatively lower concentration is sufficient and, more importantly, the approach is less susceptible to compensation based on cell signaling. MTX-23 has been designed to simultaneously bind AR's DNA binding domain (DBD) and the Von Hippel–Lindau (VHL) E3 ubiquitin ligase; it effectively degraded 50% of AR-V7 and AR-FL at the concentration of 0.37 μM and 2 μM, respectively. At the concentration of 1 μM, MTX-23 inhibited the proliferation by 30%–50% in CRPC cell lines, including the cells that express AR-V7 and are resistant to AR signaling inhibitors like abiraterone and enzalutamide. Likewise, MTX-23 was also capable of reducing AR-V7 within tumors and enhancing the enzalutamide potency *in vivo*. However, it is unknown whether and to what degree MTX-23-induced AR-V7 degradation has led to the suppression of AR signaling activity.

1.5.4. Blocking AR-V7 mediated transcription by targeting its coactivators

Bromodomain and extraterminal domain (BET) – containing protein BRD4 is a conserved member of the BET family of chromatin readers. It has a critical role in transcription by RNA polymerase II through mediating the recruitment of the positive transcription elongation factor P-TEFb[230, 231]. Knockdown of BRD4 was preliminarily found to lead to significant inhibition of AR-positive CRPC cell proliferation[232, 233], and later studies further uncovered that nuclear expression of BRD4 in clinical CRPC tumor biopsies was associated with AR-regulated gene expression and worse patient outcomes[234]. Mechanistic studies revealed direct interaction of BRD4 with AR-FL and AR-V7 through the AR-NTD, and such interaction is essential for AR-mediated transcription. Moreover, knockdown of BRD4 was also shown to reduce AR-V7 protein expression by regulating genes critical for RNA processing and alternative splicing.

The therapeutic benefits of pharmacologically targeting BRD4 in AR-V7 positive CRPC were initially explored by Chinnaiyan's group. JQ1 was a small molecule inhibitor of BRD4 which competitively binds to the bromodomain pocket in BRD4, resulting in the displacement of BRD4 from active chromatin and subsequent removal of RNA pol II from target genes[232]. In the AR-V7 expressing CRPC cell lines VCaP and 22Rv1, it inhibited AR-regulated gene transcription with an IC50 of 0.1–2.5 μM and suppressed their proliferation by 50% at the concentration of 0.05–0.2 μM. Daily i.p. treatment of JQ1 at the dosage of 50mg/kg also slowed down the VcaP tumor growth by approximately half in castrated mice, suggesting its therapeutic potential of blocking AR-V7 positive CRPC progression. A few BRD4 inhibitors are currently under development and most of them have shown antiproliferative effects in AR-V7 overexpressing cell lines, among which ZEN-3694 has entered phase Ib / Iia clinical trial[235]. 75 patients with metastatic CRPC who have

progressed on prior abiraterone and/or enzalutamide were enrolled, and they were orally treated with escalating dosages of ZEN-3694 (36 –160 mg daily) combined with 160 mg of enzalutamide. With the median duration of treatment being 3.5 months, the clinical progression-free survival in this cohort was 5.5 months, while less than 10% of patients had ⩾50% PSA decline, suggesting lacking the additive benefit of ZEN-3694 in combination with enzalutamide, and also raising questions of the compound's effect on AR-signaling blockade in CRPC patients.

p300 and CREB binding protein (p300/CBP) are other AR coactivators that are becoming promising therapeutic targets for repressing AR-V7 transcriptional activity. p300/CBP are paralogues histone acetyltransferase proteins that mediate histone acetylation at enhancer regions to lose up the chromatin and increase DNA accessibility for AR[236-238]. p300/CBP were found highly expressed in CRPC specimens and was associated with elevated AR signaling[239-242]. In the AR-V7 expressing CRPC cell lines, knockdown of p300/CBP has been reported to decrease AR-V7 expression, inhibit AR signaling and reduce tumor cell growth[241]. CCS1477 was developed by Welti and colleagues as a potent inhibitor of the conserved bromodomain of P300 and CBP[241]. CCS1477 inhibited AR signaling activity in AR-V7 expressing cell models LNCaP95 and 22Rv1 and suppressed the growth of 22Rv1 mouse xenografts. In a phase I clinical trial with metastatic CRPC patients, one patient who received 50 mg CCS1477 orally on a 3-day-on and 4-day-off schedule experienced PSA drop and AR-V7 protein reduction, whereas the other patient who had 25mg CCS1477 continuously showed rising PSA despite the treatment[243]. Therefore, the complete disclosure of clinical trial data is required to assess the potency of CCS1477 against AR-V7-driven AR signaling activity in CRPC patients.

1.6. Our research rationale and objectives

As pharmacological targeting of AR-V7 remains our opportunity and challenge for overcoming drug resistance in CRPC, we sought to explore the development of small molecule compounds targeting the AR N-terminal domain (AR-NTD) for AR-V7 inhibition. The strategic advantages of targeting AR-NTD are potentially: (1) Compared to targeting the AR DNA binding domain, AR-NTD inhibition confers less cross-reactivity with other members of the steroid receptor superfamily. (2) Compared to AR protein degradation, AR-NTD inhibition encounters less cell signaling compensation, thus potentially more enduring inhibitory effect. (3) Compared to hitting a specific AR-V7 cofactor which mediates the transcription for a subset of genes, AR-NTD inhibition evenly and broadly affects all the AR-regulated gene transcription.

Given that the AR-NTD possesses all the transactivation activity of AR and is retained in AR-V7, we aimed at achieving the following characteristics for our novel AR-NTD inhibitors: (1) Inhibit the transactivation activity of all forms of AR, including AR-V7, full-length AR, and AR ligand binding domain mutants. (2) Improve antagonistic efficacy relative to the previously reported EPI compounds. (3) Suppress the AR-V7 driven AR signaling activity in various castration resistant prostate cancer models.

Chapter 2: Discovery of a small-molecule inhibitor targeting the androgen receptor N-terminal domain for castration-resistant prostate cancer

Title

Discovery of a small-molecule inhibitor targeting the androgen receptor N-terminal domain for castration-resistant prostate cancer

Qianhui Yi[1,2], Weiguo Liu[1], Jung Hwa Seo[1], Jie Su[1], Moulay A. Alaoui-Jamali[1,2], Jun Luo[3], Rongtuan Lin[1,2] and Jian Hui Wu[1,2]*

[1]Lady Davis Institute for Medical Research, SMBD-Jewish General Hospital, McGill University, 3755 Cote-Ste-Catherine, Rd, Montreal, QC H3T 1E2, Canada

[2]Departments of Oncology and Medicine, Faculty of Medicine, McGill University, Montreal, QC, Canada

[3]Urology, Johns Hopkins University, Baltimore, MD, USA

***Corresponding author:** Jian Hui Wu, Lady Davis Institute for Medical Research, SMBD-Jewish General Hospital, McGill University, 3755 Cote-Ste-Catherine, Rd, Montreal, QC H3T 1E2, Canada. Phone: +1(514) 340-8222 ext 22148, Email: jian.h.wu@mcgill.ca

Running title: Novel AR inhibitor targeting the AR-NTD

Precis: Discovery of a novel AR inhibitor targeting the AR-NTD, with potent activity against AR splice variants and multiple clinically-relevant mutants of full-length AR, and in *vivo* efficacy against 22Rv1 xenograft in intact mice and castrated mice.

Conflict of interest: The authors declare no potential conflict of interest.

Keywords: Castration-resistant prostate cancer, Androgen Receptor, N-terminal Domain, Antiandrogen, AR-V7

2.1. Abstract

The current mainstay therapeutic strategy for advanced prostate cancer is to suppress androgen receptor (AR) signaling. However, castration-resistant prostate cancer (CRPC) invariably arises with restored AR signaling activity. To date, the AR ligand-binding domain (LBD) is the only targeted region for all of the clinically available AR signaling antagonists, such as enzalutamide and abiraterone. Major resistance mechanisms have been uncovered to sustain the AR signaling in CRPC despite these treatments, including AR amplification, AR LBD mutants, and the emergence of AR splice variants (AR-Vs), such as AR-V7. AR-V7 is a constitutively active truncated form of AR that lacks the LBD, thus can not be inhibited by AR LBD-targeting drugs. Therefore, an approach to inhibit AR through the regions outside of LBD is urgently needed. In this study, we have discovered a novel small molecule, SC428, which directly binds to the AR N-terminal domain (NTD) and exhibited pan-AR inhibitory effect. SC428 potently decreased the transactivation of AR-V7, ARv567es, as well as full-length AR (AR-FL) and its LBD mutants. SC428 substantially suppressed androgen-stimulated AR-FL nuclear translocation, chromatin binding, and AR-regulated gene transcription. Moreover, SC428 also significantly attenuated AR-V7 mediated AR signaling that does not rely on androgen, hampered AR-V7 nuclear localization, and disrupted AR-V7 homodimerization. SC428 inhibited *in vitro* proliferation and *in vivo* tumor growth of cells that expressed a high level of AR-V7 and were unresponsive to enzalutamide treatment. Together, these results indicated the potential therapeutic benefits of AR NTD targeting for overcoming drug resistance in CRPC.

2.2. Introduction

Prostate cancer is the second-most frequently diagnosed cancer with the fifth-highest mortality among men globally [244]. In the United States, prostate cancer is forecasted to cause 268,490 new cancer cases and 34,500 death in the year 2022 [245]. Although localized prostate cancer is highly curable by prostatectomy and radiation, 27%-53% of patients could suffer disease relapse and be subsequently offered androgen deprivation therapy (ADT), such as luteinizing hormone-releasing hormone agonist/antagonist and surgical castration [86]. Despite initial response to ADT, prostate cancer usually develops resistance featuring rising prostate-specific antigen (PSA) under castration level of androgen, which is clinically identified as castration-resistant prostate cancer (CRPC). Approximately 10%–20% of localized prostate cancer eventually progressed to CRPC, among which 84% was accompanied by metastasis resulting in median survival of fewer than 2 years [246].

In the past 10 years, several second-line ADT which all target androgen receptor (AR) ligand-binding domain (LBD), has been approved for treating metastatic CRPC, including the androgen biosynthesis inhibitor abiraterone (Abi), as well as antiandrogen enzalutamide (ENZ). However, their survival benefit is modest, as resistance is either pre-existing or acquired after a brief response period [103, 247]. Plus, combinational treatment of Abi and ENZ did not improve overall survival relative to monotherapy, while sequential treatment was outperformed by chemotherapy, highlighting strong cross-resistance [88, 90]. ADT treatment failure is typically manifested by continued AR signaling, and multiple mechanisms that restore AR signaling activity have been well-established in CRPC, including AR amplification, AR LBD mutation, and in this particular context, constitutively active AR splice variants (AR-Vs) with LBD truncated. On the

molecular basis, AR-Vs could leverage loss of LBD to bypass all the ADTs, among which, AR-V7 is most intensively studied due to its prevalence in CRPC patients [163, 164]. AR-V7 protein overexpression is induced following Abi and ENZ treatment in CRPC patients [167], and its nuclear expression in circulating tumor cells predicts worse outcomes from Abi and ENZ [175]. AR-V7 mRNA level is also elevated in CRPC patients [163] and is strongly associated with Abi and ENZ resistance [168]. Recent studies uncovered the emergence of AR gene rearrangements that favor AR-Vs generation in CRPC tissue [248]; such genomic change were found enriched in plasma tumor DNA from Abi and ENZ-treated patients and was linked to resistance [249]. Thus, compelling evidence has tied AR-V7 to ADT resistance in CRPC, emphasizing the urgency of AR-V7 inhibition.

AR-V7 arises from alternative splicing of AR pre-mRNA to exclude exons 4–8 that encode hinge region and LBD but include exons 1–3 and a cryptic exon 3. Exon 1 encodes the N-terminal domain (NTD) that possesses transactivation activity by serving as a hub for interaction with basal transcriptional machinery and coregulators. Exon 2–3 encodes the DNA binding domain (DBD) which facilitates dimerization and DNA binding. The unique peptide sequence derived from cryptic exon 3 confers NLS activity [250]; thus, AR-V7 is predominantly located in nucleus to constantly promote AR-regulated gene transcription and cancer cell growth regardless of androgen. Since most forms of AR, especially AR-V7, retain NTD, developing drugs that target this region is considered a promising approach for overcoming CRPC.

In this work, we report a novel small molecule SC428 that directly binds to AR NTD and inhibited transactivation of AR-V7, ARv567es, full-length AR (AR-FL) and multiple AR-FL LBD mutants. SC428 impaired androgen-induced AR-FL nuclear trafficking and chromatin binding and therefore attenuated AR-FL-regulated gene transcription. Under the castration condition, SC428

hampered AR-V7 nuclear localization and homodimerization, as well as mitigated AR-V7 mediated transcription. Because of its broad activity against AR-V7 and AR-FL, SC428 was equally effective in suppressing the proliferation across multiple prostate cancer cell lines with varying levels of AR-V7/AR-FL. Moreover, SC428 demonstrated *in vivo* activity against AR-V7 high-expressing 22Rv1 xenograft which was resistant to enzalutamide treatment.

2.3.Materials and Methods

Cell lines

293T, PC3, LNCaP, VCaP, and 22Rv1 cell lines were purchased from the ATCC and cultured as recommended. In experiments where the androgen-deprived condition was required, cells were cultured in phenol red-free medium supplemented with 10% of charcoal-stripped FBS. The stable cell lines LNCaP-AR^{WT}, LNCaP-AR^{F877L}, LNCaP-AR-V7, and LNCaP-GFP were established by transfecting pEGFP-c1-AR^{WT}, pEGFP-c1-AR^{F877L}, pEGFP-c1-AR-V7, or pEGFP-c1 empty vector plasmids into LNCaP cells with lipofectamine 3000 (Invitrogen). Cells were allowed to recover in refreshed media overnight after 48 h of transfection, and subsequently were subjected to FACS sorting for GFP using BD FACS Aria cytometer. The GFP-positive cells were cultured in media containing 150 ng/mL of G418, and the second round of GFP-sorting was performed when cells grew to 80% confluence. Counting from the second GFP-sorting, only cells that were lower than 6 passages were used in the following experiments.

Plasmids

The pEGFPc1-AR-V7 plasmid was a gift from Dr. Jun Luo (Johns Hopkins University, USA). pIRES-AR-V7 was generated by cloning the AR-V7 cDNA from pEGFPc1-AR-V7 plasmid into pIRESpuro2 vector. pcDNA-ARv567es was a gift from Dr. Stephen Plymate (University of Washington, Seattle, WA). pCMV-AR, pCMV-VP16/AR507−920, the B form of human progesterone receptor (PR-B), pCMV-MMTV-Luc, and pCMV-PSA-Luc plasmids were kind gifts from Dr. Liangnian Song (Columbia University, USA). pEGFPc1-IRF3, pEGFPc1-IRF3DBD (aa 1−133) and ISRE-Luc plasmids were gifts from Dr. Rongtuan Lin (McGill University). The pCMV-AR-T878A and pCMV-AR-H875Y plasmids were gifts from Dr. S. Srivastava (Uniformed Services University). pCMV-AR-W742C was a gift from Dr. O. Ogawa (Kyoto University). pEGFPc1-IRF3-AR^{NTD}, pCMV-VP16/$AR^{DBD+LBD}$, pEGFPc1-F877L and pCMV-AR-F877L plasmids were constructed as described in Supplementary Methods.

Compound synthesis

SC428 and its analogues were synthesized and characterized as described in the Supplementary Methods. SC428: White solid, m.p. 199-201°C, yield: 45.7%. ^{1}H NMR (500 MHz, acetone-d_6) δ 9.01 (br, 1H), 8.52 (br. d, J = 10.0 Hz, 1H), 8.28 (d, J = 2.0 Hz, 1H), 7.98 – 7.92 (m, 2H), 7.34 (dd, J_1 = 14.5 Hz, J_2 = 14.5 Hz, 1H), 7.22 (d, J = 5.0 Hz, 1H), 6.97 (dd, J_1 = 5.0 Hz, J_2 = 5.0 Hz, 1H), 6.93 (d, J = 3.5 Hz, 1H), 6.38 (d, J = 14.5 Hz, 1H). LHMS-ESI, m/z $[M+H]^+$ 338.06.

Dual luciferase reporter assay

293T, PC3, 22Rv1 or LNCaP cells were seeded into 24-well plates at least 24 h before transfection. *Firefly* luciferase reporter (PSA-Luc or MMTV-Luc) and *Renilla* luciferase reporter (pRL-TK)

alone or together with a plasmid expressing the designated transcription factor were transiently transfected into cells using lipofectamine 3000. 5 h after transfection, cell culture media was refreshed, and cells were subjected to the treatment of DMSO or designated compounds. Luciferase activities were measured using the Dual-Luciferase Reporter Assay System (Promega) on a GLOMAX 20/20 luminometer (Promega).

Cell proliferation assay

For CellTiter-Glo assay, LNCaP, VCaP, 22Rv1, or PC3 cells (3000 cells/well) were plated in 96-well plates (Thermo Scientific #167008) 24 h before compound treatment. Culture media and compounds were refreshed on day 3 and viable cells were measured using CellTiter-Glo 2.0 Assay kit (Promega) on day 6 by Synergy 4 multimode plate reader (BioTek). For BrdU assay, LNCaP stable cells (10000 cells/well) were seeded in 96-well plates (Corning #3595) 24 h before treatment. Cells were exposed to DMSO or compounds for 30 h and BrdU labeling solution was added in the last 12 h. According to the BrdU Cell Proliferation Assay Kit protocol (Cell Signaling), dividing cells were quantified by measuring the incorporated BrdU using a multimode plate reader (Perkin Elmer).

qRT-PCR analysis

2×10^6 cells were seeded in 6 cm dish and cultured in androgen-deprived media for 48 h prior to 24 h of compound treatment. Cells were then harvested and followed by total RNA extraction using RNA Neasy Mini Kit (QIAGEN), cDNA was synthesized using 5× All-In-One RT MasterMix (abm). Expression of AR regulated gene was assessed using GoTaq qPCR Master Mix

(Promega), qRT-PCR reaction was performed on 7500 Fast Real-Time PCR System (Applied Biosystems).

Confocal imaging

1×10^6 LNCaP-AR^{WT} or LNCaP-AR-V7 cells were seeded above the coverslip in 6-well plates. Cells were treated as described in the respective figure for 5 h. Confocal microscopy was performed on a fully motorized Zeiss Axio Observer Z1 microscope with confocal unit LSM-800 with a 63×1.4 NA Plan-Apochromat oil-immersion objective lens (Zeiss) using diode solid-state lasers (488 nm excitation for GFP, 405 nm for DAPI). Images were captured with GaAsP detectors and ZEN blue software. Raw data was analyzed and modifications to images for presentation purposes were made by using Fiji (Image J).

Western blot analysis

Cells were plated at 6×10^5 cells per 6 cm dish and were treated as described in the respective figures. Protein extracts were prepared using RIPA buffer supplemented with 1% Protease Inhibitor Cocktail (SIGMA) and 1mM PMSF. Protein concentration was quantified by Coomassie Protein Assay (Thermo) and samples were applied to SDS-PAGE. Western blot was performed with antibodies AR-N20 (sc-816, Santa Cruz), AR-V7 (AG10008, Precision Antibody), PSA (#2475, Cell Signaling), PARP (#46D11, Cell Signaling), phospho AR^{S81}(#04-078 Millipore), phospho ARS210/213 (ab45089, abcam) and β-actin (SIGMA). For tumor tissue, a soybean-sized piece of tissue was dissected from the tumor and was homogenized in 1mL RIPA buffer supplemented with 5% Protease Inhibitor Cocktail (SIGMA) and 2 mM PMSF, Western blot was performed with the supernatant.

Co-immunoprecipitation (Co-IP)

5×10^6 Cells were plated in 10 cm dish in androgen-deprived medium 24 h or 48 h before transfection. Cells were transfected for 5 h with corresponding plasmids using Lipofectamine 3000 (Invitrogen) and allowed to recover in refreshed media overnight. The next day, cells were exposed to the indicated treatments for 5 h, followed by lysis in RIPA buffer (50 mM Tris/Cl pH 7.5; 150 mM NaCl; 2 mM EDTA pH 8; 0.1% SDS; 1% Trito-X-100; 25 mM NaF) supplemented with 2% Protease Inhibitor Cocktail (SIGMA), 2 mM PMSF, 2.5% RQ1-RNase-Free DNase (Promega) and 2.5% RQ1 DNase 10× Reaction Buffer (Promega). GFP-tagged AR-V7 immunoprecipitation was performed using GFP-Trap A (ChromoTek, Germany) according to the manufacturer's protocol. Precipitates were eventually evaluated by western blot using AR-N20 antibody (Santa Cruz) and GFP antibody (Cell Signaling).

Animal study

All animal studies were conducted under the Animal Use Protocol approved by the Animal Care Committee of the Lady Davis Institute, Jewish General Hospital, McGill University. Six weeks old and Nu/Nu male mice were purchased from Charles River; Tumor cell implantation was done at least 1 week after animal arrival. The indicated number of tumor cells were injected subcutaneously in 200 ul solution containing 50% of PBS and 50% of Cultrex Basement Membrane Matrix, Type3 (Trevigen). Tumor length and width were measured by caliper and tumor size were calculated with the formula: $\text{Volume}=4/3\times\pi\times(\text{Length}/2)\times(\text{Width}/2)^2$. Compounds were delivered *via* intraperitoneal injection (i.p.) (at 10 ul per 1 g of mouse body weight). Compounds were formulated in saline solution contains 10% DMSO, 10% Cremophor EL, 20%

PEG400 and 1% 2-hydroxypropyl-β-cyclodextrin.

Statistical analysis

Statistical significance was calculated by the two-tailed unpaired t test using Prism Graphpad 9 , unless stated otherwise for a specific graph in the figure. Data were plotted as individual data points or summarized as average ± standard deviation (SD) of biological or technical repeats. P values considered to be significant as follows: *p<0.05, **p<0.01, ***p<0.001 and ****p<0.0001. n.s, not significant.

2.4. Results

2.4.1. SC428 inhibits the transactivation of AR-V7 and ARv567es and directly targets the AR-N terminal domain

Initial screening of our in-house compound library for anti-AR-V7 activity, using an AR-V7 dependent PSA-Luc reporter assay in 293T cells, followed by further chemical optimization, led to our lead molecule SC428 (**Fig. 1A**). SC428 and its derivatives revealed a clear structure-activity relationship against AR-V7 (**Fig. 1B**; Supplementary **Fig. S1**). In contrast to the AR LBD-targeting ENZ, which exhibited no inhibitory effect, SC428 suppressed transactivation of both AR-V7 and another AR splice variant, ARv567es, in a dose-dependent manner (**Fig. 1C**). The concentrations at which 50% of AR-V7 or ARv567es reporter activity was inhibited were 0.42 μM and 1.31 μM, respectively (**Fig. 1C**). Furthermore, SC428 also showed inhibition against ligand-stimulated activation of full-length AR but had no obvious effect on GR or PR (Supplementary **Fig. S2**), indicating that SC428 was an AR-selective inhibitor.

To assess if SC428 targets the AR NTD, we constructed a plasmid expressing chimeric

protein that fused AR NTD (amino acids 1−547, thereby removing AR LBD and DBD) to the DBD of a non-relevant transcription factor IRF3 (IRF3-AR^{NTD}). Transactivation of IRF3-AR^{NTD}, or of a corresponding control wild type IRF3, was assessed via a paired reporter that fused the interferon-stimulated response element (ISRE) to the firefly luciferase gene. When AR negative PC3 cells were transfected with this plasmid pair, SC428 treatment decreased the IRF3-AR^{NTD} dependent ISRE-Luc activity by 30% at 0.5 μM and 70% at 5 μM but showed no effect on IRF3-dependent ISRE-Luc activity (**Fig. 1D**), indicating that its inhibitory effects were dependent on the presence of AR NTD. In contrast, ENZ did not inhibit IRF3-AR^{NTD}, which was expected, as AR NTD not beings its targeted domain (**Fig. 1D**). Next, we generated a complementary reporter system, in which AR NTD was truncated, to further confirm SC428's target regions.We constructed a plasmid, which expresses another chimeric protein (VP16-$AR^{DBD+LBD}$) fusing the transactivation domain of VP16 with the DBD and LBD of AR (amino acids 540−920). Since this chimeric protein contains AR LBD, its transactivation, like AR-FL, was stimulated by DHT. Whereas ENZ and SC428 were both able to substantially inhibit DHT stimulated activation of AR-FL, only ENZ could inhibit DHT stimulated transactivation of VP16-$AR^{DBD+LBD}$ (**Fig. 1E**), confirming that SC428 specifically targets AR NTD without affecting AR DBD or LBD. In addition, we performed the surface plasmon resonance (SPR) experiment to determine the binding affinity and kinetic of SC428 with the AR NTD. The recombinant protein of AR NTD (amino acids 2−556) was immobilized on a sensor chip, and SC428 was injected into the analyte flow at a range of concentrations (0−100 μM). The SPR analysis gave an equilibrium dissociation constant, K_D value of 75 ±29 μM (**Fig. 1F**). Collectively, these results demonstrated that SC428 antagonizes AR-V7 transactivation and binds to AR NTD.

2.4.2. SC428 inhibited multiple clinically relevant LBD mutants of AR-FL

Multiple PCa patient specimens-characterized AR-FL mutants have been reported to promote the acquisition of antiandrogen resistance, including W742C, H875Y, T878A, and F877L, all of which share a conserved NTD [102]. In PC3 cells ectopically expressing wild-type or these mutant AR, SC428 inhibited the ligand-induced activation of these ARs in a concentration-dependent manner (**Fig. 2A**). SC428 showed comparable or weaker inhibition against WT, W742C, H875Y, and T878A when compared to ENZ at lower doses (1 μM and 2.5 μM) but performed equally to ENZ at higher dosages (5 μM) (**Fig. 2A**). For F877L, ENZ behaved like a partial antagonist in the presence of 10 nM DHT, whereas SC428 exhibited full antagonistic activity (**Fig. 2A**).

Next, we examined SC428's potency against F877L under androgen deprivation - a condition under which ENZ is well-known to switch from AR antagonist to agonist[251]. Unlike ENZ, which markedly increased PSA protein and mRNA expression in LNCaP-AR^{F877L} cells, SC428 suppressed AR signaling below basal levels (Supplementary **Fig. S3A, S3B**). These findings were further validated by PSA-Luc reporter assay in LNCaP-AR^{F877L} cells (Supplementary **Fig. S3C**) and in PC3 cells transiently expressing F877L (Supplementary **Fig. S3D**). When assessed by BrdU assay, SC428 indifferently inhibited the proliferation of LNCaP-AR^{WT} and LNCaP-AR^{F877L} cells cultured in androgen-free media (Supplementary **Fig. S3E**). In contrast, F877L overexpression in LNCaP cells significantly mitigated ENZ's antiproliferative ability (Supplementary **Fig. S3E**). Together, these results demonstrated that, while ENZ is converted to an agonist against F887L under castration conditions, SC428 continues to behave as a potent antagonist for this mutant.

2.4.3. SC428 suppressed AR-positive prostate cancer cell proliferation *in vitro*

To examine if inhibition of AR signaling by SC428 translated into inhibition of prostate cancer (PCa) cell growth, we compared SC428's antiproliferative activity to ENZ in a four-PCa cell lines panel: LNCaP, VCaP, 22Rv1, and PC3. Low passage LNCaP cells only express AR-FL mutant T878A [252], while VCaP cells express a high level of wild-type AR-FL and a trace amount of AR-V7 [163]. In VCaP cells, increased AR-V7 expression could be induced by androgen deprivation and antiandrogen [253], which in turn helps sustain the AR signaling activity [254]. 22Rv1 cells predominantly expresses AR-V7 rather than AR-FL due to intragenic rearrangement that enhances AR-V7 mRNA splicing [255], and is mostly reliant on AR-V7 rather than AR-FL for AR signaling and cell growth in the absence of androgen [256]. When cells were grown in androgen-free media with 0.1nM DHT, SC428 inhibited proliferation of the three AR-positive cell lines with very similar IC50 as 1.39 μM for LNCaP, 1.01 μM, and 1.13 μM for VCaP and 22Rv1(**Fig. 2B**; Supplementary **Table. S1**), respectively. Although ENZ is potent in LNCaP cells with an IC50 of 0.9 μM, its efficacy declined for more than 3-fold in VCaP cells, and is almost inactive against 22Rv1 cells (**Fig. 2B**; Supplementary **Table. S1**), which agrees with other groups' finding that AR-V7 expression is correlated to ENZ-resistant growth in PCa cell lines and PDX [200, 257]. For the AR-negative cell line PC3, SC428's antiproliferative efficacy reduced by 6-fold (IC50=6.49 μM) compared to it is in the AR-positive cells, and ENZ only showed marginal effect (IC50>10 μM) (**Fig. 2B**; Supplementary **Table. S1**). These data implied that AR-V7 expressing PCa cells are more resistant to ENZ but are equally sensitive to SC428.

2.4.4. SC428 attenuated transcription of AR-regulated genes, blocked AR-FL chromatin binding, and impaired its nuclear translocation

As SC428 has been observed to repress the transactivation of ectopically expressed AR in intrinsically AR-negative cell models, we next sought to assess if SC428 likewise also blocked the functions of endogenous AR-FL in PCa cells. Since AR is a nuclear hormone receptor whose oncogenic role is derived from its transcriptional activity, we first performed qPCR analysis on AR-regulated genes (*PSA* and *TMPRSS2*) in LNCaP-AR^{WT} cells to determine if SC428 inhibits AR-FL mediated transcription. When cells were stimulated by 10 nM DHT, both 5 μM SC428 and 10 μM ENZ substantially repressed the androgen-mediated induction of mRNA expression to be comparable or even lower than the non-androgen stimulated control (**Fig. 3A**).

We next asked whether decreased AR-regulated transcription by SC428 is due to reduced AR-chromatin binding. In the chromatin immunoprecipitation (ChIP) experiment, LNCaP-AR^{WT} cells were androgen starved for 48 hours and were then stimulated by 10 nM DHT accompanied with 10 μM ENZ, or 5 μM SC428 for another 5 h. Similar to ENZ, SC428 treatment also drastically prevented androgen-induced AR recruitment to androgen response element (ARE) in both the *PSA* enhancer and the *TMPRSS2* enhancer (**Fig. 3B**). Finally, given that AR NTD is also important for AR-nuclear localization [258], we wondered whether SC428 reduced the nuclear translocation of AR-FL. Using confocal imaging, we tracked GFP-tagged AR-FL in LNCaP-AR^{WT} cells upon DHT exposure. Like ENZ, SC428 was also capable of blocking the androgen-stimulated nuclear translocation of GFP-AR-FL (**Fig. 3C**). Together, these results suggested that by binding to the AR-NTD, SC428 impairs AR-FL nuclear trafficking and hampers its chromatin binding, hence mitigating AR-FL mediated transcription.

2.4.5. SC428 inhibited the AR signaling in AR-V7 high-expressing PCa cells and suppressed their ENZ-resistant proliferation

22Rv1 is a well-characterized CRPC cell line, featuring a high amount of endogenous AR-V7 that mediates constitutively active AR signaling independently of AR-FL [259, 260]. Using the PSA-Luc plasmid as a reporter for endogenous AR-V7 transactivation activity, we observed that treatment with SC428 (at 1, 2.5, 5 μM) for 24 hours under castration condition resulted in dose-dependent inhibition of PSA-Luc. In contrast, ENZ was completely inactive at 2.5 or 5 μM and only slightly suppressed PSA-Luc at 10 μM. (**Fig. 4A**). We then examined the expression of two canonical AR-regulated genes (*PSA* and *FKBP5*) and one AR-V7 specific gene *AKT1* to determine if SC428 impacted AR-V7 mediated transcription. In androgen starved 22Rv1 cells, 2.5 μM SC428 reduced *PSA* and *FKBP5* mRNA to approximately 50% of control, whereas 5 μM SC428 further reduced it to 10-30% of control. Moreover, 5 μM of SC428 caused a moderate but reproducible decrease of AKT1 mRNA expression. Consistent with the previous study [256], no substantial effect on *PSA*, *FKBP5* nor *AKT1* mRNA level was observed following ENZ (5 and 10 μM) treatment in 22Rv1 cells (**Fig. 4B**), suggesting that SC428, but not ENZ, blocks AR-V7 dependent AR signaling in 22Rv1 cells.

To validate the effect of SC428 against AR-V7 dependent AR signaling in a second PCa cell model, we generated a LNCaP-AR-V7 stable cell line, in which the level of GFP-tagged AR-V7 protein was approximately 2-fold higher than endogenous AR-FL protein (**Fig. 4C**). Compared to LNCaP-AR^{WT}, LNCaP-AR-V7 cells showed elevated castration-resistant AR signaling as evidenced by higher PSA level when cells were cultured in androgen-free media (**Fig. 4C**).

Although ENZ remained effective at suppressing AR signaling in LNCaP-AR-V7, its activity was notably blunted compared to in LNCaP-AR^{WT}, particularly at lower doses (0.5 μM,1 μM, and 2.5 μM) (**Fig. 4D**). Conversely, SC428 suppressed PSA-Luc with equal potency in both LNCaP-AR-V7 and LNCaP-AR^{WT} cells (**Fig. 4D**). Likewise, both ENZ and SC428 inhibited PSA gene expression in LNCaP-AR-V7 cells, but only SC428 markedly decreased mRNA level of AR-V7 specific gene *UBE2C* (**Fig. 4E**).

SC428 did not affect AR-V7 protein levels and only modestly induced AR-FL degradation when treated for longer than 20 hours at high dose (5 μM) (Supplementary **Fig. S4A**, **S4B**, **S4C**), indicating that SC428's inhibitory effect against AR signaling was not due to modulating AR-V7 protein stability. In androgen-starved LNCaP-AR-V7 and 22Rv1 cells, treatment of 5 μM SC428 for 5 h hampered the AR-NTD phosphorylation at the sites of S81 and S210/213, hinting that the post-translational modification of AR-NTD was quickly altered after binding to SC428 (Supplementary **Fig. S5A**, **S5B**, **S5C**, **S5D**).

Lastly, we compared the inhibitory effects of SC428 and ENZ on LNCaP-AR^{WT} versus LNCaP-ARV7 cell lines. Whereas ectopic expression of AR-V7 significantly diminished the antiproliferative effects of ENZ, it barely affected SC428 (**Fig. 4F**). This observation, again suggested that higher abundance of AR-V7 generally correlated with reduced ENZ potency, but had no impact on SC428 inhibited cell growth (**Fig. 2B**). These results collectively indicated that SC428 could overcome the ENZ-resistant AR signaling and cell proliferation driven by AR-V7.

2.4.6. SC428 disrupted AR-V7 homodimerization and nuclear localization

AR-V7 can form homodimer without androgen, and such dimerization is essential for AR-V7's ability to transactivate target genes and promote cell growth under castration condition [261]. A recent study further dissected that AR-V7 homodimerization does not rely on AR-FL and is therefore unaffected by AR-FL-targeting agents [196]. To assess if SC428 can disrupt AR-V7 homodimerization, we used LNCaP cells, which simultaneously express GFP-AR-V7 alongside non-tagged AR-V7 by transiently transfecting pIRES-AR-V7 plasmid into LNCaP-AR-V7 stable cells (with LNCaP-GFP cells as mock control). Next, we utilized a high GFP-affinity resin to perform the immunoprecipitation, allowing GFP-AR-V7 to serve as a bait to pull down the non-tagged AR-V7 as a prey for the purpose of detecting AR-V7 homodimer. We found that the bait GFP-AR-V7 could sufficiently coprecipitate the prey AR-V7, indicating they can form a homodimer. By comparing the relative abundance of prey pulldown, we observed that AR-V7 homodimerization was effectively mitigated by SC428 while, consistent with other group's findings [259], ENZ had no effect (**Fig. 5A**). To confirm this result in an alternative cell model, we transiently expressed GFP-AR-V7 in 22Rv1 cells (vector plasmid transfected cells as mock control) as a bait to pull down endogenous AR-V7. SC428 was again able to reduce the level of AR-V7 homodimer, whereas ENZ failed to show an effect upon (**Fig. 5B**). Intriguingly, AR-FL was not detected in the IP fraction, suggesting AR-V7 predominantly forms homodimer rather than heterodimer. This result is in concordance with Liang *et al*'s finding that only trace amount of AR-FL was associated with AR-V7 on chromatin [259]. Hence, the low abundance of AR-V7 heterodimer might be below the detection threshold in our co-IP system.

Unlike AR-FL, which requires androgen binding to initiate cytoplasm-to-nuclear translocation, AR-V7 constitutively resides in the nucleus regardless of androgen [163]. A recent study suggested that AR-V7 enters the nucleus as a monomer and subsequently homodimerizes to bind to DNA [196]. Since SC428 attenuated AR-V7 homodimerization, we wondered if SC428 also impaired AR-V7 nuclear trafficking. Confocal imaging was used to visualize the subcellular localization of GFP-AR-V7 in LNCaP-AR-V7 stable cells. The results showed that GFP-AR-V7 resided majorly within DAPI-stained nucleus in DMSO and ENZ-treated cells; however, significantly less DAPI co-localized AR-V7 was detected in SC428-treated cells (**Fig. 5C**), suggesting that SC428 impaired AR-V7 nuclear localization.

2.4.7. SC428 inhibits 22Rv1 xenograft growth *in vivo*

To assess the *in vivo* efficacy of SC428 against AR-V7 high-expressing tumors, we first examined SC428 in intact mice bearing 22Rv1 xenografts. 22Rv1 cells were subcutaneously injected into the right flank of male Nu/Nu mice. When tumor size reached 40-80 mm^3, mice received daily treatment with Vehicle, ENZ (60 mg/kg), or SC428 (60 mg/kg) intraperitoneally (IP) for 18 days. SC428 at 60 mg/kg notably slowed down tumor growth, whereas 60 mg/kg ENZ could not have any remarkable impact (**Fig. 6A**). There was no bodyweight decrease in SC428-treated mice relative to the vehicle, suggesting that SC428 was well tolerated (**Fig. 6B**). On conclusion of the experiment, SC428 at 60 mg/kg achieved approximately 50% inhibition of tumor growth when evaluated by tumor weight. In contrast, 60 mg/kg ENZ treatment yielded no significant difference (**Fig. 6C**). In addition, Western Blot analysis of tumor lysates showed that SC428, but not ENZ, reduced intratumoral PSA expression to undetectable levels, indicating that

SC428 could suppress AR signaling in 22Rv1 xenografts (**Fig. 6D**). Moreover, SC428-treated tumors also showed a higher level of cleaved-PARP, implying that SC428 induced tumor cell apoptosis *in vivo* (**Fig. 6D**).

Next, we evaluated SC428 against 22Rv1 xenograft in castrated mice to mimic the clinical CRPC setting. Male Nu/Nu mice were surgically castrated when the implanted 22Rv1 cells achieved an average tumor size of 200 mm^3, and animal health and tumor volume were closely monitored after surgery. When tumors attained an average volume of 270 mm^3, Vehicle or SC428 (90 mg/kg) was administrated daily *via* IP route 5 days a week for 3 weeks. SC428's inhibition of 22Rv1 tumor growth in castrated hosts became statistically significant on day 13 and remained so to the end of the experiment (day 21) (**Fig. 6E**). On day 21, 6/7 tumors in the Vehicle group increased greater than 100% by volume. In contrast, only 1/7 tumors in SC428 group enlarged more than 100%, while 1/7 tumors reached steady state and 2/7 tumors showed regression (**Fig. 6F**). On termination of the experiment, the average tumor weight for the SC428 group is approximately 30% of the Vehicle group (**Fig. 6G**). Furthermore, SC428 at 90 mg/kg was well-tolerated, as no obvious animal body weight loss was noted **(Fig. 6H)**. These findings showed that SC428 inhibited the growth of high AR-V7 expressing PCa xenograft under CRPC condition.

2.5. Discussion

In this work, we have demonstrated that SC428 directly binds to AR NTD and potently inhibited both AR-V7 and AR-FL activity. Importantly, SC428 had significant antiproliferative

effect against multiple ENZ-resistant cellular models, including 22Rv1, LNCaP-AR-V7 and LNCaP-AR^{F877L}. SC428 also showed antitumor activity against AR-V7 high-expressing tumors in intact mice as well as in castrated mice, demonstrating its therapeutic potential for men with CRPC that have suffered relapse from current AR targeting agents.

AR NTD being the only targeting domain of SC428 has been assessed from three complementary aspects in this study: *i*) Direct binding of SC428 to AR NTD was confirmed by surface plasmon resonance analysis; *ii*) SC428 gained inhibition on the IRF3 transciption factor when its transactivation domain was replaced by AR NTD; and *iii*) SC428 lost inhibition against AR-FL when its NTD was replaced by the transactivation domain of VP16 transcription factor. Additionally, among five steroid receptors (AR, GR, PR, MR and ER), AR NTD shares higher sequence similarity with that of GR and PR. Therefore, our observation of SC428 being inactive against GR and PR, indicates SC428 is selective towards AR NTD. However, the specific binding motif of SC428 within AR NTD remains unknow, and further work is underway to map down the precise amino acid segment that is essential for SC428 binding.

Unlike the AR LBD and DBD, which is folded protein with resolved crystal structure, AR NTD is considered “undruggable” because of its intrinsically disordered nature [213]. his poses a barrier against the use of virtual screening, which relies on the drug target's resolved 3D structure to identify hit compounds. Furthermore, intrinsically disordered protein uniquely forms poor affinity, high specificity protein-protein interaction, which limits the ability of small molecule inhibitor to simultaneously achieve both high potency and selectivity [214]. To date, EPI-001 derivatives is the only class of AR NTD inhibitors that has entered clinical trial [262]. EPI

compounds inhibit AR activity at higher μM range in cell-based experiments [215, 216]. In our study, the IC50 of SC428 in similar experiments, for instance, in the AR-Vs dependent reporter assay is around 1 μM (**Fig. 1C**), implying higher binding affinity of small molecule to AR NTD is feasible. However, the anti-proliferation IC50 of SC428 in AR-negative cells is only 6-fold higher compared to in AR-positive cells, indicating existence of off-target effect, and that further chemical modification is needed to improve specificity. EPI-001 was also found to hit non-specific target [263], highlighting the challenge of developing selective drugs towards the intrinsically disordered AR-NTD.

Dimerization is required for AR-V7 to transactivate target genes and to promote castration-resistant cell growth [261]. Recently, Cherkasov's group discovered compounds that disrupt AR-V7 dimerization by targeting the dimerization interface located in AR DBD [223]. Indeed, these inhibitors could reduce AR regulated gene transcription and suppressing PCa cell proliferation, therefore providing proof-of-concept for targeting AR-V7 dimerization. In this work, we observed that SC428 robustly reduced AR-V7 homodimers, suggesting that AR-V7 dimerization could be disrupted by targeting the AR NTD. However, Dong's group showed AR-V7 homodimerization only relys on DBD-DBD interaction [264]. One speculation is that SC428's binding to AR-V7 NTD yield a dead conformation for dimerization, though further investigation is required.

Intriguingly, SC428 induced modest degradation of AR-FL but did not affect AR-V7 protein level, hintting a discrepancy of AR-FL and AR-V7 protein stability mediated *via* AR NTD. This is consistent with known AR-FL selective degradation mechanisms, such as lysine 311

ubiquitination, which does not apply to AR-V7 [265]. Additionally, Kim and colleagues reported a PROTAC compound MTX-23 that binds to AR DBD and degraded AR-V7 at much higher rate than AR-FL[266]. These findings, together with ours, indicated that AR-V7 has distinct proteostasis comparing to AR-FL. However, SC428-induced AR-FL degradation is not the determing factor for its AR antagonism, as the treatment with SC428 only started to significantly degrade AR-FL after 20 h, whereas SC428 could already inhibit AR nuclear translocation and PSA expression as early as 4-5 h (**Fig. 3C**, Supplementary **Fig. S4A**)

In addition to suppressing AR-V7 mediated AR signaling, SC428 also showed potent efficacy for antagonizing AR-FL, suggesting that targeting AR NTD could be an a plausible approach for achieving pan-AR inhibition. This is appealing for clinical translation, as AR-V7 is found always co-overexpressed with AR-FL in patients [167, 168]. A recent study using specimens from heavily-treated CRPC patients uncovered that AR gene mutation hotspots were concentrated in LBD, and the most frequently detected mutants were W742C, H875Y, T878A and F877L [267], which are known to confer resistance to ADTs. In our previous work, we demonstrated that LBD-directed compounds could act as full antagonists for the LBD mutants [268-270]. Here, we showed these mutants could also be potently inhibited by AR NTD targeting compound, implying a potential benefit to CRPC patients habouring AR LBD mutations.

In summary, our findings indicate that SC428 is a promising AR-directed compound with potent activity against CRPC.

2.6. Figures

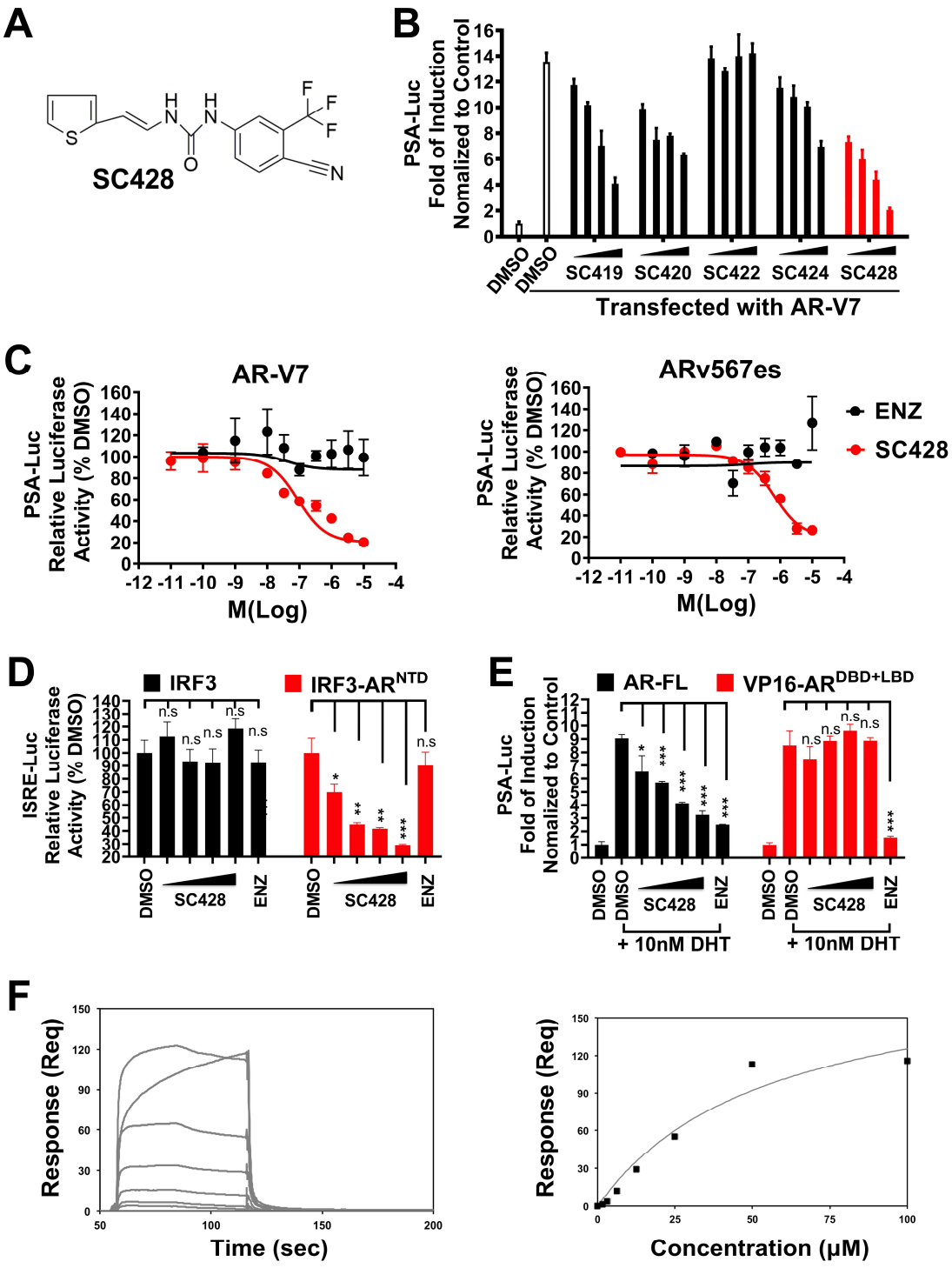
A
SC428
B
PSA-Luc
Fold of Induction
Nomalized to Control
DMSO
DMSO
SC419
SC420
SC422
SC424
SC428
Transfected with AR-V7
C
AR-V7
ARv567es
PSA-Luc
Relative Luciferase
Activity (% DMSO)
M(Log)
ENZ
SC428
D
IRF3
IRF3-AR^NTD
ISRE-Luc
Relative Luciferase
Activity (% DMSO)
n.s
DMSO
SC428
ENZ
E
AR-FL
VP16-AR^DBD+LBD
PSA-Luc
Fold of Induction
Nomalized to Control
+ 10nM DHT
F
Response (Req)
Time (sec)
Concentration (μM)

2.6.1. Figure M1-1. SC428 inhibits the transactivation of AR-V7, ARv567es and directly targets the AR N-terminal domain.

A. Chemical structure of SC428.

B. AR-V7 dependent PSA-Luc reporter assay. 293T cells were transiently transfected with PSA luciferase (PSA-Luc) reporter, pRL-TK (internal control), empty vector, or a plasmid expressing AR-V7. Cells were treated with DMSO, SC428, or its analogs at 0.5, 1, 2.5, 5 μM in androgen-deprived media for 48 h; Relative reporter activity was normalized to the empty vector control. Data represent the average ± SD of duplicate samples.

C. AR-V7 and ARv567es dependent PSA-Luc reporter assay. 293T cells were transiently transfected with PSA-Luc reporter, pRL-TK, and a plasmid expressing AR-V7 or ARv567es. Cells were treated with DMSO or SC428 at designated doses for 48 h. Relative luciferase activity was normalized to the DMSO. Data represent the average ± SD of duplicate samples.

D. IRF3 and IRF3-AR^{NTD} dependent ISRE-Luc reporter assays in PC3 cells. Cells were transiently transfected with ISRE-Luc, pRL-TK, and a plasmid expressing IRF3 or IRF3-AR^{NTD}. Cells were treated with the DMSO, 5 μM ENZ or 0.5, 1, 2.5, 5 μM SC428 in androgen-deprived media for 48 h. Data represent the average ± SD of duplicate samples.

E. AR-FL and VP16-$AR^{DBD+LBD}$ dependent PSA-Luc reporter assay in PC3 cells. Cells were transiently transfected with PSA-Luc, pRL-TK, and a plasmid expressing AR-FL or VP16-$AR^{DBD+LBD}$. Cells were pretreated with DMSO, ENZ at 5 μM, or 0.5, 1, 2.5, 5 μM SC428 for 30 min, followed by the addition of 10 nM DHT and incubation for another 48 h. Data represent the average ± SD of duplicate samples.

F. Surface plasmon resonance (SPR) analysis indicated the direct binding of SC428 with the AR-NTD. *Left panel*, representative label-free, real-time binding of compound SC428 to 10,000 RU amine-coupled AR-NTD protein (in PBS-T running buffer containing 5% DMSO), as assessed by SPR at 25 uL/min (with DMSO solvent correction). *Right panel*, representative isotherm (steady-state binding responses plotted as a function of compound concentration (*black squares*, corrected data) and then subjected to non-linear regression analysis (*grey line*, "steady-state" affinity model)) to determine the apparent equilibrium dissociation constant: K_D (AR-NTD + SC428) = 75 ±29 uM (n = 4).

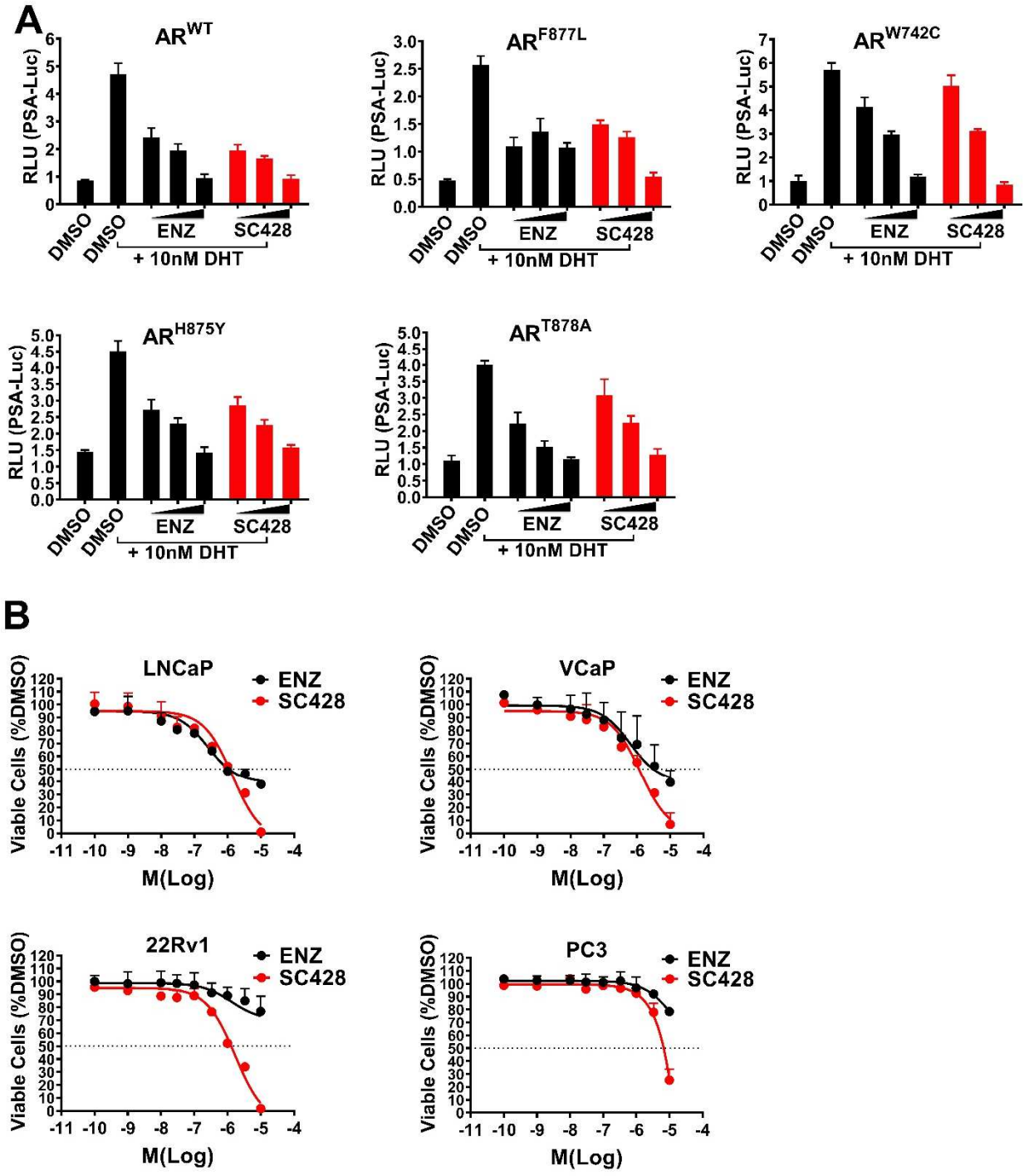
A
AR^WT
AR^F877L
AR^W742C
AR^H875Y
AR^T878A
RLU (PSA-Luc)
DMSO
DMSO
ENZ
SC428
+ 10nM DHT
B
LNCaP
VCaP
22Rv1
PC3
ENZ
SC428
Viable Cells (%DMSO)
M(Log)

2.6.2. Figure M1-2. SC428 antagonized the WT and clinically relevant mutants of AR-FL and showed antiproliferative activity towards AR-positive prostate cancer cells.

A. AR dependent PSA-Luc reporter assays in PC3 cells. PSA-Luc, pRL-TK, and plasmid expressing AR-FL WT, F877L, W742C, H875Y, or T878A were transiently transfected into PC3 cells. Cells cultured in androgen-deprived media were pretreated with DMSO, ENZ (at 1, 2.5, 5 μM), or SC428 (at 1, 2.5, 5 μM) for 30 min, followed by the addition of 10 nM DHT and incubation for another 24 h. RLU (relative luciferase unit) is calculated as PSA-Luc Firefly luciferase activity divided by pRL-TK *Renilla* luciferase activity. Data represent average ± SD of duplicate samples.

B. Cell proliferation assays to evaluate the effect of SC428 against LNCaP, VCaP, 22Rv1, and PC3 prostate cancer cells. Cells were seeded in androgen-deprived media, and 24 h later, were treated with DMSO, ENZ, or SC428 at designated doses in the presence of 0.1 nM DHT. Cell culture media and treatment were refreshed once on day 3, and viable cells were measured using the CellTiter-Glo 2.0 kit on day 6. Data represent average ± SD of three separate experiments.

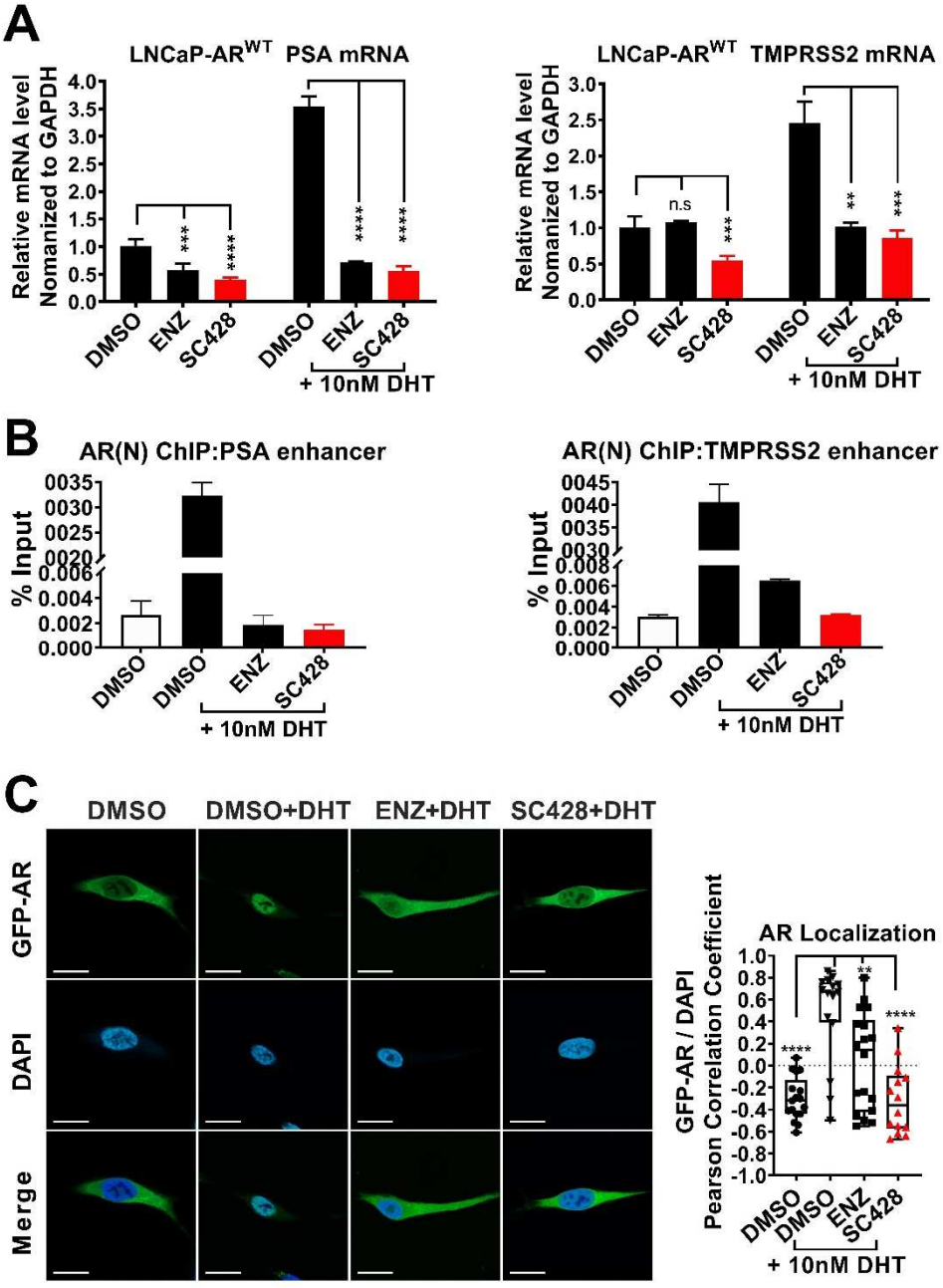
A
LNCaP-AR^WT PSA mRNA
Relative mRNA level Nomanized to GAPDH
DMSO
ENZ
SC428
+ 10nM DHT
LNCaP-AR^WT TMPRSS2 mRNA
n.s
B
AR(N) ChIP:PSA enhancer
% Input
AR(N) ChIP:TMPRSS2 enhancer
C
DMSO
DMSO+DHT
ENZ+DHT
SC428+DHT
GFP-AR
DAPI
Merge
AR Localization
GFP-AR / DAPI Pearson Correlation Coefficient

2.6.3. Figure M1-3. SC428 inhibited AR-FL transcriptional activity, attenuated AR-FL chromatin binding, and impaired its nuclear localization.

A. qRT-PCR analysis of the AR-regulated gene *PSA* and *TMPRSS2* in LNCaP-AR^{WT} cells. Cells were seeded in androgen-deprived media for 48h and subsequently were treated for an additional 24 h with DMSO, 10 μM ENZ, or 5 μM SC428 in the presence or absence of 10 nM DHT. Relative gene expression was normalized to GAPDH mRNA expression. Data represent average ± SD of three separate experiments.

B. CHIP assay of AR enrichment to AREs (*PSA* enhancer and *TMPRSS2* enhancer) in LNCaP-AR^{WT} cells, using anti-AR antibody. Cells were seeded in androgen-deprived media for 48 h and then pretreated for 30 min with DMSO, 10 μM ENZ, or 5 μM SC428, followed by the addition of 10 nM DHT and incubation for another 4.5 h. Data represent average ± SD of two separate experiments. (Beads only without antibody as the negative control).

C. Representative confocal image of GFP-tagged AR-FL in LNCaP-AR^{WT} cells (Scale bar represents 10 μm). LNCaP-AR^{WT} cells were treated as in (**B**). Pearson Correlation Coefficient between GFP and DAPI fluorescence intensity of individual cells were quantified (n=14−18) with Image J.

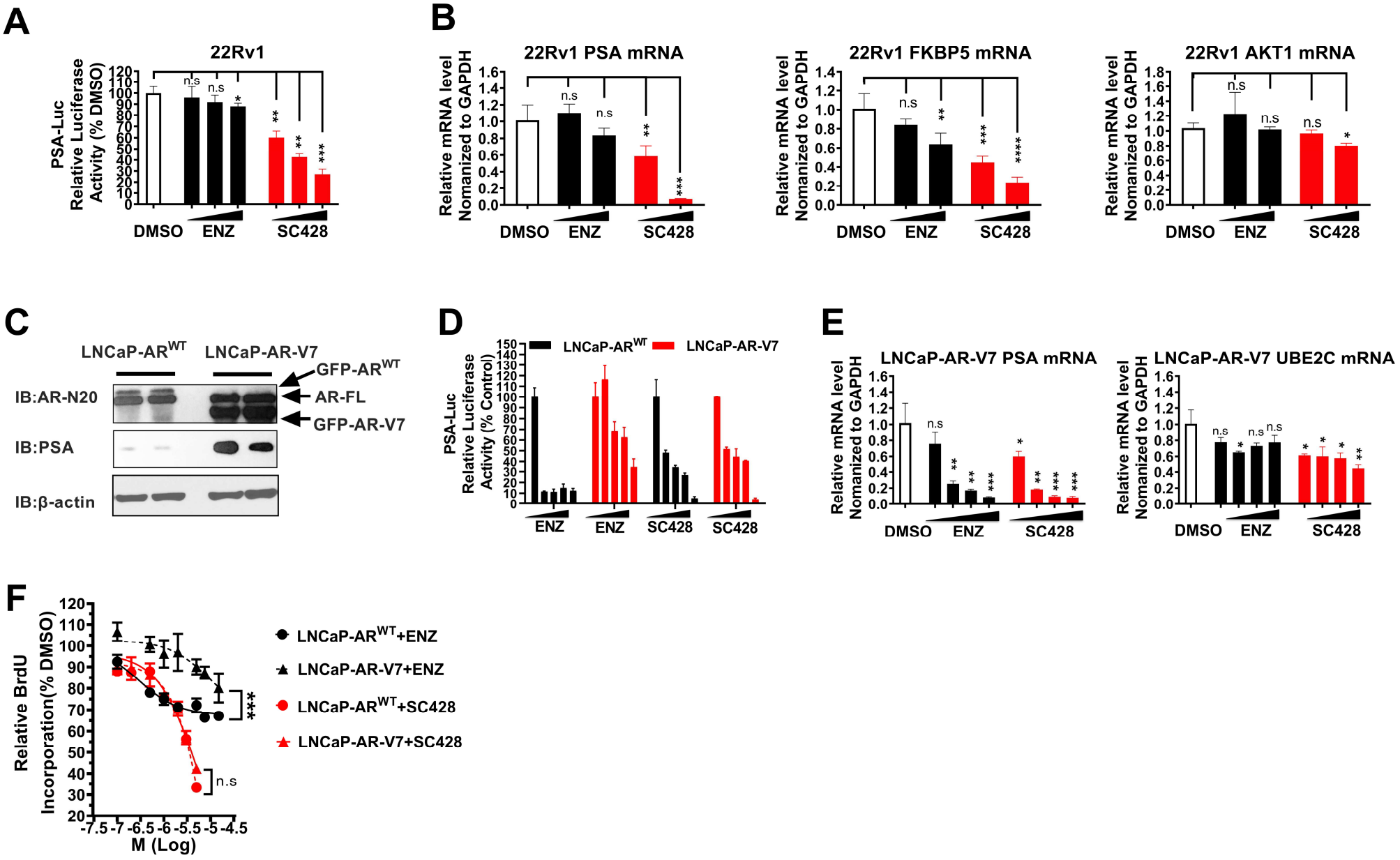
A
22Rv1
PSA-Luc Relative Luciferase Activity (% DMSO)
DMSO
ENZ
SC428
B
22Rv1 PSA mRNA
22Rv1 FKBP5 mRNA
22Rv1 AKT1 mRNA
Relative mRNA level Nomalized to GAPDH
C
LNCaP-AR^WT
LNCaP-AR-V7
GFP-AR^WT
AR-FL
GFP-AR-V7
IB:AR-N20
IB:PSA
IB:β-actin
D
PSA-Luc Relative Luciferase Activity (% Control)
E
LNCaP-AR-V7 PSA mRNA
LNCaP-AR-V7 UBE2C mRNA
F
Relative BrdU Incorporation(% DMSO)
M (Log)
LNCaP-AR^WT+ENZ
LNCaP-AR-V7+ENZ
LNCaP-AR^WT+SC428
LNCaP-AR-V7+SC428

2.6.1. Figure M1-4. SC428 suppressed the AR signaling in AR-V7 high-expressing PCa cells and suppressed their ENZ-resistant proliferation.

A. PSA-Luc reporter assay for AR-Vs-dependent AR singling activity in 22Rv1 cells. Cells were seeded in androgen-deprived medium for 48 hours before PSA-Luc and pRL-TK were transiently transfected into cells. 5 h after transfection, cells in the fresh androgen-deprived medium were treated with DMSO, ENZ (2.5, 5, 10 μM), or SC428 (1, 2.5, 5 μM) for 24 h. Bars represent the average of duplicate samples ± SD.

B. qRT-PCR analysis of AR-V7 regulated gene *PSA*, *FKBP5,* and *AKT1* expression in 22Rv1 cells. Cells were cultured in androgen-deprived medium for 48h and were treated with DMSO, ENZ (5, 10 μM), or SC428 (2.5, 5 μM) for another 24 h, in the absence of androgen. Bars represent the average of three separate experiments ± SD.

C. Western blot for AR and PSA protein expression in LNCaP-AR^{WT} and LNCaP-AR-V7 cells. Cells were cultured in androgen-deprived medium for 48 h before harvest. Duplicates represent different passages.

D. PSA-Luc reporter assay in LNCaP-AR^{WT} and LNCaP-AR-V7 cells. Cells were cultured in androgen-deprived medium for 48 h and were then transiently transfected with PSA-Luc and pRL-TK plasmids. 5 h after transfection, cells in the refreshed androgen-deprived medium were treated with DMSO, ENZ, or SC428 at 0.5, 1, 2.5, and 5 μM for another 24 h. Relative luciferase activity was normalized to DMSO vehicle control. Bars represent the average of duplicate samples ± SD.

E. qRT-PCR analysis of AR regulated gene *PSA* and AR-V7 regulated gene *UBE2C* expression in LNCaP-AR-V7 cells. Cells were cultured in androgen-deprived medium for 48h and were treated with DMSO, ENZ (0.5, 1, 2.5, 5 μM), or SC428 (0.5, 1, 2.5, 5 μM) for another 24 h, in the absence of androgen. Bars represent the average of three separate experiments ± SD.

F. BrdU assay to assess active proliferation in LNCaP-AR-V7 and LNCaP-AR^{WT} cells. Cells were cultured in androgen-deprived medium for 24 h and then treated with DMSO vehicle, ENZ, or SC428 at designated doses for another 30 h. Data represent average ± SD of triplicate samples. Paired, two-tailed t test, with pairing of data points of the same concentration for the two cell lines LNCaP-AR-V7 and LNCaP-AR^{WT}.

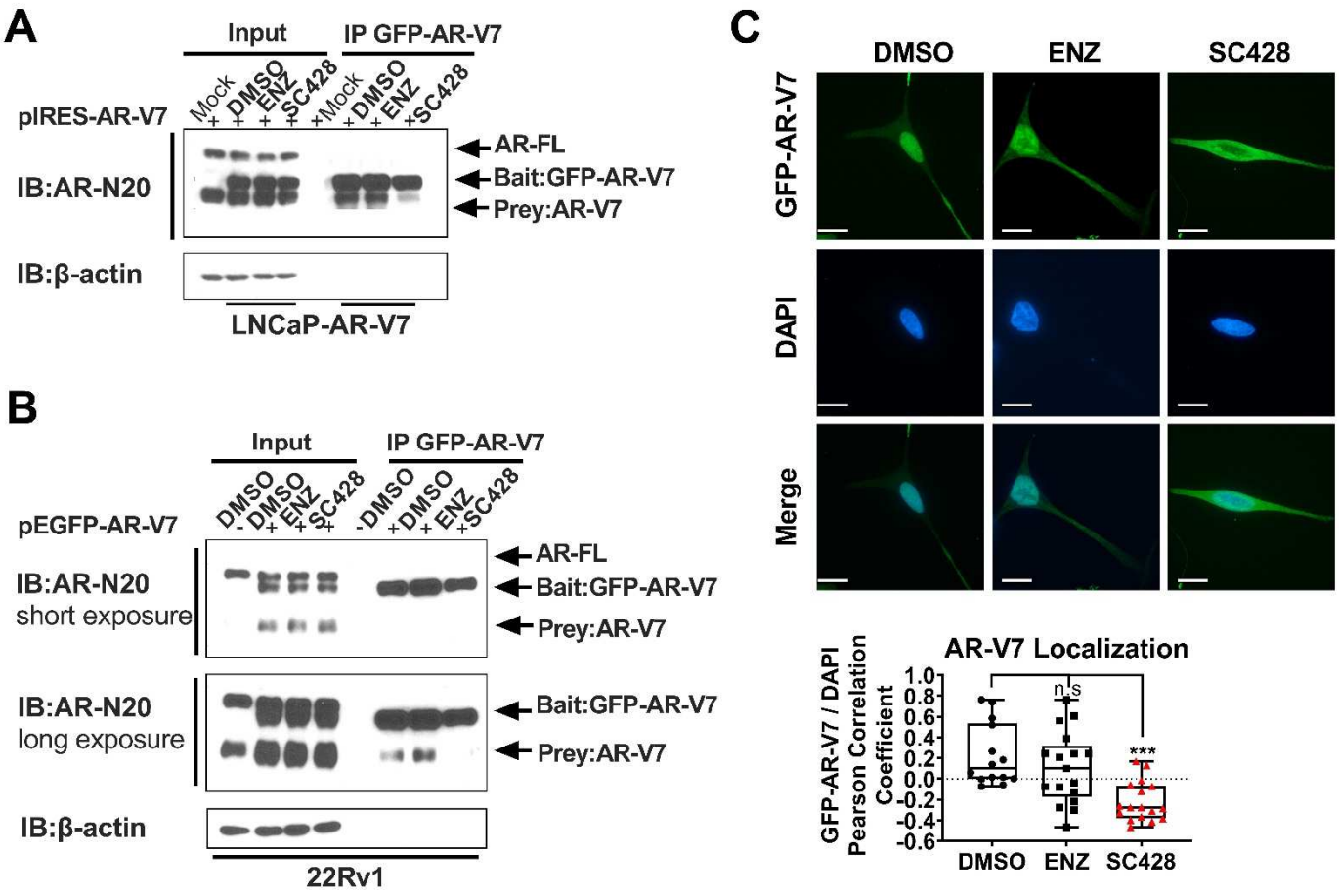
A
Input
IP GFP-AR-V7
Mock
DMSO
ENZ
SC428
Mock
DMSO
ENZ
SC428
pIRES-AR-V7
IB:AR-N20
AR-FL
Bait:GFP-AR-V7
Prey:AR-V7
IB:β-actin
LNCaP-AR-V7
B
Input
IP GFP-AR-V7
DMSO
DMSO
ENZ
SC428
DMSO
DMSO
ENZ
SC428
pEGFP-AR-V7
IB:AR-N20
short exposure
AR-FL
Bait:GFP-AR-V7
Prey:AR-V7
IB:AR-N20
long exposure
Bait:GFP-AR-V7
Prey:AR-V7
IB:β-actin
22Rv1
C
DMSO
ENZ
SC428
GFP-AR-V7
DAPI
Merge
AR-V7 Localization
GFP-AR-V7 / DAPI
Pearson Correlation
Coefficient
1.0
0.8
0.6
0.4
0.2
0.0
-0.2
-0.4
-0.6
n.s
***
DMSO
ENZ
SC428

2.6.2. Figure M1-5. SC428 disrupted AR-V7 homodimerization and nuclear localization.

A. Immunoprecipitation (IP) assay to detect AR-V7 homodimerization in LNCaP-AR-V7 cells. LNCaP-AR-V7 cell line was engineered to express GFP tagged AR-V7 stably. Cells were cultured in androgen-deprived media for 24 h and were subsequently transfected with pIRES-AR-V7 plasmid for 5 h. Cells were allowed to recover in fresh androgen-deprived media overnight, followed by 5 h treatment with DMSO, 10 μM ENZ, or 5 μM SC428. IP of GFP-tagged proteins using GFP-Trap was performed with the cell lysates, and precipitates were assessed by western blot using AR-N20 antibody. LNCaP cells stably transfected with pEGFP-c1 empty vector served as the mock control.

B. IP assay to detect AR-V7 homodimerization in 22Rv1 cells. Cells were cultured in androgen-deprived media for 48 h and were transfected with pEGFP-c1-AR-V7 plasmid for 5 h. The subsequent procedure and treatment are the same as (**D**). 22Rv1 cells transiently transfected with pEGFP-c1 empty vector served as the mock control.

C. Representative confocal image of GFP-tagged AR-V7 in LNCaP-AR-V7 cells (Scale bar represents 10 μm). LNCaP-AR-V7 cells were seeded in androgen-deprived media 48 h before 5 h treatment with DMSO, 10 μM ENZ, or 5 μM SC428. Pearson Correlation Coefficient between GFP and DAPI fluorescence intensity of individual cells were quantified (n=14−18) with Image J.

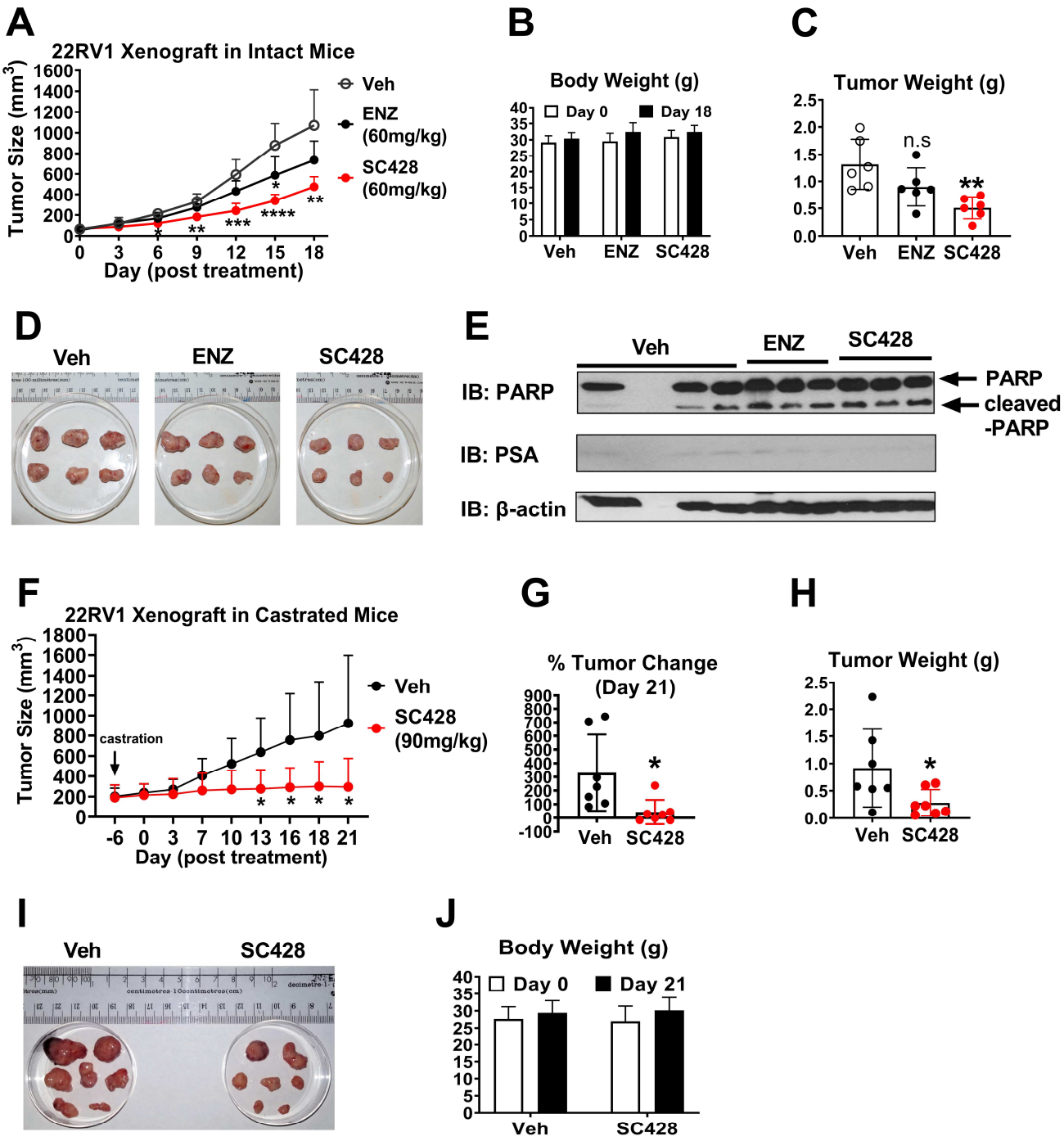
A
22RV1 Xenograft in Intact Mice
Tumor Size (mm3)
Day (post treatment)
Veh
ENZ (60mg/kg)
SC428 (60mg/kg)
B
Body Weight (g)
Day 0
Day 18
Veh
ENZ
SC428
C
Tumor Weight (g)
n.s
Veh
ENZ
SC428
D
Veh
ENZ
SC428
E
Veh
ENZ
SC428
IB: PARP
PARP
cleaved -PARP
IB: PSA
IB: β-actin
F
22RV1 Xenograft in Castrated Mice
Tumor Size (mm3)
castration
Day (post treatment)
Veh
SC428 (90mg/kg)
G
% Tumor Change (Day 21)
Veh
SC428
H
Tumor Weight (g)
Veh
SC428
I
Veh
SC428
J
Body Weight (g)
Day 0
Day 21
Veh
SC428

2.6.3. Figure M1-6. SC428 inhibits 22Rv1 xenograft growth *in vivo.*

A-E. SC428 inhibited the growth of 22Rv1 Xenograft in intact mice. 2×10^6 22Rv1 cells mixed with 50% matrigel were subcutaneously injected into the right flank of male Nu/Nu mice. When tumors reached 40–80 mm^3 in size, mice were randomized into 3 groups (n=6), which received daily IP treatment of Vehicle, 60 mg/kg ENZ, or 60 mg/kg SC428 for 18 days (first dose on day 0). Tumor size (**A**) and animal body weight (**B**) were measured every 3 days; tumor weights (**C**) were recorded, and tumor images (**D**) were taken at sacrifice. 3 out of the 6 tumors from each group were randomly picked for analysis of intratumoral PSA and cleaved-PARP by WB assay. (**E**). Unpaired, two-tailed t-test or tumor weight: p=0.0077 for vehicle-treated group versus SC428treated group, p=0.1107 for vehicle-treated group versus ENZ-treated group.

F-J. SC428 inhibited the growth of 22RV1 Xenograft in castrated mice. 5×10^6 22Rv1 cells mixed with 50% matrigel were subcutaneously injected into the right flank of male Nu/Nu mice. When tumor size reached 100–300 mm^3, mice were surgically castrated and monitored daily. After tumor resumed growing and reached the size of 150–400 mm^3 (7 days after castration), mice were randomized into 2 groups (n=7), which received 5 days per week treatment (IP) of Vehicle or SC428 (90 mg/kg) for 3 weeks. Tumor size (**F**) was measured every 3 days; % Tumor Change= (day 21 volume - day 0 volume) / day 0 volume % (**G**). At sacrifice, tumor weight (**H**) and animal body weight (**J**) were recorded, and tumor images (**I**) were taken. Unpaired, two-tailed t-test for tumor weight p=0.0451.

2.7.Supplementary information

2.7.1. Supplementary methods

1. Synthesis and characterization of SC428 and its analogues

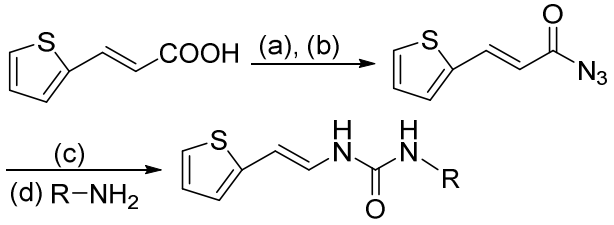

Synthesis of the SC428 and its analogues. (a) $ClCO_2Et$, Et_3N, Acetone, 0°C, 1 h; (b) NaN_3, H_2O, 0°C, 5 h; (c) Toluene, reflux, 3 h; (d) Toluene, 90°C, overnight. SC428 and its derivatives were synthesized by the following general procedure:

i) Synthesis of azide compounds.
To a mixture of acid (5 mmol, 1.08 g) and triethylamine (5.5 mmol, 0.76 mL) in dry acetone, ethyl chlorocarbamate (5.5 mmol, 0.54 mL) was added at 0℃ and the mixture was stirred at 0 ℃ for 1 h. Next, sodium azide (5.5 mmol, 0.36 g) dissolved in 7.5 mL of water was added and the mixture was stirred at 0℃ for 7 h. After the reaction was completed, the mixture was poured onto ice and the precipitated product was collected by filtration to give azide compounds.

ii) A solution of azide compound (0.5 mmol, 0.12 g) in 3 mL toluene was refluxed at 120°C for 4 h to give isocyanate compound, which didn't need further purification. After toluene was distilled off under reduced pressure, 4 mL dichloromethane and amine compound (R-NH2) (0.5 mmol) were added. To prepare SC428 or compound **19**, the mixture was stirred at 90 ℃ for 12 h and at room temperature for 1 h. To prepare compounds **20**, **22,** and **24**, the mixture was stirred at room temperature for 12 h. After the reaction was completed, 2 mL hexane was added and stirred at room temperature for 1 h. The product was filtered when the product precipitated from the reaction mixture. The product was dried under reduced pressure.

SC428: White solid, m.p. 199-201°C, yield: 45.7%. ^{1}H NMR (500 MHz, acetone-d_6) δ 9.01 (br, 1H), 8.52 (br. d, J = 10.0 Hz, 1H), 8.28 (d, J = 2.0 Hz, 1H), 7.98 – 7.92 (m, 2H), 7.34 (dd, J_1 = 14.5 Hz, J_2 = 14.5 Hz, 1H), 7.22 (d, J = 5.0 Hz, 1H), 6.97 (dd, J_1 = 5.0 Hz, J_2 = 5.0 Hz, 1H), 6.93 (d, J = 3.5 Hz, 1H), 6.38 (d, J = 14.5 Hz, 1H). LHMS-ESI, m/z $[M+H]^+$ 338.06.

SC419: White solid, m.p. 189-190°C, yield: 19.0 %. ^{1}H NMR (500 MHz, acetone-d_6) δ 9.12 (br, 1H), 8.58 (br. d, J = 10.0 Hz, 1H), 8.28 (d, J = 2.0 Hz, 1H), 8.14 (d, J = 9.0 Hz, 1H), 8.00 (dd, J_1 = 2.0 Hz, J_2 = 2.0 Hz, 1H), 7.35 (dd, J_1 = 14.5.0 Hz, J_2 = 14.5 Hz, 1H), 7.22 (d, J = 5.0 Hz, 1H), 6.98 (dd, J_1 = 5.0 Hz, J_2 = 5.0 Hz, 1H), 6.93 (d, J = 3.5 Hz, 1H), 6.39 (d, J = 14.0 Hz, 1H). LHMS-ESI, m/z $[M+H]^+$ 358.05.

SC420**:** White solid, m.p. 172-174°C, yield: 74.3 %. ^{1}H NMR (500 MHz, acetone-d_6) δ 8.58 (br, 1H), 8.36 (br. d, J = 10.0 Hz, 1H), 8.09 (s, 1H), 7.71 (dd, J_1 = 1.5 Hz, J_2 = 2.0 Hz, 1H), 7.53 (t, J = 8.0 Hz, 1H), 7.41 – 7.34 (m, 2H), 7.19 (d, J = 5.0 Hz, 1H), 6.96 (dd, J_1 = 5.0 Hz, J_2 = 5.0 Hz,

1H), 6.89 (d, J = 3.5 Hz, 1H), 6.32 (d, J = 14.5 Hz, 1H).

SC422: White solid, m.p. 171- 173℃, yield: 82.0%. ^{1}H NMR (500MHz, acetone-d_6): δ 8.19 (br, 2H), 7.56- 7.54 (m, 2H), 7.38 (dd, J_1 = 14.5 Hz, J_2 = 14.5 Hz, 1H), 7.32- 7.28 (m, 2H), 7.17 (d, J = 5.5 Hz, 1H), 7.03- 7.00 (m, 1H), 6.95 (dd, J_1 = 5.5 Hz, J_2 = 5.5 Hz, 1H), 6.87 (d, J = 3.5 Hz, 1H), 6.27 (d, J = 14.5 Hz, 1H).

SC424**:** White solid, mp. 183-185ºC, yield: 73.3 %. ^{1}H NMR (500 MHz, acetone-d_6) δ 8.68 (br, 1H), 8.36 (br. d, J = 10.0 Hz, 1H), 7.77 – 7.75 (m, 2H), 7.69 (d, J = 9.0 Hz,2H), 7.36 (dd, J_1 = 14.5 Hz, J_2 = 14.5 Hz, 1H), 7.20 (d, J = 5.0 Hz, 1H), 6.97- 6.95 (m, 1H), 6.90 (d, J = 3.5 Hz, 1H), 6.34 (d, J = 14.5 Hz, 1H). LHMS-ESI, m/z $[M+H]^+$ 270.07.

2. Plasmid Construction

To generate pEGFPc1-IRF3(DBD)-AR (1−547) (referred to in the text as IRF3-AR^{NTD}), AR cDNAs were amplified by PCR from pCMV-AR plasmid with Vent polymerase using the primer pair: 5'-ATG GAA GTG CAG TAA GGG C-3' and 5'-GAC GAA TTC TCA AAC ATG GTC CCT GGC AGT C-3' for AR amino acid 1−547. PCR products were purified and digested with *EcoRI* and cloned into *EcoRI* and *Scal* sites of pEGFPc1-IRF3(DBD) to replace the C-terminal region of IRF3. The pCMV-VP16/AR540-920 plasmid (referred to in the text as VP16-AR$^{DBD+LBD}$) was constructed using the pCMV-VP16/AR507-920 as template for a two-pairs of primers PCR reaction. Restriction sites *SacII* and *Xhol* were introduced to 5' and 3' ends respectively *via* primers of VP16-AR*SacII* forward: 5'-TCC CCG CGG CCA CCA TGG CCC CCC CGA CCG TAG TC-3' and VP16-AR*Xhol* reverse: 5'-CCG CTC GAG CTG GGT GTG GAA ATA GAT-3'. The AR507-540 deletion was introduced by using primers in AR540 conjunction, AR540 forward:5'-CGA CGC GGA TCC TTG GAG ACT GCC AGG GAC CAT G-3' and reverse: 5'-GGC AGT CTC CAA GAA TCC GCG TCG ACT GAT CCC C-3'. The PCR product of VP16-540-920 was then cloned into the pCMV vector. The pEGFPc1-F877L plasmid was constructed by introducing point mutation to the pEGFPc1-AR plasmid (Addgene #28235) using Stratagene's QuikChangeTM Site-Directed Mutagenesis Kit, and DNA sequencing was performed to confirm the mutation. The pCMV-AR-F877L plasmid was generated by subcloning from pEGFPc1-F877L.

3. Chromatin immunoprecipitation assay (ChIP assay)

1×10^6 LNCaP-AR^{WT} cells were seeded in 6 cm dish and cultured in androgen-depleted media for 48 h and then exposed to compounds for an additional 5 h. Cells were cross-linked by the addition of 450 ul of 37% formaldehyde solution into 15 mL media for 8 minutes, and then neutralized by adding 2 mL of 1 M glycine solution for 5 minutes. Subsequent experiments were done using M-Fast Chromatin Immunoprecipitation Kit (ZmTech Scientifique) according to the manufacturer's protocol, with ChIP grade androgen receptor antibody (abcam). Quantification of precipitated DNA was performed by qRT-PCR with the following primers: *PSA* enhancer forward 5'-ATG TTC ACA TTA GTA CAC CTT GCC-3', reverse 5'-TCT CAG ATC CAG GCT TGC TTA CTG TC-3'; *TMPRSS2* enhancer forward 5'- TGG TCC TGG ATG ATA AAA AAA GTT T-3', reverse 5'- GAC ATA CGC CCC ACA ACA GA-3'.

4. Surface plasmon resonance (SPR) analysis

SPR experiments were carried out in Biacore™ T200 system (McGill SPR facility). Recombinant protein of human AR-NTD (Glu2-Gln556) (LS-G26987, LSBio, WA, USA) was immobilized

onto a CM5 chip by amine-coupling. The running buffer is PBS-T, pH 7.4, containing 5% (v/v) DMSO. Titrate SC428 is in two-fold serial dilution (0-100 μM).

5. Primer sequences

The primers used for qRT-PCR assays are: *PSA* forward 5'-GTG CTT GTG GCC TCT CG-3', reverse 5'-AGC AAG ATC ACG CTT TTG TTC-3'; *TMPRSS2* forward 5'- CGC TGG CCT ACT CTG GAA-3', reverse 5'- CTG AGG AGT CGC ACT CTA TCC-3'; *FKBP5* forward 5'-GGA TAT ACG CCA ACA TGT TCA A-3', reverse 5'- CCA TTG CTT TAT TGG CCT CT-3'.

2.7.2. Supplementary figures

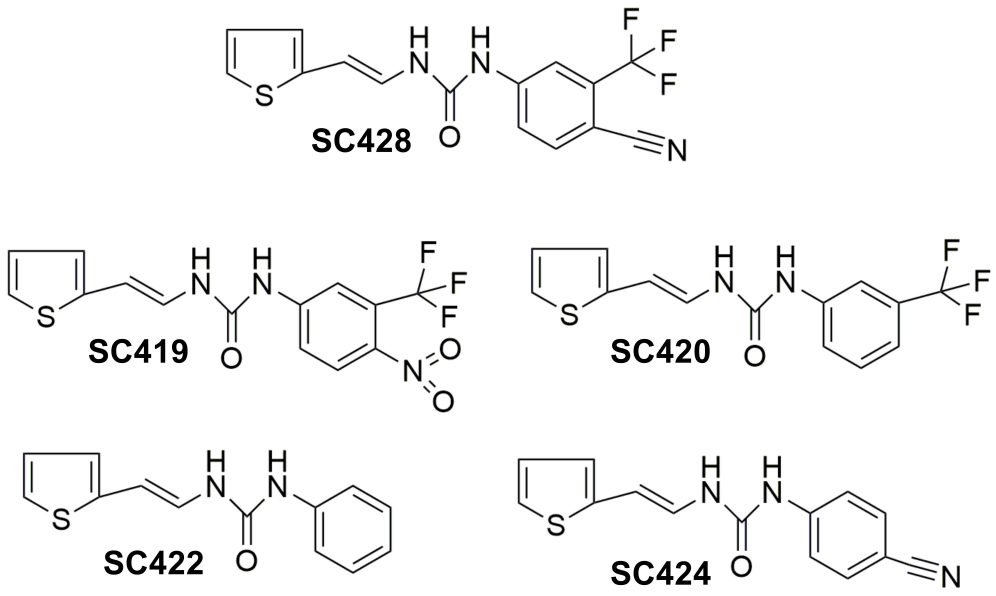

2.7.2.1. Figure M1-S1. Chemical structures of SC428 and its analogs.

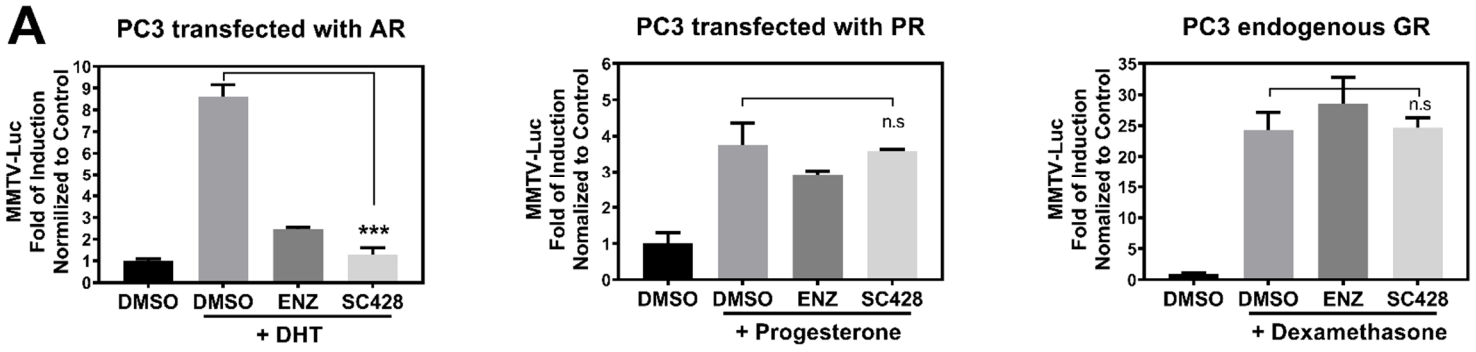

2.7.2.2. Figure -S2. SC428 potently inhibits the transactivation of AR but is inactive against PR and GR.

A. Cells were seeded in regular media, and 24 h later, cells were transiently transfected with MMTV-Luc, pRL-TK, and plasmid expressing AR or PR, or endogenous GR, as indicated. 5 h after transfection, cells in refreshed androgen-deprived media were treated with DMSO, 5 μM ENZ or 2.5 μM SC428 for 30 min, followed by addition of 10 nM DHT, 10 nM Progesterone, or 10 nM Dexamethasone and incubated M1for another 24 hour. Data represent mean ± SD of triplicate samples.

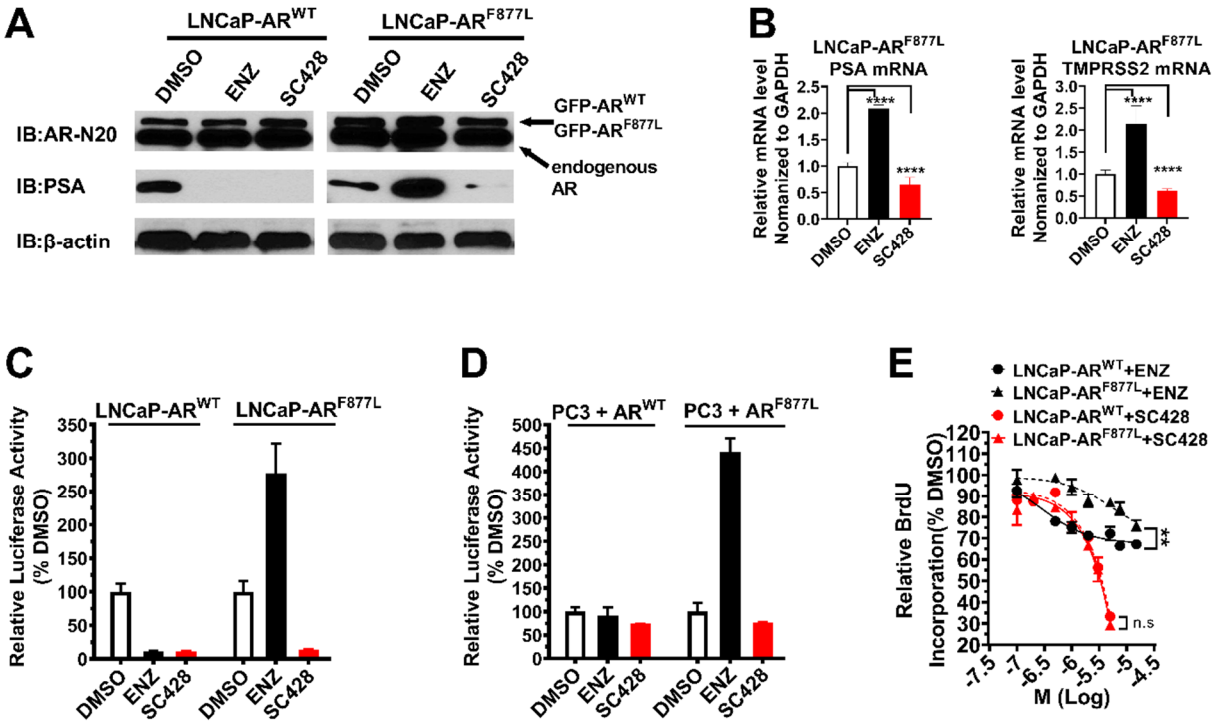
A
LNCaP-AR^WT
LNCaP-AR^F877L
DMSO
ENZ
SC428
DMSO
ENZ
SC428
IB:AR-N20
IB:PSA
IB:β-actin
GFP-AR^WT
GFP-AR^F877L
endogenous AR
B
LNCaP-AR^F877L PSA mRNA
Relative mRNA level Nomanized to GAPDH
LNCaP-AR^F877L TMPRSS2 mRNA
Relative mRNA level Nomanized to GAPDH
****
DMSO
ENZ
SC428
C
LNCaP-AR^WT
LNCaP-AR^F877L
Relative Luciferase Activity (% DMSO)
DMSO
ENZ
SC428
D
PC3 + AR^WT
PC3 + AR^F877L
Relative Luciferase Activity (% DMSO)
E
LNCaP-AR^WT+ENZ
LNCaP-AR^F877L+ENZ
LNCaP-AR^WT+SC428
LNCaP-AR^F877L+SC428
Relative BrdU Incorporation(% DMSO)
**
n.s
M (Log)

2.7.2.3. Figure M1-S3. SC428 exhibits full antagonist activity against the AR F877L mutant.

A. Western blot for AR and PSA protein expression in LNCaP-AR^{WT} and LNCaP-AR^{F877L} cells. Cells were cultured in androgen-deprived media for 48 h and were subsequently exposed to DMSO vehicle, 10 μM ENZ or 5 μM SC428 for an additional 16 h, in the absence of androgen.

B. qRT-PCR analysis of AR-regulated gene *PSA* and *TMPRSS2* in LNCaP-AR^{F877L} cells. Cells were seeded in androgen-deprived media, and 48 h later, cells were treated for 24 h with DMSO, 10 μM ENZ, or 5 μM SC428, in the absence of androgen. Relative gene expression was normalized to GAPDH mRNA level. Data represent mean ± SD of triplicate samples.

C. PSA-Luc reporter assays in LNCaP-AR^{WT} and LNCaP-AR^{F877L} cells. Cells were seeded in androgen-deprived media, and 48 h later, PSA-Luc and pRL-TK plasmids were transiently transfected into cells. Cells in refreshed androgen-deprived media were then treated with DMSO, 10 μM ENZ, or 5 μM SC428 for 24 h. Data represent mean ± SD of triplicate samples.

D. AR dependent PSA-Luc reporter assays in PC3 cells. Cells were seeded in androgen-deprived media, and 24 h later, PSA-Luc, pRL-TK, and a plasmid expressing the WT or F877L mutant of AR-FL were transiently transfected into cells. 5 h after transfection, cells in refreshed androgen-deprived media were exposed to DMSO, 10 μM ENZ, or 5 μM SC428 for an additional 24 h. Data represent mean ± SD of triplicate samples.

E. BrdU assay to assess active proliferation in LNCaP-AR^{WT} and LNCaP-AR^{F877L} cells. Cells were seeded in androgen-deprived media, and 24 h later, cells were treated with DMSO, ENZ, or SC428 at designated doses for another 30 h. Data represent mean ± SD of triplicate samples.

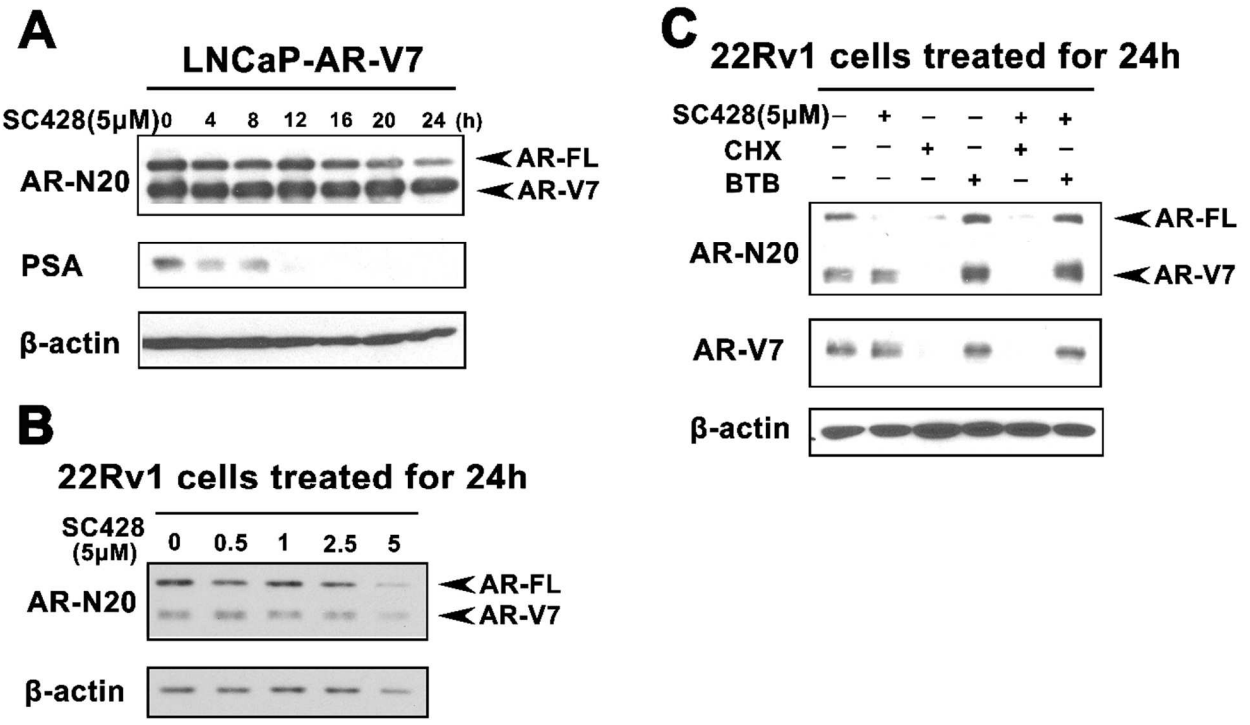

2.7.2.4. Figure M1-S4. SC428 induces modest degradation of AR-FL, but not AR-V7.

A-C. Western blot analysis to assess effects of SC428 on AR-V7 and AR-FL protein in LNCaP-AR-V7 and 22Rv1 cells. LNCaP-AR-V7 or 22Rv1 Cells were cultured in androgen-deprived media for 48 h and were treated with 5 μM SC428 for the indicated time points (**A**)**,** or with SC428 at designated doses for 24 h (**B**), or 5 μM SC428, 50 μM CHX, 100 μM BTB alone or 5 μM SC248 in the combination of with 50 μM CHX or 100 μM BTB for 24 h (**C**). CHX, Cycloheximide; BTB, Bortezomib.

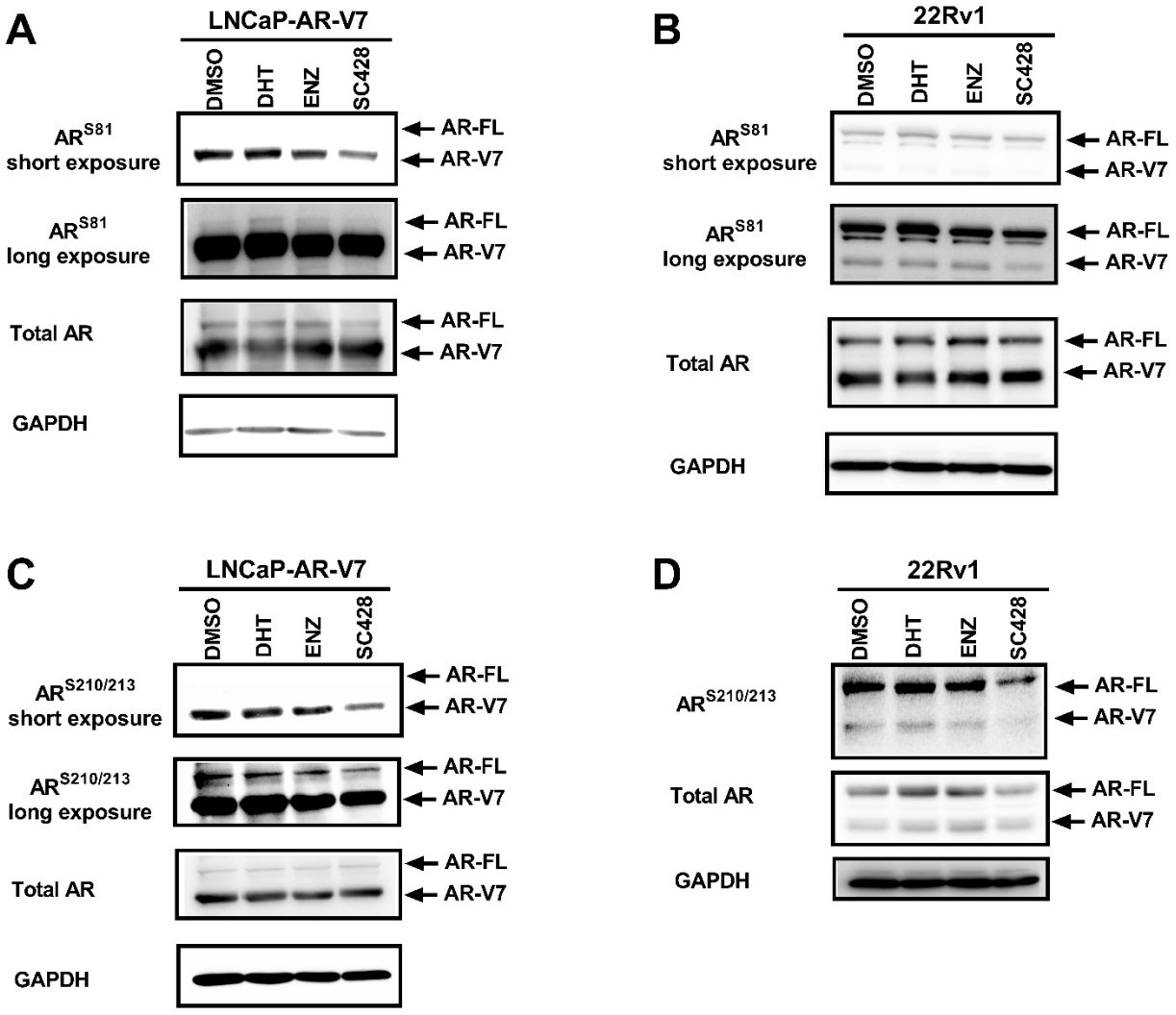

2.7.2.5. Figure M1-S5. SC428 hampered the phosphorylation of S81 and S210/213 located in AR-NTD.

A-D. Western blot analysis to evaluate the impact of SC428 on AR-NTD phosphorylation in LNCaP-AR-V7 and 22Rv1 cells. LNCaP-AR-V7 or 22Rv1 cells were cultured in androgen-deprived media for 48 h and were treated with DMSO, 10 nM DHT, 10 μM ENZ, or 5 μM SC428 for 5 h before being harvested: (**A**), S81 phosphorylated AR-FL and AR-V7 in LNCaP-AR-V7 cells. (**B**), S81 phosphorylated AR-FL and AR-V7 in 22Rv1 cells (**C**), S210/213 phosphorylated AR-FL and AR-V7 in LNCaP-AR-V7 cells. (**D**), S210/213 phosphorylated AR-FL and AR-V7 in 22Rv1 cells.

Estimated IC50 (μM)		
Cell Line	**ENZ IC50**	**SC428 IC50**
LNCaP	0.90	1.39
VCaP	3.41	1.01
22Rv1	> 10	1.13
PC3	> 10	6.49

2.7.2.6. Table M1-S1. Estimated IC50 of ENZ and SC428 for cell proliferation.

2.8.Manuscript 1 References

Sung H, Ferlay J, Siegel RL, Laversanne M, Soerjomataram I, Jemal A *et al*. Global cancer statistics 2020: GLOBOCAN estimates of incidence and mortality worldwide for 36 cancers in 185 countries2021; 71: 209-249.

2 Siegel RL, Miller KD, Fuchs HE, Jemal A. Cancer statistics, 2022. *CA: A Cancer Journal for Clinicians* 2022; 72: 7-33.

3 Cornford P, van den Bergh RC, Briers E, Van den Broeck T, Cumberbatch MG, De Santis M *et al*. EAU-EANM-ESTRO-ESUR-SIOG guidelines on prostate cancer. Part II—2020 update: treatment of relapsing and metastatic prostate cancer. *European urology* 2021; 79: 263-282.

4 Labriola MK, Atiq S, Hirshman N, Bitting RL. Management of men with metastatic castration-resistant prostate cancer following potent androgen receptor inhibition: A review of novel investigational therapies. *Prostate Cancer and Prostatic Diseases* 2021; 24: 301-309.

5 De Bono JS, Logothetis CJ, Molina A, Fizazi K, North S, Chu L *et al*. Abiraterone and increased survival in metastatic prostate cancer. *New England Journal of Medicine* 2011; 364: 1995-2005.

6 Scher HI, Fizazi K, Saad F, Taplin M-E, Sternberg CN, Miller K *et al*. Increased survival with enzalutamide in prostate cancer after chemotherapy. *New England Journal of Medicine* 2012; 367: 1187-1197.

7 Attard G, Borre M, Gurney H, Loriot Y, Andresen-Daniil C, Kalleda R *et al*. Abiraterone alone or in combination with enzalutamide in metastatic castration-resistant prostate cancer with rising prostate-specific antigen during enzalutamide treatment. *Journal of Clinical Oncology* 2018; 36: 2639.

8 de Wit R, de Bono J, Sternberg CN, Fizazi K, Tombal B, Wülfing C *et al*. Cabazitaxel versus abiraterone or enzalutamide in metastatic prostate cancer. *New England Journal of Medicine* 2019; 381: 2506-2518.

9 Hu R, Dunn TA, Wei S, Isharwal S, Veltri RW, Humphreys E *et al*. Ligand-independent androgen receptor variants derived from splicing of cryptic exons signify hormone-refractory prostate cancer. *Cancer research* 2009; 69: 16-22.

10 Guo Z, Yang X, Sun F, Jiang R, Linn DE, Chen H *et al*. A novel androgen receptor splice variant is up-regulated during prostate cancer progression and promotes androgen depletion–resistant growth. *Cancer research* 2009; 69: 2305-2313.

11 Sharp A, Coleman I, Yuan W, Sprenger C, Dolling D, Rodrigues DN *et al*. Androgen receptor splice variant-7 expression emerges with castration resistance in prostate cancer. *The Journal of clinical investigation* 2019; 129: 192-208.

12 Scher HI, Graf RP, Schreiber NA, McLaughlin B, Lu D, Louw J *et al*. Nuclear-specific AR-V7 protein localization is necessary to guide treatment selection in metastatic castration-resistant prostate cancer. *European urology* 2017; 71: 874-882.

13 Antonarakis ES, Lu C, Wang H, Luber B, Nakazawa M, Roeser JC *et al*. AR-V7 and resistance to enzalutamide and abiraterone in prostate cancer. *New England Journal of Medicine* 2014; 371: 1028-1038.

14 Li Y, Yang R, Henzler CM, Ho Y, Passow C, Auch B *et al*. Diverse AR gene rearrangements mediate resistance to androgen receptor inhibitors in metastatic prostate cancer. *Clinical Cancer Research* 2020; 26: 1965-1976.

15 Annala M, Taavitsainen S, Khalaf DJ, Vandekerkhove G, Beja K, Sipola J *et al*. Evolution of castration-resistant prostate cancer in ctDNA during sequential androgen receptor pathway inhibition. *Clinical Cancer Research* 2021; 27: 4610-4623.

16 Armstrong CM, Gao AC. Current strategies for targeting the activity of androgen receptor variants. *Asian Journal of Urology* 2019; 6: 42-49.

17 Watson PA, Arora VK, Sawyers CL. Emerging mechanisms of resistance to androgen receptor inhibitors in prostate cancer. *Nature Reviews Cancer* 2015; 15: 701-711.

18 Korpal M, Korn JM, Gao X, Rakiec DP, Ruddy DA, Doshi S *et al*. An F876L mutation in androgen receptor confers genetic and phenotypic resistance to MDV3100 (enzalutamide). *Cancer discovery* 2013; 3: 1030-1043.

19 Gaddipati JP, McLeod DG, Heidenberg HB, Sesterhenn IA, Finger MJ, Moul JW *et al*. Frequent detection of codon 877 mutation in the androgen receptor gene in advanced prostate cancers. *Cancer research* 1994; 54: 2861-2864.

20 Hu R, Lu C, Mostaghel EA, Yegnasubramanian S, Gurel M, Tannahill C *et al*. Distinct transcriptional programs mediated by the ligand-dependent full-length androgen receptor and its splice variants in castration-resistant prostate cancer. *Cancer research* 2012; 72: 3457-3462.

21 Yu Z, Chen S, Sowalsky AG, Voznesensky OS, Mostaghel EA, Nelson PS *et al*. Rapid induction of androgen receptor splice variants by androgen deprivation in prostate cancer. *Clinical cancer research* 2014; 20: 1590-1600.

22 Li Y, Alsagabi M, Fan D, Bova GS, Tewfik AH, Dehm SM. Intragenic rearrangement and altered RNA splicing of the androgen receptor in a cell-based model of prostate cancer progression. *Cancer research* 2011; 71: 2108-2117.

23 Li Y, Chan SC, Brand LJ, Hwang TH, Silverstein KA, Dehm SM. Androgen receptor splice variants mediate enzalutamide resistance in castration-resistant prostate cancer cell lines. *Cancer research* 2013; 73: 483-489.

24 Zhu Y, Dalrymple SL, Coleman I, Zheng SL, Xu J, Hooper JE *et al*. Role of androgen receptor splice variant-7 (AR-V7) in prostate cancer resistance to 2nd-generation androgen receptor signaling inhibitors. *Oncogene* 2020; 39: 6935-6949.

25 Cao B, Qi Y, Zhang G, Xu D, Zhan Y, Alvarez X *et al*. Androgen receptor splice variants activating the full-length receptor in mediating resistance to androgen-directed therapy. *Oncotarget* 2014; 5: 1646.

26 Dar JA, Masoodi KZ, Eisermann K, Isharwal S, Ai J, Pascal LE *et al*. The N-terminal domain of the androgen receptor drives its nuclear localization in castration-resistant prostate cancer cells. *The Journal of steroid biochemistry and molecular biology* 2014; 143: 473-480.

27 Liang J, Wang L, Poluben L, Nouri M, Arai S, Xie L *et al*. Androgen receptor splice variant 7 functions independently of the full length receptor in prostate cancer cells. *Cancer Letters* 2021; 519: 172-184.

28 Hu R, Isaacs WB, Luo JJTP. A snapshot of the expression signature of androgen receptor splicing variants and their distinctive transcriptional activities2011; 71: 1656-1667.

29 Xu D, Zhan Y, Qi Y, Cao B, Bai S, Xu W *et al*. Androgen Receptor Splice Variants Dimerize to Transactivate Target Genes. *Cancer Res* 2015; 75: 3663-3671.

30 Roggero CM, Jin L, Cao S, Sonavane R, Kopplin NG, Ta HQ *et al*. A detailed characterization of stepwise activation of the androgen receptor variant 7 in prostate cancer cells. *Oncogene* 2021; 40: 1106-1117.

31 Tsafou K, Tiwari P, Forman-Kay J, Metallo SJ, Toretsky J. Targeting intrinsically disordered transcription factors: changing the paradigm. *Journal of molecular biology* 2018; 430: 2321-2341.

32 Sadar MD. Discovery of drugs that directly target the intrinsically disordered region of the androgen receptor. *Expert opinion on drug discovery* 2020; 15: 551-560.

33 Le Moigne R, Pearson P, Lauriault V, Chi K, Ianotti N, Pachynski R *et al*. Pre-Clinical and clinical pharmacology of EPI-7386, an androgen receptor N-terminal domain inhibitor for castration-resistant prostate cancer. *J Clin Oncol* 2021; 39: 119.

34 Andersen RJ, Mawji NR, Wang J, Wang G, Haile S, Myung J-K *et al*. Regression of castrate-recurrent prostate cancer by a small-molecule inhibitor of the amino-terminus domain of the androgen receptor. *Cancer cell* 2010; 17: 535-546.

35 Myung J-K, Banuelos CA, Fernandez JG, Mawji NR, Wang J, Tien AH *et al*. An androgen receptor N-terminal domain antagonist for treating prostate cancer. *The Journal of clinical investigation* 2013; 123: 2948-2960.

36 Brand LJ, Olson ME, Ravindranathan P, Guo H, Kempema AM, Andrews TE *et al*. EPI-001 is a selective peroxisome proliferator-activated receptor-gamma modulator with inhibitory effects on androgen receptor expression and activity in prostate cancer. *Oncotarget* 2015; 6: 3811-3824.

37 Dalal K, Ban F, Li H, Morin H, Roshan-Moniri M, Tam KJ *et al*. Selectively targeting the dimerization interface of human androgen receptor with small-molecules to treat castration-resistant prostate cancer. *Cancer Letters* 2018; 437: 35-43.

38 Xu D, Zhan Y, Qi Y, Cao B, Bai S, Xu W *et al*. Androgen receptor splice variants dimerize to transactivate target genes. *Cancer research* 2015: canres. 0381.2015.

39 McClurg UL, Cork DM, Darby S, Ryan-Munden CA, Nakjang S, Mendes Côrtes L *et al*. Identification of a novel K311 ubiquitination site critical for androgen receptor transcriptional activity. *Nucleic acids research* 2017; 45: 1793-1804.

40 Lee GT, Nagaya N, Desantis J, Madura K, Sabaawy HE, Kim W-J *et al*. Effects of MTX-23, a novel PROTAC of androgen receptor splice variant-7 and androgen receptor, on CRPC resistant to second-line antiandrogen therapy. *Molecular cancer therapeutics* 2021; 20: 490-499.

41 Tukachinsky H, Madison RW, Chung JH, Gjoerup OV, Severson EA, Dennis L *et al*. Genomic analysis of circulating tumor DNA in 3,334 patients with advanced prostate cancer identifies targetable BRCA alterations and AR resistance mechanisms. *Clinical Cancer Research* 2021; 27: 3094-3105.

42 Liu W, Zhou J, Geng G, Lin R, Wu JH. Synthesis and in vitro characterization of ionone-based compounds as dual inhibitors of the androgen receptor and NF-kappaB. *Invest New Drugs* 2014; 32: 227-234.

43 Liu W, Zhou J, Geng G, Shi Q, Sauriol F, Wu JH. Antiandrogenic, maspin induction, and antiprostate cancer activities of tanshinone IIA and its novel derivatives with modification in ring A. *J Med Chem* 2012; 55: 971-975.

44 Liu B, Geng G, Lin R, Ren C, Wu JH. Learning from estrogen receptor antagonism: structure-based identification of novel antiandrogens effective against multiple clinically relevant androgen receptor mutants. *Chem Biol Drug Des* 2012; 79: 300-312.

Bridging Text 1

In the same drug screening workflow, we discovered another class of small molecules that has a completely distinct chemical structure than SC428. Following the chemical optimization, we discovered a second lead compound (SC912) for targeting AR NTD. While both SC428 and SC912 target AR NTD, our data indicates that they target different regions of AR-NTD. Specifically, SC912 target the AR-NTD region that is closer to the DNA-binding domain. Importantly, both compounds lead to potent inhibition of AR-V7 activity, demonstrating that there are multiple potential strategies by which AR-NTD could be targeted by small molecules to achieve AR-V7 antagonism.

Chapter 3: SC912 inhibits AR-V7 activity in castration-resistant prostate cancer by targeting androgen receptor N-terminal domain

SC912 inhibits AR-V7 activity in castration-resistant prostate cancer by targeting androgen receptor N-terminal domain

Qianhui Yi[1,2], Xiaojun Han[1], Henry G. Yu[1,2], Huei-Yu Chen[1,2], Dinghong Qiu[1], Jie Su[1], Moulay A. Alaoui-Jamali[1,2], Rongtuan Lin[1,2], Gerald Batist[1,2], and Jian Hui Wu[1,2]*

[1]Lady Davis Institute for Medical Research, SMBD-Jewish General Hospital, McGill University, 3755 Cote-Ste-Catherine, Rd, Montreal, QC H3T 1E2, Canada

[2]Departments of Oncology and Medicine, Faculty of Medicine, McGill University, Montreal, QC, Canada

***Corresponding author:** Jian Hui Wu, Lady Davis Institute for Medical Research, SMBD-Jewish General Hospital, McGill University, 3755 Cote-Ste-Catherine, Rd, Montreal, QC H3T 1E2, Canada. Phone: +1(514) 340-8222 ext 22148, Email: jian.h.wu@mcgill.ca

3.1. Abstract

Second-generation androgen deprivation therapies (ADT) are the mainstay treatments for castration-resistant prostate cancer (CRPC). They function to suppress the androgen receptor (AR) signaling by blocking androgen biosynthesis or by directly inhibiting AR through its ligand-binding domain (LBD). However, their effect is short-lived, as the AR signaling inevitably rises again which is frequently coupled with AR-V7 overexpression. AR-V7 is a truncated form of AR that lacks the LBD, thus being constitutively active without androgen and irresponsive to AR-LBD inhibitors. Though compelling evidence has tied AR-V7 to drug resistance in CRPC, pharmacological inhibition of AR-V7 is still an unmet need. In this study, we discovered a small molecule SC912 which binds to the AR N-terminal domain (NTD) and inhibited the transactivation of multiple forms of AR, especially AR-V7. This pan-AR inhibition relied on the presence of amino acids 507-531 in AR-NTD. SC912 also disrupted AR-V7 transcriptional activity, together with impaired AR-V7 nuclear localization and DNA binding. In the AR-V7 positive CRPC cells, SC912 suppressed proliferation, induced cell-cycle arrest and apoptosis. In the AR-V7 expressing CRPC xenografts, SC912 attenuated tumor growth and antagonized intratumoral AR signaling. Together, these results suggested the therapeutic potential of SC912 for repressing the AR-V7 driven AR signaling in CRPC.

3.2. Introduction

Castration-resistant prostate cancer (CRPC) is a relapsed form of prostate cancer from initial androgen deprivation therapies (ADT); its progression manifests reactivated AR signaling activity despite the castration level of androgen. When CRPC develops, second-line ADT is offered to patients to regain AR signaling blockade[86], including androgen biosynthesis inhibitor abiraterone (Abi) [271], and antiandrogens such as Enzalutamide (ENZ) that compete for the androgen binding pocket in the AR ligand-binding domain (LBD)[101]. However, resistance almost always occurs after a brief response period, featured with rising PSA as a sign of restored AR signaling activity [103, 247]. The underlying mechanisms contributing to Abi and ENZ resistance are AR gene amplification, AR-LBD mutations, and AR splicing variants (AR-Vs) with LBD truncated. The recently FDA-approved antiandrogen (darolutamide) showed higher LBD binding affinity that was not altered in the LBD mutants [104], hence may provide some relief to the drug resistance fueled by AR amplification and LBD mutation. However, AR-Vs are still undrugged.

Among many documented AR-Vs, AR-V7 is the best-established resistance driver in CRPC [272]. From the molecular perspective, AR-V7 possesses full transcriptional activity derived from the AR N-terminal domain (NTD), and the ability to bind androgen response elements (ARE) in AR-regulated genes through the DNA binding domain (DBD). Moreover, loss of LBD unleashes AR-V7 from the constraint of ligand-dependent activation [180], and the acquisition of a unique peptide that reconstitutes NLS permits AR-V7 constant nuclear localization [273]. Therefore, unlike full length-AR (AR-FL), whose activation is androgen-dependent and prone to antiandrogen inhibition, AR-V7 is constitutively active regardless of androgen, and is irresponsive to any antiandrogen. From the clinical perspective, AR-V7 mRNA and protein were both found overexpressed in Abi and ENZ-treated CRPC patients and were predictive of worse outcome [165, 167, 168, 171]. The more recent studies uncovered that, AR genomic rearrangements which preferentially give rise to AR-Vs were detectable in CRPC tissues [274]; these AR intragenetic abberations were particularly enriched in Abi and ENZ-treated patients and were associated with drug resistance [275]. Therefore, mounting evidence highlighted the urgency of AR-V7 inhibition.

Tremendous efforts have been dedicated to exploring the pharmacological inhibition of AR-V7's function, and the currently reported approaches can be categorized into: (1) direct targeting of AR-V7, *via* AR-NTD [215] or AR-DBD [222, 223]; (2) reducing the AR-V7 abundance, by degrading its protein [226, 228, 276] or disturbing its pre-mRNA splicing [277]; (3) abolishing AR-V7 mediated transcription, by targeting the cofactors [232, 241]. Among these approaches, direct targeting is conceptually the most desirable because fewer compensation pathways are present and there would be fewer non-specific effects. However, when targeting the very conserved AR-DBD, avoiding cross-reactivity with other hormone receptors is difficult [50]. Meanwhile, AR-NTD is composed mostly of "undruggable" intrinsically disordered protein [22, 213].

Since the transcriptional activity of all forms of AR resides entirely in their NTD [201], targeting this domain is still actively pursued despite the technical challenges. To date, EPI compounds are the only class of AR-NTD inhibitor that has entered the clinical trial. Although EPI-506 achieved PSA response in some CRPC patients, the trial was terminated for high pill burden [214]. Concordantly, a high micromolar concentration of EPI-002 was also required to inhibit AR signaling activity in cell-based experiments [216], emphasizing improved potency is demanded for AR-NTD inhibitors. We previously reported a small molecule SC428 that binds to AR-NTD and inhibits AR-FL/AR-V7 biological functions in 1–5 μM range. Additionally, SC428 also proved the concept that an AR-NTD inhibitor can indeed sufficiently block AR-V7 mediated AR signaling in CRPC cells.

In the present study, we discovered the other AR-NTD inhibitor SC912 that has a different chemical backbone from SC428. SC912 inhibited transactivation of AR-FL, AR-LBD mutants, AR-V7, and ARv567es, with the AR-NTD amino acids 507-531 being indispensable for its inhibitory effects. Mechanistically, SC912 impaired AR-V7 mediated transcription, and blocked AR-V7 nuclear trafficking and ARE binding. For the AR-V7 expressing CRPC cells, SC912 antagonized their AR signaling activity and mitigated their castration-resistant growth both *in vitro* and *in vivo*, suggesting its therapeutic potential in CRPC.

3.3.Result

3.3.1. SC912 inhibited AR-V7 and AR-FL transactivation without cross-reactivity to other hormone receptors

To identify AR-NTD inhibitors, we developed a cell-based AR-Vs transactivation assay to select compounds that have antagonistic activity against the two most well-known AR splice variants AR-V7 and ARv567es. Using an AR-responsive luciferase reporter, cotransfected with AR-V7 or ARv567es expression plasmid into 293T cells, we discovered compound SC912 potently inhibited both AR-V7 and ARv567es transactivation with nanomolar IC50. In contrast, the AR-LBD targeting agent ENZ showed no inhibitory activity even at the highest tested concentration of 10 μM (**Fig. 1A**). AR-FL transactivation assays were also performed with wild-type AR, and a panel of AR-LBD mutants that were previously discovered to confer resistance to antiandrogen drugs: including flutamide-resistant T878A and H875Y, bicalutamide-resistant W742C, and ENZ-resistant F877L [102]. SC912 inhibited dihydrotestosterone (DHT)-induced activation of wild-type AR, T878A mutant, and W742C mutant with a comparable level of potency to ENZ. However, for the F877L mutant, ENZ was weaker by approximately 3-fold relative to the wild-type AR at the concentration of 3 μM, whereas SC912 maintained a similar magnitude of inhibition (**Supplementary Fig. 1**).

To assess the receptor specificity, PC3 cells were transfected with a pan hormone receptor-responsive luciferase reporter for the endogenous glucocorticoid receptor (GR) activity or paired with AR or progesterone receptor (PR) expression plasmid, and the corresponding ligands of AR, PR, or GR was then employed respectively. Within the concentration range 0.1 –10 μM, SC912 selectively suppressed ligand stimulated AR activation and showed no inhibitory effect against GR and PR transactivation (**Fig. 1B**). Given that the DNA binding domain is highly conserved among hormone receptors, SC912's selectivity to AR argued that the binding motif of SC912 might not locate in AR-DBD.

The direct binding of SC912 to AR in prostate cancer cells was assessed by the cellular thermal shift assay (CETSA). In LNCaP cells, 10 nM DHT caused a drastic thermal shift of intracellular AR-FL protein, increasing its T_m from ~45 °C to ~51 °C, whereas the addition of 10 μM ENZ or SC912 decreased that T_m back to ~47 °C (**Fig. 1C**) This observation is consistent with Shaw's report that androgen-induced thermal stabilization of AR-FL is reversed by ENZ binding, and further revealed that SC912 binds to AR-FL with an affinity comparable to ENZ. Similarly, in 22Rv1 cells, 30 μM SC912 also caused a thermal shift of the endogenous AR-V7, resulting in the T_m dropping from ~51 °C to ~48 °C, whereas 30 μM ENZ had no impact (**Fig. 1D**). These results implied that the SC912-bound AR-FL and AR-V7 protein undergo conformational changes, leading to susceptibility to denaturalization.

3.3.2. AR-NTD amino acids 507-531 are indispensable for SC912's full inhibitory capacity

Our primary objective was to develop a small molecule targeting AR-NTD without interfering with the AR-LBD or AR-DBD. To investigate the interacting motif of SC912 on AR, we constructed a series of plasmids expressing chimeric proteins with various segments of AR-NTD fused to the DNA binding domain of the transcriptional factor IRF3. Using an interferon-responsive gene-based luciferase reporter, we observed that in PC3 cells, SC912 substantially inhibited the transactivation of IRF3-AR1-547 and IRF3-AR361-547 in contrast to no to marginal activity on wild-type IRF3 and IRF3-AR1-370, suggesting SC912's interacting motif on AR is majorly located within the amino acids 361-547 (**Fig. 2A**). To further narrow down this range, we generated another set of plasmids expressing AR protein which bear different deletions within amino acids 361-547 and are fused to the transactivation domain of the transcriptional factor VP16. When utilizing PSA-Luc as a reporter, SC912 attenuated androgen-stimulated transactivation of VP16-AR508-920 in PC3 cells, whereas it had no impact on VP16-AR530-920 nor VP16-AR540-920, indicating the importance of AR-NTD amino acid 508-530 for SC912's inhibitory effect (**Fig. 2B**).

Next, we sought to investigate if amino acid 508-530 would impair SC912's antagonistic activity against AR-FL and AR-V7. The plasmids AR-FL-del(507-531) and AR-V7-del(507-531) were constructed to express AR-FL or AR-V7 protein without the amino acids 507-531. SC912 only substantially inhibited DHT-stimulated transactivation of AR-FL but not AR-FL-del(507-531) in the range of 0.3–3 μM (**Fig. 2C**). Likewise, a similar selectivity of SC912 was also observed in suppressing AR-V7 transactivation but not in AR-V7-del(507-531) (**Fig. 2D**). Interestingly, no pronounced change in AR-FL nor AR-V7 transactivation activity appeared upon amino acids 507-531 deletion (**Fig. 2C-2D**), implying such deletion is not deleterious to the overall structure of AR protein.

Lastly, we determined the influence of amino acid 507-531 on SC912's binding to AR. We transitly expressed AR-FL/AR-V7 proteins and their amino acid 507-531 deleted counterparts in 293T cells, respectively. Deletion of amino acid 507-531 compeltely abolished SC912's interaction with both AR-FL and AR-V7, evidenced by no thermal distablization of AR protein was detected by CETSA assay in the concentration range 0.03—100 μM. On the contrary, the compound EC50 for heat-denaturalizing wildtype AR-FL and AR-V7 were 1.1 μM and 0.3 μM (**Fig. 1E-1F**), respectively, highlighted the prensence of AR-NTD amino acid 507-531 segement determines the SC912's target engagement.

3.3.3. SC912 blocked AR-V7 driven AR signaling in CRPC cells

To evaluate if SC912's inhibition of AR-FL/AR-V7 transactivation in ectopic expression models is transferable to endogenous cell models, we added SC912 to three CRPC cell lines expressing different amounts of AR-V7: LNCaP cells can acquire some AR-V7 expression and castration resistance at high passage (HP-LNCaP) [278]; VCaP cells are inherently castration-resistant *via* modest but rapid AR-V7 overexpression after castration or antiandrogen treatments [279], 22Rv1 cells are irresponsive to all of those treatments due to their high intrinsic level of AR-V7 [280]. Within these three CRPC cell lines, higher basal AR-V7 level correlated with less response to ENZ's inhibition on AR signaling, whereas SC912 demonstrated similar inhibitory activity (**Supplementary Fig. 2**). When assessed by qPCR assay of three canonical AR-regulated genes

(*PSA, FKBP5,* and *TMPRSS2*), SC912 dose-dependently (0.3–3 μM) attenuated their transcription in all three CRPC cell lines, with the effect being most pronounced on *PSA* and *FKBP5* that 1 μM of SC912 suppressed their mRNA expression by more than 40% (**Fig. 3A**). Next, we asked if SC912 could also impair the transcription of AR-V7 specifically regulated genes. We quantified the mRNA of three tumor suppressor genes (*B4GALT1*, *SLC30A7,* and *HIF1A*) whose transcription is reported to be specifically repressed by AR-V7 in LNCaP-95 [207]. Indeed, SC912 at 3 μM significantly elevated the expression of *B4GALT1* and *HIF1A* in HP-LNCaP, while even greater changes were observed in cell lines expressing more AR-V7. In VCaP as well as our LNCaP-AR-V7 stable cells, the mRNA levels of all three AR-V7 repressed genes spiked upon SC912 treatment (**Fig. 3B**). Collectively, these data indicated that SC912 suppressed AR-V7 transcriptional activity in CRPC cells.

Lastly, to isolate SC912's inhibitory effect on AR-V7 alone, we built two stable 22Rv1 cell lines with doxycycline-inducible knockdown of AR-FL or AR-V7, respectively (**Fig. 3C**). The mRNA quantification of canonical AR-regulated genes revealed that AR-FL knockdown did not mitigate AR signaling activity in 22Rv1 cells, whereas a drastic decline of such was noted following AR-V7 knockdown (**Fig. 3D**). These observations aligned with the previous discoveries that AR signaling activity is predominantly driven by AR-V7 rather than AR-FL in 22Rv1 cells [259, 281]. More importantly, 3 μM of SC912 markedly reduced AR signaling activity in control and shAR-FL cells but its potency was significantly diminished in shAR-V7 cells. On the contrary, 10 μM of ENZ inhibited AR signaling in neither the control nor the knockdown cells (**Fig. 3D**), demonstrating that SC912 but not ENZ was capable of blocking AR-V7 mediated AR signaling activity in CRPC cells.

3.3.4. SC912 hampered the nuclear localization and chromatin binding for both AR-V7 and AR-FL

AR nuclear translocation and subsequent DNA-binding are two prerequisite steps happening before AR-initiated transcription. Since SC912 inhibited AR transcriptional activity, we wondered if such inhibition is associated with hampering those upper stream events as well. Therefore, we first examined if SC912 treatment reduced AR chromatin binding. In the chromatin

immunoprecipitation assay with LNCaP-AR-FL stable cells, androgen-induced AR-FL recruitment to AREs (PSA enhancer and *TMPRSS2* enhancer) was partially prevented by 3 μM of SC912, while completely blocked by 5 μM of ENZ. Next, we assessed the capability of SC912 in reducing androgen-independent AR-FL/AR-V7 DNA binding (**Fig. 4A**). In LNCaP-AR-V7 cells, SC912 at 3 μM lowered the AR-FL/AR-V7 chromatin recruitment by more than 50%; whereas ENZ at 5 μM only had a marginal effect yet was not statistically significant (**Fig. 4B**). Furthermore, in the shFL-22Rv1 cells, SC912 also potently diminished AR-V7 binding to AREs, in contrast to ENZ showed no inhibition at all (**Fig. 4C**). Lastly, we examined if SC912 also affects the nuclear localization of AR-FL and AR-V7. GFP tagged AR-FL or AR-V7 were transiently expressed in PC3 cells, respectively, and their subcellular localization was visualized using confocal microscopy. Though being weaker than 5 μM of ENZ, 3 μM of SC912 significantly reduced androgen-stimulated nuclear translocation of AR-FL (**Fig. 4D**). More importantly, SC912 also markedly attenuated the androgen-independent nuclear localization of AR-V7 which ENZ failed to affect (**Fig. 4E**). These results suggested that, though androgen-induced nuclear translocation and DNA binding of AR-FL were mitigated by both SC912 and ENZ, these events for androgen-independent AR-V7 were only disturbed by SC912.

3.3.5. SC912 caused proliferation arrest and apoptosis in AR-V7 positive CRPC cells

The antiproliferative potency of SC912 in CRPC cells was assessed in three AR-FL/AR-V7 expressing cell lines HP-LNCaP, VCaP, 22Rv1, and an AR-negative cell line PC3. When cells were grown in androgen-free media for 6 days, SC912 inhibited the proliferation of all three AR-positive cell lines with nanomolar IC50 (0.3 – 0.9 μM), whereas much higher IC50 (5.77 μM) was noted in PC3 cells. ENZ suppressed HP-LNCaP proliferation with an IC50 of 1.76 μM, in contrast to being less potent in VCaP (IC50 = 9.88 μM) and almost inactive in 22Rv1 and PC3 (**Fig. 5A** and **Supplementary Fig. 3**). To validate these findings, the four CRPC cell lines were next treated with DMSO, ENZ, or SC912 for 48 hours before being applied to cell cycle analysis using flow cytometry. 1 μM of SC912 caused a substantial amount of AR-positive cells to stall at G1/S transition, while no remarkable effect on the cell cycling was observed in AR-negative cells. In comparison, 5 μM of ENZ led to G1-phase arrest only in HP-LNCaP but had no obvious impact

on other cell lines (**Fig. 5B** and **Supplementary Fig. 4**), suggesting SC912 but not ENZ is broadly effective in blocking AR-V7 positive CRPC cell growth.

1 μM of SC912 also induced apoptosis in the three AR-V7 positive CRPC cell lines, evidenced by the emergence of PARP cleavage in cell lysate western blot, which conversely, was not detectable in PC3 cells (**Fig. 5C**). Furthermore, consistent with its antiproliferative results, ENZ also only induced apoptosis in HP-LNCaP but not in the other CRPC cell lines (**Fig. 5C**). In summary, these findings agreed with previous discoveries that prostate cancer cells and PDX with higher AR-V7 expression are more resistant to ENZ [257]; nonetheless, our study further revealed that they could be similarly susceptible to SC912 triggered growth arrest and cell death.

3.3.6. SC912 repressed tumor growth and interrupted AR signaling in AR-V7 expressing CRPC xenografts

In considering of SC912's therapeutic activity in CRPC tumors, we first assessed the effect of SC912 on VCaP xenografts. Male NOD-SCID mice implanted with VCaP cells were subsequently castrated when tumor sizes reached 250–500 mm^3. Compounds were given intraperitoneally 5-times a week for 3-weeks once VCaP tumors resumed growing in castrated hosts. Strikingly, the first three dosages of SC912 (60mg/kg) immediately halted the castration-resistant growth of VCaP tumors, which lasted to the endpoint. In contrast, the tumor volume in the vehicle group increased by approximately 150% on average (**Fig. 6A**). When compared by weight, the tumors in the SC912 group were about 40% of that of the vehicle group (**Fig. 6B**); furthermore, SC912 treatment did not cause obvious animal body weight loss, indicating that SC912 at 60mg/kg is effective and well-tolerated (**Fig. 6C**).

Next, we explored how the AR signaling in VCaP tumors was influenced by SC912 treatment. In the serum of SC912 treated mice, a sizeable drop in human PSA concentration was detected by ELISA (28.1 ng/mL v.s 12.7 ng/mL) (**Fig. 6D**). Additionally, qPCR analysis of the intratumoral mRNA also demonstrated a reduction of *PSA* expression, and concordantly, an upregulation of AR-V7 repressed gene *B4GALT1* (**Fig. 6E**), suggesting that androgen-independent AR signaling in VCaP xenografts was inhibited by SC912. Moreover, within SC912 treated tumors, a 3.2-fold

increase of AR-FL protein and a 2.6-fold increase of AR-V7 protein was shown by western blot (**Fig. 6F-6G**), coupled with a statistically insignificant but observable bump of AR-FL and AR-V7 mRNA (**Fig. 6H**). These data collectively implied that CRPC tumors responded to SC912 inhibited AR signaling with AR overexpression.

Lastly, we evaluated SC912's potency against 22Rv1 xenografts which are more castration-resistant and express a higher amount of AR-V7. As expected, 22Rv1 tumor progression was not paused by castrating host mice, however, it was markedly mitigated by 90mg/kg of SC912. After 10 days of treatment, the tumor inhibitory effect of SC912 became statistically significant, followed by the p-value dropping below 0.01 in the next 3 days and remaining so to the end of the experiment (**Fig. 6I**). The average tumor weight for the SC912 group is approximately 45% of the vehicle group (**Fig. 6J**), and no decline in animal body weight was observed (**Fig. 6K**). These findings demonstrated that SC912 was capable of repressing the growth of CRPC tumors that express high levels of AR-V7.

3.4. Discussion

Persistent AR signaling activity is a widely recognized cause of Abi and ENZ resistance in CRPC. While mounting evidence emphasized AR-V7's role as a key driver of sustaining AR signaling in CRPC, chemical inhibition of AR-V7 remains unavailable. In this work, we have demonstrated that SC912 potently inhibited the biological functions of AR-V7, and the AR-NTD amino acids 507-531 are essential for its inhibitory effect. SC912 blocked AR-V7 mediated AR signaling in CRPC cells *in vitro* and repressed their tumor growth in castrated mice, demonstrating its potential benefit to men with CRPC that relapsed from current AR signaling inhibitors.

The AR-NTD amino acids 507-531 were found to be indespensible for SC912's antagonistic effect on both AR-FL and AR-V7, nevertheless, the influence from redisues outside of this region can not be ruled out. Deletion of amino acids 507-531 did not compeletely abolished SC912's inhibition, evidenced by 3 μM of SC912 still caused a ~15% reduction of transactivation for AR-FL bearing this deletion (**Fig. 2C**). Plus, 3 μM of SC912 also caused a mild dip in IRF3-AR1-370 transactivation (**Fig. 2A**), hinting to the possibility of a secondary motif that conducts SC912 and

AR-NTD interaction exisiting within aa 1-370. Furthermore, as the amino acids 507-531 predominantly determined SC912's efficacy, we do not know if they function by directly interacting with SC912 or by facilitating the formation of a compound interacting surface. Since conformational plasticity and lacking of folded structure is the nature of intrinsically disordered proteins like AR-NTD [282], we also can not distinguish if SC912 bound to a pre-formed structure, or if the binding pocket spontaneously formed upon encountering SC912. Further exploration is ongoing, using molecular simulation to predict binding sites within and around aa 507-531, followed by point mutation and direct binding assay with recombinant protein, which will provide better resolution on the interaction pattern between SC912 and AR-NTD.

SC912 exhibited comparable potency to ENZ in repressing androgen-stimulated AR-FL transactivation (**Fig. 1C** and **Supplementrary Fig. 1**), but relatively weaker inhibition against AR-FL nuclear translocation and DNA binding (**Fig. 4A, 4D**). This observation hinted that in SC912 treated cells, androgen exposure still led to a proportion of AR-FL going into nucleus and binding to AREs, but these AR-FL were somehow not transcriptionally viable. One possibility is that SC912 disrupted AR-mediated transcription initiation, such as by blocking the recruitment of transcriptional machinery and co-regulators to AR-NTD [283, 284]. Though it is conceivable for SC912 to attenuate these protein interactions occurring with its targeted region, future study is necessary to elucidate its mechanism of action involved in the sequential events required by AR-mediated transcription.

Overexpression of AR was induced by SC912 in all VCaP tumors (**Fig. 6F**), which is consistent with the previously described negative feedback loop between AR signaling and AR expression [285], highlighting that on-target inhibition of AR signaling was achieved by SC912 in CRPC xenografts. However, it is worth noting that SC912-caused AR overexpression is distinct from that of the conventional AR signaling inhibitors. Castration condition, ENZ, and Abi were all reported to preferentially trigger more AR-V7 upregulation rather than AR-FL in VCaP [181, 279]; conversely, SC912 induced AR-V7 and AR-FL overexpression to similar extents with a moderate bias towards AR-FL (**Fig. 6G**). This discrepancy is likely rooted in the AR-V7 antagonism that was uniquely applied to SC912 treated VCaP. One hypothesis could be, CRPC cells do not favor

AR-V7 overexpression when AR-V7 and AR-FL are indifferently targeted, instead, evenly enriching both forms of AR might convey more survival benefits.

In conclusion, our findings suggested a potential for developing SC912 as an AR-V7 inhibitor against the constitutively active AR signaling in CRPC.

3.5. Materials and Methods

Cell lines

293T, PC3, LNCaP, VCaP, and 22Rv1 cell lines were purchased from the ATCC and cultured as recommended. In experiments where the androgen-deprived condition was required, cells were cultured in phenol red-free medium supplemented with 10% of charcoal-stripped FBS. HP-LNCaP is derived from *in vitro* culturing of LNCaP for 80 passages. The stable cell lines LNCaP-AR^{WT}, and LNCaP-AR-V7 were established as previously described. The doxycycline inducible shAR-FL-22Rv1 and shAR-V7-22Rv1 cell lines were built by cloning the foward and reverse shAR-FL or shAR-V7 oligonucleotides into pLKO-Tet-On (addgene: #21915) vector. The AR-FL-pLKO-Tet-On and AR-V7-pLKO-Tet-Lentivirus particles were produced by transfecting the above plasmids along with psPax2 and pMD2.G packaging vectors into HEK293T cells. 22Rv1 cells were transudced with lentirivus particles in the presence of 4ng/mL polybrene (Millipore Sigma). AR-FL or AR-V7 knockdown was induced using 100ng/mL doxycycline (Millipore Sigma) and verified by Western Blot.

Plasmids

The pEGFPc1-AR-V7 plasmid was a gift from Dr. Jun Luo (Johns Hopkins University, USA). pIRES-AR-V7 was generated by cloning the AR-V7 cDNA from pEGFPc1-AR-V7 plasmid into pIRthe ESpuro2 vector. pcDNA-ARv567es was a gift from Dr. Stephen Plymate (University of Washington, Seattle, WA). pCMV-AR, pCMV-VP16/AR507−920, the B form of human progesterone receptor (PR-B), pCMV-MMTV-Luc, and pCMV-PSA-Luc plasmids were kind gifts from Dr. Liangnian Song (Columbia University, USA). pEGFPc1-IRF3, pEGFPc1-IRF3DBD (aa 1−133) and ISRE-Luc plasmids were gifts from Dr. Rongtuan Lin (McGill University). The pCMV-AR-T878A and pCMV-AR-H875Y plasmids were gifts from Dr. S. Srivastava (Uniformed Services University). pCMV-AR-W742C was a gift from Dr. O. Ogawa (Kyoto University). pEGFPc1-IRF3-AR1-547, pCMV-VP16-AR540-920, and pCMV-AR-F877L plasmids were constructed as previously described in section 2.7.1. The construction of pEGFPc1-IRF3-AR1-370, pEGFPc1-IRF3-AR361-547 and pCMV-VP16-AR530-920 plasmids is described in supplementary methods.

Dual luciferase reporter assay

Cells were seeded into 24-well plates at least 24 h before transfection. *Firefly* luciferase reporter (PSA-Luc, MMTV-Luc or ISRE-Luc) and *Renilla* luciferase reporter (pRL-TK) together with a plasmid expressing the designated transcription factor were transiently transfected into cells using lipofectamine 3000. 5 h after transfection, cell culture media was refreshed, and cells were subjected to the treatment of DMSO or designated compounds. Luciferase activities were measured using the Dual-Luciferase Reporter Assay System (Promega) on a GLOMAX 20/20 luminometer (Promega).

qRT-PCR analysis

2×10^6 cells were seeded in 6 cm dish and cultured in androgen-deprived media for 48 h prior to 24 h of compound treatment. Cells were then harvested and followed by total RNA extraction using RNAqueous™ Total RNA Isolation Kit (Applied Biosystems), and cDNA was synthesized using iScript cDNA Synthesis Kit (BIO-RAD). For tumor tissue, frozen tissue was grounded in liquid N2 with mortar and pestle before being applied to RNA extraction. Extracted RNA samples were subjected to DNase treatment (Promega) before reverse transcription. cDNA was assessed using GoTaq qPCR Master Mix (Promega); qRT-PCR reaction was performed on 7500 Fast Real-Time PCR System (Applied Biosystems). The primer sequences for the analyzed genes are included in the supplementary methods.

Confocal imaging

1×10^6 LNCaP-AR^{WT} or LNCaP-AR-V7 cells were seeded above the coverslip in 6-well plates. Cells were treated as described in the respective figure for 5 h. Confocal microscopy was performed on a fully motorized Zeiss Axio Observer Z1 microscope with confocal unit LSM-800 with a 63×1.4 NA Plan-Apochromat oil-immersion objective lens (Zeiss) using diode solid-state lasers (488 nm excitation for GFP, 405 nm for DAPI). Images were captured with GaAsP detectors and ZEN blue software. Raw data was analyzed and modifications to images for presentation purposes were made by using Fiji (Image J).

Cell proliferation assay

Cells (3000 cells/well) were plated in 96-well plates (Corning #3595) 24 h before compound treatment. Culture media and compounds were refreshed on day 3 and viable cells were measured using CellTiter-Glo 2.0 Assay kit (Promega) on day 6 by Synergy 4 multimode plate reader (BioTek).

Cell-cycle flow cytometry

5×10^5 cells were seeded in 6cm dishes and cultured in androgen-free medium for 48 h before 24 h treatment. Cells were then pulsed with BrDU for 1h prior to harvest and were thereafter permeabilized for Alexa 647 anti-Brdu (Biolegends) and DAPI staining. Samples were run on BD LSRFortessa (Becton Dickson), and the results were analyzed using FlowJo V9.

Western blot analysis

Cells were plated at 6×10^5 cells per 6cm dish and were treated as described in the respective figures. Protein extracts were prepared using RIPA buffer supplemented with 1% Protease Inhibitor Cocktail (SIGMA) and 1mM PMSF. Protein concentration was quantified by Coomassie Protein Assay (Thermo) and samples were applied to SDS-PAGE. Western Blot was performed with antibodies AR-N20 (sc-816, Santa Cruz), AR-V7 (AG10008, Precision Antibody), PSA (#2475, Cell Signaling), PARP (#46D11, Cell Signaling), and β-actin (SIGMA). For tumor tissue, a soybean-sized piece of tissue was dissected from the tumor and was homogenized in 1mL RIPA buffer supplemented with 5% Protease Inhibitor Cocktail (SIGMA) and 2 mM PMSF; western blot was performed with the supernatant.

Animal study

All animal studies were conducted under the Animal Use Protocol approved by the Animal Care Committee of the Lady Davis Institute, Jewish General Hospital, McGill University. Six weeks old NOD-SCID or Nu/Nu male mice were purchased from Charles River. Tumor cell implantation was done at least 1 week after animal arrival. The VCaP cells were passaged in castrated mice once and cultured *in vitro* in complete media for 5 passages before being used for this experiment. The indicated number of tumor cells were injected subcutaneously in 200 µl solution containing 50% of PBS and 50% of Cultrex Basement Membrane Matrix, Type3 (Trevigen). Tumor length

and width were measured by caliper and tumor size was calculated with the formula: Volume=4/3×π×(Length/2) ×(Width/2)^2. Compounds were delivered *via* intraperitoneal injection (i.p.) (at 10 μl per 1 g of mouse body weight). Compounds were formulated in saline solution contains 10% DMSO, 10% Cremophor EL, 20% PEG400 and 1% 2-hydroxypropyl-β-cyclodextrin.

Statistical analysis

Statistical significance was calculated by the two-tailed unpaired t test using Graphpad Prism 9, unless stated otherwise for a specific graph in the figure. Data were plotted as individual data points or summarized as average ± standard deviation (SD) of biological or technical repeats. P values considered to be significant as follows: *p<0.05, **p<0.01, ***p<0.001 and ****p<0.0001. n.s, not significant.

3.6.Figures

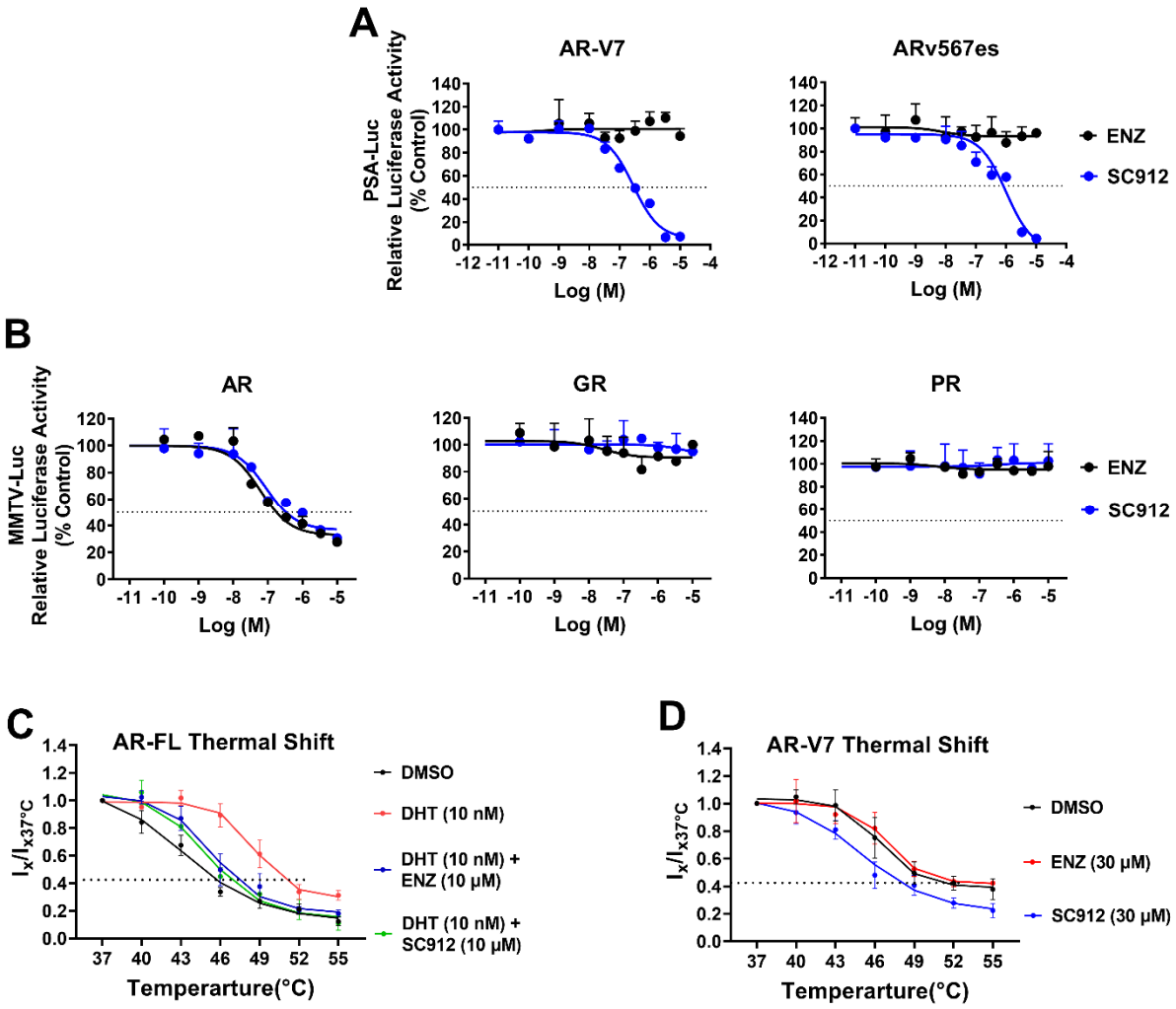
A
AR-V7
ARv567es
PSA-Luc
Relative Luciferase Activity
(% Control)
Log (M)
ENZ
SC912
B
AR
GR
PR
MMTV-Luc
Relative Luciferase Activity
(% Control)
Log (M)
ENZ
SC912
C
AR-FL Thermal Shift
$I_x/I_{x37°C}$
Temperarture(°C)
DMSO
DHT (10 nM)
DHT (10 nM) +
ENZ (10 μM)
DHT (10 nM) +
SC912 (10 μM)
D
AR-V7 Thermal Shift
$I_x/I_{x37°C}$
Temperarture(°C)
DMSO
ENZ (30 μM)
SC912 (30 μM)

3.6.1. Figure M2-1. SC912 inhibited AR-V7 and AR-FL transactivation without cross-reactivity to other hormone receptors.

A. AR-Vs transactivation-based PSA-Luc reporter assay. 293T cells were transiently transfected with AR-V7 or ARv567es expressing plasmid paired with PSA-Luc *Renila* luciferase reporter plasmid; pRL-TK *firefly* luciferase reporter plasmid was co-transfected as an internal control. Cells were treated with ENZ or SC912 at designated doses for 48 h in androgen-free media; Relative PSA-Luc reporter activity was normalized to the DMSO treated samples. Data represent the average ± SD of two separate experiments.
B. Hormone receptor transactivation-based MMTV-Luc reporter assay. PC3 cells were transiently transfected with MMTV-Luc *Renila* luciferase reporter plasmid, pRL-TK, and a plasmid expressing AR or PR, or endogenous GR as indicated. Cells were pretreated in androgen-free media with ENZ or SC912 at designated doses for 30 min, followed by the addition of 10 nM DHT, 10 nM Progesterone, or 10 nM Dexamethasone respectively for another 24 h. Relative MMTV-Luc reporter activity was normalized to the DMSO-treated samples. Data represent the average ± SD of duplicate samples.
C-D. Cellular thermal stability assay (CETSA) for assessing in-cell AR and compound binding. LNCaP (**C**) or 22Rv1 (**D**) cells were exposed to designated treatments for 1h followed by 3 min of heat shocks at the indicated temperature. Thermostable AR-FL (**C**) or AR-V7 (**D**) was quantified by western blots (relative to β-actin) and normalized to the blot intensity of the 37 °C samples. Data represent the average ± SD of two biological repeats.

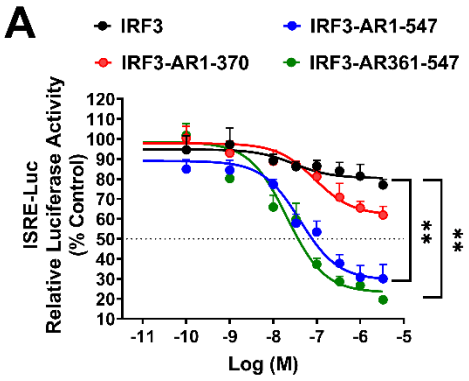
A
IRF3
IRF3-AR1-547
IRF3-AR1-370
IRF3-AR361-547
ISRE-Luc
Relative Luciferase Activity
(% Control)
Log (M)
**
**

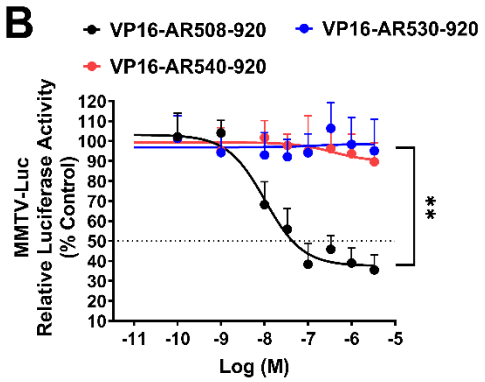
B
VP16-AR508-920
VP16-AR530-920
VP16-AR540-920
MMTV-Luc
Relative Luciferase Activity
(% Control)
Log (M)
**

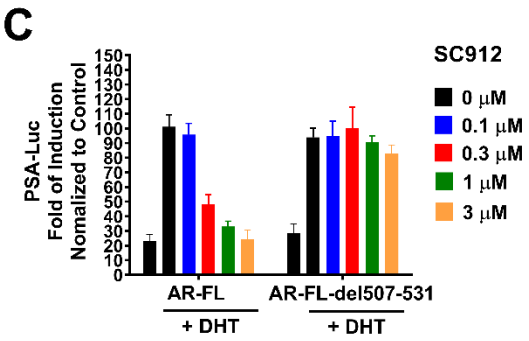
C
PSA-Luc
Fold of Induction
Nomalized to Control
SC912
0 μM
0.1 μM
0.3 μM
1 μM
3 μM
AR-FL
AR-FL-del507-531
+ DHT
+ DHT

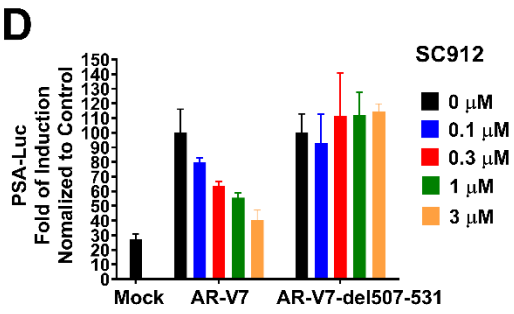
D
PSA-Luc
Fold of Induction
Nomalized to Control
SC912
0 μM
0.1 μM
0.3 μM
1 μM
3 μM
Mock
AR-V7
AR-V7-del507-531

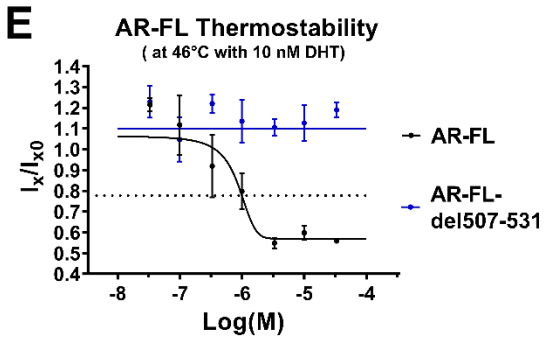
E
AR-FL Thermostability
(at 46°C with 10 nM DHT)
Ix/Ix0
Log(M)
AR-FL
AR-FL-
del507-531

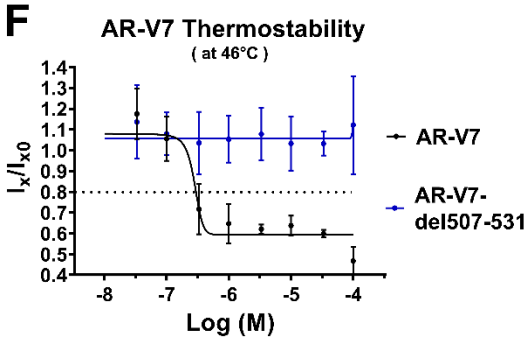
F
AR-V7 Thermostability
(at 46°C)
Ix/Ix0
Log (M)
AR-V7
AR-V7-
del507-531

3.6.2. Figure M2-2. AR-NTD amino acids 507-531 are indispensable for SC912's full inhibitory capacity

A. IRF3-AR transactivation-based ISRE-Luc reporter assays. PC3 cells were transfected with ISRE-Luc *Renila* luciferase reporter plasmid, pRL-TK, and a plasmid expressing IRF3, IRF3-AR (1–547), IRF3-AR (1–370), or IRF3-AR (361–547) fusion protein. Cells were treated with ENZ or SC912 at designated doses for 24 h in androgen-free media; Relative ISRE-Luc reporter activity was normalized to the DMSO treated samples. Data represent the average ± SD of duplicate samples.
B. VP16-AR transactivation-based PSA-Luc reporter assay. PC3 cells were transiently transfected with PSA-Luc, pRL-TK, and a plasmid expressing VP16-AR(508-920), VP16-AR(530-920), or VP16-AR(540-920) fusion protein. Cells were pretreated with SC912 at designated doses in androgen-free media for 30 min before the addition of 10 nM DHT for another 24 h. Relative PSA-Luc reporter activity was normalized to the samples without DHT. Data represent the average ± SD of duplicate samples.
C. AR-FL transactivation-based PSA-Luc reporter assay. PC3 cells were transfected with PSA-Luc and pRL-TK reporter plasmids, and a plasmid expressing AR-FL or corresponding amino acid 507-531 deleted counterparts: AR-FL-del507-531. Cells were pretreated with SC912 (0, 0.1, 0.3, 1.0, 3.0 μM) in androgen-free media for 30 min followed by the addition of 10 nM DHT for another 48 h. Relative PSA-Luc reporter activity was normalized to 0 μM SC912 treated cells, and no DHT stimulated cells were used as the negative control. Data represent the average ± SD of triplicate samples.
D. AR-V7 transactivation-based PSA-Luc reporter assay Right panel: PC3 cells were transfected with PSA-Luc and pRL-TK reporter plasmids, and a plasmid expressing AR-V7 or corresponding amino acid 507-531 deleted counterparts: AR-V7-del507-531. Cells were treated with SC912 (0, 0.1, 0.3, 1.0, 3.0 μM) in androgen deprived medium for 48 h, Relative PSA-Luc reporter activity was normalized to 0 μM SC912 treated cells, and cells transfected with empty expression vector were used as the negative control. Data represent the average ± SD of triplicate samples.
E-F. Cellular thermal stability assay (CETSA) for assessing the effect of AR-NTD amino acids 507-531 on the target engagement of SC912. **E,** 293T cells transiently expressing AR-FL or AR-FL-del507-531 were treated with 10 nM DHT together with SC912 (0.03 μM —33.33 μM). **F,** 293T cells transiently expressing AR-V7 or AR-V7-del507-531 were treated with SC912 (0.03 μM —100 μM). After 1h of treatment, cells were harvested and subjected to 3 min of heat shock at 46 °C. Thermostable AR-FL or AR-V7 were quantified by western blots (relative to β-actin) and normalized to the blot intensity of the non-treated samples. Data represent the average ± SD of two biological repeats.

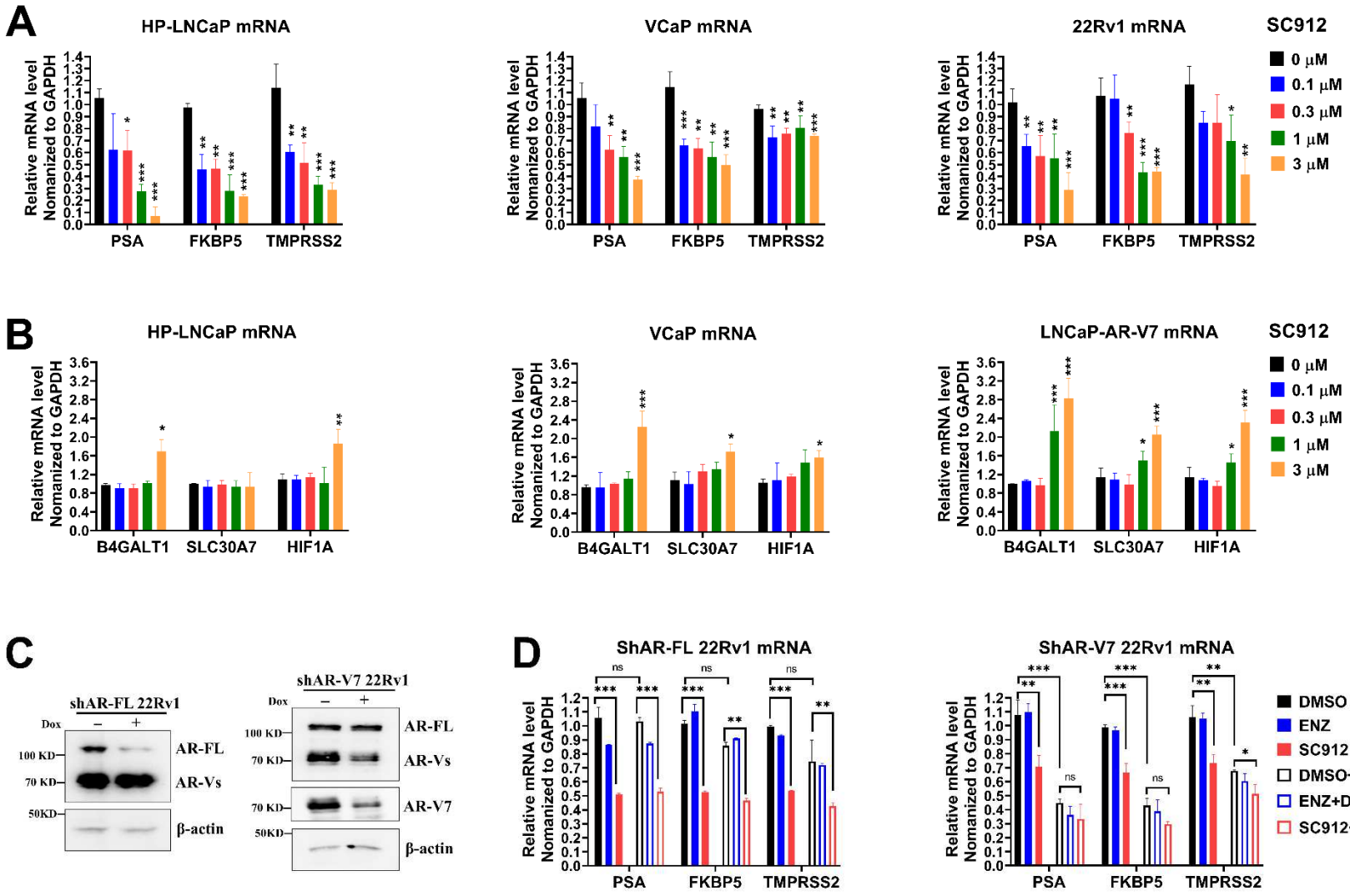
A
HP-LNCaP mRNA
VCaP mRNA
22Rv1 mRNA
SC912
0 μM
0.1 μM
0.3 μM
1 μM
3 μM
Relative mRNA level
Nomanized to GAPDH
PSA
FKBP5
TMPRSS2
B
HP-LNCaP mRNA
VCaP mRNA
LNCaP-AR-V7 mRNA
SC912
B4GALT1
SLC30A7
HIF1A
C
shAR-FL 22Rv1
shAR-V7 22Rv1
Dox
100 KD
70 KD
50KD
AR-FL
AR-Vs
AR-V7
β-actin
D
ShAR-FL 22Rv1 mRNA
ShAR-V7 22Rv1 mRNA
ns
DMSO
ENZ
SC912
DMSO+DOX
ENZ+DOX
SC912+DOX

3.6.3. Figure M2-3. SC912 blocked AR-V7 driven AR signaling in CRPC cells.

A. qRT-PCR analysis of canonical AR-regulated genes. HP-LNCaP, VCaP, and 22Rv1 cells were cultured in androgen-free media for 48 h before being treated with SC912 (0, 0.1, 0.3, 1.0, 3.0 μM) for another 24 h. Data represent the average ± SD of three separate experiments

B. qRT-PCR analysis of AR-V7 specifically regulated genes. HP-LNCaP, VCaP, and LNCaP-AR-V7 cells were treated the same as in **3A**. Data represent the average ± SD of three separate experiments.

C. Western blot validation of ShAR-FL 22Rv1 and ShAR-V7 22Rv1 stable cell lines. Cells were treated with 50 ng/mL doxycycline for 48 h in androgen-free media before harvest.

D. qRT-PCR analysis of canonical AR-regulated genes in ShAR-FL 22Rv1 and ShAR-V7 22Rv1 cells. Cells were processed the same as in **3C** before being subjected to refreshing the media and adding DMSO, 10 μM ENZ, or 3 μM SC912, cells were then treated for 24 h before harvest. Data represent the average ± SD of three separate experiments.

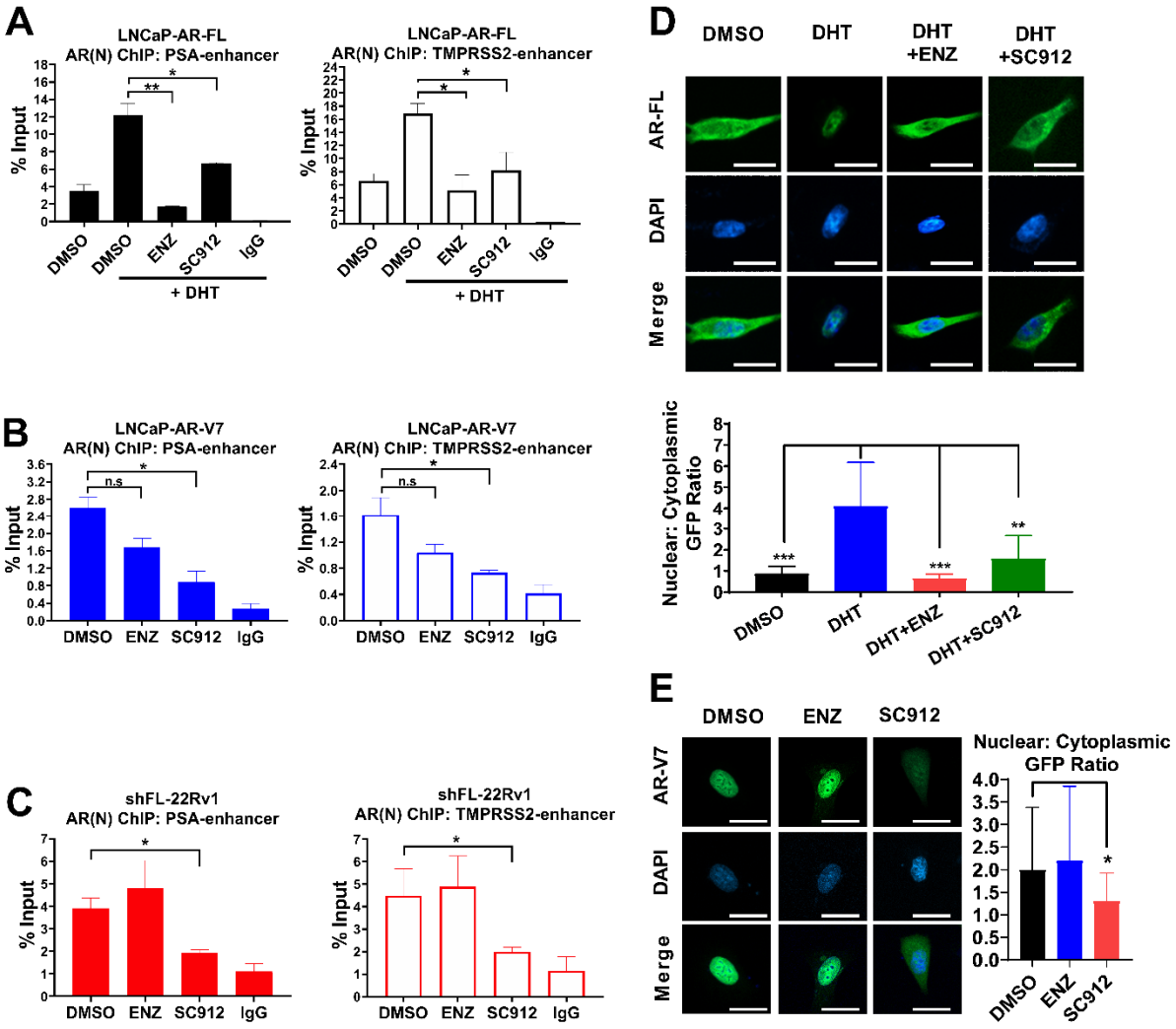

3.6.4. Figure M2-4. SC912 hampered the nuclear localization and chromatin binding for both AR-V7 and AR-FL.

A ChIP assay for androgen stimulated AR-FL enrichment to AREs. LNCaP-AR-FL cells were cultured in androgen-free media for 48 h and were then pretreated for 30 min with DMSO control, 5 μM ENZ, or 3 μM SC912, followed by the addition of 10 nM DHT and incubation for another 4.5 h before harvest. Data represent the average ± SD of two biological repeats.

B, ChIP assay for androgen-independent AR-FL/AR-V7 enrichment to AREs. LNCaP-AR-V7 cells were cultured in androgen-free media for 48 h before being treated with DMSO, 5 μM ENZ, or 3 μM SC912 for 5 h. Data represent the average ± SD of two biological repeats.

C, ChIP assay of androgen-independent AR-V7 enrichment to AREs. shAR-FL 22Rv1 cells were incubated in androgen-free media containing 50 ng/mL doxycycline for 48 h before being treated the same as **4B**. Data represent the average ± SD of two biological repeats.

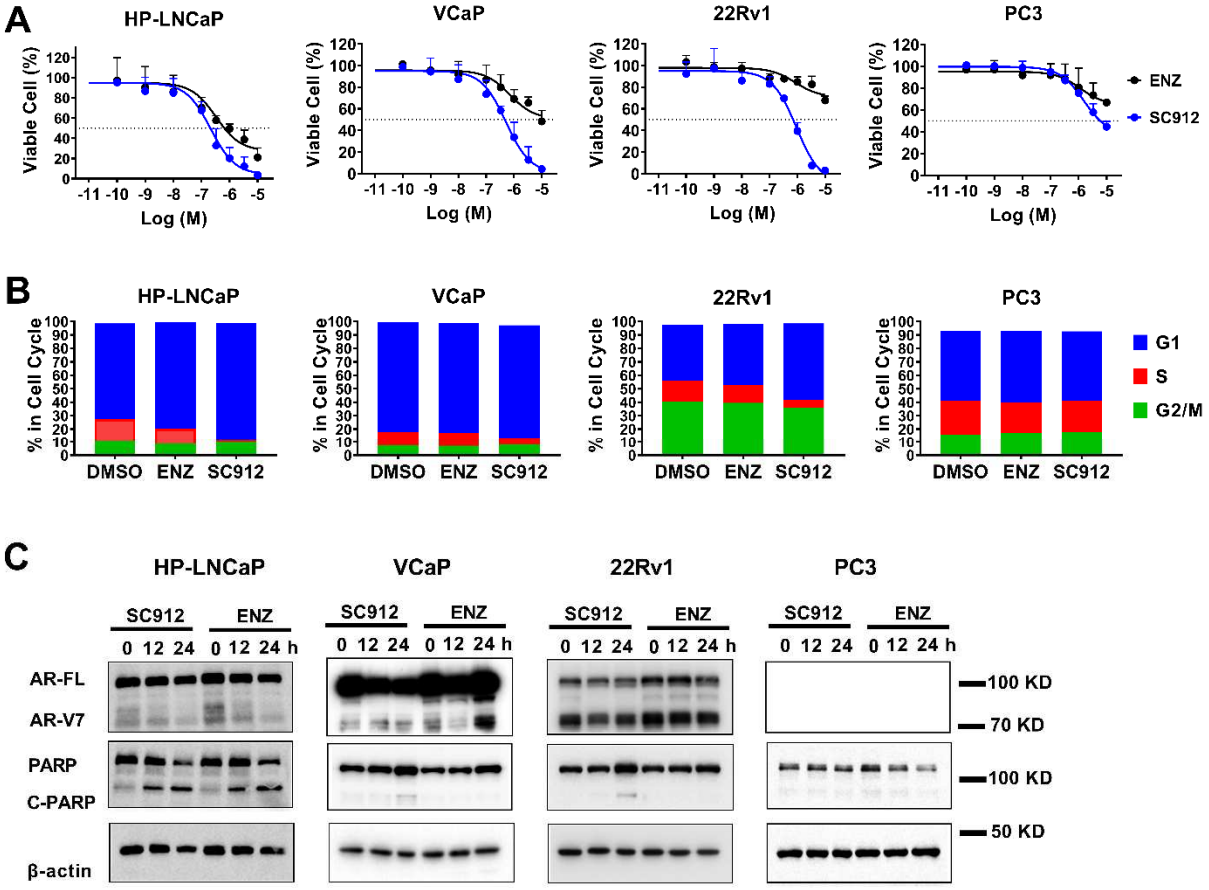
A
HP-LNCaP
VCaP
22Rv1
PC3
Viable Cell (%)
Log (M)
ENZ
SC912
B
% in Cell Cycle
DMSO
ENZ
SC912
G1
S
G2/M
C
SC912
ENZ
0 12 24 0 12 24 h
AR-FL
AR-V7
PARP
C-PARP
β-actin
100 KD
70 KD
100 KD
50 KD

3.6.5. Figure M2-5. SC912 caused proliferation arrest and apoptosis in AR-V7 positive CRPC cells.

A. CellTiter-Glo assays for evaluating the antiproliferative effect of SC912 in CRPC cells. HP-LNCaP, VCaP, 22Rv1, and PC3 cells were seeded in androgen-free media for 24 h before being treated with DMSO, ENZ, or SC912 at designated doses. Cell culture media and corresponding treatments were refreshed once on day 3, and cell viability was measured on day 6. Data represent the average ± SD of three separate experiments.

B. Cell cycle compartment flow cytometry for assessing SC912 induced growth arrest in CRPC cells. HP-LNCaP, VCaP, 22Rv1, and PC3 cells were cultured in androgen-free media for 48 h before being treated with DMSO, 3 μM ENZ, or 1 μM SC912 for 24 h. Cells were pulsed with BrDU for 1h prior to harvest. G1 and G2/M-phase cells were defined as cells that show no BrDU staining and possess 1N/2N DNA content respectively. S-phase cells were defined as cells that were positive for BrdU staining.

C. Western blot analysis of SC912 induced apoptosis in CRPC cells. HP-LNCaP, VCaP, 22Rv1, and PC3 cells were cultured in androgen-free media for 48 h and subsequently treated with 3 μM ENZ or 1 μM SC912 for 0, 12, or 24 h before being harvested.

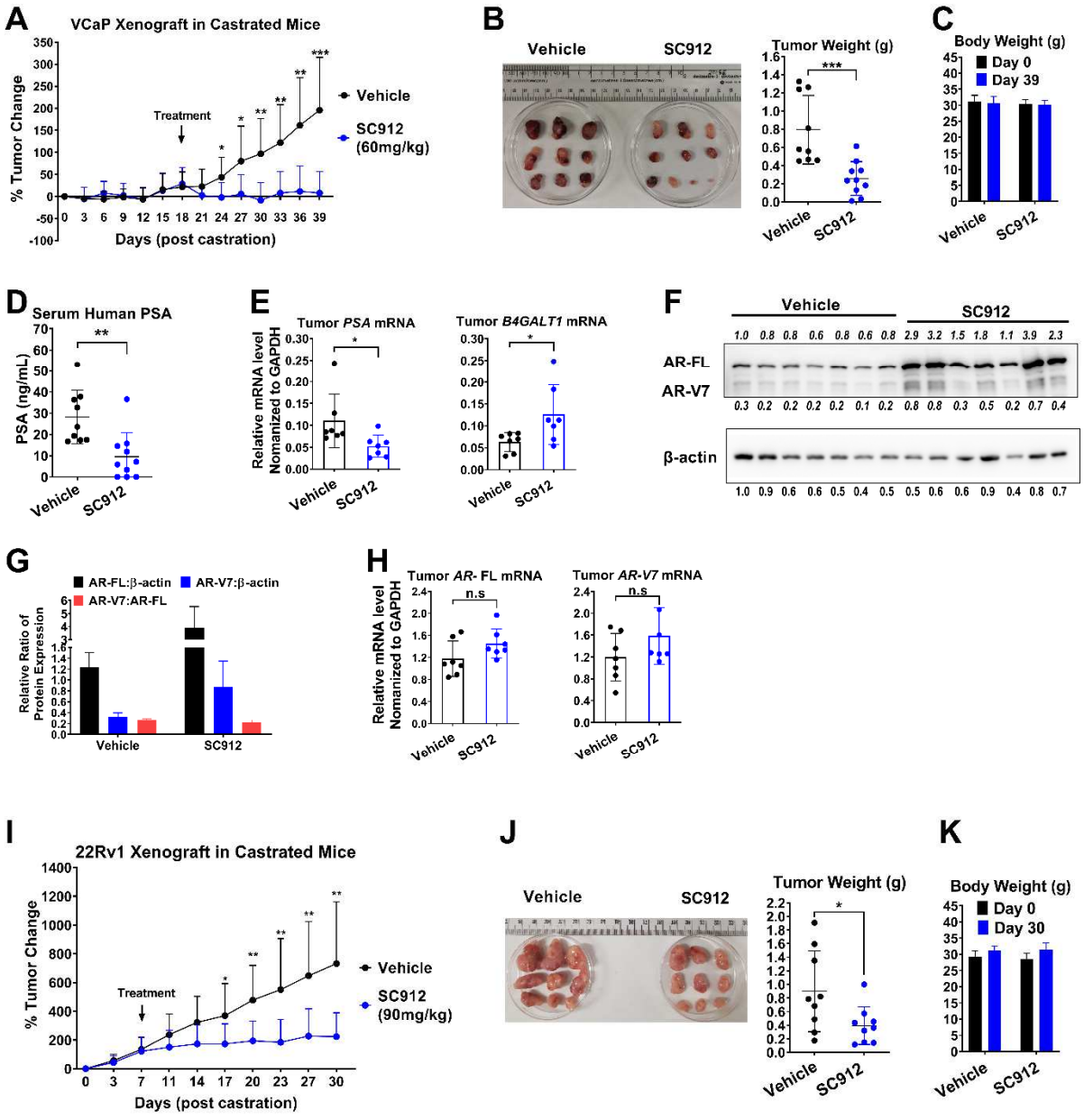
A
VCaP Xenograft in Castrated Mice
% Tumor Change
Treatment
Vehicle
SC912 (60mg/kg)
Days (post castration)
B
Vehicle
SC912
Tumor Weight (g)
C
Body Weight (g)
Day 0
Day 39
D
Serum Human PSA
PSA (ng/mL)
E
Tumor PSA mRNA
Tumor B4GALT1 mRNA
Relative mRNA level Nomanized to GAPDH
F
AR-FL
AR-V7
β-actin
G
AR-FL:β-actin
AR-V7:β-actin
AR-V7:AR-FL
Relative Ratio of Protein Expression
H
Tumor AR- FL mRNA
Tumor AR-V7 mRNA
n.s
I
22Rv1 Xenograft in Castrated Mice
SC912 (90mg/kg)
J
K
Body Weight (g)
Day 0
Day 30

3.6.6. Figure M2-6. SC912 repressed tumor growth and interrupted AR signaling in AR-V7 expressing CRPC xenografts.

A-H. SC912 abolished the growth of VCaP xenografts in castrated mice. 1×10^7 VCaP cells mixed with 50% matrigel were subcutaneously injected into the right flank of male NOD-SCID mice. When tumor size reached 250−500 mm^3, mice were surgically castrated and monitored daily (Day 0). After the tumors resumed growing and reached the size of 300−600 mm^3 (Day 18), mice were randomized into 2 groups (n=9-10), which received 5 days per week treatment (i.p.) of vehicle or SC912 (60 mg/kg) for 3 weeks before sacrifice (Day 39). **A,** VCaP tumor growth curve (n=9-10). The % Tumor Change was calculated as (Day39- Day0)/Day0 %. **B,** Tumor image and weight on Day 39 (n=9-10). **C,** ELISA assay of human PSA concentration in mouse serum (n=9-10). **D,** Mouse body weight comparison on Day 0 and Day 39 (n=9-10). **E,** qRT-PCR analysis of AR-regulated gene expression in tumors (n=7). **F,** Western blot analysis of AR-FL and AR-V7 protein expression in tumor (n=7). **G,** Quantification of AR-FL and AR-V7 protein levels (n=7). **H,** qRT-PCR analysis of AR-FL and AR-V7 mRNA expression in tumors (n=7).

G-J. SC912 suppressed the growth of AR-V7 high-expressing 22Rv1 tumors in castrated mice. 5×10^6 22Rv1 cells mixed with 50% matrigel were subcutaneously injected into the right flank of male Nu/Nu mice. When tumor size reached 100−300 mm^3, mice were surgically castrated and monitored daily (Day 0). Animals were allowed to recover from surgery for one week and tumors reached the size of 150−450 mm^3. Mice were then randomized into 2 groups (n=9), which received treatment (i.p.) of vehicle or SC912 (90 mg/kg) 5 days a week for 3 weeks before sacrifice (Day 30). **I,** 22Rv1 tumor growth curve (n=9). **J,** Tumor image and weights on Day 30 (n=9). **K,** Mouse body weight comparison on Day 0 and Day 30 (n=9).

3.7. Supplementary Information

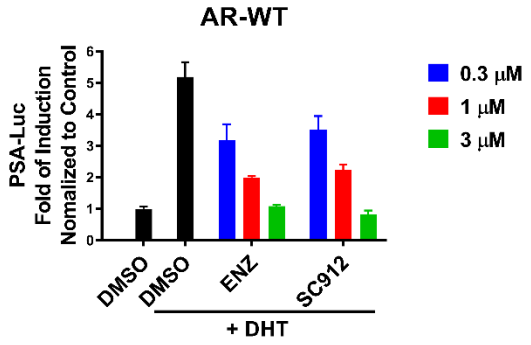

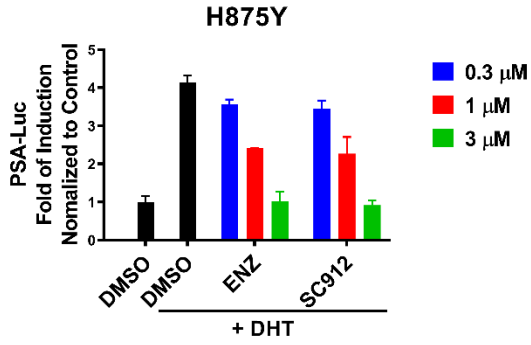

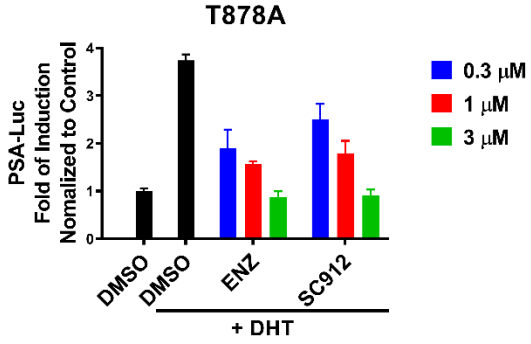

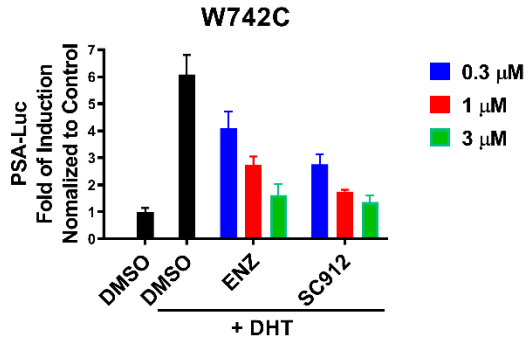

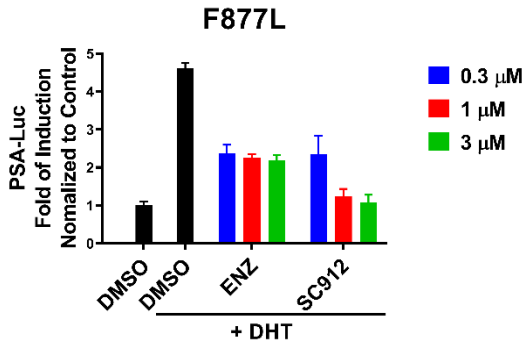

3.7.1. Figure M2-S1. SC912 inhibited the transactivation of AR-FL and its clinically relevant LBD mutants.

PC3 cells were transiently transfected with PSA-Luc reporter plasmid, pRL-TK, and a plasmid expressing AR-FL or its LBD mutants as indicated in the specific panel. Cells were pretreated in androgen-free media with DMSO, ENZ (0.3, 1, 3 μM), or SC912 (0.3, 1, 3 μM) for 30 min, followed by the addition of 10 nM DHT for 24 h. Relative PSA-Luc reporter activity was normalized to the DMSO treated without DHT stimulated samples. Data represent the average ± s.d. of duplicate samples.

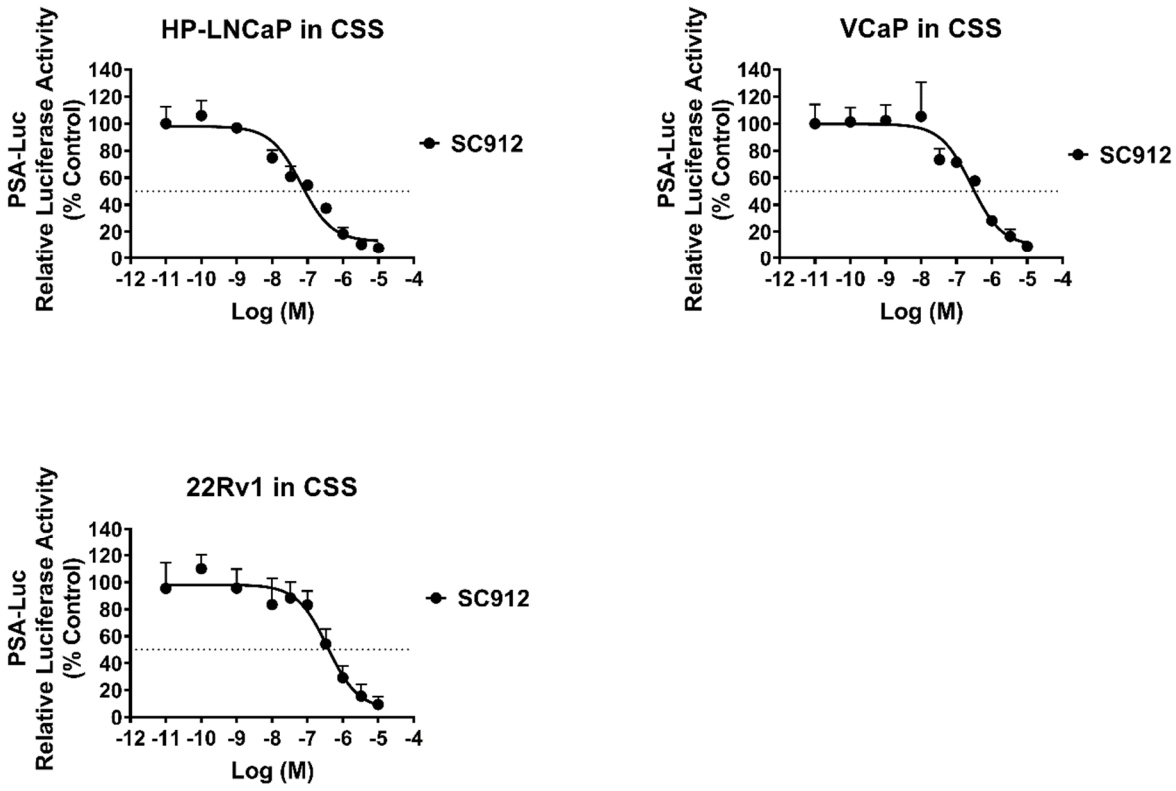

3.7.2. Figure M2-S2. SC912 inhibited the androgen-independent AR signaling in CRPC cell lines.

HP-LNCaP, VCaP, or 22Rv1 cells were cultured in androgen-free media for 48 h before being transfected with PSA-Luc and pRL-TK reporter plasmids. Cells were then treated with ENZ or SC912 at designated doses for 24 h. Relative PSA-Luc reporter activity was normalized to the DMSO treated samples. Data represent the average ± SD of duplicate samples.

Estimated IC50 (μM)		
Cell Line	ENZ IC50	SC112 IC50
HP-LNCaP	1.76	0.31
VCaP	9.88	0.60
22Rv1	28.90	0.86
PC3	27.74	5.77

3.7.3. Figure M2-S3. Estimated antiproliferation IC50 of SC912 in CRPC cell lines.

The IC50 of SC912 and ENZ from the CellTiter-Glo assay in **Figure. 5A** was calculated using GraphPad Prism 9.0, based on the nonlinear fit curve presented in **Figure. 5A**.

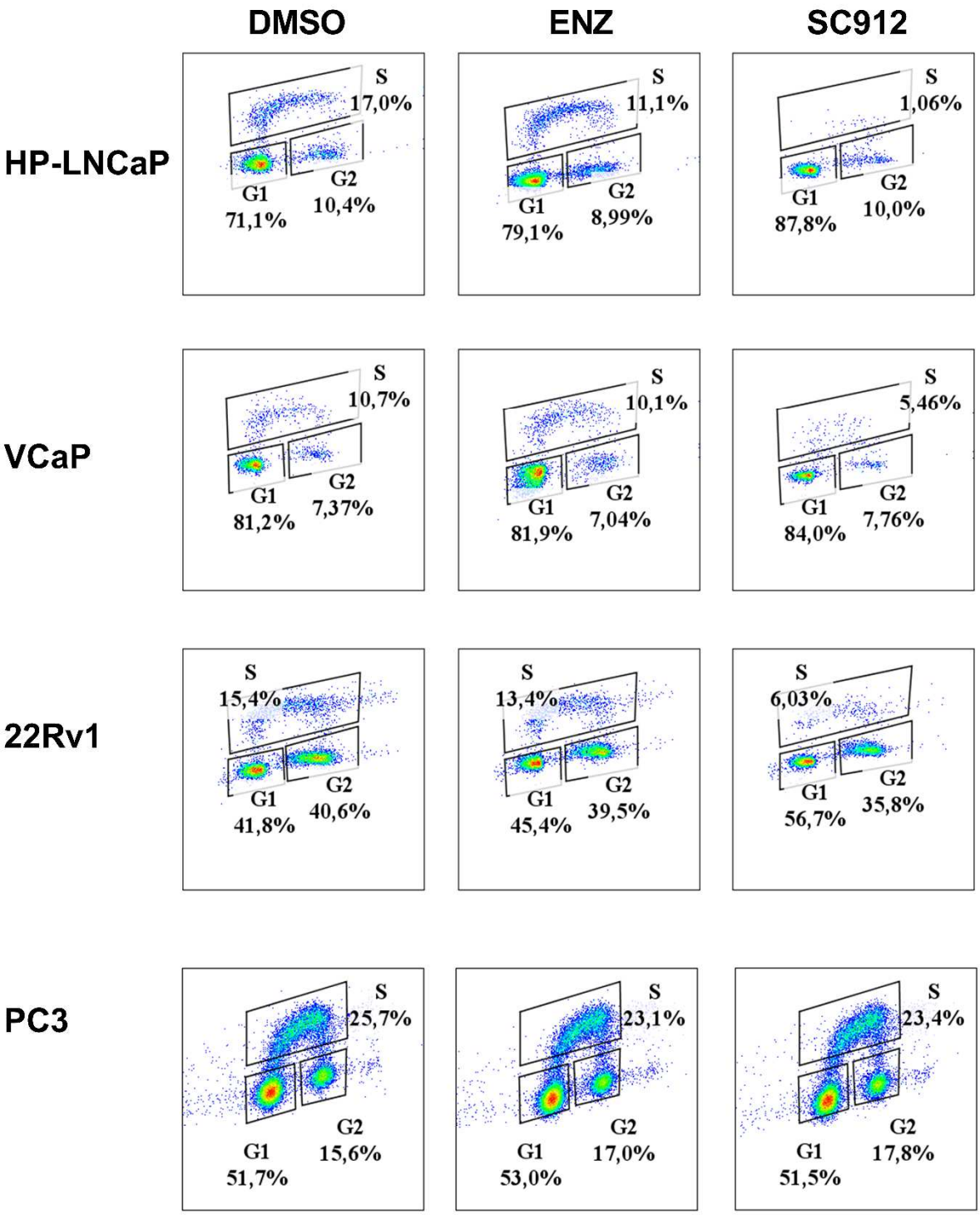

3.7.4. Figure M2-S4. SC912 caused cell cycle arrest in CRPC cell lines.

The flow cytometry scatterplots for the bar graph in **Figure. 5B,** which summarizes SC912 treatment induced G1 arrest in AR-V7 positive CRPC cells.

3.8.Manuscript 2 References

1 Andersen RJ, Mawji NR, Wang J, Wang G, Haile S, Myung J-K *et al*. Regression of castrate-recurrent prostate cancer by a small-molecule inhibitor of the amino-terminus domain of the androgen receptor. Cancer cell 2010; 17: 535-546.

2 Annala M, Taavitsainen S, Khalaf DJ, Vandekerkhove G, Beja K, Sipola J *et al*. Evolution of Castration-Resistant Prostate Cancer in ctDNA during Sequential Androgen Receptor Pathway InhibitionProstate Cancer Evolution during Sequential AR Inhibition. Clinical Cancer Research 2021; 27: 4610-4623.

3 Antonarakis ES, Lu C, Wang H, Luber B, Nakazawa M, Roeser JC *et al*. AR-V7 and resistance to enzalutamide and abiraterone in prostate cancer. New England Journal of Medicine 2014; 371: 1028-1038.

4 Antonarakis ES, Lu C, Luber B, Wang H, Chen Y, Nakazawa M *et al*. Androgen receptor splice variant 7 and efficacy of taxane chemotherapy in patients with metastatic castration-resistant prostate cancer. JAMA oncology 2015; 1: 582-591.

5 Asangani IA, Dommeti VL, Wang X, Malik R, Cieslik M, Yang R *et al*. Therapeutic targeting of BET bromodomain proteins in castration-resistant prostate cancer. Nature 2014; 510: 278-282.

6 Cato L, de Tribolet-Hardy J, Lee I, Rottenberg JT, Coleman I, Melchers D *et al*. ARv7 represses tumor-suppressor genes in castration-resistant prostate cancer. Cancer cell 2019; 35: 401-413. e406.

7 Chan SC, Li Y, Dehm SM. Androgen receptor splice variants activate androgen receptor target genes and support aberrant prostate cancer cell growth independent of canonical androgen receptor nuclear localization signal. Journal of Biological Chemistry 2012; 287: 19736-19749.

8 Cornford P, van den Bergh RC, Briers E, Van den Broeck T, Cumberbatch MG, De Santis M *et al*. EAU-EANM-ESTRO-ESUR-SIOG guidelines on prostate cancer. Part II—2020 update: treatment of relapsing and metastatic prostate cancer. European urology 2021; 79: 263-282.

9 Dalal K, Che M, Que NS, Sharma A, Yang R, Lallous N *et al*. Bypassing Drug Resistance Mechanisms of Prostate Cancer with Small Molecules that Target Androgen Receptor–Chromatin InteractionsTargeting Androgen Receptor Interactions with Chromatin. Molecular cancer therapeutics 2017; 16: 2281-2291.

10 Dalal K, Ban F, Li H, Morin H, Roshan-Moniri M, Tam KJ *et al*. Selectively targeting the dimerization interface of human androgen receptor with small-molecules to treat castration-resistant prostate cancer. Cancer Letters 2018; 437: 35-43.

11 De Bono JS, Logothetis CJ, Molina A, Fizazi K, North S, Chu L *et al*. Abiraterone and increased survival in metastatic prostate cancer. New England Journal of Medicine 2011; 364: 1995-2005.

12 De Mol E, Szulc E, Di Sanza C, Martínez-Cristóbal P, Bertoncini CW, Fenwick RB *et al*. Regulation of androgen receptor activity by transient interactions of its transactivation domain with general transcription regulators. Structure 2018; 26: 145-152. e143.

13 Dehm SM, Schmidt LJ, Heemers HV, Vessella RL, Tindall DJ. Splicing of a novel androgen receptor exon generates a constitutively active androgen receptor that mediates prostate cancer therapy resistance. Cancer research 2008; 68: 5469-5477.

14 Esquenet M, Swinnen JV, Heyns W, Verhoeven G. LNCaP prostatic adenocarcinoma cells derived from low and high passage numbers display divergent responses not only to androgens but also to retinoids. The Journal of steroid biochemistry and molecular biology 1997; 62: 391-399.

15 Hu R, Isaacs WB, Luo J. A snapshot of the expression signature of androgen receptor splicing variants and their distinctive transcriptional activities. The Prostate 2011; 71: 1656-1667.

16 Kanayama M, Lu C, Luo J, Antonarakis ES. AR splicing variants and resistance to AR targeting agents. Cancers 2021; 13: 2563.

17 Lavery DN, McEwan IJ. Structural characterization of the native NH2-terminal transactivation domain of the human androgen receptor: a collapsed disordered conformation underlies structural plasticity and protein-induced folding. Biochemistry 2008; 47: 3360-3369.

18 Lee GT, Nagaya N, Desantis J, Madura K, Sabaawy HE, Kim W-J *et al*. Effects of MTX-23, a Novel PROTAC of Androgen Receptor Splice Variant-7 and Androgen Receptor, on CRPC Resistant to Second-Line Antiandrogen TherapyMTX-23, a Novel PROTAC That Degrades AR-V7 and AR-FL. Molecular cancer therapeutics 2021; 20: 490-499.

19 Li Y, Yang R, Henzler CM, Ho Y, Passow C, Auch B *et al*. Diverse AR Gene Rearrangements Mediate Resistance to Androgen Receptor Inhibitors in Metastatic Prostate CancerAR Gene Rearrangements in Prostate Cancer. Clinical Cancer Research 2020; 26: 1965-1976.

20 Liang J, Wang L, Poluben L, Nouri M, Arai S, Xie L *et al*. Androgen receptor splice variant 7 functions independently of the full length receptor in prostate cancer cells. Cancer Letters 2021; 519: 172-184.

21 Liu C, Armstrong CM, Ning S, Yang JC, Lou W, Lombard AP *et al*. ARVib suppresses growth of advanced prostate cancer via inhibition of androgen receptor signaling. Oncogene 2021; 40: 5379-5392.

22 Liu L, Xie N, Sun S, Plymate S, Mostaghel E, Dong X. Mechanisms of the androgen receptor splicing in prostate cancer cells. Oncogene 2014; 33: 3140-3150.

23 Melnyk JE, Steri V, Nguyen HG, Hwang YC, Gordan JD, Hann B *et al*. Targeting a splicing-mediated drug resistance mechanism in prostate cancer by inhibiting transcriptional regulation by PKCβ1. Oncogene 2022; 41: 1536-1549.

24 Moilanen A-M, Riikonen R, Oksala R, Ravanti L, Aho E, Wohlfahrt G *et al*. Discovery of ODM-201, a new-generation androgen receptor inhibitor targeting resistance mechanisms to androgen signaling-directed prostate cancer therapies. Scientific reports 2015; 5: 1-11.

25 Mollica L, Bessa LM, Hanoulle X, Jensen MR, Blackledge M, Schneider R. Binding mechanisms of intrinsically disordered proteins: theory, simulation, and experiment. Frontiers in molecular biosciences 2016; 3: 52.

26 Monaghan AE, McEwan IJ. A sting in the tail: the N-terminal domain of the androgen receptor as a drug target. Asian Journal of Andrology 2016; 18: 687.

27 Myung J-K, Banuelos CA, Fernandez JG, Mawji NR, Wang J, Tien AH *et al*. An androgen receptor N-terminal domain antagonist for treating prostate cancer. The Journal of clinical investigation 2013; 123: 2948-2960.

28 Ponnusamy S, He Y, Hwang D-J, Thiyagarajan T, Houtman R, Bocharova V *et al*. Orally Bioavailable Androgen Receptor Degrader, Potential Next-Generation Therapeutic for Enzalutamide-Resistant Prostate CancerA Novel AR Degrader for the Treatment of Prostate Cancer. Clinical Cancer Research 2019; 25: 6764-6780.

29 Potter GA, Barrie SE, Jarman M, Rowlands MG. Novel steroidal inhibitors of human cytochrome P45017. alpha.-Hydroxylase-C17, 20-lyase): potential agents for the treatment of prostatic cancer. Journal of medicinal chemistry 1995; 38: 2463-2471.

30 Reid J, Murray I, Watt K, Betney R, McEwan IJ. The androgen receptor interacts with multiple regions of the large subunit of general transcription factor TFIIF. Journal of Biological Chemistry 2002; 277: 41247-41253.

31 Sadar MD. Discovery of drugs that directly target the intrinsically disordered region of the androgen receptor. Expert opinion on drug discovery 2020; 15: 551-560.

32 Scher HI, Fizazi K, Saad F, Taplin M-E, Sternberg CN, Miller K *et al*. Increased survival with enzalutamide in prostate cancer after chemotherapy. New England Journal of Medicine 2012; 367: 1187-1197.

33 Schweizer MT, Antonarakis ES, Wang H, Ajiboye AS, Spitz A, Cao H *et al*. Effect of bipolar androgen therapy for asymptomatic men with castration-resistant prostate cancer: results from a pilot clinical study. Science translational medicine 2015; 7: 269ra262-269ra262.

34 Shaffer PL, Jivan A, Dollins DE, Claessens F, Gewirth DT. Structural basis of androgen receptor binding to selective androgen response elements. Proceedings of the National Academy of Sciences 2004; 101: 4758-4763.

35 Sharp A, Coleman I, Yuan W, Sprenger C, Dolling D, Rodrigues DN *et al*. Androgen receptor splice variant-7 expression emerges with castration resistance in prostate cancer. The Journal of clinical investigation 2019; 129: 192-208.

36 Tran C, Ouk S, Clegg NJ, Chen Y, Watson PA, Arora V *et al*. Development of a second-generation antiandrogen for treatment of advanced prostate cancer. Science 2009; 324: 787-790.

37 Tsafou K, Tiwari P, Forman-Kay J, Metallo SJ, Toretsky J. Targeting intrinsically disordered transcription factors: changing the paradigm. Journal of molecular biology 2018; 430: 2321-2341.

38 Uo T, Plymate SR, Sprenger CC. The potential of AR-V7 as a therapeutic target. Expert Opinion on Therapeutic Targets 2018; 22: 201-216.

39 Watson PA, Arora VK, Sawyers CL. Emerging mechanisms of resistance to androgen receptor inhibitors in prostate cancer. Nature Reviews Cancer 2015; 15: 701-711.

40 Welti J, Rodrigues DN, Sharp A, Sun S, Lorente D, Riisnaes R *et al*. Analytical validation and clinical qualification of a new immunohistochemical assay for androgen receptor splice variant-7 protein expression in metastatic castration-resistant prostate cancer. European urology 2016; 70: 599-608.

41 Welti J, Sharp A, Brooks N, Yuan W, McNair C, Chand SN *et al*. Targeting the p300/CBP Axis in Lethal Prostate CancerTargeting the p300/CBP Axis in Lethal Prostate Cancer. Cancer discovery 2021; 11: 1118-1137.

42 Yu Z, Chen S, Sowalsky AG, Voznesensky OS, Mostaghel EA, Nelson PS *et al*. Rapid Induction of Androgen Receptor Splice Variants by Androgen Deprivation in Prostate CancerAndrogen Repression of AR Splice Variant. Clinical cancer research 2014; 20: 1590-1600.

43 Zhu Y, Dalrymple SL, Coleman I, Zheng SL, Xu J, Hooper JE *et al*. Role of androgen receptor splice variant-7 (AR-V7) in prostate cancer resistance to 2nd-generation androgen receptor signaling inhibitors. Oncogene 2020; 39: 6935-6949.

Bridging Text 2

In addition to the above projects dedicated to the discovery of AR-NTD-targeting inhibitors, a secondary aspect of my PhD studies was devoted to exploring the therapeutic potential of inducing T-cell mediated anti-tumoral immunity, through a novel chemical agonist of Stimulator of Interferon Gene (STING). Below is a brief background summary of current understanding of the immune landscape in prostate cancer and STING biology followed by a manuscript detailing the preliminary results of STING agonist discovery.

Prostate cancer microenvironment

Prostate cancer is considered particularly "immune-cold", evidenced by the immunosuppressive microenvironment and unresponsiveness to immune checkpoint blockade in clinical trials. Pathologic examination of prostate cancer specimens revealed the tumor infiltrated lymphocyte was skewed towards a regulatory T cell and T helper 17 population [286], which were known to suppress antitumor immune responses, and has been associated with shorter disease-free survival in prostate cancer patients[287]. Mechanistic studies and clinical analysis further uncovered that androgen deprivation therapy (ADT)-induced pro-immune response in the early post-treatment period featured increased tumor infiltration of various immune cells including $CD4^+$ T cells, $CD8^+$ T cells, NK cells, and macrophages[288, 289]. However, this ADT-induced immune-stimulating response quickly diminished as treatment resistance emerged[290, 291]. Moreover, a recent clinical study observed down-regulated antigen presentation during castration-resistant prostate cancer (CRPC) progression; furthermore, in CRPC biopsy, tumor cell MHC class I expression is inversely correlated with nuclear AR concentration and AR-regulated gene expression[292]. These

findings suggested that prostate cancer acquires immune resistance during progression towards CRPC and hinted at possible mutual resistance drivers for ADT and immunotherapy.

Immunotherapy in prostate cancer

Immune checkpoint blockade has revolutionized the cancer treatment paradigm, inducing an unprecedented response rate with durable anti-tumor immunity in solid tumors. Unfortunately, immunotherapy treatments reported largely disappointing efficacies in patients with prostate cancer. To date, sipuleucel-T represents the only immunotherapy approved by FDA for metastatic CRPC, however, the use of this agent is relatively limited in clinical practice. Furthermore, multiple immune checkpoint inhibitors assessed in clinical trials demonstrated very moderate benefits. In two phase III trials, the cytotoxic T-lymphocyte antigen-4 (CTLA-4) inhibitors Ipilimumab did not improve overall survival for radiotherapy-relapsed nor chemotherapy-naïve CRPC patients[293, 294]. In a phase II trial, the monoclonal antibody against programmed death receptor 1 (PD-1) pembrolizumab only achieved partial disease control in a small subset of metastatic CRPC patients[295]. Similarly, the monoclonal antibody against programmed death-ligand 1 (PD-L1) atezolizumab also failed to show significant benefits in patients with metastatic CRPC[296]. The dual inhibition of immune checkpoints of CTLA-4 and PD-1 (ipilimumab plus nivolumab) for metastatic CRPC only yielded complete response in 4 out of 90 patients, suggesting limited efficacy even for combinational immune therapies[297]. Interestingly, it is noteworthy that prostate cancer under treatment of abiraterone showed a downregulation of PD-L1 expression in the tumors. The variations in PD-L1 expression in prostate tumors partly suggest that the levels of immune checkpoint molecule expression vary in different stages of prostate cancer progression, in response to ADT[291]. Therefore, current mainstay immunotherapy of checkpoint blockade

demonstrated limited efficacy in prostate cancer, and alternative approaches of improving effector T cell function was required for immunotherapy against CRPC.

STING as innate cytosolic DNA sensor for tumor surveillance

STING was originally identified as a mediator of mammalian cell defense against microbial infections. Canonically, after pathogens invade a host cell, bacterial cyclic dinucleotides (CDNs) directly bind to and activate host-STING, leading to IFN (interferon) and other proinflammatory signaling cascades. In addition to bacterial CDNs, follow-up discoveries have proven that STING is also involved in detecting other sources of cytosolic DNA, such as viral DNA and host self-DNA. Moreover, subsequent studies have also indicated that STING pathway is even capable of mediating anti-tumor immunity through recognizing tumor-derived DNA in tumor infiltrated DCs (dendritic cells).

Multiple clinical observations confirmed that the presence of infiltrating $CD8^+$ T cells in tumor biopsy is associated with favorable outcomes [298, 299]. Gene expression analysis of clinical tumors further revealed that a type-I IFN gene signature positively correlates with the tumor infiltration of $CD8^+$ T cell [300], which together implies that the priming of $CD8^+$ T cells is initiated or aided by an upstream event leading to type-I IFN release. A mechanistic study using IFN gene knockout mice showed abolished T cell response against tumor antigens accompanied by increased tumor incidence [301]. The failure of T-cell response in $IFN^{-/-}$ mice has been traced down to being caused by a lack of intratumoral $CD8^+\alpha$ DC that normally serves as APC (antigen-presenting cell) for T-cell cross-priming [302]. These studies together hinted that there indeed exists a type-I IFN pathway within the DC leading to spontaneous T-cell response, which is indispensable for immune sensing of tumors.

Follow-up research have attributed the STING pathway as the main type-I IFN synthesis pathway in DCs and confirmed its essential role in anti-tumor immunity. Hyperactive STING mutants were recently identified in patients with inflammatory syndrome characterized by excessive IFN production [303]. More recent studies demonstrated that $STING^{-/-}$ mice have substantially reduced IFN gene signature in tumor tissue and more aggressive tumor growth [304]. In a landmark study, Woo and colleagues have established that STING-deficient mice are defective in T-cell cross-priming against tumor antigens and consequently more susceptible to tumorigenic events [305]. Furthermore, they have detected tumor-derived DNA within the cytosol of most tumor-resident DCs [305]. Overall, these observations bridged STING's role in tumor DNA detection with immune suppression of tumor growth.

Collectively, these pioneer studies depict a new model of tumor immune surveillance: upon entering DC cytosol, tumor-derived DNA is recognized by STING, consequently inducing IFN production that leads to further APC activation, presenting of tumor specific antigens to naïve $CD8^+$ T cells, and cumulating in a spontaneous anti-tumor T-cell response. The clinical translation for STING stimulation was therefore encouraged under the hypothesis that adequate STING induction in TME is very likely to have immuno-therapeutic potential.

Clinical trials of STING agonists

The first breakthrough study exhibiting the clinical potential of STING activation used a small molecule STING-agonist compound DMXAA [306] to induce almost complete mouse tumor regression. However, there remained ambiguity as to whether DMXAA's antitumor was due to STING or through an alternate mechanism, given DMXAA is also a vascular disrupting agent. Later investigation firmly established that DMXAA's primary mode of action is via STING

induction by comparing treatment efficacy between wild type, STING-deficient, and typeI IFN receptor deficient mice. In addition to a greater degree of tumor shrinkage, DMXAA-treated wild-type mice also displayed a greater number of tumor-antigen specific $CD8^+$ T cells among the splenocyte, which represents elevated tumor-oriented immunity [307]. Despite potent antitumor activity on mice, DMXAA failed human clinical trials because of its species-specific binding affinity which only limits to mouse but not human STING.

The current strategy of human STING agonist development is synthetic cyclic dinucleotide compounds that mimic the structure of bacterial CDNs with modifications for improving potency and biostability[307, 308]. The initial effect in animal studies are impressive; intertumoral injection of synthetic CDNs directly activated STING in TME, promoted robust tumor-antigen specific $CD8^+$ T cells generation and resulted in striking tumor regression in a wide spectrum of tumor models[307]. Encouragingly, local administration of synthetic CDNs was found to harness systemic immune responses which consolidated immunologic memory and metastasis blockage[307].

Two CDN-based-STING agonists ADU-S100 (Aduro) and MK1454 (Merck), are in multiple ongoing clinical studies. According to results of phase I trial (NCT02675439) aiming at determining safety and dosage, ADU-S100 only demonstrated limited therapeutic effect as monotherapy in advanced melanoma patients who have relapsed after or are refectory to anti-PD-1 antibodies. 2/41 patients experienced partial response and 11/41 patients showed stable disease. The other phase Ib trial (NCT03172936) in patients with advanced or metastatic solid tumors or lymphoma, ADU-S100 was co-treatment with spartalizumab an anti-PD-L1 antibody. The rationale of combination therapy is backed up by early synergistic antitumor effect of STING

agonist and immune checkpoint inhibitors in preclinical models. When combined with spartalizumab, partial response was observed in patients with PD-1-naïve TNBC and PD-1-relapsed/refractory melanoma. Based on the similar premise, a phase 2 trial (NCT03937141) of coupling ADU-S100 with Pembrolizumab (anti-PD-L1 antibody) is currently in the enrolling stage of patients with metastatic head and neck squamous cell carcinoma. The other STING agonist MK-1454 is tested in a Phase I clinical trial (NCT03010176) as monotherapy and in combination with Pembrolizumab in patients with solid tumor or lymphoma. Patients who received MK-1454 alone did not exhibit a complete or partial response, while 20% of the patients showed stable disease. Patients who received MK-1454 plus Pembrolizumab showed a partial response in 24% of patients (6/25, including 3 with HNSCC, 1 with TNBC, and 2 with anaplastic thyroid carcinoma) and 24% of patients (6/25) showed stable disease. Induction of systemic type-I interferon response has been demonstrated; however, little intra-tumor data has been disclosed. Given the encouraging efficacy and acceptable safety profile of MK-1454 and Pembrolizumab combination, another Phase II clinical trial (NCT04220866) of such treatment paradigm is currently recruiting metastatic or recurrent head and neck squamous cell carcinoma.

Both STING agonists as monotherapy only demonstrated marginal therapeutic effect in patients, in contrary to their drastic anti-tumor immunity stimulating compacity demonstrated in preclinical models. The possible contributing factors of such a difference could include serval aspects: CDNs are suspectable to degradation by extracellular phosphodiesterase at the phosphodiester linkage of cAMP and cGMP[309, 310]. Therefore, pharmacological stimulation of STING using natural CDNs was discouraged when rapid clearance was found for intratumorally delivered CDNs and only marginally efficacy was shown for intravenously injected CDNs. Through chemical modification of phosphodiester bond into phosphorothioate bond, ADU-S100 possesses

remarkably improved hydrolytic stability comparing to pathogen-derived CDNs, therefore is more appealing for clinical development. Nonetheless, the lack of biostability remains a bottleneck for ADU-S100, as intratumoral injection is the only viable route in clinical trials whereas systemic administration of such drugs is still not enabled. Therefore, the necessity for intratumoral injection to achieve maximal therapeutic effect narrowed the drug evaluation and application only to the accessible tumors, such as melanoma, lymphoma, head and neck carcinoma and breast cancer. While most types of tumors missed the chance to be assessed for the discovery of potentially more responsive tumor types. Likewise, lack of feasibility for systemic delivery also limited the efficacy of ADU-S100 in patients with metastasis, a major hurdle given that metastatic dissemination remains the leading cause of cancer-associated mortality[311]. In addition to inadequate drug concentration in the distal lesion, tumor genetic divergence[312, 313] and microenvironment variation are potential factors which limit anti-tumoral immunity response at metastatic sites. Lastly, tumor heterogeneity increases the likelihood of immune escaping, it was also recently demonstrated that patients with more heterogenous tumors respond less to checkpoint blockade immunotherapy [314]. Naturally arising tumors in patients possess highly diverse subclones relative to cell line implantation-derived murine tumors used in CDN preclinical evaluation, thus intrinsic tumor heterogeneity could theoretically also be a cause of dampened therapeutic effect of CDN-based drugs in clinical trials.

Approaches for improving STING agonist monotherapy

On the premise to enable the systemic administration and enhance the intracellular delivery of STING agonist, efforts have been devoted in developing optimal drug carriers for CDN compounds. CDNs could be encapsulated in lipophilic nanoparticles that readily penetrate cell

membrane and subsequently disassemble in response to endolysosomal acidification to promote cytosolic release of CDN. Preclinical evaluation of these nanoparticle vehicles revealed promising results. One STING-activating nanoparticle enhanced CDN immunotherapeutic efficacy against melanoma via intravenous injection[315]. Another cGAMP formulated nanoparticle enabled targeted delivery to APCs residing in breast cancer lung metastases via inhalation, resulting in immunogenic TME and tumor repression in lung metastasis sites[316].

Lastly, the approach of STING stimulation by true small molecules that are not CDN derived, hence are more drug like has also been explored. Among which, the Amidobenzimidazole-based STING agonist is the only candidate that has advanced to clinic trial stage. Amidobenzimidazole was reported suitable for systemic administration. In syngeneic colon tumor mouse model, it led to adaptive $CD8^+$ T cell response and elicited strong anti-tumor activity[317]. In an ongoing Phase I trial, this small molecule STING agonist is intravenously injected as a monotherapy or coupled with Pembrolizumab for patients with advanced solid tumor.

STING activity facilitates immune suppression

It is well established that STING stimulation in DCs indirectly promotes effector T cell clonal expansion via antigen cross-presentation-mediated T-cell activation. Contrarily, several recent studies revealed antiproliferative and proapoptotic functions of endogenous STING activation in T cells, highlighting another possible cause for undurable antitumor immunity in patients treated with STING agonists. A constitutive active STING mutant was discovered to impair CD4+ T cell proliferation[318]. Likewise, another gain of function STING mutation was reported to cause spontaneous activation and apoptotic cell death in both $CD4^+$ and $CD8^+$ T cells[319]. Another

study further explain that STING agonist only primes apoptosis in $CD4^{+}$T cells and cancerous T cells but not in innate immune cells such as DCs and macrophages, indicating that STING activation promoted apoptosis is T cell specific. The underlying mechanism of such selectivity is substantially higher STING protein level in T cells that conveys intensified STING response upon stimulation, therefore determines the proapoptotic cell fate. These studies collectively hinted the necessity of precise intensity controlled for STING signaling agonism to achieve sufficient innate immune cell activation while avoiding exhausting T cells[320]. Indeed, a study using various dosages of clinical CDN (ADU-S100) discovered that the magnitude of STING signaling determines the induction of apoptotic programs in T cells; lower dosing regimen is more immunogenic by mitigating T cell death and improving T cell activation[321].

Emerging evidence also unveiled that STING activity in tumor cells may play a crucial role in facilitating an immune-suppressive tumor microenvironment. The Hou lab uncovered a clinically observable upregulated STING expression during the progression of HPV+ tongue squamous small cell carcinoma (SSCC). Additionally, activation of STING in SSCC cells promoted secretion of immunosuppressive cytokines which drives the infiltration of Tregs[322]. Concordantly, the Weichselbaum lab discovered that radiotherapy-induced STING activation in colon tumor cells enhances suppressive inflammation in tumors by facilitating the influx of circulating myeloid derived suppressor cells (MDSC), which results in tumor radioresistance[323]. However, Cui and collogues found, in nasopharyngeal carcinoma, that tumor endogenous STING functions to repress tumor resident MDSC differentiation thus helping to maintain immunogenic microenvironment[324]. These conflicting studies painted a mixed picture of tumor cell STING's role in shaping the immune landscape in tumor microenvironment, thus additional studies will be required to optimize the treatment regimen of STING agonist for specific tumor types.

Tumor cells acquire immune quiescence status in response to STING agonist

While immune cells response to STING stimulation has long been the major focus of assessing antitumor effect of STING agonist, little is known about the outcome of tumor cells' autonomous response to their intrinsic STING pathway activation. Recent works have revealed an important link between tumor cell STING activation and acquired T cell resistance, thus helping tumor cells bypass immune surveillance. Intratumoral injection of synthetic CDN was observed to trigger markedly upregulated PD-L1 expression on B16 melanoma cells, and combination treatment of CDN based STING agonist with PD-L1 inhibitor was shown to cure poorly immunogenic CT26 colon cancer tumors that do not respond to PD-L1 blockade alone[325]. Moreover, Lim and collogues have discovered that proinflammatory cytokine TNF-α mediates deubiquitylation and stabilization of PD-L1 in 4T1 breast cancer tumor and convey T cell suppression[326]. Although the correlation with STING was not directly proven, TNF-α is one of the key cytokines secreted by tumor cells upon STING pathway activation[327], which raises a unique prospect of STING pathway in cancer cells to modulate immune checkpoint molecules for immune invasion. Concordantly, multiple studies reported synergy between STING agonist and immune checkpoint inhibitors in different mouse tumor models [328] [315, 321] [329], which also agrees with improved therapeutic effect when pairing ADU-S100 with anti-PD-L1 in clinic trails.

STING activation in tumor cells plays bipolar roles

In addition to STING's role in regulating immune cells, another emerging element to consider is cancer-cell intrinsic activation of STING, which has been demonstrated to either suppress or promote tumor progression depending on the specific context[330]. Indeed, analysis of cGAS/STING mRNA protein levels in cancer tissues revealed mixed results. In colorectal cancer

[331] and melanoma [332], lower cGAS/STING levels correlated with cancer progression, while reverse trends are seen in pancreatic ductal adenocarcinoma [333] and head-and-neck squamous cell carcinoma [334], highlighting that the phenotypical outcome of tumor cell autonomous STING activation is likely very diverse and should also be taken into consideration when designing the treatment regime for STING agonist.

Tumor cells generally harbour high magnitude of chromosomal instability, which is the main source of cytosolic DNA to activate STING [335]. STING pathway activation leads to IRF3 and NF-κB mediated transcription of pro-inflammatory genes, triggering cell senescence, autonomous tumor cell death and immune-mediated clearance which is well documented and reviewed [336]; thus, cancer cells are commonly found with adaptations to dampen STING expression/activity and to tolerate chromosomal instability. Uncovered mechanisms include epigenetic silencing of STING gene [337], STING protein post-translational modification [338], STING protein degradation [339], and disrupting STING pathway downstream cascade [340] [341]. STING gene promoter was found hyper methylated in a subset of patient tumors compared to normal tissue counterparts [342], suggesting epigenetic silencing being a mechanism of tumor cells downregulating STING on the transcriptional level. In KRAS mutated NSCLC (non-small cell lung cancer) cell lines, DNA hypermethylation is uniquely concentrated in STING promoter region and leads to suppressed STING expression; ectopic expression of STING restored the cell ability of sensing pathologic accumulation of mitochondria dsDNA and consequently impaired the fitness of those cells [337]. In ovarian cancer cell lines, deubiquitinase USP35 was found to bind to and inactivate STING by catalyzing the removal of ubiquitin moieties from STING protein. Silencing of USP35 harnessed the STING pathway activation and sensitized ovarian cancer xenografts to DNA-damage by the chemotherapeutic drug cisplatin. The clinical relevance was

indicated by overexpression of USP35 transcriptome and protein in ovarian cancer patients, as well as its correlation with reduced $CD8^+$ T cell infiltration and poor overall survival [338]. In nasopharyngeal carcinoma (NPC), where high concentration of Galectin-9 are associated with shortened survival of NPC patients, Galentin-9 was found secreted by NPC cells to mediate STING degradation via directly interacting with STING C-terminal domain thus enhancing protein ubiquitination [339]. In these specific contexts mentioned above where STING activity is suppressed for better tumor cell fitness, pharmacological STING stimulation might restore STING activity and induce autonomous tumor cell death, thus potentially synergizing with immune-mediated clearance.

Emerging evidence now also support a pro-tumor progression role of tumor cell internal STING pathway activity. STING activates the pro-inflammatory transcriptional factor NF-kB [343], which is well known to have overlapping function in regulating inflammation related tumor cell survival and metastasis. Indeed, recent work has demonstrated an important link between chronic cGAS-STING activation and metastasis. Bakhoum and colleagues uncovered that breast cancer cells utilize micronuclei as a source of cytosolic DNA to acquire constitutive activation of cGAS-STING and downstream NF-κB signaling, which promotes metastasis for MDA-MB-231 and 4T1 breast cancer tumors as well as triple-negative breast cancer PDX xenografts [344]. This study indicated another challenge for clinical application of STING agonist: that precise modulation of STING activity is required to avoid pro-metastasis downstream effector program in tumor cells.

STING activation in tumor cells leads to three potential downstream pathways with distinct outcomes

There are at least two major contributing factors to the unpredictable outcome of STING activation in cancer cells. The first is that the outcome of STING stimulation is mediated via downstream activation of three parallel signaling pathways: 1) IRF3, 2) "canonical" NF-kB mediated via the relA/p50 NF-kB subunits, and 3) "non-canonical" NF-kB mediated via the relB/p100 subunits [345-348]. While IRF3 and canonical NF-kB promotes interferon response, noncanonical NF-kB was found to suppress interferons [349]. In general, IRF3 or canonical NF-kB stimulates the interferon response, which can directly induce cell death in malignant cells via apoptosis [350] [351]. Conversely, activation of non-canonical NF-κB in cancer cells has mostly oncogenic effects. For instance, in MDA-MB-231 breast cancer cells, chromosomal instability activated STING promoted tumor metastasis via the non-canonical NF-kB pathway[352]. Likewise, activation of non-canonical NF-kB was shown to promote immunosuppression in MC38 and B16l murine tumor models in response to radiotherapy, while canonical NF-kB had the opposite effect[353]. As such, activation of STING in cancer cells can elicit different sets of downstream responses that have opposing effects on cancer cell viability.

A key determining factor influencing the specificity of downstream STING axis is STING's C-terminal tail (CTT) domain. STING CTT varies across species and impacts the capacity of STING to directly interact with its interacting partners [354]. For instance, a chimera STING made by incorporating a DPVETTDY motif from the CTT of zebrafish potentiated STING's interaction with TRAF6 to shift the balance of IRF3/NF-kB signaling towards the latter [355]. This agrees with cryo-electron microscopy resolution of STING-TBK1 interaction showing that STING interacts with TBK1 via its CTT [356]. A critical motif within STING's CTT is a pLxIS consensus motif conserved between MAVS, STING, and TRIF that when phosphorylated (S366 in STING),

specifically triggers a downstream IRF3 response [357, 358]. In addition, STING-ubiquitination on its lysine residues by ubiquitin protein ligases is another type of post-translational modification that can favor activation of IRF3 or NF-kB [359, 360]. This suggests that STING agonists may be potentially engineered to elicit a specific downstream response by targeting specific STING-regulatory residues.

There are numerous other strategies that could potentially be used to activate or inhibit STING in a way that favors specific downstream pathways. For instance, small molecule kinase inhibitors of MAPKAPK2/5 selectively inhibited IRF3, but not NF-κB translocation, suggesting that other targets downstream of STING itself are potentially also options for circumventing undesirable effects of modulating STING activity. Additionally, compared to IRF3 or canonical NF-κB, non-canonical NF-kB pathway activation appears to be preferentially dependent on Tumor necrosis factor receptor (TNFR)-associated factor 6 (TRAF6) [355, 360, 361], suggesting that TRAF6 may be a target for enhancing the anti-tumoral effects of STING. Since TRAF6 plays a prominent role in mediating non-canonical STING activation in response to DNA damage, STING antagonists could potentially augment the effects of PARP inhibitors, etoposide, or radiotherapy [360]. Lastly, administration of STING agonists or inhibitors may be personalized based on the rate of chromosomal instability in patient tumors, as in principle, chromosomally unstable cells are exposed to cytosolic DNA at high frequency and as such may consist of cells that are already resistant to STING-induced cell death.

STING activation is intimately connected with autophagy, another determining factor for cancer growth or inhibition

The second likely reason for STING's paradoxical role in cancer cells is that regulation of cGAS-STING activation is intimately connected with stimulation of autophagy, a process that much like STING, can have double-edged effects on cancer growth and survival [362]. Indeed, STING activated autophagy can occur independently of STING CTT or TBK1, and the autophagy induction of STING likely precedes its interferon-promoting functions[363, 364]. There is strong evidence supporting reciprocal-regulation between STING and core autophagy factors to fine-tune the innate immune response. Upon stimulation, STING is trafficked to the perinuclear region [364], where it can directly promote autophagy via its LC-3 interacting domain [365]. In turn, activation of autophagy triggers lysosome-mediated degradation of STING to act as feedback to limit sustained STING activation [358, 366]. Notably, the autophagy regulator ULK1/2, like TBK1, can also phosphorylate STING on S366 to selectively modulate the IRF3 pathway activity [358].

Activation of autophagy has a dual role in cancer. Autophagy induction can promote tumor cell survival in response to stress related to protein misfolding or energy balance [367, 368]. However, there are also nonprotective forms of autophagy that, when activated, results in cytostatic or cytotoxic effects on cancer cells [369]. Given the integrated role between STING and autophagy, the dichotomous outcome of autophagy activation likely also contributes to variations in the outcome of STING activation in cancer cells. While the mechanisms underlying the STING-autophagy connection is still being resolved, their connection can potentially be exploited to devise combination treatments between STING agonists and drugs that stimulates or inhibits autophagy such as the mTOR inhibitor everolimus or chloroquine [370, 371].

Chapter 4: Stimulation of STING by Novel Small Molecules for Antitumor Immunity

Stimulation of STING by Novel Small Molecules for Antitumor Immunity

Qianhui Yi[1,2], Xiaojun Han[1], Rongtuan Lin[1,2], Gerald Batist[1,2], and Jian Hui Wu[1,2]*

[1]Lady Davis Institute for Medical Research, SMBD-Jewish General Hospital, McGill University, 3755 Cote-Ste-Catherine, Rd, Montreal, QC H3T 1E2, Canada

[2]Departments of Oncology and Medicine, Faculty of Medicine, McGill University, Montreal, QC, Canada

***Corresponding author:** Jian Hui Wu, Lady Davis Institute for Medical Research, SMBD-Jewish General Hospital, McGill University, 3755 Cote-Ste-Catherine, Rd, Montreal, QC H3T 1E2, Canada. Phone: +1(514) 340-8222 ext 22148, Email: jian.h.wu@mcgill.ca

4.1. Abstract

The stimulator of interferon genes (STING) pathway is a major component of the innate immune system. It functions in dendritic cells (DCs) through sensing the existing tumor DNA to alert the tumor immune surveillance: upon entering DC cytosol, tumor-derived DNA is recognized by STING and consequently induces IFN production that leads to antigen-presenting cell activation. Activated DCs then present tumor-specific antigens to naïve $CD8^+$ T cells and cumulate in a spontaneous anti-tumor T-cell response. The clinical translation for STING stimulation was therefore encouraged under the hypothesis that adequate STING induction in the tumor microenvironment is very likely to enrich the tumor-infiltrated T cells, thus transforming the "immune cold" tumors, such as prostate cancer, to an "immune hot" phenotype. Prior drug development of STING agonists has focused on modifying the natural cyclic dinucleotides (CDN), which are native ligands of STING derived from bacteria or humans. However, synthetic CDNs are large molecules that lack drug-like features, are susceptible to enzymatic degradation, and are impermeable to cell membranes, and therefore have limited therapeutic potential. In this study, we discovered a small molecule STING agonist #716, that potently activated human STING signaling in both ectopic cell models and human peripheral blood mononuclear cells (PBMC). #716 treatment enhanced PBMCs killing of prostate cancer cells *in vitro* and suppressed prostate cancer allografts growing *in vivo*. More importantly, #716 significantly enriched the anti-tumor T cell population in the tumor-bearing mice, suggesting it is a promising chemical structure for further optimization.

4.2. Introduction

Current immune therapy approaches have focused on boosting adaptive immunity majorly by enhancing T-cell response. The immune checkpoint inhibitors anti-PD-L1, anti-PD-1, and anti-CTLA-4 monoclonal antibody, as well as chimeric antigen receptor-based T cell (CAR-T) therapy have demonstrated great clinical success in multiple types of tumors but have shown great limitations in prostate cancer[372, 373]. Therefore, expanding the toolbox of immune therapy is essential for achieving a more robust and enduring antitumor response. T cells are not autonomous in their effector function, their adequate and sustained activation relies on the innate immune response[374]. Innate immunity involves various types of cells from the myeloid lineage, including dendritic cells (DCs), monocytes, macrophages etc. The interplay between innate and adaptive immunity in cancer is manifested by the key role of antigen-presenting DCs in eliciting the function of tumor-specific $CD8^+$ T cells[375]. Thus, novel immune therapy developments using the strategy of harnessing tumor recognition by DCs to further prime T-cell response has gained increasing interest.

STING – stimulator of interference genes - is an endoplasmic reticulum-resident for sensing the presence of cytosolic DNA, commonly generated *via* cellular DNA damage or pathogen infection. Cytosolic DNA binds to the cyclic GMP-AMP synthase (cGAS) to generate cyclic GMP-AMP (cGAMP). cGAMP binds and activates STING, resulting in the phosphorylation of its direct binding partner TANK-binding kinase 1 (TBK1)[346]. Furthermore, activation of STING results in endosomal trafficking of the STING complex from the surface of the endoplasmic reticulum to the perinuclear membrane, where TBK1 phosphorylates interferon regulatory transcription factor 3 (IRF3)[376]. The end product of this cascade is the activation of anti-tumoral innate immunity

via two distinct mechanisms. In tumor cells, STING mediates the process whereby DNA damage response leads to the upregulation of ligands for the recruitment of natural killer cells[377]. In antigen-presenting cells, especially the DCs, activation of STING results in the secretion of type 1 interferons (IFN-β), leading to an antitumor adaptive immunity[307, 378]. Therefore, STING has a central role in mobilizing immune response in suppressing tumor development.

The potency of STING-activation against cancer was discovered serendipitously. Pre-clinical studies using the small molecule DMXAA showed impressive effects including full rejection of both transplantable and inducible tumors in animal models. At the time, the anti-tumor effects were postulated to be due to the inhibition of multiple angiogenesis-related kinases such as VEGFR. However, the pre-clinical effects were not replicated in human clinical trials[379], and only in the retrospective study was the discovery that DMXAA's anti-tumor effects in mice were largely due to activation of STING rather than kinase inhibition. DMXAA is a potent inducer of STING in animal models, but a later study revealed that its effect was limited to mouse STING[306, 380]. On the other hand, further studies have proven that inducing activation of human STING - using synthetic cGAMP - can indeed generate activation of similar downstream pathways as in mouse STING[381, 382]. However, the use of synthetic cyclic nucleotides (CDN) to activate STING in a clinical setting would be difficult due to the prohibitive cost of the product and the lack of an efficient delivery method[383]. On this basis, we aim to develop a viable small molecule to achieve human STING activation where DMXAA could not.

In this study, we reported a novel small molecule compound #716 which robustly agonized human STING in ectopic cell models and induced human STING signaling activation in primary human

immune cells. #716 demonstrated an anti-tumor effect in a syngeneic mouse model of prostate cancer, alongside causing a significant induction of type-I IFN in mouse serum. More importantly, intraperitoneal injection of #716 into tumor-bearing mice elevated the production of tumor-antigen-specific $CD8^+$ T cells, indicating that #716's *in vivo* efficacy is mediated through boosting anti-tumor immunity.

4.3.Materials and Methods

Cell lines and plasmids

293T, THP-1, E.G7-OVA, TRAMP-C1, and Raw264.7 cell lines were purchased from the ATCC and cultured as recommended. Human PBMC were extracted from freshly collected patient blood in Jewish General Hospital (Montreal, Quebec). PBMC were purified by centrifuging blood at 800g for 30 min and removing the top layer containing plasma. Then, the remaining blood was diluted with an equal volume of PBS (pH 7.4), containing 0.05 M EDTA. 12.5 ml of diluted blood was layered over 25 ml of the Ficoll-Paque (GE Healthcare). The gradients were centrifuged at 400g for 30 min at 18-20 °C in a swinging-bucket rotor without the brake applied. PBMC interfaces were removed *via* pipetting and washing with PBS-EDTA and centrifugation at 400g for 15 min. The PBMC pellets were suspended in 3 mL of ammonium chloride-potassium (ACK) lysing buffer (Invitrogen) and incubated for 2 min at room temperature with gentle mixing to lyse contaminating red blood cells. Then the pellets were washed and centrifuged twice with PBS-EDTA. The cell number and viability of purified PBMCs were determined using a Countess Automated Cell Counter (Invitrogen) together with trypan blue staining. The extracted PBMC were immediately preserved in liquid nitrogen with FBS containing 10 % DMSO and stored until required for downstream analyses. PcDNA-human STING, pcDNA-mouse STING, and ISRE-Luc

plasmids were gifts from Dr. Rongtuan Lin (McGill University). Puno.1-human STING-HAQ was purchased from InvivoGen.

Dual-luciferase reporter assay

293T cells were seeded into 24-well plates at least 24 h before transfection. *Firefly* luciferase reporter ISRE-Luc and *Renilla* luciferase reporter pRL-TK (internal control) together with a plasmid expressing the designated forms of STING were transiently transfected into cells using lipofectamine 3000. 5 h after transfection, cell culture media was refreshed, and cells were subjected to the treatment of DMSO or designated compounds treatments. Luciferase activities were measured using the Dual-Luciferase Reporter Assay System (Promega) on a GLOMAX 20/20 luminometer (Promega).

qRT-PCR analysis

2×10^7 PBMC cells were seeded in 6-cm dish and cultured for 24 h prior to compound treatment. Cells were then harvested and used for total RNA extraction using mirVana miRNA Isolation Kit (Life technologies). Thereafter, the extracted RNA was subjected to DNA clearance using RQ1 RNase-Free DNase (Promega). cDNA was then synthesized using 5× All-In-One RT MasterMix (abm), and the remaining RNA was digested by the RNase H (Biolabs). Expression of IFN-β gene was assessed using GoTaq qPCR Master Mix (Promega), with the primers: forward 5'-AAA CTC ATG AGC AGT CTG CA-3' and reverse 5'-AGG AGA TCT TCA GTT TCG GCG G-3'. The qRT-PCR reaction was performed on 7500 Fast Real-Time PCR System (Applied Biosystems).

Western blot analysis

Cells were plated at the density of 6×10^6 cells per 6 cm dish and were treated as described in the respective figures. Protein extracts were prepared using RIPA buffer supplemented with 1% Protease Inhibitor Cocktail (SIGMA) and 1mM PMSF. Protein concentration was quantified by Coomassie Protein Assay (Thermo) and samples were applied to SDS-PAGE. Western blot was performed with antibodies: phospho-TBK1 (#5483, Cell Signaling), TBK1 (#3504, Cell Signaling), phospho-IRF3 (#4947, Cell Signaling), IRF3 (#4302, Cell Signaling), phospho-STAT1(#9167, Cell Signaling), and STAT1 (#9172, Cell Signaling).

Animal study

All animal studies were conducted under the Animal Use Protocol approved by the Animal Care Committee of the Lady Davis Institute, Jewish General Hospital, McGill University. Six weeks old C57L/6 male mice were purchased from Charles River; Tumor cell implantation was done at least 1 week after animal arrival. 10×10^6 TRAMP-C1 cells were injected subcutaneously in 200 ul of PBS. Tumor length and width were measured by caliper and tumor size was calculated with the formula: $\text{Volume}=4/3\times\pi\times(\text{Length}/2)\times(\text{Width}/2)^2$. Compounds were delivered *via* intraperitoneal injection (i.p.) (at 10 µl per 1 g of mouse body weight). Compounds were formulated in saline solution contains 10% DMSO, 10% Cremophor EL, 20% PEG400 and 1% 2-hydroxypropyl-β-cyclodextrin. At sacrifice, the mouse blood was withdrawn *via* cardiac puncture and the serum cytokine IFN-β concentration was quantified using VeriKine Mouse IFN Beta ELISA Kit (Pbl Assay Science).

Pentamer Staining for tumor antigen-specific $CD8^+$ T cell

Splenocytes were analyzed 5 days after the last injection of #716. For OVA-pentamer staining, splenocytes were preincubated for 15 min with purified anti-mouse CD16/32 antibody (93,

Biolegend) to block potential nonspecific binding and labeled with PE MHC class I pentamer (Proimmune) consisting of H-2Kb complexed to SIINFEKL (Ovalbumin 257-264) peptide, APC anti-mouse TCRβ chain Antibody (H57-597, BioLegend), Pacific Blue anti-mouse CD8a Antibody (53-6.7, BioLegend), and the Fixable Viability Dye eFluor 450 (Bioscience). Stained cells were analyzed using LSR II cytometer with FACSDiva software (BD Biosciences). Data analysis was conducted with FlowJo software.

4.4. Result

4.4.1. Compound #178 directly bonded and modestly activated human STING

We screened a library of compounds designed to target potential ligand binding pockets in the known STING 3D structure (**Fig. 1A**). As an initial proof of concept, we used the surface plasmon resonance (SPR) technique to confirm that our candidate compounds directly interact with human STING (**Fig. 1B**). After the drug-protein interaction was confirmed, we then sought to utilize cellular models to select the compounds that were capable of activating the STING signaling pathway.

To verify STING activation, we utilized two cell line models: a human monocytic cell line THP-1 and the cell line 293T transfected with either human or mouse STING for our screening purposes. Our initial results showed some potential candidates, including compounds #348 and #408, which were able to induce a mild activation of STING at the concentration of 20 μM (**Fig. 1C**). We then used a luciferase-reporter assay to detect the activation of interferon-stimulated response elements (ISRE) as a secondary method to quantify STING activation. In 293T, #178, #348 and #408

increased the reporter activity by 2–5 folds in human STING, with lesser effect against mouse STING (**Fig. 1A**), indicating further chemical modification is required for improving their potency.

4.4.2. Compound #716 demonstrated substantially improved STING activating potency

Subsequent chemical modification on the backbone the of #178 compound family led to the discovery of a new compound #716, which demonstrated greater capacity in stimulating STING. At the concentration of 10 and 20 μM, the #716 induced a 20 and 50-fold induction of human STING-dependent ISRE reporter activity, respectively, whereas the mouse STING agonist DMXAA showed no effect. On the other hand, 20 μM of DMXAA drastically induced mouse STING activation by 60-fold, whereas #716 at the same concentration only achieved a 10-fold mouse STING activation. For the human STING haplotype HAQ[384] (hSTING-HAQ), 20 μM of #716 also only stimulated its activation by around 10-fold, while consistently, DMXAA had no agonistic effect (**Fig. 2A**).

To confirm that the induction of ISRE-Luc reporter activity was mediated through enhancing the canonical STING pathway, we used western blot to quantify the phosphorylation of downstream targets, TBK1, IRF3, and STAT1. In 293T cells transfected with human STING expressing plasmid, #716 induced phosphorylation of TBK1, IRF3, and STAT1 comparably to the endogenous STING ligand cGAMP, while DMXAA had no impact (**Fig. 2B**). Overall, these initial results suggested that #716 was highly potent for the wild-type human STING and induced a downstream signaling cascade following STING activation.

4.4.3. #716 induced STING-dependent signaling in primary immune cells and enhanced immune cell-mediated prostate cancer cell killing

Given #716 was observed to activate STING in human cell lines, we next wondered if its STING agonistic activity was also appliable to primary immune cells. Human peripheral blood mononuclear cells (PBMC) were extracted from patient donors' blood and were subsequently treated with 20 μM of #716 for 0, 4, 6, or 8 hours (**Fig. 3A**). STING signaling activation, evidenced by elevated phosphorylation of TBK1, IRF3, and STAT1, became observable as early as 4 hours of treatment and peaked at 6–8 hours. Likewise, in the human monocyte cells THP-1, 20 μM of #716 induced a 20-fold overexpression of the interferon beta (IFN-β) gene (**Fig. 3B**), indicating hyperactivation of the STING pathway in human immune cells following #716 treatment.

Next, we sought to explore if this STING activation caused by #716 in immune cells could enhance their anti-tumor response. PBMC is a mixture of multiple immune cell types, including lymphocytes (T cells, B cells, and natural killer cells), monocytes, and dendritic cells. Therefore, in vitro co-culturing of PBMC with tumor cells would also facilitate the tumor cell killing that mimics the T cell priming by the tumor antigen-presenting dendritic cells in vivo. Indeed, when human PBMC were cultured together with human prostate cancer cells 22Rv1 and treated with 20 μM of #716 for 24 hours, the viable 22Rv1 reduced by approximately 50% compared to DMSO treated cells (**Fig. 3C**). More importantly, when the pre-cocultured and treated PBMC were harvested and subsequently added to another fresh batch of 22Rv1, these PBMC were also able to facilitate prostate cancer cell killing with very similar potency (**Fig. 3D**), suggesting that #176 treatment enhanced antitumor immunity as well as immunological memory in PBMC.

4.4.4. Compound # 716 exhibited anti-tumor efficacy in mouse prostate cancer allografts

Given that #716 appeared to have a stronger stimulatory effect on human STING compared to mouse STING when those were ectopically expressed 293T cells, we sought to establish whether #716 would be capable of stimulating mouse STING in mouse immune cells, as this is a major consideration before proceeding with any mouse-based *in vivo* studies. The murine macrophage cells RAW264.7 were treated with 10 μM of #716 for 8 hours before being harvested for western blot analysis, DMSO, and 10 μM of DMXAA treated cells were included as the negative and positive controls, respectively. Though weaker than DMXAA, #716 substantially elevated the level of P-TBK1(**Fig. 4A**), suggesting #716 could antagonize the STING signaling in murine immune cells.

Next, we evaluated the anti-tumor potency of #716 in the prostate cancer allograft model. Male C578L/6 mice were subcutaneously injected with TRAMP-C1 mouse prostate cancer cells. Tumors became palpable 10 days after the implantation of TRAMP-C1 cells, and tumor-bearing mice were randomized into three groups to receive every other day dosages of the vehicle or 25mg/kg #716 or two dosages of 25mg DMXAA. At the conclusion of the experiment, the tumor growth was markedly suppressed in the #716 treated mice when compared to that of the vehicle group, while tumors in the DMXAA-treated group showed full regression with of 1/3 tumor completely disappeared (**Fig. 4B-4E**). Furthermore, #716 and DMXAA also strongly induced IFN-β cytokine secretion when evaluated by the mouse serum ELISA (**Fig. 4F**), implying the anti-tumor efficacy of #716 was probably derived from activating the STING pathway in dendritic cells *in vivo*.

4.4.5. #716 stimulated the generation of tumor antigen-specific $CD8^+$ T cells in mice

As #716 treatment might have induced antigen-presenting dendritic cell activation *in vivo*, evidenced by elevated IFN-β concentration in mice serum, we wondered if this could lead to the presenting of tumor-specific antigens to naïve $CD8^+$ T cells, and cumulating in a spontaneous anti-tumor T-cell response. To answer this question, we utilized the E.G7-OVA tumor system. E.G7-OVA cells express the chicken OVA (ovalbumin neotumor antigen) - the dominant MHC class I peptide from ovalbumin (SINKFEKL) that has been well characterized in C57BL/6 mice. C57BL/6 mice immunized with E.G7-OVA cells give rise to H-2Kb restricted cytotoxic lymphocytes specific for the OVA 258-276 peptide[385] and for which tetramers are available to specifically track these cells. E.G7-OVA tumor-bearing mice were treated (i.p) with two dosages of the vehicle or 30mg/kg #716 or a single dosage of 20mg/kg DMXAA. 5 days after the last treatment, the mice were sacrificed and their splenocytes were harvested. For FACS analysis, the SINKFEKL tumor antigen-specific cytotoxic T lymphocytes within splenocytes were quantified by gating on $CD8^+$/ $pentamer^+$ lymphocytes. In the #716 treated mice, the percentage of $CD8^+$/ $pentamer^+$ lymphocytes increased by approximately 3-fold in comparison to the vehicle-treated mice, while DMXAA treatment induced a greater enrichment (~6-fold) of such T cells (**Fig. 5**). These data confirmed that, although weaker than the mouse STING agonist DMXAA, #716 harnessed the anti-tumor T cell response *in vivo*.

4.5. Discussion

Presently, our lead compound #716 has shown a great capacity to induce the activation of the human STING signaling pathway *in vitro*. However, its potency in stimulating the mouse STING is rather modest by comparison, therefore, the magnitude of anti-tumor immunity that could be potentially achieved by #716 in humans was theoretically underrepresented by these *in vivo* results obtained from mouse models. For continuing the preclinical development of STING agonists, chemical optimization on the #716 structure is needed for achieving a unified agonistic activity on all forms of STING, including mouse STING, human STING, and multiple human STING haplotypes. Moreover, the other challenge is the building up of more representative cell and animal models to further investigate the compound's mechanistic effects. The lack of a normal dendritic cell line means we currently rely on ectopic expression of human STING in 293T to test compound activation. This model is sufficient for initial screening, as the downstream kinases TBK1 and IRF3 were phosphorylated in response to compound treatment. However, inherent differences between available cell models and true antigen-presenting cells, such as dendritic cells, could obfuscate our understanding of these compounds' efficacy in a physiological setting.

#716 was demonstrated to suppress tumor growth and stimulate anti-tumor T cell generation *in vivo*, however, how much of its tumor suppression effect was derived from anti-tumor immunity requires further dissection. Moreover, given that STING activation in the dendritic cells is the determining factor for anti-tumor immunity[386-388], future works also need to characterize the dendritic cell population *in vivo* post the compound treatment.

Latest studies suggested STING activation can be a double-edged sword when manipulated as cancer immunotherapy. Serval research groups reported the antiproliferative and proapoptotic function of endogenous STING activation in T cells[389-391], highlighting the possibility of T cell exhaustion upon STING stimulation *in vivo*, which could lead to antitumor immunity being unendurable. Emerging evidence also unveiled that STING activity in tumor cells may play a crucial role in facilitating an immune-suppressive tumor microenvironment by secreting proinflammatory cytokines and recruiting immunosuppressive immune cells[392], such as Treg cells[334, 393] and myeloid-derived suppressor cells[394, 395]. More recent works also found an important link between STING activation within tumor cells and acquired T cell resistance *via* overexpression of immune checkpoints[396-398], such as PD-L1, thus helping tumor cells bypass immune surveillance. These mechanistic studies, together with the disappointingly modest efficacy of synthetic CDN STING agonists as monotherapy in the clinical trials[399, 400], raised considerable skepticism about STING still being a validated immune target for cancer therapy.

4.6. Figures

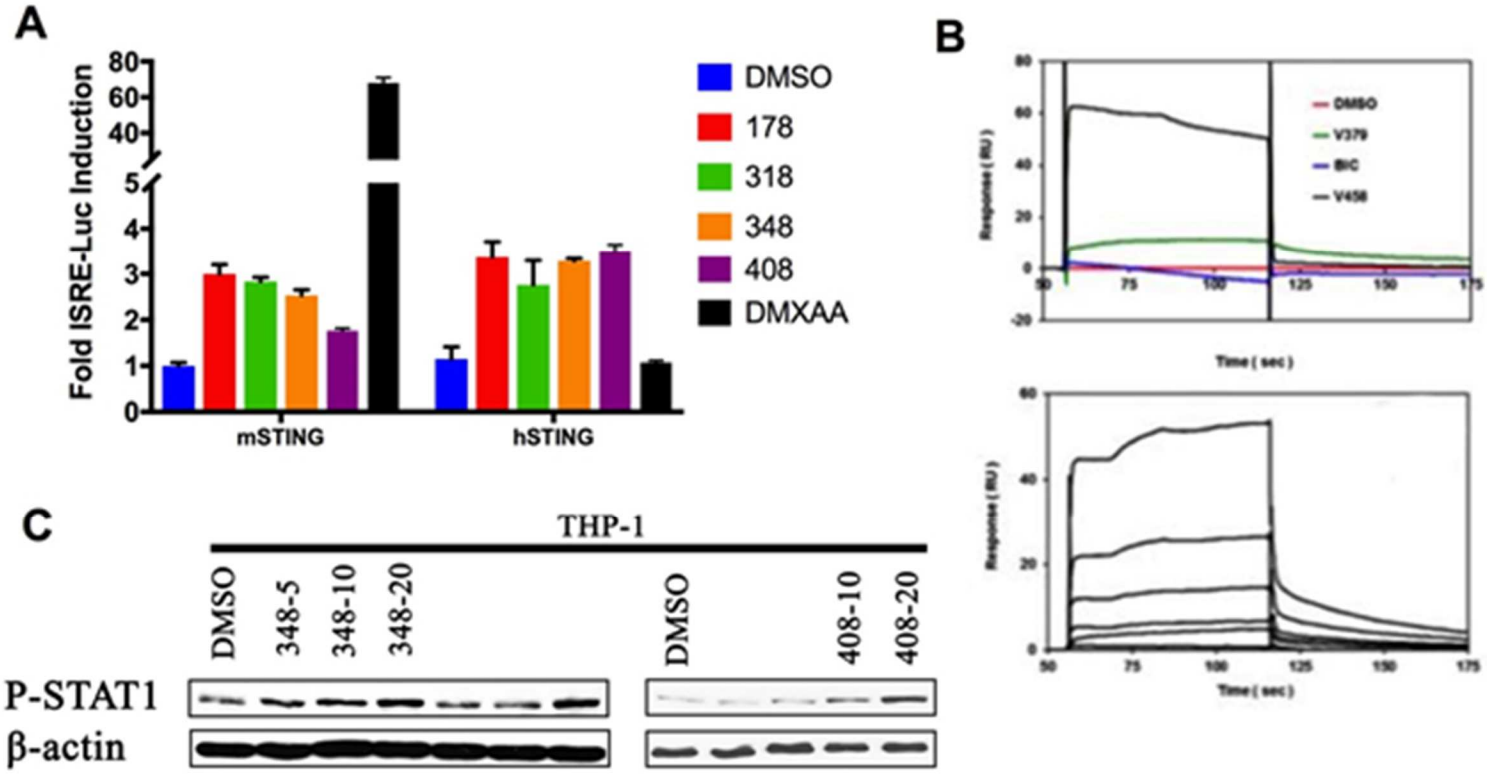

4.6.1. Figure M3-1. Initial candidate molecule directly bound to hSTING and stimulated the STING signaling pathway.

(A) 293T cells were transfected with indicated STING alleles and ISRE-luciferase reporter. After 5 hours, cells were stimulated for 24 hours with indicated compounds (20 μM) and assessed for ISRE-luciferase activity. Another co-transfected pRL-TK luciferase reporter served as internal control. **(B)** Specific, dose-dependent binding of **#178** (with concentration from 0 to 50 μM, 2-fold dilution series in PBST running buffer containing 5% DMSO) to amine-coupled STING (8,700 RU) at 25 μL/min (reference-subtracted data with DMSO solvent correction), as assessed by SPR; **(C)** THP-1 cells were treated with indicated compounds (5-10 μM) for 16 hours before being collected for western blot.

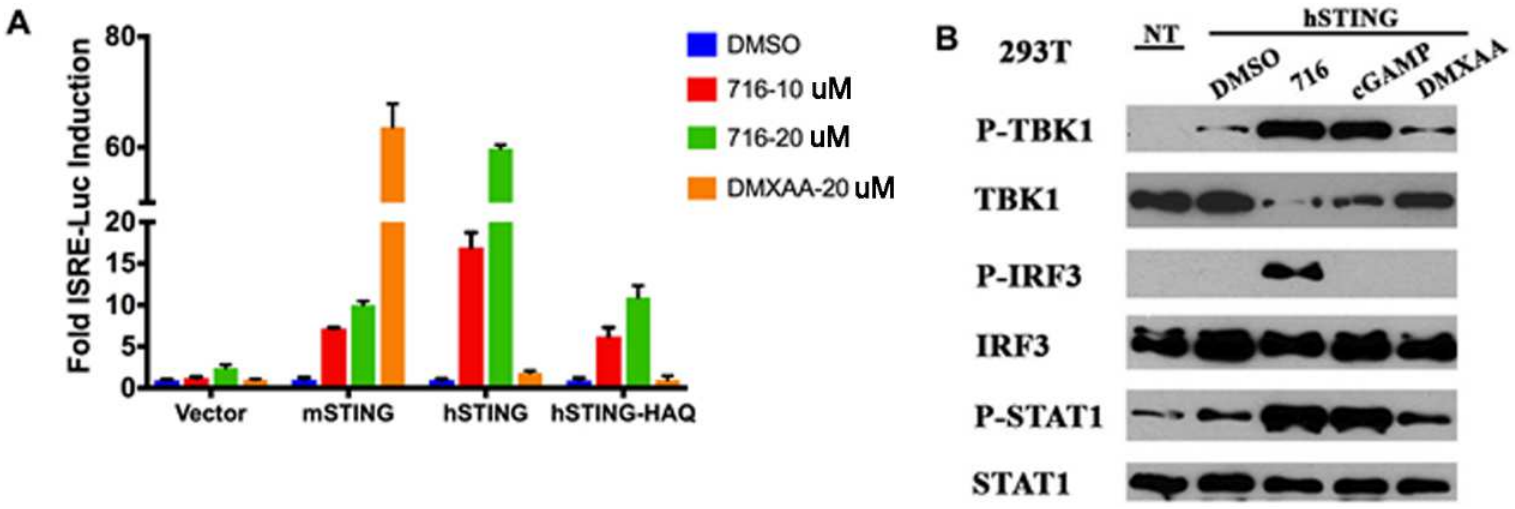

4.6.2. Figure M3-2. Compound #716 demonstrated substantially improved STING agonist potency.

(A) 293T cells were transfected with indicated STING alleles and ISRE-luciferase reporter. After 5 hours, cells were stimulated for 24 hours with indicated compounds (10-–20 μM) and assessed for ISRE-luciferase activity. Another co-transfected pRL-TK luciferase reporter served as internal control. (B) 293T cells were transfected with human STING construct for 5 hours, cells were then cultured in fresh medium with indicated compounds (20 μM for #716 and DMXAA, 10μM for cGAMP) for 24 hours before being harvested for western blot analysis.

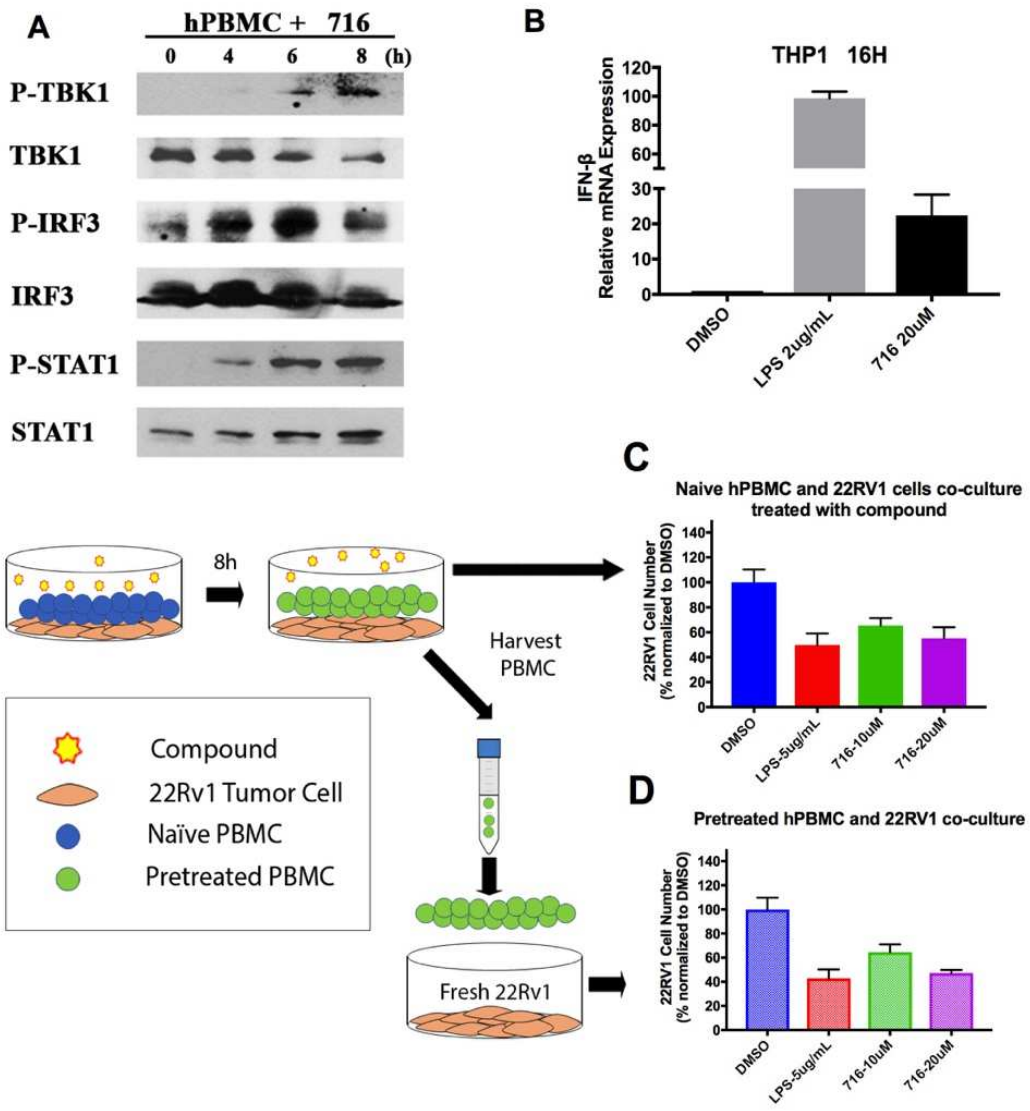

4.6.3. Figure M3-3 Compound #716 induced STING-dependent signaling in human immune cells and enhanced immune cell-mediated prostate cancer cell killing

(A) Human PBMCs treated with 20μM 716 were harvested at indicated time points for western blot analysis. **(B)** THP-1 monocytes were stimulated with 2μg/ml LPS or 20μM 716 for 16 hours, fold of induction of IFN-β was measured by qRT-PCR and relative normalized expression was determined by comparison with untreated control. **(C)** 22RV1 cells (2×10^4 per well) were seeded in 12-well plates 24 hours before adding 2×10^5 naïve human PBMC into each well. The co-culture was then treated with indicated compounds for 24 hours, or **(D)** pre-treated PBMCs were taken out after 8 hours and subsequently co-cultured with another fresh equal batch of 22RV1 cells for 24 hours. PBMCs were then completely removed from each well and 22RV1 cell number was counted by trypan blue exclusion method.

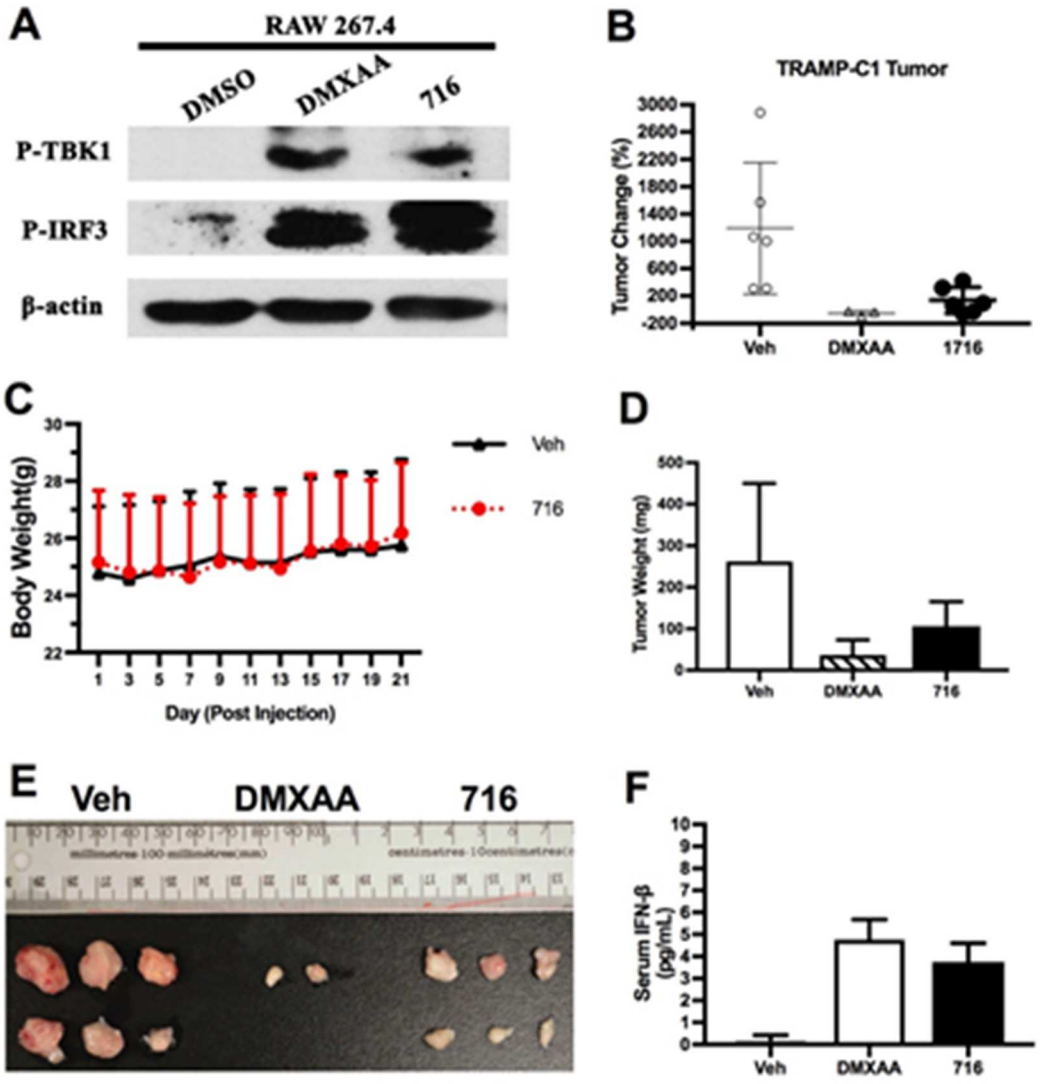

4.6.4. Figure M3-4. Compound # 716 exhibited anti-tumor efficacy in murine TRAMP-C1 prostate cancer and trigged cytokine production in tumor-bearing mice.

(A) RAW 264.7 cells were treated with indicated compounds (10μM) for 8 hours before being collected for western blot analysis. **(B-F)** 10×10^6 TRAMP-C1 cells were implanted subcutaneously into the right flank of the C578L/6 mice. When tumors were palpable, mice received two i.p doses of 25mg/kg DMXAA (n=3) or every other day i.p dose of 25mg/kg #716 (n=6); animals treated with vehicle (n=6) every other day served as the control group. **(B)** Percentage of change in individual tumor volumes after 21 days. **(C)** Mice body weight was measured twice weekly. **(D)** Mice were sacrificed on Day 21 and tumors were harvested for weight measurement. **(E)** Tumor image (one tumor disappeared in DMXAA treated group). **(F)** Mice blood was collected by cardiac puncture on Day 21 and the amount of IFN-β in serum was measured by ELISA.

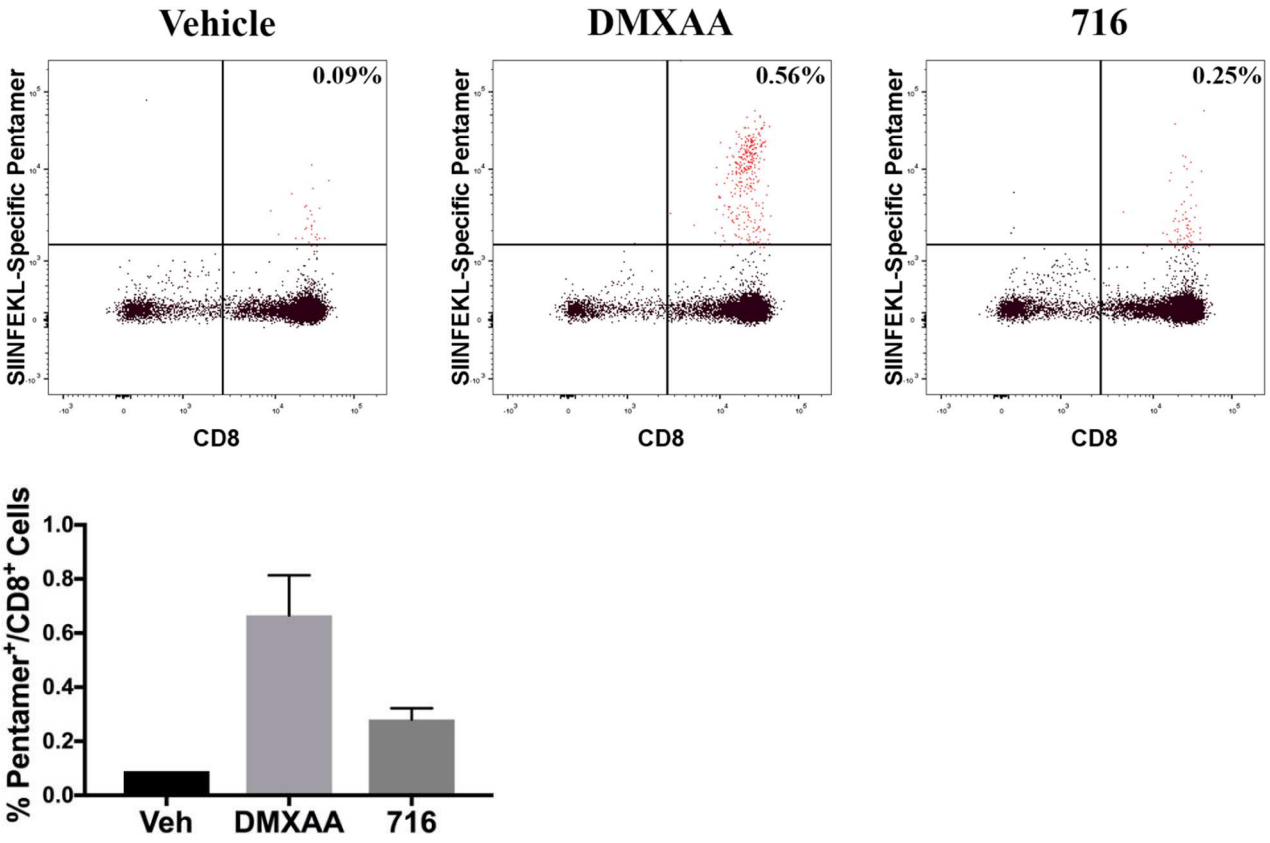
Vehicle
DMXAA
716
0.09%
0.56%
0.25%
SIINFEKL-Specific Pentamer
CD8
% Pentamer+/CD8+ Cells
1.0
0.8
0.6
0.4
0.2
0.0
Veh
DMXAA
716

4.6.5. Figure M3-5. #716 stimulated the generation of tumor antigen-specific CD8+ T cells in mice.

EG7-OVA tumor-bearing C57BL/6 mice (n=1 for DMSO, n=2 for DMXAA and #716) were intraperitoneally treated with vehicle, 20mg/kg DMXAA or 60mg/kg #716; 3 days later #716-treated animal received a second dose of 30mg/kg #716. 5 days after the initial treatment, mouse splenocytes were harvested and stained with antibodies against TCR-β, CD4, CD8, and OVA peptide SIINFEKL specific pentamer. The percentage of tumor antigen-specific $CD8^+$ T cells was determined by first gating on TCR-β positive lymphocytes and then gating on CD4 negative $CD8^+$/$pentamer^+$ lymphocytes.

4.7. Manuscript 3 References

1 Barber GN. STING: infection, inflammation and cancer. Nature Reviews Immunology 2015; 15: 760-770.

2 Cerboni S, Jeremiah N, Gentili M, Gehrmann U, Conrad C, Stolzenberg M-C *et al*. Intrinsic antiproliferative activity of the innate sensor STING in T lymphocytes. Journal of Experimental Medicine 2017; 214: 1769-1785.

3 Chen Q, Sun L, Chen ZJ. Regulation and function of the cGAS–STING pathway of cytosolic DNA sensing. Nature immunology 2016; 17: 1142-1149.

4 Cheng AN, Cheng L-C, Kuo C-L, Lo YK, Chou H-Y, Chen C-H *et al*. Mitochondrial Lon-induced mtDNA leakage contributes to PD-L1–mediated immunoescape via STING-IFN signaling and extracellular vesicles. Journal for immunotherapy of cancer 2020; 8.

5 Conlon J, Burdette DL, Sharma S, Bhat N, Thompson M, Jiang Z *et al*. Mouse, but not human STING, binds and signals in response to the vascular disrupting agent 5, 6-dimethylxanthenone-4-acetic acid. The Journal of Immunology 2013; 190: 5216-5225.

6 Corrales L, Glickman LH, McWhirter SM, Kanne DB, Sivick KE, Katibah GE *et al*. Direct activation of STING in the tumor microenvironment leads to potent and systemic tumor regression and immunity. Cell reports 2015; 11: 1018-1030.

7 Demaria O, De Gassart A, Coso S, Gestermann N, Di Domizio J, Flatz L *et al*. STING activation of tumor endothelial cells initiates spontaneous and therapeutic antitumor immunity. Proceedings of the National Academy of Sciences 2015; 112: 15408-15413.

8 Demaria O, Cornen S, Daëron M, Morel Y, Medzhitov R, Vivier E. Harnessing innate immunity in cancer therapy. Nature 2019; 574: 45-56.

9 Diamond MS, Kinder M, Matsushita H, Mashayekhi M, Dunn GP, Archambault JM *et al*. Type I interferon is selectively required by dendritic cells for immune rejection of tumors. Journal of Experimental Medicine 2011; 208: 1989-2003.

10 Domvri K, Petanidis S, Zarogoulidis P, Anestakis D, Tsavlis D, Bai C *et al*. Treg-dependent immunosuppression triggers effector T cell dysfunction via the STING/ILC2 axis. Clinical Immunology 2021; 222: 108620.

11 Du S-S, Chen G-W, Yang P, Chen Y-X, Hu Y, Zhao Q-Q *et al*. Radiation Therapy Promotes Hepatocellular Carcinoma Immune Cloaking via PD-L1 Upregulation Induced by cGAS-

STING Activation. International Journal of Radiation Oncology* Biology* Physics 2022; 112: 1243-1255.

12 Fuertes MB, Kacha AK, Kline J, Woo S-R, Kranz DM, Murphy KM *et al*. Host type I IFN signals are required for antitumor CD8+ T cell responses through CD8α+ dendritic cells. Journal of Experimental Medicine 2011; 208: 2005-2016.

13 Garris CS, Luke JJ. Dendritic Cells, the T-cell-inflamed Tumor Microenvironment, and Immunotherapy Treatment ResponseDendritic Cells and Immunotherapy Response. Clinical Cancer Research 2020; 26: 3901-3907.

14 Gulen MF, Koch U, Haag SM, Schuler F, Apetoh L, Villunger A *et al*. Signalling strength determines proapoptotic functions of STING. Nature communications 2017; 8: 1-10.

15 Hargadon KM, Johnson CE, Williams CJ. Immune checkpoint blockade therapy for cancer: an overview of FDA-approved immune checkpoint inhibitors. International immunopharmacology 2018; 62: 29-39.

16 Harrington K, Brody J, Ingham M, Strauss J, Cemerski S, Wang M *et al*. Preliminary results of the first-in-human (FIH) study of MK-1454, an agonist of stimulator of interferon genes (STING), as monotherapy or in combination with pembrolizumab (pembro) in patients with advanced solid tumors or lymphomas. Annals of Oncology 2018; 29: viii712.

17 Kim S, Li L, Maliga Z, Yin Q, Wu H, Mitchison TJ. Anticancer flavonoids are mouse-selective STING agonists. ACS chemical biology 2013; 8: 1396-1401.

18 Lara Jr PN, Douillard J-Y, Nakagawa K, Von Pawel J, McKeage MJ, Albert I *et al*. Randomized phase III placebo-controlled trial of carboplatin and paclitaxel with or without the vascular disrupting agent vadimezan (ASA404) in advanced non–small-cell lung cancer. Journal of Clinical Oncology 2011; 29: 2965-2971.

19 Li T, Cheng H, Yuan H, Xu Q, Shu C, Zhang Y *et al*. Antitumor activity of cGAMP via stimulation of cGAS-cGAMP-STING-IRF3 mediated innate immune response. Scientific reports 2016; 6: 1-14.

20 Liang D, Xiao-Feng H, Guan-Jun D, Er-Ling H, Sheng C, Ting-Ting W *et al*. Activated STING enhances Tregs infiltration in the HPV-related carcinogenesis of tongue squamous cells via the c-jun/CCL22 signal. Biochimica et Biophysica Acta (BBA)-Molecular Basis of Disease 2015; 1852: 2494-2503.

21 Liang H, Deng L, Hou Y, Meng X, Huang X, Rao E *et al*. Host STING-dependent MDSC mobilization drives extrinsic radiation resistance. Nature communications 2017; 8: 1-10.

22 Lim S-O, Li C-W, Xia W, Cha J-H, Chan L-C, Wu Y *et al*. Deubiquitination and stabilization of PD-L1 by CSN5. Cancer cell 2016; 30: 925-939.

23 Marcus A, Mao AJ, Lensink-Vasan M, Wang L, Vance RE, Raulet DH. Tumor-derived cGAMP triggers a STING-mediated interferon response in non-tumor cells to activate the NK cell response. Immunity 2018; 49: 754-763. e754.

24 Meric-Bernstam F, Sandhu SK, Hamid O, Spreafico A, Kasper S, Dummer R *et al*. Phase Ib study of MIW815 (ADU-S100) in combination with spartalizumab (PDR001) in patients (pts) with advanced/metastatic solid tumors or lymphomas. American Society of Clinical Oncology, 2019.

25 Moore MW, Carbone FR, Bevan MJ. Introduction of soluble protein into the class I pathway of antigen processing and presentation. Cell 1988; 54: 777-785.

26 Motedayen Aval L, Pease JE, Sharma R, Pinato DJ. Challenges and opportunities in the clinical development of STING agonists for cancer immunotherapy. Journal of Clinical Medicine 2020; 9: 3323.

27 Motwani M, Pesiridis S, Fitzgerald KA. DNA sensing by the cGAS–STING pathway in health and disease. Nature Reviews Genetics 2019; 20: 657-674.

28 Pitt JM, Vétizou M, Daillère R, Roberti MP, Yamazaki T, Routy B *et al*. Resistance mechanisms to immune-checkpoint blockade in cancer: tumor-intrinsic and-extrinsic factors. Immunity 2016; 44: 1255-1269.

29 Woo S-R, Fuertes MB, Corrales L, Spranger S, Furdyna MJ, Leung MY *et al*. STING-dependent cytosolic DNA sensing mediates innate immune recognition of immunogenic tumors. Immunity 2014; 41: 830-842.

30 Woo S-R, Corrales L, Gajewski TF. The STING pathway and the T cell-inflamed tumor microenvironment. Trends in immunology 2015; 36: 250-256.

31 Wu J, Chen Y-J, Dobbs N, Sakai T, Liou J, Miner JJ *et al*. STING-mediated disruption of calcium homeostasis chronically activates ER stress and primes T cell death. Journal of Experimental Medicine 2019; 216: 867-883.

32 Yi G, Brendel VP, Shu C, Li P, Palanathan S, Cheng Kao C. Single nucleotide polymorphisms of human STING can affect innate immune response to cyclic dinucleotides. PloS one 2013; 8: e77846.

33 Zhang C-x, Ye S-b, Ni J-j, Cai T-t, Liu Y-n, Huang D-j *et al*. STING signaling remodels the tumor microenvironment by antagonizing myeloid-derived suppressor cell expansion. Cell Death & Differentiation 2019; 26: 2314-2328.

Comprehensive discussion

The current therapies for castration-resistant prostate cancer (CRPC) are androgen deprivation therapies (ADT), such as enzalutamide and abiraterone, which focus on inhibiting AR activity and blocking downstream signaling pathways to suppress tumor growth [86] [271] [101]. However, the selective pressure imposed by ADT drugs also drives cancer cells to adapt by developing mechanisms to circumvent ADT [87]. Among many resistant mechanisms, the generation of AR splicing variants, especially AR-V7 is being recognized as a key player in the CRPC progression. AR-V7 arises from alternative splicing of AR pre-mRNA and intragenic rearrangement of the AR gene which results in truncation of the ligand binding domain (LBD) [102, 163]. Mechanistically, the antagonism of ADT against AR depends on competing with androgen for the androgen-binding pocket located in AR-LBD [86] [271] [101]. Therefore, the absence of AR-LBD in AR-V7 creates a form of AR that is constitutively active without androgen and irresponsive to all the currently available ADT, resulting in ADT-resistant tumor cell growth [102, 163]. The high prevalence of AR-V7 and its correlation with worse treatment outcomes in CRPC patients have highlighted the urgency of AR-V7 inhibition.

In the last 5-10 years, a substantial amount of effort has been dedicated to exploring the strategies of AR-V7 inhibition, including (1) direct targeting *via* AR N-terminal domain (AR-NTD) [215] or AR DNA binding domain (AR-DBD) [222, 223], (2) reducing AR-V7 protein level by inducing degradation [226, 228, 276] or inhibiting its mRNA splicing [277], (3) and blocking AR-V7 transcriptional activity by interfering in AR-V7 co-activators [232, 241]. While the clinical efficacy of the compounds corresponding to each targeting strategy is under investigation, none of them has reached Phase III clinical trial. A commonly observed obstacle for these compounds is

lacking profound potency, evidenced by the relatively low PSA responding rate and short PSA responding time in CRPC patients. Therefore, improving the inhibitory potency should be a high priority for developing the AR-V7 inhibitor.

In this study, we explored the AR-V7 inhibition approach of AR-NTD direct targeting. In our opinion, a directing targeting approach has several advantages when compared to indirect approaches. For instance, the AR-V7 degrader niclosamide downregulates the AR-V7 protein level *via* HSP70/STUB1 mediated E3 ubiquitin-proteasome pathway [226]. However, it is conceivable that the other AR interacting chaperone proteins (HSP90 and HSP40), or even ubiquitin-conjugating enzymes can theoretically compensate for this compound-induced degradation [401]. The other example is targeting the AR-V7 transcriptional co-activator BRD4 with a small molecule inhibitor JQ1 [232]. JQ1 binds to BRD4 resulting in its displacement of active chromatin and subsequent removal of RNA pol II from AR-regulated genes [232]. However, the transcriptomic change of prostate cancer cells treated with JQ1 did not largely recapitulate the AR transcriptome with only a subset of AR-regulated genes alongside many nonspecific genes being affected [241]. This observation hinted that the co-activator BRD4, although important for AR-mediated transcription, it is not equally indispensable for all the AR-regulated genes. Some AR-regulated genes may preferentially rely on other pioneer factors, epigenetic readers, or epigenetic modifiers for improving chromatin accessibility other than BRD4. Therefore, it would be unsurprising if targeting a single AR co-activator is insufficient to block the full spectrum of AR signaling.

In the thesis, we described the discovery of two AR-NTD small molecule inhibitors: SC428 and SC912. Though having distinct chemical backbone structures, both SC428 and SC912 potently

inhibited transactivation of AR-V7, ARv567es, full-length AR (AR-FL), and multiple AR-LBD mutants. SC428 impaired androgen-induced AR-FL nuclear trafficking and chromatin binding and therefore attenuated AR-FL-regulated gene transcription. Under the castration condition, SC428 hampered AR-V7 nuclear localization and homodimerization, as well as mitigated AR-V7 mediated transcription. Because of its broad activity against AR-V7 and AR-FL, SC428 was equally effective in suppressing the proliferation across multiple prostate cancer cell lines with varying levels of AR-V7/AR-FL. Moreover, SC428 demonstrated *in vivo* activity against high AR-V7 high-expressing 22Rv1 xenograft which was resistant to enzalutamide treatment. With the second AR-NTD inhibitor SC912, we found an identifiable segment of amino acids 507-531 within the AR-NTD being indispensable for its inhibitory effects. Mechanistically, SC912 impaired AR-V7 mediated transcription and blocked AR-V7 nuclear trafficking and chromatin binding. For the AR-V7 expressing CRPC cells, SC912 antagonized their AR signaling activity and mitigated their castration-resistant growth both *in vitro* and *in vivo*, suggesting its therapeutic potential in CRPC.

Both SC428 and SC912 possess improved potency in inhibiting AR-V7 mediated AR signaling activity and CRPC cell proliferation, with the IC50 being around 1 μM in blocking AR-V7 transactivation and suppressing the growth of AR-V7 expressing CRPC cells, which is approximately a 20-fold increase of efficacy comparing to previously reported EPI compounds [215, 216]. Moreover, SC428 and SC912 inhibited mRNA expression of canonic AR-regulated genes as well as AR-V7 specifically regulated genes in CRPC cells, suggesting these AR-NTD inhibitors are indeed capable of abolishing persistent AR signaling activity driven by AR-V7 in CRPC. Lastly, SC428 and SC912 demonstrated a similar magnitude of antagonism against various

forms of AR, including wildtype AR, clinically relevant AR-LBD mutants, and AR splicing variants, thus proving the concept that AR-NTD targeting could indeed achieve pan-AR inhibition. Therefore, AR-NTD inhibitor when becoming available in the clinic is expected to overcome the ADT resistance fueled by all these AR alteration-based mechanisms in CRPC.

AR-NTD being an intrinsically disordered protein (IDP) imposed a great challenge for its pharmacological targeting [213]. Without the 3D structure being resolved for virtual docking, our initial drug screening process completely relied on cellular assays, which are low-throughput and time, and labor consuming. Moreover, the direct binding of the compounds and AR-NTD was also difficult to confirm, as the KD value of a direct binding assay, such as surface plasmon resonance (SPR), cannot reflect the IC50 of cell-based experiments. Firstly, the recombinant protein used in SPR does not reconstitute the natural conformations of AR-NTD; The recombinant protein was expressed and extracted from E. coli, which means the post-translational modifications which are extremely enriched in AR-NTD were not present, therefore, the recombinant protein cannot reconstitute the AR-NTD conformation with high fidelity. Additionally, AR-NTD being an IDP can add another layer of complication [214]. IDP is well-known for being structurally flexible and heterogenous, which means IDP simultaneously adopts various conformations in its natural environment [213]. However, the recombinant protein used in the *ex vivo* binding assay can only represent one single structure and fail to capture the large density of the possible IDP ensembles. Secondly, the co-interactors are missing in SPR assay to recapitulate the native binding state between AR-NTD and compound; AR-NTD is a hub for cofactors interaction, and its native conformations are substantially shaped by these binding partners. Hence, the binding affinity of a compound to AR-NTD could be fundamentally altered when these cofactors are absent.

In our experience, we have not observed any correlation between the KD value of a direct-binding assay and the IC50 of a cellular assay from AR-NTD inhibitors. The other interesting observation was that we have not encountered false-positive compounds in SPR assay, but the potential false-negatives were rather frequent. Taken together, we, therefore, can not select any direct binding assay as a drug-screening tool for this study, while mostly using it as a confirmative method to complement the cellular experiments.

Although having similar potency, the two compounds SC428 and SC912 probably have distinct binding fashion to AR-NTD. With SC428, we failed to identify a specific segment in AR-NTD that conducts the compound binding. As we performed various lengths of deletion on AR-NTD (amino acid 1-370, amino acid 181-547, amino acid 370-547), these deletions all caused a partial but not complete loss of SC428's inhibitory effect, implying SC428 may bind to AR-NTD through multiple motifs. Coincidentally, the other AR-NTD inhibitor EPI-001 was also reported to bind to AR-NTD through at least three regions [214]. In contrast, we mapped down to the amino acid 507-531 being indispensable for SC912's inhibition against wildtype AR and AR-V7, indicating a single fragment on AR-NTD determined the binding of SC912. The amino acid 507-531 fragment is close to the conjunction of AR-NTD and AR-DBD, and interestingly, may have some folded secondary structure according to the conformation prediction based on amino acid composition[214]. Therefore, future investigation on the interacting pattern of SC912 and amino acid 507-531 may help uncover a druggable site on the intrinsically disordered AR-NTD.

Conclusion and summary

In this thesis, we discovered two small molecule compounds targeting the AR N-terminal domain (AR-NTD) for AR-V7 inhibition. Though having distinctive chemical backbones, SC428 and SC912 both exhibited pan-AR inhibition capability against various resistant driving AR mutants, including AR-V7, full-length AR, and AR ligand binding domain mutants. SC428 and SC912 possess substantially improved potency compared to previously reported AR-NTD inhibitors and suppressed the AR-V7-driven AR signaling activity in various castration-resistant prostate cancer models *in vitro* and *in vivo*, highlighting their therapeutic potential for overcoming drug resistance in castration-resistant prostate cancer.

References for background and discussion

1 Sung H, Ferlay J, Siegel RL, Laversanne M, Soerjomataram I, Jemal A *et al*. Global cancer statistics 2020: GLOBOCAN estimates of incidence and mortality worldwide for 36 cancers in 185 countries. *CA: a cancer journal for clinicians* 2021; 71: 209-249.

2 Wolf AM, Wender RC, Etzioni RB, Thompson IM, D'Amico AV, Volk RJ *et al*. American Cancer Society guideline for the early detection of prostate cancer: update 2010. *CA: a cancer journal for clinicians* 2010; 60: 70-98.

3 Foster C, Bostwick D, Bonkhoff H, Damber J-E, Van der Kwast T, Montironi R *et al*. Cellular and molecular pathology of prostate cancer precursors. *Scandinavian Journal of Urology and Nephrology* 2000; 34: 19-43.

4 Litvinov IV, De Marzo AM, Isaacs JT. Is the Achilles' heel for prostate cancer therapy a gain of function in androgen receptor signaling? *The Journal of Clinical Endocrinology & Metabolism* 2003; 88: 2972-2982.

5 Isaacs JT. Resolving the Coffey Paradox: what does the androgen receptor do in normal vs. malignant prostate epithelial cells? *American Journal of Clinical and Experimental Urology* 2018; 6: 55.

6 Vander Griend DJ, D'Antonio J, Gurel B, Antony L, DeMarzo AM, Isaacs JT. Cell‐autonomous intracellular androgen receptor signaling drives the growth of human prostate cancer initiating cells. *The Prostate* 2010; 70: 90-99.

7 Tomlins SA, Rhodes DR, Perner S, Dhanasekaran SM, Mehra R, Sun X-W *et al*. Recurrent fusion of TMPRSS2 and ETS transcription factor genes in prostate cancer. *science* 2005; 310: 644-648.

8 Magi‐Galluzzi C, Tsusuki T, Elson P, Simmerman K, LaFargue C, Esgueva R *et al*. TMPRSS2–ERG gene fusion prevalence and class are significantly different in prostate cancer of caucasian, african‐american and japanese patients. *The Prostate* 2011; 71: 489-497.

9 Blattner M, Liu D, Robinson BD, Huang D, Poliakov A, Gao D *et al*. SPOP mutation drives prostate tumorigenesis in vivo through coordinate regulation of PI3K/mTOR and AR signaling. *Cancer cell* 2017; 31: 436-451.

10 Dai X, Gan W, Li X, Wang S, Zhang W, Huang L *et al*. Prostate cancer–associated SPOP mutations confer resistance to BET inhibitors through stabilization of BRD4. *Nature medicine* 2017; 23: 1063-1071.

11 Grasso CS, Wu Y-M, Robinson DR, Cao X, Dhanasekaran SM, Khan AP *et al*. The mutational landscape of lethal castration-resistant prostate cancer. *Nature* 2012; 487: 239-243.

12 Robinson D, Van Allen EM, Wu Y-M, Schultz N, Lonigro RJ, Mosquera J-M *et al*. Integrative clinical genomics of advanced prostate cancer. *Cell* 2015; 161: 1215-1228.

13 Cerami E, Gao J, Dogrusoz U, Gross BE, Sumer SO, Aksoy BA *et al*. The cBio cancer genomics portal: an open platform for exploring multidimensional cancer genomics data. *Cancer discovery* 2012; 2: 401-404.

14 Huggins C, Hodges CV. Studies on prostatic cancer. I. The effect of castration, of estrogen and of androgen injection on serum phosphatases in metastatic carcinoma of the prostate. *Cancer research* 1941; 1: 293-297.

15 Denmeade SR, Lin XS, Isaacs JT. Role of programmed (apoptotic) cell death during the progression and therapy for prostate cancer. *The Prostate* 1996; 28: 251-265.

16 Lin C, Yang L, Tanasa B, Hutt K, Ju B-g, Ohgi KA *et al*. Nuclear receptor-induced chromosomal proximity and DNA breaks underlie specific translocations in cancer. *Cell* 2009; 139: 1069-1083.

17 Haffner MC, Aryee MJ, Toubaji A, Esopi DM, Albadine R, Gurel B *et al*. Androgen-induced TOP2B-mediated double-strand breaks and prostate cancer gene rearrangements. *Nature genetics* 2010; 42: 668-675.

18 Taylor BS, Schultz N, Hieronymus H, Gopalan A, Xiao Y, Carver BS *et al*. Integrative genomic profiling of human prostate cancer. *Cancer cell* 2010; 18: 11-22.

19 Gelmann EP. Molecular biology of the androgen receptor. *Journal of Clinical Oncology* 2002; 20: 3001-3015.

20 Schoch CL, Ciufo S, Domrachev M, Hotton CL, Kannan S, Khovanskaya R *et al*. NCBI Taxonomy: a comprehensive update on curation, resources and tools. *Database* 2020; 2020.

21 Sayers EW, Cavanaugh M, Clark K, Ostell J, Pruitt KD, Karsch-Mizrachi I. GenBank. *Nucleic acids research* 2019; 47: D94-D99.

22 Lavery DN, McEwan IJ. Structural characterization of the native NH2-terminal transactivation domain of the human androgen receptor: a collapsed disordered conformation underlies structural plasticity and protein-induced folding. *Biochemistry* 2008; 47: 3360-3369.

23 Reid J, Kelly SM, Watt K, Price NC, McEwan IJ. Conformational analysis of the androgen receptor amino-terminal domain involved in transactivation: influence of structure-stabilizing solutes and protein-protein interactions. *Journal of Biological Chemistry* 2002; 277: 20079-20086.

24 Uversky VN. Multitude of binding modes attainable by intrinsically disordered proteins: a portrait gallery of disorder-based complexes. *Chemical Society Reviews* 2011; 40: 1623-1634.

25 Giorgetti E, Lieberman AP. Polyglutamine androgen receptor-mediated neuromuscular disease. *Cellular and molecular life sciences* 2016; 73: 3991-3999.

26 Baldassarri M, Picchiotti N, Fava F, Fallerini C, Benetti E, Daga S *et al*. Shorter androgen receptor polyQ alleles protect against life-threatening COVID-19 disease in European males. *EBioMedicine* 2021; 65: 103246.

27 Luo J, Attard G, Balk SP, Bevan C, Burnstein K, Cato L *et al*. Role of androgen receptor variants in prostate cancer: report from the 2017 mission androgen receptor variants meeting. *European urology* 2018; 73: 715-723.

28 Tan M, Li J, Xu HE, Melcher K, Yong E-l. Androgen receptor: structure, role in prostate cancer and drug discovery. *Acta Pharmacologica Sinica* 2015; 36: 3-23.

29 Roy A, Lavrovsky Y, Song C, Chen S, Jung M, Velu N *et al*. Regulation of androgen action. *Vitamins & Hormones* 1998; 55: 309-352.

30 Quigley CA, De Bellis A, Marschke KB, El-Awady MK, Wilson EM, French FS. Androgen receptor defects: historical, clinical, and molecular perspectives. *Endocrine reviews* 1995; 16: 271-321.

31 De Bellis A, Quigley C, Marschke KB, El-Awady M, Lane MV, Smith EP *et al*. Characterization of mutant androgen receptors causing partial androgen insensitivity syndrome. *The Journal of Clinical Endocrinology & Metabolism* 1994; 78: 513-522.

32 Feng Q, He B. Androgen receptor signaling in the development of castration-resistant prostate cancer. *Frontiers in oncology* 2019; 9: 858.

33 Wilson E, French F. Binding properties of androgen receptors. Evidence for identical receptors in rat testis, epididymis, and prostate. *Journal of Biological Chemistry* 1976; 251: 5620-5629.

34 Smith DF, Toft DO. Minireview: the intersection of steroid receptors with molecular chaperones: observations and questions. *Molecular endocrinology* 2008; 22: 2229-2240.

35 Russo JW, Liu X, Ye H, Calagua C, Chen S, Voznesensky O *et al*. Phosphorylation of androgen receptor serine 81 is associated with its reactivation in castration-resistant prostate cancer. *Cancer letters* 2018; 438: 97-104.

36 Callewaert L, Van Tilborgh N, Claessens F. Interplay between two hormone-independent activation domains in the androgen receptor. *Cancer research* 2006; 66: 543-553.

37 Groner AC, Cato L, de Tribolet-Hardy J, Bernasocchi T, Janouskova H, Melchers D *et al*. TRIM24 is an oncogenic transcriptional activator in prostate cancer. *Cancer cell* 2016; 29: 846-858.

38 Bevan CL, Hoare S, Claessens F, Heery DM, Parker MG. The AF1 and AF2 domains of the androgen receptor interact with distinct regions of SRC1. *Molecular and cellular biology* 1999; 19: 8383-8392.

39 Slagsvold T, Kraus I, Bentzen T, Palvimo J, Saatcioglu F. Mutational analysis of the androgen receptor AF-2 (activation function 2) core domain reveals functional and mechanistic differences of conserved residues compared with other nuclear receptors. *Molecular Endocrinology* 2000; 14: 1603-1617.

40 Panaretou B, Prodromou C, Roe SM, O'Brien R, Ladbury JE, Piper PW *et al*. ATP binding and hydrolysis are essential to the function of the Hsp90 molecular chaperone in vivo. *The EMBO journal* 1998; 17: 4829-4836.

41 He B, Kemppainen JA, Wilson EM. FXXLF and WXXLF sequences mediate the NH2-terminal interaction with the ligand binding domain of the androgen receptor. *Journal of Biological Chemistry* 2000; 275: 22986-22994.

42 He B, Bowen NT, Minges JT, Wilson EM. Androgen-induced NH2-and COOH-terminal interaction inhibits p160 coactivator recruitment by activation function 2. *Journal of Biological Chemistry* 2001; 276: 42293-42301.

43 Langley E, Zhou Z-x, Wilson EM. Evidence for an Anti-parallel Orientation of the Ligand-activated Human Androgen Receptor Dimer (∗). *Journal of Biological Chemistry* 1995; 270: 29983-29990.

44 He B, Minges JT, Lee LW, Wilson EM. The FXXLF motif mediates androgen receptor-specific interactions with coregulators. *Journal of Biological Chemistry* 2002; 277: 10226-10235.

45 Leung JK, Sadar MD. Non-genomic actions of the androgen receptor in prostate cancer. *Frontiers in endocrinology* 2017; 8: 2.

46 Heinlein CA, Chang C. Androgen receptor (AR) coregulators: an overview. *Endocrine reviews* 2002; 23: 175-200.

47 Deng Q, Zhang Z, Wu Y, Yu W-y, Zhang J, Jiang Z-m *et al*. Non-genomic action of androgens is mediated by rapid phosphorylation and regulation of androgen receptor trafficking. *Cellular Physiology and Biochemistry* 2017; 43: 223-236.

48 Ueda T, Mawji NR, Bruchovsky N, Sadar MD. Ligand-independent activation of the androgen receptor by interleukin-6 and the role of steroid receptor coactivator-1 in prostate cancer cells. *Journal of Biological Chemistry* 2002; 277: 38087-38094.

49 van Royen ME, Cunha SM, Brink MC, Mattern KA, Nigg AL, Dubbink HJ *et al*. Compartmentalization of androgen receptor protein–protein interactions in living cells. *The Journal of cell biology* 2007; 177: 63-72.

50 Shaffer PL, Jivan A, Dollins DE, Claessens F, Gewirth DT. Structural basis of androgen receptor binding to selective androgen response elements. *Proceedings of the National Academy of Sciences* 2004; 101: 4758-4763.

51 Centenera MM, Harris JM, Tilley WD, Butler LM. Minireview: the contribution of different androgen receptor domains to receptor dimerization and signaling. *Molecular endocrinology* 2008; 22: 2373-2382.

52 Nadal M, Prekovic S, Gallastegui N, Helsen C, Abella M, Zielinska K *et al*. Structure of the homodimeric androgen receptor ligand-binding domain. *Nature communications* 2017; 8: 1-14.

53 El Kharraz S, Helsen C, Dubois V, Libert C, Poutanen M, Claessens F. LBD Dimerization of the Androgen Receptor but Not N/C Interaction Is Crucial for Normal Male Development in Mice. *Journal of the Endocrine Society* 2021; 5: A822-A822.

54 Ozanne DM, Brady ME, Cook S, Gaughan L, Neal DE, Robson CN. Androgen receptor nuclear translocation is facilitated by the f-actin cross-linking protein filamin. *Molecular endocrinology* 2000; 14: 1618-1626.

55 Kaku N, Matsuda K-i, Tsujimura A, Kawata M. Characterization of nuclear import of the domain-specific androgen receptor in association with the importin α/β and Ran-guanosine 5′-triphosphate systems. *Endocrinology* 2008; 149: 3960-3969.

56 Gregory CW, Johnson Jr RT, Mohler JL, French FS, Wilson EM. Androgen receptor stabilization in recurrent prostate cancer is associated with hypersensitivity to low androgen. *Cancer research* 2001; 61: 2892-2898.

57 Gong Y, Wang D, Dar JA, Singh P, Graham L, Liu W *et al*. Nuclear export signal of androgen receptor (NESAR) regulation of androgen receptor level in human prostate cell lines via ubiquitination and proteasome-dependent degradation. *Endocrinology* 2012; 153: 5716-5725.

58 Lv S, Song Q, Chen G, Cheng E, Chen W, Cole R *et al*. Regulation and targeting of androgen receptor nuclear localization in castration-resistant prostate cancer. *The Journal of clinical investigation* 2021; 131.

59 Wilson S, Qi J, Filipp FV. Refinement of the androgen response element based on ChIP-Seq in androgen-insensitive and androgen-responsive prostate cancer cell lines. *Scientific reports* 2016; 6: 1-15.

60 Wang Q, Li W, Liu XS, Carroll JS, Jänne OA, Keeton EK *et al*. A hierarchical network of transcription factors governs androgen receptor-dependent prostate cancer growth. *Molecular cell* 2007; 27: 380-392.

61 Bolton EC, So AY, Chaivorapol C, Haqq CM, Li H, Yamamoto KR. Cell-and gene-specific regulation of primary target genes by the androgen receptor. *Genes & development* 2007; 21: 2005-2017.

62 Massie CE, Adryan B, Barbosa‐Morais NL, Lynch AG, Tran MG, Neal DE *et al*. New androgen receptor genomic targets show an interaction with the ETS1 transcription factor. *EMBO reports* 2007; 8: 871-878.

63 Pique-Regi R, Degner JF, Pai AA, Gaffney DJ, Gilad Y, Pritchard JK. Accurate inference of transcription factor binding from DNA sequence and chromatin accessibility data. *Genome research* 2011; 21: 447-455.

64 Jolma A, Yin Y, Nitta KR, Dave K, Popov A, Taipale M *et al*. DNA-dependent formation of transcription factor pairs alters their binding specificity. *Nature* 2015; 527: 384-388.

65 Li J, Fu J, Toumazou C, Yoon H-G, Wong J. A role of the amino-terminal (N) and carboxyl-terminal (C) interaction in binding of androgen receptor to chromatin. *Molecular endocrinology* 2006; 20: 776-785.

66 Urbanucci A, Sahu B, Seppälä J, Larjo A, Latonen L, Waltering K *et al*. Overexpression of androgen receptor enhances the binding of the receptor to the chromatin in prostate cancer. *Oncogene* 2012; 31: 2153-2163.

67 Tewari AK, Yardimci GG, Shibata Y, Sheffield NC, Song L, Taylor BS *et al*. Chromatin accessibility reveals insights into androgen receptor activation and transcriptional specificity. *Genome biology* 2012; 13: 1-17.

68 Gao N, Zhang J, Rao MA, Case TC, Mirosevich J, Wang Y *et al*. The role of hepatocyte nuclear factor-3α (Forkhead Box A1) and androgen receptor in transcriptional regulation of prostatic genes. *Molecular endocrinology* 2003; 17: 1484-1507.

69 Sahu B, Laakso M, Ovaska K, Mirtti T, Lundin J, Rannikko A *et al*. Dual role of FoxA1 in androgen receptor binding to chromatin, androgen signalling and prostate cancer. *The EMBO journal* 2011; 30: 3962-3976.

70 Zhao JC, Fong K-W, Jin H-J, Yang YA, Kim J, Yu J. FOXA1 acts upstream of GATA2 and AR in hormonal regulation of gene expression. *Oncogene* 2016; 35: 4335-4344.

71 Robinson JL, Hickey TE, Warren AY, Vowler SL, Carroll T, Lamb AD *et al*. Elevated levels of FOXA1 facilitate androgen receptor chromatin binding resulting in a CRPC-like phenotype. *Oncogene* 2014; 33: 5666-5674.

72 Lupien M, Eeckhoute J, Meyer CA, Wang Q, Zhang Y, Li W *et al*. FoxA1 translates epigenetic signatures into enhancer-driven lineage-specific transcription. *Cell* 2008; 132: 958-970.

73 Chamberlain NL, Driver ED, Miesfeld RL. The length and location of CAG trinucleotide repeats in the androgen receptor N-terminal domain affect transactivation function. *Nucleic acids research* 1994; 22: 3181-3186.

74 Wu D, Zhang C, Shen Y, Nephew KP, Wang Q. Androgen receptor-driven chromatin looping in prostate cancer. *Trends in Endocrinology & Metabolism* 2011; 22: 474-480.

75 McEwan IJ, Gustafsson J-Å. Interaction of the human androgen receptor transactivation function with the general transcription factor TFIIF. *Proceedings of the National Academy of Sciences* 1997; 94: 8485-8490.

76 He B, Lanz RB, Fiskus W, Geng C, Yi P, Hartig SM *et al*. GATA2 facilitates steroid receptor coactivator recruitment to the androgen receptor complex. *Proceedings of the National Academy of Sciences* 2014; 111: 18261-18266.

77 Wang Q, Carroll JS, Brown M. Spatial and temporal recruitment of androgen receptor and its coactivators involves chromosomal looping and polymerase tracking. *Molecular cell* 2005; 19: 631-642.

78 Hsieh C-L, Fei T, Chen Y, Li T, Gao Y, Wang X *et al*. Enhancer RNAs participate in androgen receptor-driven looping that selectively enhances gene activation. *Proceedings of the National Academy of Sciences* 2014; 111: 7319-7324.

79 Litwin MS, Tan H-J. The diagnosis and treatment of prostate cancer: a review. *Jama* 2017; 317: 2532-2542.

80 Edge SB, Compton CC. The American Joint Committee on Cancer: the 7th edition of the AJCC cancer staging manual and the future of TNM. *Annals of surgical oncology* 2010; 17: 1471-1474.

81 Epstein JI, Zelefsky MJ, Sjoberg DD, Nelson JB, Egevad L, Magi-Galluzzi C *et al*. A contemporary prostate cancer grading system: a validated alternative to the Gleason score. *European urology* 2016; 69: 428-435.

82 Moch H, Cubilla AL, Humphrey PA, Reuter VE, Ulbright TM. The 2016 WHO classification of tumours of the urinary system and male genital organs—part A: renal, penile, and testicular tumours. *European urology* 2016; 70: 93-105.

83 Mohler JL, Antonarakis ES, Armstrong AJ, D'Amico AV, Davis BJ, Dorff T *et al*. Prostate cancer, version 2.2019, NCCN clinical practice guidelines in oncology. *Journal of the National Comprehensive Cancer Network* 2019; 17: 479-505.

84 Albertsen PC. Observational studies and the natural history of screen-detected prostate cancer. *Current opinion in urology* 2015; 25: 232-237.

85 Mottet N, van den Bergh RC, Briers E, Van den Broeck T, Cumberbatch MG, De Santis M *et al*. EAU-EANM-ESTRO-ESUR-SIOG guidelines on prostate cancer—2020 update. Part 1: screening, diagnosis, and local treatment with curative intent. *European urology* 2021; 79: 243-262.

86 Cornford P, van den Bergh RC, Briers E, Van den Broeck T, Cumberbatch MG, De Santis M *et al*. EAU-EANM-ESTRO-ESUR-SIOG guidelines on prostate cancer. Part II—2020 update: treatment of relapsing and metastatic prostate cancer. *European urology* 2021; 79: 263-282.

87 James ND, Spears MR, Clarke NW, Dearnaley DP, De Bono JS, Gale J *et al*. Survival with newly diagnosed metastatic prostate cancer in the "docetaxel era": data from 917 patients in the control arm of the STAMPEDE trial (MRC PR08, CRUK/06/019). *European urology* 2015; 67: 1028-1038.

88 de Wit R, de Bono J, Sternberg CN, Fizazi K, Tombal B, Wülfing C *et al*. Cabazitaxel versus abiraterone or enzalutamide in metastatic prostate cancer. *New England Journal of Medicine* 2019; 381: 2506-2518.

89 Schrader AJ, Boegemann M, Ohlmann C-H, Schnoeller TJ, Krabbe L-M, Hajili T *et al*. Enzalutamide in castration-resistant prostate cancer patients progressing after docetaxel and abiraterone. *European urology* 2014; 65: 30-36.

90 Attard G, Borre M, Gurney H, Loriot Y, Andresen-Daniil C, Kalleda R *et al*. Abiraterone alone or in combination with enzalutamide in metastatic castration-resistant prostate

cancer with rising prostate-specific antigen during enzalutamide treatment. *Journal of Clinical Oncology* 2018; 36: 2639.

91 Khalaf DJ, Annala M, Taavitsainen S, Finch DL, Oja C, Vergidis J *et al*. Optimal sequencing of enzalutamide and abiraterone acetate plus prednisone in metastatic castration-resistant prostate cancer: a multicentre, randomised, open-label, phase 2, crossover trial. *The Lancet Oncology* 2019; 20: 1730-1739.

92 Flitsch J, Bernreuther C, Hagel C, Lüdecke DK. Hypophysectomy for prostate cancer: a revival of old knowledge?: Case report. *Journal of neurosurgery* 2008; 109: 760-764.

93 Montgomery RB, Mostaghel EA, Vessella R, Hess DL, Kalhorn TF, Higano CS *et al*. Maintenance of intratumoral androgens in metastatic prostate cancer: a mechanism for castration-resistant tumor growth. *Cancer research* 2008; 68: 4447-4454.

94 Attard G, Belldegrun AS, De Bono JS. Selective blockade of androgenic steroid synthesis by novel lyase inhibitors as a therapeutic strategy for treating metastatic prostate cancer. *BJU international* 2005; 96: 1241-1246.

95 Attard G, Reid A, Yap T, Raynaud F, Dowsett M. Re: Phase I clinical trial of a selective inhibitor of CYP17, abiraterone acetate, confirms that castration-resistant prostrate cancer commonly remains hormone driven. *Journal of clinical oncology* 2008; 26: 4563-4571.

96 Barrie S, Potter G, Goddard P, Haynes B, Dowsett M, Jarman M. Pharmacology of novel steroidal inhibitors of cytochrome P45017α (17α-hydroxylase/C17–20 lyase). *The Journal of steroid biochemistry and molecular biology* 1994; 50: 267-273.

97 Fizazi K, Scher HI, Molina A, Logothetis CJ, Chi KN, Jones RJ *et al*. Abiraterone acetate for treatment of metastatic castration-resistant prostate cancer: final overall survival analysis of the COU-AA-301 randomised, double-blind, placebo-controlled phase 3 study. *The lancet oncology* 2012; 13: 983-992.

98 Ryan CJ, Smith MR, Fizazi K, Saad F, Mulders PF, Sternberg CN *et al*. Abiraterone acetate plus prednisone versus placebo plus prednisone in chemotherapy-naive men with metastatic castration-resistant prostate cancer (COU-AA-302): final overall survival analysis of a randomised, double-blind, placebo-controlled phase 3 study. *The Lancet Oncology* 2015; 16: 152-160.

99 Shore ND, Chowdhury S, Villers A, Klotz L, Siemens DR, Phung D *et al*. Efficacy and safety of enzalutamide versus bicalutamide for patients with metastatic prostate cancer (TERRAIN): a randomised, double-blind, phase 2 study. *The Lancet Oncology* 2016; 17: 153-163.

100 Penson DF, Armstrong AJ, Concepcion R, Agarwal N, Olsson C, Karsh L *et al*. Enzalutamide versus bicalutamide in castration-resistant prostate cancer: the STRIVE trial. *Journal of Clinical Oncology* 2016; 34: 2098-2106.

101 Tran C, Ouk S, Clegg NJ, Chen Y, Watson PA, Arora V *et al*. Development of a second-generation antiandrogen for treatment of advanced prostate cancer. *Science* 2009; 324: 787-790.

102 Watson PA, Arora VK, Sawyers CL. Emerging mechanisms of resistance to androgen receptor inhibitors in prostate cancer. *Nature Reviews Cancer* 2015; 15: 701-711.

103 Scher HI, Fizazi K, Saad F, Taplin M-E, Sternberg CN, Miller K *et al*. Increased survival with enzalutamide in prostate cancer after chemotherapy. *New England Journal of Medicine* 2012; 367: 1187-1197.

104 Moilanen A-M, Riikonen R, Oksala R, Ravanti L, Aho E, Wohlfahrt G *et al*. Discovery of ODM-201, a new-generation androgen receptor inhibitor targeting resistance mechanisms to androgen signaling-directed prostate cancer therapies. *Scientific reports* 2015; 5: 1-11.

105 Clegg NJ, Wongvipat J, Joseph JD, Tran C, Ouk S, Dilhas A *et al*. ARN-509: A Novel Antiandrogen for Prostate Cancer TreatmentDevelopment of Antiandrogen ARN-509. *Cancer research* 2012; 72: 1494-1503.

106 Smith MR, Saad F, Chowdhury S, Oudard S, Hadaschik BA, Graff JN *et al*. Apalutamide treatment and metastasis-free survival in prostate cancer. *New England Journal of Medicine* 2018; 378: 1408-1418.

107 Smith MR, Hussain M, Saad F, Fizazi K, Sternberg CN, Crawford ED *et al*. Darolutamide and survival in metastatic, hormone-sensitive prostate cancer. *New England Journal of Medicine* 2022; 386: 1132-1142.

108 Borgmann H, Lallous N, Ozistanbullu D, Beraldi E, Paul N, Dalal K *et al*. Moving towards precision urologic oncology: targeting enzalutamide-resistant prostate cancer and mutated forms of the androgen receptor using the novel inhibitor darolutamide (ODM-201). *European Urology* 2018; 73: 4-8.

109 Pienta KJ. Preclinical mechanisms of action of docetaxel and docetaxel combinations in prostate cancer. *Seminars in oncology*, vol. 28. Elsevier, 2001, pp 3-7.

110 Friedland D, Cohen J, Miller Jr R, Voloshin M, Gluckman R, Lembersky B *et al*. A phase II trial of docetaxel (Taxotere) in hormone-refractory prostate cancer: correlation of antitumor effect to phosphorylation of Bcl-2. *Seminars in oncology*, vol. 26, 1999, pp 19-23.

111 Tannock IF, De Wit R, Berry WR, Horti J, Pluzanska A, Chi KN *et al*. Docetaxel plus prednisone or mitoxantrone plus prednisone for advanced prostate cancer. *New England Journal of Medicine* 2004; 351: 1502-1512.

112 Mita AC, Figlin R, Mita MM. Cabazitaxel: More Than a New Taxane for Metastatic Castrate-Resistant Prostate Cancer? Cabazitaxel Drug Update. *Clinical Cancer Research* 2012; 18: 6574-6579.

113 Pezaro CJ, Omlin AG, Altavilla A, Lorente D, Ferraldeschi R, Bianchini D *et al*. Activity of cabazitaxel in castration-resistant prostate cancer progressing after docetaxel and next-generation endocrine agents. *European urology* 2014; 66: 459-465.

114 Mita AC, Denis LJ, Rowinsky EK, DeBono JS, Goetz AD, Ochoa L *et al*. Phase I and pharmacokinetic study of XRP6258 (RPR 116258A), a novel taxane, administered as a 1-hour infusion every 3 weeks in patients with advanced solid tumors. *Clinical Cancer Research* 2009; 15: 723-730.

115 Bissery M, Bouchard H, Riou J, Vrignaud P, Combeau C, Bourzat J *et al*. Preclinical evaluation of TXD258, a new taxoid. *Proc Am Assoc Cancer Res*, vol. 41, 2000, p 214.

116 Bissery M. Preclinical evaluation of new taxoids. *Current pharmaceutical design* 2001; 7: 1251.

117 De Bono JS, Oudard S, Ozguroglu M, Hansen S, Machiels J-P, Kocak I *et al*. Prednisone plus cabazitaxel or mitoxantrone for metastatic castration-resistant prostate cancer progressing after docetaxel treatment: a randomised open-label trial. *The Lancet* 2010; 376: 1147-1154.

118 Oudard S, Fizazi K, Sengeløv L, Daugaard G, Saad F, Hansen S *et al*. Cabazitaxel versus docetaxel as first-line therapy for patients with metastatic castration-resistant prostate cancer: a randomized phase III trial—FIRSTANA. *Journal of Clinical Oncology* 2017; 35: 3189-3197.

119 Kantoff PW, Schuetz TJ, Blumenstein BA, Glode LM, Bilhartz DL, Wyand M *et al*. Overall survival analysis of a phase II randomized controlled trial of a Poxviral-based PSA-targeted immunotherapy in metastatic castration-resistant prostate cancer. *Journal of Clinical Oncology* 2010; 28: 1099.

120 Cheever MA, Higano CS. PROVENGE (Sipuleucel-T) in Prostate Cancer: The First FDA-Approved Therapeutic Cancer VaccineTherapeutic Prostate Cancer Vaccine. *Clinical Cancer Research* 2011; 17: 3520-3526.

121 Kantoff PW, Higano CS, Shore ND, Berger ER, Small EJ, Penson DF *et al*. Sipuleucel-T immunotherapy for castration-resistant prostate cancer. *New England Journal of Medicine* 2010; 363: 411-422.

122 Caram ME, Ross R, Lin P, Mukherjee B. Factors associated with use of sipuleucel-T to treat patients with advanced prostate cancer. *JAMA network open* 2019; 2: e192589-e192589.

123 Roodman GD. Mechanisms of bone metastasis. *New England journal of medicine* 2004; 350: 1655-1664.

124 Logothetis CJ, Lin S-H. Osteoblasts in prostate cancer metastasis to bone. *Nature Reviews Cancer* 2005; 5: 21-28.

125 Bruland ØS, Nilsson S, Fisher DR, Larsen RH. High-linear energy transfer irradiation targeted to skeletal metastases by the α-emitter 223Ra: adjuvant or alternative to conventional modalities? *Clinical cancer research* 2006; 12: 6250s-6257s.

126 Henriksen G, Breistøl K, Bruland ØS, Fodstad Ø, Larsen RH. Significant antitumor effect from bone-seeking, α-particle-emitting 223Ra demonstrated in an experimental skeletal metastases model. *Cancer research* 2002; 62: 3120-3125.

127 Liepe K. Alpharadin, a 223Ra-based alpha-particle-emitting pharmaceutical for the treatment of bone metastases in patients with cancer. *Current opinion in investigational drugs (London, England: 2000)* 2009; 10: 1346-1358.

128 Deshayes E, Roumiguié M, Thibault C, Beuzeboc P, Cachin F, Hennequin C *et al*. Radium 223 dichloride for prostate cancer treatment. *Drug design, development and therapy* 2017; 11: 2643.

129 Parker Ca, Nilsson S, Heinrich D, Helle SI, O'sullivan J, Fosså SD *et al*. Alpha emitter radium-223 and survival in metastatic prostate cancer. *New England Journal of Medicine* 2013; 369: 213-223.

130 Morris MJ, Corey E, Guise TA, Gulley JL, Kevin Kelly W, Quinn DI *et al*. Radium-223 mechanism of action: implications for use in treatment combinations. *Nature Reviews Urology* 2019; 16: 745-756.

131 Smith M, Parker C, Saad F, Miller K, Tombal B, Ng QS *et al*. Addition of radium-223 to abiraterone acetate and prednisone or prednisolone in patients with castration-resistant prostate cancer and bone metastases (ERA 223): a randomised, double-blind, placebo-controlled, phase 3 trial. *The Lancet Oncology* 2019; 20: 408-419.

132 EMA. EMA Restricts Use of Prostate Cancer Medicine XOFIGO.

133 Emmett L, Willowson K, Violet J, Shin J, Blanksby A, Lee J. Lutetium 177 PSMA radionuclide therapy for men with prostate cancer: a review of the current literature and discussion of practical aspects of therapy. *Journal of medical radiation sciences* 2017; 64: 52-60.

134 Sartor O, De Bono J, Chi KN, Fizazi K, Herrmann K, Rahbar K *et al*. Lutetium-177–PSMA-617 for metastatic castration-resistant prostate cancer. *New England Journal of Medicine* 2021; 385: 1091-1103.

135 Chandran E, Figg WD, Madan R. Lutetium-177-PSMA-617: A Vision of the Future. *Cancer Biology & Therapy* 2022; 23: 186-190.

136 Messina C, Cattrini C, Soldato D, Vallome G, Caffo O, Castro E *et al*. BRCA mutations in prostate cancer: prognostic and predictive implications. *Journal of Oncology* 2020; 2020.

137 Mateo J, Boysen G, Barbieri CE, Bryant HE, Castro E, Nelson PS *et al*. DNA repair in prostate cancer: biology and clinical implications. *European urology* 2017; 71: 417-425.

138 Boussios S, Karihtala P, Moschetta M, Abson C, Karathanasi A, Zakynthinakis-Kyriakou N *et al*. Veliparib in ovarian cancer: a new synthetically lethal therapeutic approach. *Investigational new drugs* 2020; 38: 181-193.

139 Kunkel TA, Erie DA. Eukaryotic mismatch repair in relation to DNA replication. *Annual review of genetics* 2015; 49: 291.

140 Yang K, Guo R, Xu D. Non-homologous end joining: advances and frontiers. *Acta Biochimica et Biophysica Sinica* 2016; 48: 632-640.

141 van Gent DC, Hoeijmakers JH, Kanaar R. Chromosomal stability and the DNA double-stranded break connection. *Nature Reviews Genetics* 2001; 2: 196-206.

142 Hatano Y, Tamada M, Matsuo M, Hara A. Molecular trajectory of BRCA1 and BRCA2 mutations. *Frontiers in Oncology* 2020; 10: 361.

143 Lozano R, Castro E, Aragón IM, Cendón Y, Cattrini C, López-Casas PP *et al*. Genetic aberrations in DNA repair pathways: A cornerstone of precision oncology in prostate cancer. *British journal of cancer* 2021; 124: 552-563.

144 Ashworth A, Lord CJ. Synthetic lethal therapies for cancer: what's next after PARP inhibitors? *Nature reviews Clinical oncology* 2018; 15: 564-576.

145 Castro E, Romero-Laorden N, Del Pozo A. Re: PROREPAIR-B: A Prospective Cohort Study of the Impact of Germline DNA Repair Mutations on the Outcomes of Patients with Metastatic Castration-resistant Prostate Cancer. *J Clin Oncol* 2019; 37: 490-503.

146 Beltran H, Yelensky R, Frampton GM, Park K, Downing SR, MacDonald TY *et al*. Targeted next-generation sequencing of advanced prostate cancer identifies potential therapeutic targets and disease heterogeneity. *European urology* 2013; 63: 920-926.

147 Mateo J, Carreira S, Sandhu S, Miranda S, Mossop H, Perez-Lopez R *et al*. DNA-repair defects and olaparib in metastatic prostate cancer. *New England Journal of Medicine* 2015; 373: 1697-1708.

148 de Bono J, Mateo J, Fizazi K, Saad F, Shore N, Sandhu S *et al*. Olaparib for metastatic castration-resistant prostate cancer. *New England Journal of Medicine* 2020; 382: 2091-2102.

149 Abida W, Patnaik A, Campbell D, Shapiro J, Bryce AH, McDermott R *et al*. Rucaparib in men with metastatic castration-resistant prostate cancer harboring a BRCA1 or BRCA2 gene alteration. *Journal of Clinical Oncology* 2020; 38: 3763.

150 Abida W, Campbell D, Patnaik A, Shapiro JD, Sautois B, Vogelzang NJ *et al*. Non-BRCA DNA Damage Repair Gene Alterations and Response to the PARP Inhibitor Rucaparib in Metastatic Castration-Resistant Prostate Cancer: Analysis From the Phase II TRITON2 StudyRucaparib in mCRPC with a Non-BRCA DDR Gene Alteration. *Clinical Cancer Research* 2020; 26: 2487-2496.

151 Koivisto P, Kononen J, Palmberg C, Tammela T, Hyytinen E, Isola J *et al*. Androgen receptor gene amplification: a possible molecular mechanism for androgen deprivation therapy failure in prostate cancer. *Cancer research* 1997; 57: 314-319.

152 Visakorpi T, Hyytinen E, Koivisto P, Tanner M, Keinänen R, Palmberg C *et al*. In vivo amplification of the androgen receptor gene and progression of human prostate cancer. *Nature genetics* 1995; 9: 401-406.

153 Attard G, Swennenhuis JF, Olmos D, Reid AH, Vickers E, A'Hern R *et al*. Characterization of ERG, AR and PTEN gene status in circulating tumor cells from patients with castration-resistant prostate cancer. *Cancer research* 2009; 69: 2912-2918.

154 Leversha MA, Han J, Asgari Z, Danila DC, Lin O, Gonzalez-Espinoza R *et al*. Fluorescence in situ hybridization analysis of circulating tumor cells in metastatic prostate cancer. *Clinical cancer research* 2009; 15: 2091-2097.

155 Linja MJ, Savinainen KJ, Saramäki OR, Tammela TL, Vessella RL, Visakorpi T. Amplification and overexpression of androgen receptor gene in hormone-refractory prostate cancer. *Cancer research* 2001; 61: 3550-3555.

156 Chen CD, Welsbie DS, Tran C, Baek SH, Chen R, Vessella R *et al*. Molecular determinants of resistance to antiandrogen therapy. *Nature medicine* 2004; 10: 33-39.

157 Kawata H, Ishikura N, Watanabe M, Nishimoto A, Tsunenari T, Aoki Y. Prolonged treatment with bicalutamide induces androgen receptor overexpression and androgen hypersensitivity. *The Prostate* 2010; 70: 745-754.

158 Veldscholte J, Ris-Stalpers C, Kuiper G, Jenster G, Berrevoets C, Claassen E *et al*. A mutation in the ligand binding domain of the androgen receptor of human INCaP cells affects steroid binding characteristics and response to anti-androgens. *Biochemical and biophysical research communications* 1990; 173: 534-540.

159 Newmark JR, Hardy DO, Tonb DC, Carter BS, Epstein JI, Isaacs WB *et al*. Androgen receptor gene mutations in human prostate cancer. *Proceedings of the National Academy of Sciences* 1992; 89: 6319-6323.

160 Barbieri CE, Baca SC, Lawrence MS, Demichelis F, Blattner M, Theurillat J-P *et al*. Exome sequencing identifies recurrent SPOP, FOXA1 and MED12 mutations in prostate cancer. *Nature genetics* 2012; 44: 685-689.

161 Tan J-a, Sharief Y, Hamil KG, Gregory CW, Zang D-Y, Sar M *et al*. Dehydroepiandrosterone activates mutant androgen receptors expressed in the androgen-dependent human prostate cancer xenograft CWR22 and LNCaP cells. *Molecular Endocrinology* 1997; 11: 450-459.

162 van de Wijngaart DJ, Molier M, Lusher SJ, Hersmus R, Jenster G, Trapman J *et al*. Systematic Structure-Function Analysis of Androgen Receptor Leu701 Mutants Explains the Properties of the Prostate Cancer Mutant L701H 2. *Journal of Biological Chemistry* 2010; 285: 5097-5105.

163 Hu R, Dunn TA, Wei S, Isharwal S, Veltri RW, Humphreys E *et al*. Ligand-independent androgen receptor variants derived from splicing of cryptic exons signify hormone-refractory prostate cancer. *Cancer research* 2009; 69: 16-22.

164 Guo Z, Yang X, Sun F, Jiang R, Linn DE, Chen H *et al*. A novel androgen receptor splice variant is up-regulated during prostate cancer progression and promotes androgen depletion–resistant growth. *Cancer research* 2009; 69: 2305-2313.

165 Welti J, Rodrigues DN, Sharp A, Sun S, Lorente D, Riisnaes R *et al*. Analytical validation and clinical qualification of a new immunohistochemical assay for androgen receptor splice variant-7 protein expression in metastatic castration-resistant prostate cancer. *European urology* 2016; 70: 599-608.

166 Efstathiou E, Titus M, Wen S, Hoang A, Karlou M, Ashe R *et al*. Molecular characterization of enzalutamide-treated bone metastatic castration-resistant prostate cancer. *European urology* 2015; 67: 53-60.

167 Sharp A, Coleman I, Yuan W, Sprenger C, Dolling D, Rodrigues DN *et al*. Androgen receptor splice variant-7 expression emerges with castration resistance in prostate cancer. *The Journal of clinical investigation* 2019; 129: 192-208.

168 Antonarakis ES, Lu C, Wang H, Luber B, Nakazawa M, Roeser JC *et al*. AR-V7 and resistance to enzalutamide and abiraterone in prostate cancer. *New England Journal of Medicine* 2014; 371: 1028-1038.

169 Antonarakis ES, Lu C, Luber B, Wang H, Chen Y, Zhu Y *et al*. Clinical significance of androgen receptor splice variant-7 mRNA detection in circulating tumor cells of men with metastatic castration-resistant prostate cancer treated with first-and second-line abiraterone and enzalutamide. *Journal of Clinical Oncology* 2017; 35: 2149.

170 Armstrong AJ, Halabi S, Luo J, Nanus DM, Giannakakou P, Szmulewitz RZ *et al*. Prospective multicenter validation of androgen receptor splice variant 7 and hormone therapy resistance in high-risk castration-resistant prostate cancer: the PROPHECY study. *Journal of Clinical Oncology* 2019; 37: 1120.

171 Antonarakis ES, Lu C, Luber B, Wang H, Chen Y, Nakazawa M *et al*. Androgen receptor splice variant 7 and efficacy of taxane chemotherapy in patients with metastatic castration-resistant prostate cancer. *JAMA oncology* 2015; 1: 582-591.

172 Armstrong AJ, Luo J, Nanus DM, Giannakakou P, Szmulewitz RZ, Danila DC *et al*. Prospective multicenter study of circulating tumor cell AR-V7 and taxane versus hormonal treatment outcomes in metastatic castration-resistant prostate cancer. *JCO Precision Oncology* 2020; 4: 1285-1301.

173 Kessel K, Seifert R, Weckesser M, Roll W, Humberg V, Schlack K *et al*. Molecular analysis of circulating tumor cells of metastatic castration-resistant Prostate Cancer Patients receiving 177Lu-PSMA-617 Radioligand Therapy. *Theranostics* 2020; 10: 7645.

174 Scher HI, Lu D, Schreiber NA, Louw J, Graf RP, Vargas HA *et al*. Association of AR-V7 on circulating tumor cells as a treatment-specific biomarker with outcomes and survival in castration-resistant prostate cancer. *JAMA oncology* 2016; 2: 1441-1449.

175 Scher HI, Graf RP, Schreiber NA, McLaughlin B, Lu D, Louw J *et al*. Nuclear-specific AR-V7 protein localization is necessary to guide treatment selection in metastatic castration-resistant prostate cancer. *European urology* 2017; 71: 874-882.

176 Scher HI, Graf RP, Schreiber NA, Jayaram A, Winquist E, McLaughlin B *et al*. Assessment of the validity of nuclear-localized androgen receptor splice variant 7 in circulating tumor cells as a predictive biomarker for castration-resistant prostate cancer. *JAMA oncology* 2018; 4: 1179-1186.

177 Libertini SJ, Tepper CG, Rodriguez V, Asmuth DM, Kung H-J, Mudryj M. Evidence for calpain-mediated androgen receptor cleavage as a mechanism for androgen independence. *Cancer research* 2007; 67: 9001-9005.

178 Cai C, He HH, Chen S, Coleman I, Wang H, Fang Z *et al*. Androgen receptor gene expression in prostate cancer is directly suppressed by the androgen receptor through recruitment of lysine-specific demethylase 1. *Cancer cell* 2011; 20: 457-471.

179 Metzger E, Wissmann M, Yin N, Müller JM, Schneider R, Peters AH *et al*. LSD1 demethylates repressive histone marks to promote androgen-receptor-dependent transcription. *Nature* 2005; 437: 436-439.

180 Uo T, Plymate SR, Sprenger CC. The potential of AR-V7 as a therapeutic target. *Expert Opinion on Therapeutic Targets* 2018; 22: 201-216.

181 Liu L, Xie N, Sun S, Plymate S, Mostaghel E, Dong X. Mechanisms of the androgen receptor splicing in prostate cancer cells. *Oncogene* 2014; 33: 3140-3150.

182 Wang B, Lo UG, Wu K, Kapur P, Liu X, Huang J *et al*. Developing new targeting strategy for androgen receptor variants in castration resistant prostate cancer. *International journal of cancer* 2017; 141: 2121-2130.

183 Jones D, Noble M, Wedge SR, Robson CN, Gaughan L. Aurora A regulates expression of AR-V7 in models of castrate resistant prostate cancer. *Scientific reports* 2017; 7: 1-11.

184 Li S, Qi Y, Yu J, Hao Y, He B, Zhang M *et al*. Nuclear Aurora kinase A switches m6A reader YTHDC1 to enhance an oncogenic RNA splicing of tumor suppressor RBM4. *Signal transduction and targeted therapy* 2022; 7: 1-15.

185 Lee ECY, Frolov A, Li R, Ayala G, Greenberg NM. Targeting Aurora kinases for the treatment of prostate cancer. *Cancer research* 2006; 66: 4996-5002.

186 Nadiminty N, Tummala R, Liu C, Lou W, Evans CP, Gao AC. NF-κB2/p52: c-Myc: hnRNPA1 Pathway Regulates Expression of Androgen Receptor Splice Variants and Enzalutamide Sensitivity in Prostate CancerHnRNPA1 Regulates Alternative Splicing of Androgen Receptor. *Molecular cancer therapeutics* 2015; 14: 1884-1895.

187 Zhang Z, Zhou N, Huang J, Ho T-T, Zhu Z, Qiu Z *et al*. Regulation of androgen receptor splice variant AR3 by PCGEM1. *Oncotarget* 2016; 7: 15481.

188 Wang R, Sun Y, Li L, Niu Y, Lin W, Lin C *et al*. Preclinical study using Malat1 small interfering RNA or androgen receptor splicing variant 7 degradation enhancer ASC-J9® to suppress enzalutamide-resistant prostate cancer progression. *European urology* 2017; 72: 835-844.

189 Li Y, Hwang TH, Oseth L, Hauge A, Vessella RL, Schmechel SC *et al*. AR intragenic deletions linked to androgen receptor splice variant expression and activity in models of prostate cancer progression. *Oncogene* 2012; 31: 4759-4767.

190 Henzler C, Li Y, Yang R, McBride T, Ho Y, Sprenger C *et al*. Truncation and constitutive activation of the androgen receptor by diverse genomic rearrangements in prostate cancer. *Nature communications* 2016; 7: 1-12.

191 Liu C, Lou W, Yang JC, Liu L, Armstrong CM, Lombard AP *et al*. Proteostasis by STUB1/HSP70 complex controls sensitivity to androgen receptor targeted therapy in advanced prostate cancer. *Nature communications* 2018; 9: 1-16.

192 Liu C, Yang JC, Armstrong CM, Lou W, Liu L, Qiu X *et al*. AKR1C3 Promotes AR-V7 Protein Stabilization and Confers Resistance to AR-Targeted Therapies in Advanced Prostate CancerAKR1C3 Regulates AR-V7 and Confers Resistance. *Molecular cancer therapeutics* 2019; 18: 1875-1886.

193 Gao L, Zhang W, Zhang J, Liu J, Sun F, Liu H *et al*. KIF15-mediated stabilization of AR and AR-V7 contributes to enzalutamide resistance in prostate cancer. *Cancer research* 2021; 81: 1026-1039.

194 Liu Y, Yu C, Shao Z, Xia X, Hu T, Kong W *et al*. Selective degradation of AR-V7 to overcome castration resistance of prostate cancer. *Cell death & disease* 2021; 12: 1-13.

195 Li Y, Xie N, Gleave ME, Rennie PS, Dong X. AR-v7 protein expression is regulated by protein kinase and phosphatase. *Oncotarget* 2015; 6: 33743.

196 Roggero CM, Jin L, Cao S, Sonavane R, Kopplin NG, Ta HQ *et al*. A detailed characterization of stepwise activation of the androgen receptor variant 7 in prostate cancer cells. *Oncogene* 2021; 40: 1106-1117.

197 Özgün F, Kaya Z, Morova T, Geverts B, Abraham TE, Houtsmuller AB *et al*. DNA binding alters ARv7 dimer interactions. *Journal of cell science* 2021; 134: jcs258332.

198 Xu D, Zhan Y, Qi Y, Cao B, Bai S, Xu W *et al*. Androgen Receptor Splice Variants Dimerize to Transactivate Target GenesDimerization of Androgen Receptor Splice Variants. *Cancer research* 2015; 75: 3663-3671.

199 Zhan Y, Zhang G, Wang X, Qi Y, Bai S, Li D *et al*. Interplay between Cytoplasmic and Nuclear Androgen Receptor Splice Variants Mediates Castration ResistanceAR-V Interactions Impact Castration Resistance. *Molecular Cancer Research* 2017; 15: 59-68.

200 Cao B, Qi Y, Zhang G, Xu D, Zhan Y, Alvarez X *et al*. Androgen receptor splice variants activating the full-length receptor in mediating resistance to androgen-directed therapy. *Oncotarget* 2014; 5: 1646.

201 Monaghan AE, McEwan IJ. A sting in the tail: the N-terminal domain of the androgen receptor as a drug target. *Asian Journal of Andrology* 2016; 18: 687.

202 Magani F, Peacock SO, Rice MA, Martinez MJ, Greene AM, Magani PS *et al*. Targeting AR Variant–Coactivator Interactions to Exploit Prostate Cancer VulnerabilitiesTargeting AR Variant Coactivation in CRPC. *Molecular cancer research* 2017; 15: 1469-1480.

203 Wang Q, Li W, Zhang Y, Yuan X, Xu K, Yu J *et al*. Androgen receptor regulates a distinct transcription program in androgen-independent prostate cancer. *Cell* 2009; 138: 245-256.

204 Chen Z, Wu D, Thomas-Ahner JM, Lu C, Zhao P, Zhang Q *et al*. Diverse AR-V7 cistromes in castration-resistant prostate cancer are governed by HoxB13. *Proceedings of the National Academy of Sciences* 2018; 115: 6810-6815.

205 Wei J, Shi Z, Na R, Wang C-H, Resurreccion WK, Zheng SL *et al*. Germline HOXB13 G84E mutation carriers and risk to twenty common types of cancer: results from the UK Biobank. *British journal of cancer* 2020; 123: 1356-1359.

206 Krause WC, Shafi AA, Nakka M, Weigel NL. Androgen receptor and its splice variant, AR-V7, differentially regulate FOXA1 sensitive genes in LNCaP prostate cancer cells. *The international journal of biochemistry & cell biology* 2014; 54: 49-59.

207 Cato L, de Tribolet-Hardy J, Lee I, Rottenberg JT, Coleman I, Melchers D *et al*. ARv7 represses tumor-suppressor genes in castration-resistant prostate cancer. *Cancer cell* 2019; 35: 401-413. e406.

208 Jenster G, van der Korput HA, van Vroonhoven C, van der Kwast TH, Trapman J, Brinkmann AO. Domains of the human androgen receptor involved in steroid binding, transcriptional activation, and subcellular localization. *Molecular endocrinology* 1991; 5: 1396-1404.

209 Jenster G, van der Korput HA, Trapman J, Brinkmann AO. Identification of Two Transcription Activation Units in the N-terminal Domain of the Human Androgen Receptor (∗). *Journal of Biological Chemistry* 1995; 270: 7341-7346.

210 Simental J, Sar M, Lane M, French F, Wilson E. Transcriptional activation and nuclear targeting signals of the human androgen receptor. *Journal of Biological Chemistry* 1991; 266: 510-518.

211 Kumar R, McEwan IJ. Allosteric modulators of steroid hormone receptors: structural dynamics and gene regulation. *Endocrine reviews* 2012; 33: 271-299.

212 Oldfield CJ, Uversky VN, Dunker AK, Kurgan L. Introduction to intrinsically disordered proteins and regions. *Intrinsically Disordered Proteins*. Elsevier, 2019, pp 1-34.

213 Tsafou K, Tiwari P, Forman-Kay J, Metallo SJ, Toretsky J. Targeting intrinsically disordered transcription factors: changing the paradigm. *Journal of molecular biology* 2018; 430: 2321-2341.

214 Sadar MD. Discovery of drugs that directly target the intrinsically disordered region of the androgen receptor. *Expert opinion on drug discovery* 2020; 15: 551-560.

215 Andersen RJ, Mawji NR, Wang J, Wang G, Haile S, Myung J-K *et al*. Regression of castrate-recurrent prostate cancer by a small-molecule inhibitor of the amino-terminus domain of the androgen receptor. *Cancer cell* 2010; 17: 535-546.

216 Myung J-K, Banuelos CA, Fernandez JG, Mawji NR, Wang J, Tien AH *et al*. An androgen receptor N-terminal domain antagonist for treating prostate cancer. *The Journal of clinical investigation* 2013; 123: 2948-2960.

217 Yang YC, Banuelos CA, Mawji NR, Wang J, Kato M, Haile S *et al*. Targeting Androgen Receptor Activation Function-1 with EPI to Overcome Resistance Mechanisms in Castration-Resistant Prostate CancerEPI Overcomes Resistance Mechanisms in CRPC. *Clinical Cancer Research* 2016; 22: 4466-4477.

218 Brand LJ, Olson ME, Ravindranathan P, Guo H, Kempema AM, Andrews TE *et al*. EPI-001 is a selective peroxisome proliferator-activated receptor-gamma modulator with inhibitory effects on androgen receptor expression and activity in prostate cancer. *Oncotarget* 2015; 6: 3811.

219 Vaishampayan U, Montgomery R, Gordon M, Smith D, Barber K, de Haas-Amatsaleh A *et al*. EPI-506 (ralaniten acetate), a novel androgen receptor (AR) N-terminal domain (NTD) inhibitor, in men with metastatic castration-resistant prostate cancer (mCRPC): Phase 1 update on safety, tolerability, pharmacokinetics and efficacy. *Annals of Oncology* 2017; 28: v274.

220 Le Moigne R, Pearson P, Lauriault V, Chi K, Ianotti N, Pachynski R *et al*. Pre-Clinical and clinical pharmacology of EPI-7386, an androgen receptor N-terminal domain inhibitor for castration-resistant prostate cancer. *J Clin Oncol* 2021; 39.

221 Khorasanizadeh S, Rastinejad F. Nuclear-receptor interactions on DNA-response elements. *Trends in biochemical sciences* 2001; 26: 384-390.

222 Dalal K, Che M, Que NS, Sharma A, Yang R, Lallous N *et al*. Bypassing Drug Resistance Mechanisms of Prostate Cancer with Small Molecules that Target Androgen Receptor–

Chromatin InteractionsTargeting Androgen Receptor Interactions with Chromatin. *Molecular cancer therapeutics* 2017; 16: 2281-2291.

223 Dalal K, Ban F, Li H, Morin H, Roshan-Moniri M, Tam KJ *et al*. Selectively targeting the dimerization interface of human androgen receptor with small-molecules to treat castration-resistant prostate cancer. *Cancer Letters* 2018; 437: 35-43.

224 Radaeva M, Ban F, Zhang F, LeBlanc E, Lallous N, Rennie PS *et al*. Development of novel inhibitors targeting the d-box of the dna binding domain of androgen receptor. *International journal of molecular sciences* 2021; 22: 2493.

225 Liu C, Lou W, Zhu Y, Nadiminty N, Schwartz CT, Evans CP *et al*. Niclosamide Inhibits Androgen Receptor Variants Expression and Overcomes Enzalutamide Resistance in Castration-Resistant Prostate CancerNiclosamide Overcomes Resistance to Enzalutamide. *Clinical cancer research* 2014; 20: 3198-3210.

226 Liu C, Armstrong CM, Ning S, Yang JC, Lou W, Lombard AP *et al*. ARVib suppresses growth of advanced prostate cancer via inhibition of androgen receptor signaling. *Oncogene* 2021; 40: 5379-5392.

227 Parikh M, Liu C, Wu C-Y, Evans CP, Dall'Era M, Robles D *et al*. Phase Ib trial of reformulated niclosamide with abiraterone/prednisone in men with castration-resistant prostate cancer. *Scientific reports* 2021; 11: 1-7.

228 Lee GT, Nagaya N, Desantis J, Madura K, Sabaawy HE, Kim W-J *et al*. Effects of MTX-23, a Novel PROTAC of Androgen Receptor Splice Variant-7 and Androgen Receptor, on CRPC Resistant to Second-Line Antiandrogen TherapyMTX-23, a Novel PROTAC That Degrades AR-V7 and AR-FL. *Molecular cancer therapeutics* 2021; 20: 490-499.

229 Burslem GM, Crews CM. Proteolysis-targeting chimeras as therapeutics and tools for biological discovery. *Cell* 2020; 181: 102-114.

230 Dawson MA, Prinjha RK, Dittmann A, Giotopoulos G, Bantscheff M, Chan W-I *et al*. Inhibition of BET recruitment to chromatin as an effective treatment for MLL-fusion leukaemia. *Nature* 2011; 478: 529-533.

231 Filippakopoulos P, Qi J, Picaud S, Shen Y, Smith WB, Fedorov O *et al*. Selective inhibition of BET bromodomains. *Nature* 2010; 468: 1067-1073.

232 Asangani IA, Dommeti VL, Wang X, Malik R, Cieslik M, Yang R *et al*. Therapeutic targeting of BET bromodomain proteins in castration-resistant prostate cancer. *Nature* 2014; 510: 278-282.

233 Chan SC, Selth LA, Li Y, Nyquist MD, Miao L, Bradner JE *et al*. Targeting chromatin binding regulation of constitutively active AR variants to overcome prostate cancer resistance to endocrine-based therapies. *Nucleic acids research* 2015; 43: 5880-5897.

234 Welti J, Sharp A, Yuan W, Dolling D, Nava Rodrigues D, Figueiredo I *et al*. Targeting Bromodomain and Extra-Terminal (BET) Family Proteins in Castration-Resistant Prostate Cancer (CRPC) Targeting BET Family Proteins in CRPC. *Clinical Cancer Research* 2018; 24: 3149-3162.

235 Aggarwal RR, Schweizer MT, Nanus DM, Pantuck AJ, Heath EI, Campeau E *et al*. A Phase Ib/IIa Study of the Pan-BET Inhibitor ZEN-3694 in Combination with Enzalutamide in Patients with Metastatic Castration-resistant Prostate CancerBET Inhibitor ZEN-3694 Plus Enzalutamide in mCRPC. *Clinical Cancer Research* 2020; 26: 5338-5347.

236 Fu M, Rao M, Wang C, Sakamaki T, Wang J, Di Vizio D *et al*. Acetylation of androgen receptor enhances coactivator binding and promotes prostate cancer cell growth. *Molecular and cellular biology* 2003; 23: 8563-8575.

237 Ianculescu I, Wu D-Y, Siegmund KD, Stallcup MR. Selective roles for cAMP response element-binding protein binding protein and p300 protein as coregulators for androgen-regulated gene expression in advanced prostate cancer cells. *Journal of Biological Chemistry* 2012; 287: 4000-4013.

238 Fu M, Wang C, Reutens AT, Wang J, Angeletti RH, Siconolfi-Baez L *et al*. p300 and p300/cAMP-response element-binding protein-associated factor acetylate the androgen receptor at sites governing hormone-dependent transactivation. *Journal of Biological Chemistry* 2000; 275: 20853-20860.

239 Debes JD, Sebo TJ, Lohse CM, Murphy LM, Haugen DAL, Tindall DJ. p300 in prostate cancer proliferation and progression. *Cancer research* 2003; 63: 7638-7640.

240 Comuzzi B, Nemes C, Schmidt S, Jasarevic Z, Lodde M, Pycha A *et al*. The androgen receptor co-activator CBP is up-regulated following androgen withdrawal and is highly expressed in advanced prostate cancer. *The Journal of Pathology: A Journal of the Pathological Society of Great Britain and Ireland* 2004; 204: 159-166.

241 Welti J, Sharp A, Brooks N, Yuan W, McNair C, Chand SN *et al*. Targeting the p300/CBP Axis in Lethal Prostate CancerTargeting the p300/CBP Axis in Lethal Prostate Cancer. *Cancer discovery* 2021; 11: 1118-1137.

242 Jin L, Garcia J, Chan E, de la Cruz C, Segal E, Merchant M *et al*. Therapeutic Targeting of the CBP/p300 Bromodomain Blocks the Growth of Castration-Resistant Prostate CancerCBP/p300 Inhibitors for the Treatment of Prostate Cancer. *Cancer research* 2017; 77: 5564-5575.

243 De Bono JS, Cojocaru E, Plummer ER, Knurowski T, Clegg K, Ashby F *et al*. An open label phase I/IIa study to evaluate the safety and efficacy of CCS1477 as monotherapy and in combination in patients with advanced solid/metastatic tumors. American Society of Clinical Oncology, 2019.

244 Sung H, Ferlay J, Siegel RL, Laversanne M, Soerjomataram I, Jemal A *et al*. Global cancer statistics 2020: GLOBOCAN estimates of incidence and mortality worldwide for 36 cancers in 185 countries2021; 71: 209-249.

245 Siegel RL, Miller KD, Fuchs HE, Jemal A. Cancer statistics, 2022. *CA: A Cancer Journal for Clinicians* 2022; 72: 7-33.

246 Labriola MK, Atiq S, Hirshman N, Bitting RL. Management of men with metastatic castration-resistant prostate cancer following potent androgen receptor inhibition: A review of novel investigational therapies. *Prostate Cancer and Prostatic Diseases* 2021; 24: 301-309.

247 De Bono JS, Logothetis CJ, Molina A, Fizazi K, North S, Chu L *et al*. Abiraterone and increased survival in metastatic prostate cancer. *New England Journal of Medicine* 2011; 364: 1995-2005.

248 Li Y, Yang R, Henzler CM, Ho Y, Passow C, Auch B *et al*. Diverse AR gene rearrangements mediate resistance to androgen receptor inhibitors in metastatic prostate cancer. *Clinical Cancer Research* 2020; 26: 1965-1976.

249 Annala M, Taavitsainen S, Khalaf DJ, Vandekerkhove G, Beja K, Sipola J *et al*. Evolution of castration-resistant prostate cancer in ctDNA during sequential androgen receptor pathway inhibition. *Clinical Cancer Research* 2021; 27: 4610-4623.

250 Armstrong CM, Gao AC. Current strategies for targeting the activity of androgen receptor variants. *Asian Journal of Urology* 2019; 6: 42-49.

251 Korpal M, Korn JM, Gao X, Rakiec DP, Ruddy DA, Doshi S *et al*. An F876L mutation in androgen receptor confers genetic and phenotypic resistance to MDV3100 (enzalutamide). *Cancer discovery* 2013; 3: 1030-1043.

252 Gaddipati JP, McLeod DG, Heidenberg HB, Sesterhenn IA, Finger MJ, Moul JW *et al*. Frequent detection of codon 877 mutation in the androgen receptor gene in advanced prostate cancers. *Cancer research* 1994; 54: 2861-2864.

253 Hu R, Lu C, Mostaghel EA, Yegnasubramanian S, Gurel M, Tannahill C *et al*. Distinct transcriptional programs mediated by the ligand-dependent full-length androgen

receptor and its splice variants in castration-resistant prostate cancer. *Cancer research* 2012; 72: 3457-3462.

254 Yu Z, Chen S, Sowalsky AG, Voznesensky OS, Mostaghel EA, Nelson PS *et al*. Rapid induction of androgen receptor splice variants by androgen deprivation in prostate cancer. *Clinical cancer research* 2014; 20: 1590-1600.

255 Li Y, Alsagabi M, Fan D, Bova GS, Tewfik AH, Dehm SM. Intragenic rearrangement and altered RNA splicing of the androgen receptor in a cell-based model of prostate cancer progression. *Cancer research* 2011; 71: 2108-2117.

256 Li Y, Chan SC, Brand LJ, Hwang TH, Silverstein KA, Dehm SM. Androgen receptor splice variants mediate enzalutamide resistance in castration-resistant prostate cancer cell lines. *Cancer research* 2013; 73: 483-489.

257 Zhu Y, Dalrymple SL, Coleman I, Zheng SL, Xu J, Hooper JE *et al*. Role of androgen receptor splice variant-7 (AR-V7) in prostate cancer resistance to 2nd-generation androgen receptor signaling inhibitors. *Oncogene* 2020; 39: 6935-6949.

258 Dar JA, Masoodi KZ, Eisermann K, Isharwal S, Ai J, Pascal LE *et al*. The N-terminal domain of the androgen receptor drives its nuclear localization in castration-resistant prostate cancer cells. *The Journal of steroid biochemistry and molecular biology* 2014; 143: 473-480.

259 Liang J, Wang L, Poluben L, Nouri M, Arai S, Xie L *et al*. Androgen receptor splice variant 7 functions independently of the full length receptor in prostate cancer cells. *Cancer Letters* 2021; 519: 172-184.

260 Hu R, Isaacs WB, Luo JJTP. A snapshot of the expression signature of androgen receptor splicing variants and their distinctive transcriptional activities2011; 71: 1656-1667.

261 Xu D, Zhan Y, Qi Y, Cao B, Bai S, Xu W *et al*. Androgen Receptor Splice Variants Dimerize to Transactivate Target Genes. *Cancer Res* 2015; 75: 3663-3671.

262 Le Moigne R, Pearson P, Lauriault V, Chi K, Ianotti N, Pachynski R *et al*. Pre-Clinical and clinical pharmacology of EPI-7386, an androgen receptor N-terminal domain inhibitor for castration-resistant prostate cancer. *J Clin Oncol* 2021; 39: 119.

263 Brand LJ, Olson ME, Ravindranathan P, Guo H, Kempema AM, Andrews TE *et al*. EPI-001 is a selective peroxisome proliferator-activated receptor-gamma modulator with inhibitory effects on androgen receptor expression and activity in prostate cancer. *Oncotarget* 2015; 6: 3811-3824.

264 Xu D, Zhan Y, Qi Y, Cao B, Bai S, Xu W *et al*. Androgen receptor splice variants dimerize to transactivate target genes. *Cancer research* 2015: canres. 0381.2015.

265 McClurg UL, Cork DM, Darby S, Ryan-Munden CA, Nakjang S, Mendes Côrtes L *et al*. Identification of a novel K311 ubiquitination site critical for androgen receptor transcriptional activity. *Nucleic acids research* 2017; 45: 1793-1804.

266 Lee GT, Nagaya N, Desantis J, Madura K, Sabaawy HE, Kim W-J *et al*. Effects of MTX-23, a novel PROTAC of androgen receptor splice variant-7 and androgen receptor, on CRPC resistant to second-line antiandrogen therapy. *Molecular cancer therapeutics* 2021; 20: 490-499.

267 Tukachinsky H, Madison RW, Chung JH, Gjoerup OV, Severson EA, Dennis L *et al*. Genomic analysis of circulating tumor DNA in 3,334 patients with advanced prostate cancer identifies targetable BRCA alterations and AR resistance mechanisms. *Clinical Cancer Research* 2021; 27: 3094-3105.

268 Liu W, Zhou J, Geng G, Lin R, Wu JH. Synthesis and in vitro characterization of ionone-based compounds as dual inhibitors of the androgen receptor and NF-kappaB. *Invest New Drugs* 2014; 32: 227-234.

269 Liu W, Zhou J, Geng G, Shi Q, Sauriol F, Wu JH. Antiandrogenic, maspin induction, and antiprostate cancer activities of tanshinone IIA and its novel derivatives with modification in ring A. *J Med Chem* 2012; 55: 971-975.

270 Liu B, Geng G, Lin R, Ren C, Wu JH. Learning from estrogen receptor antagonism: structure-based identification of novel antiandrogens effective against multiple clinically relevant androgen receptor mutants. *Chem Biol Drug Des* 2012; 79: 300-312.

271 Potter GA, Barrie SE, Jarman M, Rowlands MG. Novel steroidal inhibitors of human cytochrome P45017. alpha.-Hydroxylase-C17, 20-lyase): potential agents for the treatment of prostatic cancer. *Journal of medicinal chemistry* 1995; 38: 2463-2471.

272 Kanayama M, Lu C, Luo J, Antonarakis ES. AR splicing variants and resistance to AR targeting agents. *Cancers* 2021; 13: 2563.

273 Chan SC, Li Y, Dehm SM. Androgen receptor splice variants activate androgen receptor target genes and support aberrant prostate cancer cell growth independent of canonical androgen receptor nuclear localization signal. *Journal of Biological Chemistry* 2012; 287: 19736-19749.

274 Li Y, Yang R, Henzler CM, Ho Y, Passow C, Auch B *et al*. Diverse AR Gene Rearrangements Mediate Resistance to Androgen Receptor Inhibitors in Metastatic Prostate CancerAR Gene Rearrangements in Prostate Cancer. *Clinical Cancer Research* 2020; 26: 1965-1976.

275 Annala M, Taavitsainen S, Khalaf DJ, Vandekerkhove G, Beja K, Sipola J *et al*. Evolution of Castration-Resistant Prostate Cancer in ctDNA during Sequential Androgen Receptor Pathway InhibitionProstate Cancer Evolution during Sequential AR Inhibition. *Clinical Cancer Research* 2021; 27: 4610-4623.

276 Ponnusamy S, He Y, Hwang D-J, Thiyagarajan T, Houtman R, Bocharova V *et al*. Orally Bioavailable Androgen Receptor Degrader, Potential Next-Generation Therapeutic for Enzalutamide-Resistant Prostate CancerA Novel AR Degrader for the Treatment of Prostate Cancer. *Clinical Cancer Research* 2019; 25: 6764-6780.

277 Melnyk JE, Steri V, Nguyen HG, Hwang YC, Gordan JD, Hann B *et al*. Targeting a splicing-mediated drug resistance mechanism in prostate cancer by inhibiting transcriptional regulation by PKCβ1. *Oncogene* 2022; 41: 1536-1549.

278 Esquenet M, Swinnen JV, Heyns W, Verhoeven G. LNCaP prostatic adenocarcinoma cells derived from low and high passage numbers display divergent responses not only to androgens but also to retinoids. *The Journal of steroid biochemistry and molecular biology* 1997; 62: 391-399.

279 Yu Z, Chen S, Sowalsky AG, Voznesensky OS, Mostaghel EA, Nelson PS *et al*. Rapid Induction of Androgen Receptor Splice Variants by Androgen Deprivation in Prostate CancerAndrogen Repression of AR Splice Variant. *Clinical cancer research* 2014; 20: 1590-1600.

280 Dehm SM, Schmidt LJ, Heemers HV, Vessella RL, Tindall DJ. Splicing of a novel androgen receptor exon generates a constitutively active androgen receptor that mediates prostate cancer therapy resistance. *Cancer research* 2008; 68: 5469-5477.

281 Hu R, Isaacs WB, Luo J. A snapshot of the expression signature of androgen receptor splicing variants and their distinctive transcriptional activities. *The Prostate* 2011; 71: 1656-1667.

282 Mollica L, Bessa LM, Hanoulle X, Jensen MR, Blackledge M, Schneider R. Binding mechanisms of intrinsically disordered proteins: theory, simulation, and experiment. *Frontiers in molecular biosciences* 2016; 3: 52.

283 Reid J, Murray I, Watt K, Betney R, McEwan IJ. The androgen receptor interacts with multiple regions of the large subunit of general transcription factor TFIIF. *Journal of Biological Chemistry* 2002; 277: 41247-41253.

284 De Mol E, Szulc E, Di Sanza C, Martínez-Cristóbal P, Bertoncini CW, Fenwick RB *et al*. Regulation of androgen receptor activity by transient interactions of its transactivation domain with general transcription regulators. *Structure* 2018; 26: 145-152. e143.

285 Schweizer MT, Antonarakis ES, Wang H, Ajiboye AS, Spitz A, Cao H *et al*. Effect of bipolar androgen therapy for asymptomatic men with castration-resistant prostate cancer: results from a pilot clinical study. *Science translational medicine* 2015; 7: 269ra262-269ra262.

286 Sfanos KS, Bruno TC, Maris CH, Xu L, Thoburn CJ, DeMarzo AM *et al*. Phenotypic analysis of prostate-infiltrating lymphocytes reveals TH17 and Treg skewing. *Clinical Cancer Research* 2008; 14: 3254-3261.

287 Flammiger A, Weisbach L, Huland H, Tennstedt P, Simon R, Minner S *et al*. High tissue density of FOXP3+ T cells is associated with clinical outcome in prostate cancer. *European journal of cancer* 2013; 49: 1273-1279.

288 Mercader M, Bodner BK, Moser MT, Kwon PS, Park ES, Manecke RG *et al*. T cell infiltration of the prostate induced by androgen withdrawal in patients with prostate cancer. *Proceedings of the National Academy of Sciences* 2001; 98: 14565-14570.

289 Gannon PO, Poisson AO, Delvoye N, Lapointe R, Mes-Masson A-M, Saad F. Characterization of the intra-prostatic immune cell infiltration in androgen-deprived prostate cancer patients. *Journal of immunological methods* 2009; 348: 9-17.

290 Calagua C, Russo J, Sun Y, Schaefer R, Lis R, Zhang Z *et al*. Expression of PD-L1 in Hormone-naïve and Treated Prostate Cancer Patients Receiving Neoadjuvant Abiraterone Acetate plus Prednisone and LeuprolideNeoadjuvant Abi/Prednisone/Leuprolide Reduces PD-L1 in PCa. *Clinical Cancer Research* 2017; 23: 6812-6822.

291 Pu Y, Xu M, Liang Y, Yang K, Guo Y, Yang X *et al*. Androgen receptor antagonists compromise T cell response against prostate cancer leading to early tumor relapse. *Science translational medicine* 2016; 8: 333ra347-333ra347.

292 Carretero FJ, Del Campo AB, Flores-Martín JF, Mendez R, García-Lopez C, Cozar JM *et al*. Frequent HLA class I alterations in human prostate cancer: molecular mechanisms and clinical relevance. *Cancer Immunology, Immunotherapy* 2016; 65: 47-59.

293 Kwon ED, Drake CG, Scher HI, Fizazi K, Bossi A, Van den Eertwegh AJ *et al*. Ipilimumab versus placebo after radiotherapy in patients with metastatic castration-resistant prostate cancer that had progressed after docetaxel chemotherapy (CA184-043): a multicentre, randomised, double-blind, phase 3 trial. *The lancet oncology* 2014; 15: 700-712.

294 Beer TM, Kwon ED, Drake CG, Fizazi K, Logothetis C, Gravis G *et al*. Randomized, double-blind, phase III trial of ipilimumab versus placebo in asymptomatic or minimally

symptomatic patients with metastatic chemotherapy-naive castration-resistant prostate cancer. *J Clin Oncol* 2017; 35: 40-47.

295 Antonarakis ES, Piulats JM, Gross-Goupil M, Goh J, Ojamaa K, Hoimes CJ *et al*. Pembrolizumab for treatment-refractory metastatic castration-resistant prostate cancer: multicohort, open-label phase II KEYNOTE-199 study. *Journal of Clinical Oncology* 2020; 38: 395.

296 Kim JW, Shaffer DR, Massard C, Powles T, Harshman LC, Braiteh FS *et al*. A phase Ia study of safety and clinical activity of atezolizumab (atezo) in patients (pts) with metastatic castration-resistant prostate cancer (mCRPC). American Society of Clinical Oncology, 2018.

297 Sharma P, Pachynski RK, Narayan V, Fléchon A, Gravis G, Galsky MD *et al*. Nivolumab plus ipilimumab for metastatic castration-resistant prostate cancer: preliminary analysis of patients in the CheckMate 650 trial. *Cancer cell* 2020; 38: 489-499. e483.

298 Zhang L, Conejo-Garcia JR, Katsaros D, Gimotty PA, Massobrio M, Regnani G *et al*. Intratumoral T cells, recurrence, and survival in epithelial ovarian cancer2003; 348: 203-213.

299 Galon J, Costes A, Sanchez-Cabo F, Kirilovsky A, Mlecnik B, Lagorce-Pagès C *et al*. Type, density, and location of immune cells within human colorectal tumors predict clinical outcome2006; 313: 1960-1964.

300 Harlin H, Meng Y, Peterson AC, Zha Y, Tretiakova M, Slingluff C *et al*. Chemokine expression in melanoma metastases associated with CD8+ T-cell recruitment2009; 69: 3077-3085.

301 Fuertes MB, Kacha AK, Kline J, Woo S-R, Kranz DM, Murphy KM *et al*. Host type I IFN signals are required for antitumor CD8+ T cell responses through CD8α+ dendritic cells2011; 208: 2005-2016.

302 Diamond MS, Kinder M, Matsushita H, Mashayekhi M, Dunn GP, Archambault JM *et al*. Type I interferon is selectively required by dendritic cells for immune rejection of tumors2011; 208: 1989-2003.

303 Liu Y, Jesus AA, Marrero B, Yang D, Ramsey SE, Montealegre Sanchez GA *et al*. Activated STING in a vascular and pulmonary syndrome2014; 371: 507-518.

304 Zhu Q, Man SM, Gurung P, Liu Z, Vogel P, Lamkanfi M *et al*. Cutting edge: STING mediates protection against colorectal tumorigenesis by governing the magnitude of intestinal inflammation2014; 193: 4779-4782.

305 Woo S-R, Corrales L, Gajewski TFJTii. The STING pathway and the T cell-inflamed tumor microenvironment2015; 36: 250-256.

306 Conlon J, Burdette DL, Sharma S, Bhat N, Thompson M, Jiang Z *et al*. Mouse, but not human STING, binds and signals in response to the vascular disrupting agent 5, 6-dimethylxanthenone-4-acetic acid. *The Journal of Immunology* 2013; 190: 5216-5225.

307 Corrales L, Glickman LH, McWhirter SM, Kanne DB, Sivick KE, Katibah GE *et al*. Direct activation of STING in the tumor microenvironment leads to potent and systemic tumor regression and immunity. *Cell reports* 2015; 11: 1018-1030.

308 Fu J, Kanne DB, Leong M, Glickman LH, McWhirter SM, Lemmens E *et al*. STING agonist formulated cancer vaccines can cure established tumors resistant to PD-1 blockade. *Science translational medicine* 2015; 7: 283ra252-283ra252.

309 Maurice DH, Ke H, Ahmad F, Wang Y, Chung J, Manganiello VCJNrDd. Advances in targeting cyclic nucleotide phosphodiesterases2014; 13: 290-314.

310 Li L, Yin Q, Kuss P, Maliga Z, Millán JL, Wu H *et al*. Hydrolysis of 2′ 3′-cGAMP by ENPP1 and design of nonhydrolyzable analogs2014; 10: 1043-1048.

311 Gupta P, Mani S, Yang J, Hartwell K, Weinberg R. The evolving portrait of cancer metastasis. *Cold Spring Harbor symposia on quantitative biology*, vol. 70. Cold Spring Harbor Laboratory Press, 2005, pp 291-297.

312 Stoecklein NH, Klein CAJIjoc. Genetic disparity between primary tumours, disseminated tumour cells, and manifest metastasis2010; 126: 589-598.

313 Turajlic S, Swanton CJS. Metastasis as an evolutionary process2016; 352: 169-175.

314 McGranahan N, Furness AJ, Rosenthal R, Ramskov S, Lyngaa R, Saini SK *et al*. Clonal neoantigens elicit T cell immunoreactivity and sensitivity to immune checkpoint blockade2016; 351: 1463-1469.

315 Shae D, Becker KW, Christov P, Yun DS, Lytton-Jean AK, Sevimli S *et al*. Endosomolytic polymersomes increase the activity of cyclic dinucleotide STING agonists to enhance cancer immunotherapy2019; 14: 269-278.

316 Liu Y, Crowe WN, Wang L, Lu Y, Petty WJ, Habib AA *et al*. An inhalable nanoparticulate STING agonist synergizes with radiotherapy to confer long-term control of lung metastases2019; 10: 1-15.

317 Ramanjulu JM, Pesiridis GS, Yang J, Concha N, Singhaus R, Zhang S-Y *et al*. Design of amidobenzimidazole STING receptor agonists with systemic activity2018; 564: 439-443.

318 Cerboni S, Jeremiah N, Gentili M, Gehrmann U, Conrad C, Stolzenberg M-C *et al*. Intrinsic antiproliferative activity of the innate sensor STING in T lymphocytes2017; 214: 1769-1785.

319 Wu J, Chen Y-J, Dobbs N, Sakai T, Liou J, Miner JJ *et al*. STING-mediated disruption of calcium homeostasis chronically activates ER stress and primes T cell deathSTING-mediated ER stress primes T cell death2019; 216: 867-883.

320 Gulen MF, Koch U, Haag SM, Schuler F, Apetoh L, Villunger A *et al*. Signalling strength determines proapoptotic functions of STING2017; 8: 1-10.

321 Sivick KE, Desbien AL, Glickman LH, Reiner GL, Corrales L, Surh NH *et al*. Magnitude of therapeutic STING activation determines CD8+ T cell-mediated anti-tumor immunity2018; 25: 3074-3085. e3075.

322 Liang D, Xiao-Feng H, Guan-Jun D, Er-Ling H, Sheng C, Ting-Ting W *et al*. Activated STING enhances Tregs infiltration in the HPV-related carcinogenesis of tongue squamous cells via the c-jun/CCL22 signal2015; 1852: 2494-2503.

323 Liang H, Deng L, Hou Y, Meng X, Huang X, Rao E *et al*. Host STING-dependent MDSC mobilization drives extrinsic radiation resistance2017; 8: 1-10.

324 Zhang C-x, Ye S-b, Ni J-j, Cai T-t, Liu Y-n, Huang D-j *et al*. STING signaling remodels the tumor microenvironment by antagonizing myeloid-derived suppressor cell expansion2019; 26: 2314-2328.

325 Fu J, Kanne DB, Leong M, Glickman LH, McWhirter SM, Lemmens E *et al*. STING agonist formulated cancer vaccines can cure established tumors resistant to PD-1 blockade2015; 7: 283ra252-283ra252.

326 Lim S-O, Li C-W, Xia W, Cha J-H, Chan L-C, Wu Y *et al*. Deubiquitination and stabilization of PD-L1 by CSN52016; 30: 925-939.

327 Zhao L, Ching L, Kestell P, Baguley BJBjoc. The antitumour activity of 5, 6-dimethylxanthenone-4-acetic acid (DMXAA) in TNF receptor-1 knockout mice2002; 87: 465-470.

328 Ager CR, Reilley MJ, Nicholas C, Bartkowiak T, Jaiswal AR, Curran MAJCir. Intratumoral STING activation with T-cell checkpoint modulation generates systemic antitumor immunity2017; 5: 676-684.

329 Ghaffari A, Peterson N, Khalaj K, Vitkin N, Robinson A, Francis J-A *et al*. STING agonist therapy in combination with PD-1 immune checkpoint blockade enhances response to carboplatin chemotherapy in high-grade serous ovarian cancer2018; 119: 440-449.

330 Bakhoum SF, Cantley LC. The multifaceted role of chromosomal instability in cancer and its microenvironment. *Cell* 2018; 174: 1347-1360.

331 Xia T, Konno H, Ahn J, Barber GN. Deregulation of STING signaling in colorectal carcinoma constrains DNA damage responses and correlates with tumorigenesis. *Cell reports* 2016; 14: 282-297.

332 Xia T, Konno H, Barber GN. Recurrent loss of STING signaling in melanoma correlates with susceptibility to viral oncolysis. *Cancer research* 2016; 76: 6747-6759.

333 Baird JR, Friedman D, Cottam B, Dubensky TW, Kanne DB, Bambina S *et al*. Radiotherapy combined with novel STING-targeting oligonucleotides results in regression of established tumors. *Cancer research* 2016; 76: 50-61.

334 Liang D, Xiao-Feng H, Guan-Jun D, Er-Ling H, Sheng C, Ting-Ting W *et al*. Activated STING enhances Tregs infiltration in the HPV-related carcinogenesis of tongue squamous cells via the c-jun/CCL22 signal. *Biochimica et Biophysica Acta (BBA)-Molecular Basis of Disease* 2015; 1852: 2494-2503.

335 Bakhoum SF, Cantley LCJC. The multifaceted role of chromosomal instability in cancer and its microenvironment2018; 174: 1347-1360.

336 Paludan SR, Reinert LS, Hornung VJNRI. DNA-stimulated cell death: implications for host defence, inflammatory diseases and cancer2019; 19: 141-153.

337 Kitajima S, Ivanova E, Guo S, Yoshida R, Campisi M, Sundararaman SK *et al*. Suppression of STING associated with LKB1 loss in KRAS-driven lung cancer2019; 9: 34-45.

338 Zhang J, Chen Y, Chen X, Zhang W, Zhao L, Weng L *et al*. Deubiquitinase USP35 restrains STING-mediated interferon signaling in ovarian cancer2020: 1-17.

339 Zhang C-x, Huang D-j, Baloche V, Zhang L, Xu J-x, Li B-w *et al*. Galectin-9 promotes a suppressive microenvironment in human cancer by enhancing STING degradation2020; 9: 1-14.

340 Wu S, Zhang Q, Zhang F, Meng F, Liu S, Zhou R *et al*. HER2 recruits AKT1 to disrupt STING signalling and suppress antiviral defence and antitumour immunity2019; 21: 1027-1040.

341 Kim H, Kim H, Feng Y, Li Y, Tamiya H, Tocci S *et al*. PRMT5 control of cGAS/STING and NLRC5 pathways defines melanoma response to antitumor immunity2020; 12.

342 Konno H, Yamauchi S, Berglund A, Putney RM, Mulé JJ, Barber GNJO. Suppression of STING signaling through epigenetic silencing and missense mutation impedes DNA damage mediated cytokine production2018; 37: 2037-2051.

343 Abe T, Barber GNJJov. Cytosolic-DNA-mediated, STING-dependent proinflammatory gene induction necessitates canonical NF-κB activation through TBK12014; 88: 5328-5341.

344 Bakhoum SF, Ngo B, Laughney AM, Cavallo J-A, Murphy CJ, Ly P *et al*. Chromosomal instability drives metastasis through a cytosolic DNA response2018; 553: 467-472.

345 Shih VF-S, Tsui R, Caldwell A, Hoffmann A. A single NFκB system for both canonical and non-canonical signaling. *Cell research* 2011; 21: 86-102.

346 Chen Q, Sun L, Chen ZJ. Regulation and function of the cGAS–STING pathway of cytosolic DNA sensing. *Nature immunology* 2016; 17: 1142-1149.

347 Ishikawa H, Barber GN. STING is an endoplasmic reticulum adaptor that facilitates innate immune signalling. *Nature* 2008; 455: 674-678.

348 Galluzzi L, Vanpouille-Box C, Bakhoum SF, Demaria S. Snapshot: cGAS-STING signaling. *Cell* 2018; 173: 276-276. e271.

349 Jin J, Hu H, Li HS, Yu J, Xiao Y, Brittain GC *et al*. Noncanonical NF-κB pathway controls the production of type I interferons in antiviral innate immunity. *Immunity* 2014; 40: 342-354.

350 Chawla-Sarkar M, Lindner DJ, Liu Y-F, Williams B, Sen GC, Silverman RH *et al*. Apoptosis and interferons: role of interferon-stimulated genes as mediators of apoptosis. *Apoptosis* 2003; 8: 237-249.

351 Kotredes KP, Gamero AM. Interferons as inducers of apoptosis in malignant cells. *Journal of Interferon & Cytokine Research* 2013; 33: 162-170.

352 Bakhoum SF, Ngo B, Laughney AM, Cavallo J-A, Murphy CJ, Ly P *et al*. Chromosomal instability drives metastasis through a cytosolic DNA response. *Nature* 2018; 553: 467-472.

353 Hou Y, Liang H, Rao E, Zheng W, Huang X, Deng L *et al*. Non-canonical NF-κB antagonizes STING sensor-mediated DNA sensing in radiotherapy. *Immunity* 2018; 49: 490-503. e494.

354 Ergun SL, Fernandez D, Weiss TM, Li L. STING polymer structure reveals mechanisms for activation, hyperactivation, and inhibition. *Cell* 2019; 178: 290-301. e210.

355 de Oliveira Mann CC, Orzalli MH, King DS, Kagan JC, Lee AS, Kranzusch PJ. Modular architecture of the STING C-terminal tail allows interferon and NF-κB signaling adaptation. *Cell reports* 2019; 27: 1165-1175. e1165.

356 Zhang C, Shang G, Gui X, Zhang X, Bai X-c, Chen ZJ. Structural basis of STING binding with and phosphorylation by TBK1. *Nature* 2019; 567: 394-398.

357 Liu S, Cai X, Wu J, Cong Q, Chen X, Li T *et al*. Phosphorylation of innate immune adaptor proteins MAVS, STING, and TRIF induces IRF3 activation. *Science* 2015; 347.

358 Konno H, Konno K, Barber GN. Cyclic dinucleotides trigger ULK1 (ATG1) phosphorylation of STING to prevent sustained innate immune signaling. *Cell* 2013; 155: 688-698.

359 Ni G, Konno H, Barber GN. Ubiquitination of STING at lysine 224 controls IRF3 activation. *Science immunology* 2017; 2.

360 Dunphy G, Flannery SM, Almine JF, Connolly DJ, Paulus C, Jønsson KL *et al*. Non-canonical activation of the DNA sensing adaptor STING by ATM and IFI16 mediates NF-κB signaling after nuclear DNA damage. *Molecular cell* 2018; 71: 745-760. e745.

361 Balka KR, Louis C, Saunders TL, Smith AM, Calleja DJ, D'Silva DB *et al*. TBK1 and IKKε Act Redundantly to Mediate STING-Induced NF-κB Responses in Myeloid Cells. *Cell Reports* 2020; 31: 107492.

362 Singh SS, Vats S, Chia AY-Q, Tan TZ, Deng S, Ong MS *et al*. Dual role of autophagy in hallmarks of cancer. *Oncogene* 2018; 37: 1142-1158.

363 Margolis SR, Wilson SC, Vance RE. Evolutionary origins of cGAS-STING signaling. *Trends in immunology* 2017; 38: 733-743.

364 Gui X, Yang H, Li T, Tan X, Shi P, Li M *et al*. Autophagy induction via STING trafficking is a primordial function of the cGAS pathway. *Nature* 2019; 567: 262-266.

365 Liu D, Wu H, Wang C, Li Y, Tian H, Siraj S *et al*. STING directly activates autophagy to tune the innate immune response. *Cell Death & Differentiation* 2019; 26: 1735-1749.

366 Prabakaran T, Bodda C, Krapp C, Zhang Bc, Christensen MH, Sun C *et al*. Attenuation of c GAS‐STING signaling is mediated by a p62/SQSTM 1‐dependent autophagy pathway activated by TBK1. *The EMBO journal* 2018; 37: e97858.

367 Mathew R, Karantza-Wadsworth V, White E. Role of autophagy in cancer. *Nature Reviews Cancer* 2007; 7: 961-967.

368 White E, DiPaola RS. The double-edged sword of autophagy modulation in cancer. *Clinical cancer research* 2009; 15: 5308-5316.

369 Gewirtz DA. The four faces of autophagy: implications for cancer therapy. *Cancer research* 2014; 74: 647-651.

370 Crazzolara R, Bradstock KF, Bendall LJ. RAD001 (Everolimus) induces autophagy in acute lymphoblastic leukemia. *Autophagy* 2009; 5: 727-728.

371 Mauthe M, Orhon I, Rocchi C, Zhou X, Luhr M, Hijlkema K-J *et al*. Chloroquine inhibits autophagic flux by decreasing autophagosome-lysosome fusion. *Autophagy* 2018; 14: 1435-1455.

372 Hargadon KM, Johnson CE, Williams CJ. Immune checkpoint blockade therapy for cancer: an overview of FDA-approved immune checkpoint inhibitors. *International immunopharmacology* 2018; 62: 29-39.

373 Pitt JM, Vétizou M, Daillère R, Roberti MP, Yamazaki T, Routy B *et al*. Resistance mechanisms to immune-checkpoint blockade in cancer: tumor-intrinsic and-extrinsic factors. *Immunity* 2016; 44: 1255-1269.

374 Demaria O, Cornen S, Daëron M, Morel Y, Medzhitov R, Vivier E. Harnessing innate immunity in cancer therapy. *Nature* 2019; 574: 45-56.

375 Garris CS, Luke JJ. Dendritic Cells, the T-cell-inflamed Tumor Microenvironment, and Immunotherapy Treatment ResponseDendritic Cells and Immunotherapy Response. *Clinical Cancer Research* 2020; 26: 3901-3907.

376 Motwani M, Pesiridis S, Fitzgerald KA. DNA sensing by the cGAS–STING pathway in health and disease. *Nature Reviews Genetics* 2019; 20: 657-674.

377 Marcus A, Mao AJ, Lensink-Vasan M, Wang L, Vance RE, Raulet DH. Tumor-derived cGAMP triggers a STING-mediated interferon response in non-tumor cells to activate the NK cell response. *Immunity* 2018; 49: 754-763. e754.

378 Woo S-R, Fuertes MB, Corrales L, Spranger S, Furdyna MJ, Leung MY *et al*. STING-dependent cytosolic DNA sensing mediates innate immune recognition of immunogenic tumors. *Immunity* 2014; 41: 830-842.

379 Lara Jr PN, Douillard J-Y, Nakagawa K, Von Pawel J, McKeage MJ, Albert I *et al*. Randomized phase III placebo-controlled trial of carboplatin and paclitaxel with or without the vascular disrupting agent vadimezan (ASA404) in advanced non–small-cell lung cancer. *Journal of Clinical Oncology* 2011; 29: 2965-2971.

380 Kim S, Li L, Maliga Z, Yin Q, Wu H, Mitchison TJ. Anticancer flavonoids are mouse-selective STING agonists. *ACS chemical biology* 2013; 8: 1396-1401.

381 Demaria O, De Gassart A, Coso S, Gestermann N, Di Domizio J, Flatz L *et al*. STING activation of tumor endothelial cells initiates spontaneous and therapeutic antitumor immunity. *Proceedings of the National Academy of Sciences* 2015; 112: 15408-15413.

382 Li T, Cheng H, Yuan H, Xu Q, Shu C, Zhang Y *et al*. Antitumor activity of cGAMP via stimulation of cGAS-cGAMP-STING-IRF3 mediated innate immune response. *Scientific reports* 2016; 6: 1-14.

383 Motedayen Aval L, Pease JE, Sharma R, Pinato DJ. Challenges and opportunities in the clinical development of STING agonists for cancer immunotherapy. *Journal of Clinical Medicine* 2020; 9: 3323.

384 Yi G, Brendel VP, Shu C, Li P, Palanathan S, Cheng Kao C. Single nucleotide polymorphisms of human STING can affect innate immune response to cyclic dinucleotides. *PloS one* 2013; 8: e77846.

385 Moore MW, Carbone FR, Bevan MJ. Introduction of soluble protein into the class I pathway of antigen processing and presentation. *Cell* 1988; 54: 777-785.

386 Fuertes MB, Kacha AK, Kline J, Woo S-R, Kranz DM, Murphy KM *et al*. Host type I IFN signals are required for antitumor CD8+ T cell responses through CD8α+ dendritic cells. *Journal of Experimental Medicine* 2011; 208: 2005-2016.

387 Diamond MS, Kinder M, Matsushita H, Mashayekhi M, Dunn GP, Archambault JM *et al*. Type I interferon is selectively required by dendritic cells for immune rejection of tumors. *Journal of Experimental Medicine* 2011; 208: 1989-2003.

388 Woo S-R, Corrales L, Gajewski TF. The STING pathway and the T cell-inflamed tumor microenvironment. *Trends in immunology* 2015; 36: 250-256.

389 Cerboni S, Jeremiah N, Gentili M, Gehrmann U, Conrad C, Stolzenberg M-C *et al*. Intrinsic antiproliferative activity of the innate sensor STING in T lymphocytes. *Journal of Experimental Medicine* 2017; 214: 1769-1785.

390 Wu J, Chen Y-J, Dobbs N, Sakai T, Liou J, Miner JJ *et al*. STING-mediated disruption of calcium homeostasis chronically activates ER stress and primes T cell death. *Journal of Experimental Medicine* 2019; 216: 867-883.

391 Gulen MF, Koch U, Haag SM, Schuler F, Apetoh L, Villunger A *et al*. Signalling strength determines proapoptotic functions of STING. *Nature communications* 2017; 8: 1-10.

392 Barber GN. STING: infection, inflammation and cancer. *Nature Reviews Immunology* 2015; 15: 760-770.

393 Domvri K, Petanidis S, Zarogoulidis P, Anestakis D, Tsavlis D, Bai C *et al*. Treg-dependent immunosuppression triggers effector T cell dysfunction via the STING/ILC2 axis. *Clinical Immunology* 2021; 222: 108620.

394 Zhang C-x, Ye S-b, Ni J-j, Cai T-t, Liu Y-n, Huang D-j *et al*. STING signaling remodels the tumor microenvironment by antagonizing myeloid-derived suppressor cell expansion. *Cell Death & Differentiation* 2019; 26: 2314-2328.

395 Liang H, Deng L, Hou Y, Meng X, Huang X, Rao E *et al*. Host STING-dependent MDSC mobilization drives extrinsic radiation resistance. *Nature communications* 2017; 8: 1-10.

396 Lim S-O, Li C-W, Xia W, Cha J-H, Chan L-C, Wu Y *et al*. Deubiquitination and stabilization of PD-L1 by CSN5. *Cancer cell* 2016; 30: 925-939.

397 Cheng AN, Cheng L-C, Kuo C-L, Lo YK, Chou H-Y, Chen C-H *et al*. Mitochondrial Lon-induced mtDNA leakage contributes to PD-L1–mediated immunoescape via STING-IFN signaling and extracellular vesicles. *Journal for immunotherapy of cancer* 2020; 8.

398 Du S-S, Chen G-W, Yang P, Chen Y-X, Hu Y, Zhao Q-Q *et al*. Radiation Therapy Promotes Hepatocellular Carcinoma Immune Cloaking via PD-L1 Upregulation Induced by cGAS-STING Activation. *International Journal of Radiation Oncology* Biology* Physics* 2022; 112: 1243-1255.

399 Meric-Bernstam F, Sandhu SK, Hamid O, Spreafico A, Kasper S, Dummer R *et al*. Phase Ib study of MIW815 (ADU-S100) in combination with spartalizumab (PDR001) in patients (pts) with advanced/metastatic solid tumors or lymphomas. American Society of Clinical Oncology, 2019.

400 Harrington K, Brody J, Ingham M, Strauss J, Cemerski S, Wang M *et al*. Preliminary results of the first-in-human (FIH) study of MK-1454, an agonist of stimulator of interferon genes (STING), as monotherapy or in combination with pembrolizumab (pembro) in patients with advanced solid tumors or lymphomas. *Annals of Oncology* 2018; 29: viii712.

401 Eftekharzadeh B, Banduseela VC, Chiesa G, Martínez-Cristóbal P, Rauch JN, Nath SR *et al*. Hsp70 and Hsp40 inhibit an inter-domain interaction necessary for transcriptional activity in the androgen receptor. *Nature communications* 2019; 10: 1-14.